UNIVERSITA' DEGLI STUDI DI NAPOLI "FEDERICO II"

SCUOLA POLITECNICA E DELLE SCIENZE DI BASE

Corso di Laurea Magistrale in Ingegneria Edile

Tesi di Laurea Magistrale in

Earthquake Engineering and Structural Control

DESIGN OPTIMIZATION OF HIGH-RISE BUILDINGS EQUIPPED WITH OUTRIGGER SYSTEMS AND SHEAR LINK BOZZO DEVICES (SLB)

RELATORI:

Ch.mo Prof. Ing. Giorgio Serino

Ch.mo. Prof. Ing. Antonio Formisano

CANDIDATA:

Francesca Del Vecchio

Matr. N51/0926

CORRELATORE:

Prof. Luis Bozzo, Phd

Anno Accademico 2022/2023

Alla mia Napoli,

questo è il nostro anno.

Alle mie compagne di avventura

Mesa, Carmen, Mariangela e Annamaria.

ABSTRACT

The development of tall buildings is constantly increasing around the world, introducing new challenges that must be addressed through engineering judgment. The design of high and slender structures is controlled by three determining factors - *strength, rigidity and functionality* - produced by the action of lateral load. The overall geometry of a building often determines what factor governs the design. There are numerous lateral structural systems used in the design of buildings, the one analyzed in this thesis is the ***Outrigger system***. These are rigid horizontal structures designed to improve the stiffness of the structure and the resistance to overturning of the building, connecting the central core to the perimeter columns. Historically used in the construction of canoes, there has been a gradual use in tall buildings and skyscrapers, with the aim of improving the structural response by adding stability. The processing of the system was realized with the addition of seismic energy dissipation devices, the ***Shear Link Bozzo device*** (widely used in Mexico, Peru, Ecuador) which have brought an advantage in the field of application, reducing vibration and concentrating most of the damage inside the device, preserving the remaining structural elements. The theoretical study of this system is analyzed through its application in a real case study of a reinforced concrete building located in *Nuevo Vallarta (Mexico)*, whose treatment highlights how the system represents an excellent solution for the seismic protection of tall buildings. The analysis highlights the convenience in the use of this system for significant structural improvements in terms of interstory drift, displacements, shear and accelerations, as well as providing a large energy dissipation capacity thanks to the presence of SLB heatsinks and determining a cost-effectiveness that defines, at the same construction cost, a more rigid structure and more resistant to horizontal forces.

LIST OF CONTENTS

LIST OF FIGUERES

LIST OF TABLES

1. INTRODUCTION

Mankind has always been fascinated by heights and throughout our history, we have constantly sought to metaphorically reach for the stars. From ancient pyramids to today's modern skyscraper, the power and wealth of a civilization has been repeatedly expressed through massive and monumental structures. Today the symbol of economic power and leadership is the skyscraper.

The development of tall buildings is rapidly increasing worldwide, introducing new challenges that must be addressed through engineering judgement.

The design of tall, slender structures is controlled by three determinants, strength (material capacity), stiffness (drift), and functionality (perception of motion and accelerations), produced by the action of lateral loading, such as wind or earthquake. The overall geometry of a building often determines which factor governs the overall design. As a building gets taller and leaner, drift considerations become more significant.

There are a number of lateral structural systems used in the design of high-rise buildings such as: shear frames, shear truss, shear core frames, framed pipes, lattice pipes, super frames etc.

Outrigger systems have been used extensively in super-tall buildings constructed since the 1980s, eclipsing the previously favoured tube-frame systems. For high-rise buildings, especially in active seismic zone or with dominant wind load, this system can be chosen as the appropriate structure. However, Outriggers are not listed as a seismic lateral load resistant system in any code. Design guidelines are not available. An experimental analysis was therefore carried out to define the correct system to be used in the structure.

A shear dissipator has been incorporated into this system which allows the energy deriving from a lateral load from an earthquake or wind to be dissipated.

Historically, the seismic design of structures has been based on a combination of strength and ductility. For small and frequent seismic perturbations, the structure should remain in the elastic range, with all stresses well below the yield points. However, it is not reasonable to expect a traditional structure to respond elastically

when subjected to a large earthquake. Instead, the design engineer relies on the inherent ductility of buildings to prevent catastrophic failure, while still accepting some level of structural and non-structural damage. This philosophy has led to the development of seismic design codes characterized by lateral force methods and inelastic design response spectra. With this approach the structure is designed to withstand an equivalent static load.

However, new and innovative structural protection concepts have been advanced in recent years and are in various stages of development. Modern structural protection systems can be divided into three main groups:

- ***Seismic Isolation Systems***

  A seismic isolation system is typically placed at the foundation of the structure and, due to its flexibility and energy absorption capacity, reflects and partially absorbs a portion of the earthquake input energy before it can be transmitted to the structure. The net effect is a reduction in the demand for energy dissipation on the structural system.

- ***Passive energy dissipation systems***

  The research and development of passive energy dissipation devices for structural applications has nearly 50 years of history. The basic function of these devices, when incorporated into the superstructure of a building, is to absorb a part of the incoming seismic energy thus reducing the demand for energy dissipation on the primary structural elements and minimizing possible structural damage. Unlike seismic isolation, these devices can also be effective against wind-induced motion and earthquake motion.

- ***Semi-active and active systems***

  Semi-active and active structural control is an area of structural protection in which the movement of a structure is controlled or modified by the action of a control system via an external energy supply. The difference between semi-active and fully active systems is that the first type of devices cannot add energy to the structure.

This thesis work proposes a study of the behavior of the Outriggers, the optimization of their position and the efficiency and improvement that the structure receives when two or three Outriggers are used in it. This system is coupled to passive energy

dissipation systems and in particular attention is paid to hysteretic metal devices, to which the Bozzo Shear Link device belongs.

For this reason:

- Chapter 2 deals with the description of Outrigger systems through an analysis of the stiffness, their evolution and their possible position within a generic structure;

- Chapter 3 deals with passive dissipation systems and metallic devices in which their basic principles and classification are introduced;

- Chapter 4 defines a more detailed focus on the Shear Link Bozzo device, through a description of the four generations, up to the modelling of the same;

- Chapter 5 describes the case study of the thesis: a new reinforced concrete skyscraper located in Nuevo Vallarta, Nayarit (Mexico). The purpose of the study is twofold: firstly, it intends to highlight the advantages associated with the application of the Outrigger system and the use of Bozzo Shear Link devices; a comparison is proposed between the bare frame structure, with 2 Outrigger systems and with 3 Outrigger systems;

2. OUTRIGGERS SYSTEM

2.1 Structural System for tall buildings

Since the beginning of the 20th century, skyscrapers have become part of the history of construction and their presence, initially confined to the urban fabric of the United States, has gradually spread to cities all over the world. There are several reasons behind the development of tall buildings, starting from a height of almost 50m up to the current 800m, with an average annual increase of 6.8m/year. However, the height of the building has not evolved gradually over time, but there are significant accelerations throughout history, due to various factors, in particular the progress of structural engineering and materials, and also of construction technologies.

From an urban planning and architectural point of view, tall buildings have developed over time due to the need for larger volumes available with limited building surfaces as well as the need to have a characterizing element in the city landscape.

In tall buildings, the structure has to support not only normal gravitational loads such as self-weight, permanent and variable loads, but also horizontal actions, such as wind and earthquakes, which are much more relevant than in normal buildings. For this reason, bracing systems must be created to contain inter-floor displacements, total displacements and reduce accelerations, in order to guarantee the well-being of customers and maximize the usable areas.

Tall buildings can have different uses: defensive (towers), communicative (bell towers), engineering (chimneys or antennas), residential, for the tertiary sector or as a landmark (e.g. the Eiffel Tower).

From the point of view of the construction material used to build the structural system, tall buildings can be divided into:

- *Steel Structures*: Supertall buildings are usually made of steel due to its high mechanical properties, light weight, and ease of assembly;
- *Reinforced concrete structures*: most of the tall buildings are made of reinforced concrete because it is cheaper than other materials but with very good properties (especially high-performance concrete);

- *Hybrid concrete-steel structures*: the advantage in this case is the possibility of creating very rigid elements (columns or walls) with reduced dimensions, a fundamental property for maximizing the available surfaces.

Given the importance of the cooperation between structural parts and architectural parts, in tall buildings it is possible to recognize two main types of mutually interacting systems:

- Structural systems designed to support gravitational loads (eg.floors, pillars and walls);
- Structural systems created to support horizontal actions (bracing systems) which are all the more relevant the higher the structure is, sometimes also influencing the architectural form.

Various structural systems have been introduced in tall buildings to overcome lateral and vertical loads. These structural systems are divided into external and internal structural systems.

The external structural systems such as tube, framed tube, reinforced tube, bundle tube, tube in tube, diagrid, space truss, super-frame and exoskeleton (Figure 2.1).

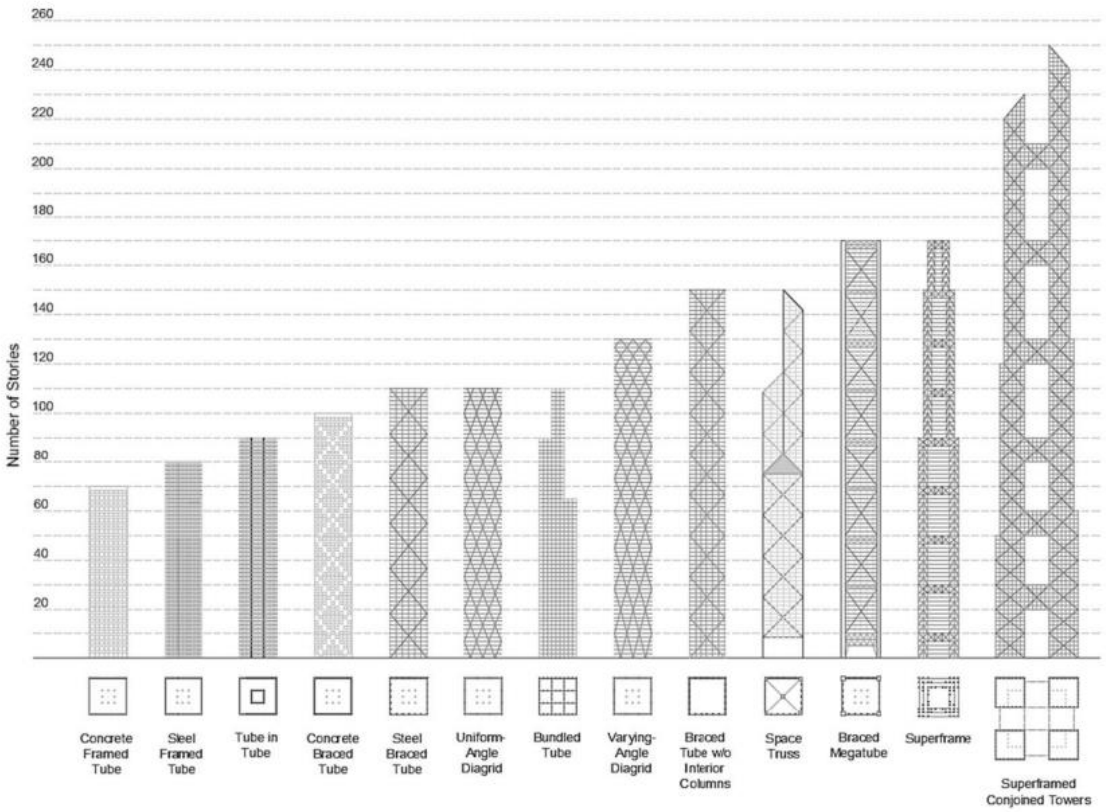

Figures 1 external structural system

The internal structural systems are moment resisting frame, braced frames, concentrically braced frames, shear walls, rigid frame, frame tube, braced tube, bundle tube and stabilizing systems which can be used to improve lateral strength in tall buildings (Figure 2.2).

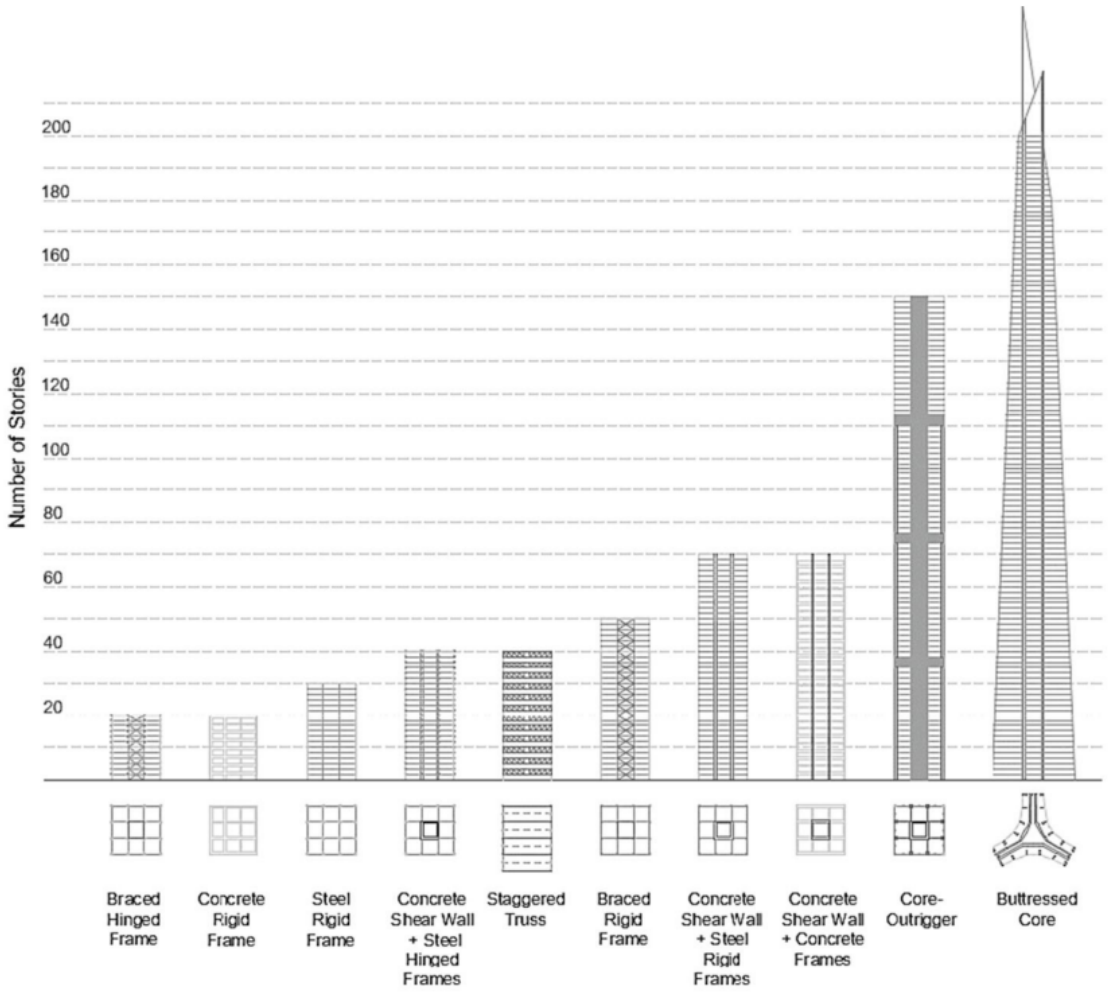

Figure 2. 2Internal structural system

Depending on the bracing system involved, another fictional classification of the heights that can be achieved with the different structural schemes presented is also possible:

- ***Semi-rigid frames***: pillars, beams and, in part, links are all interested in supporting horizontal actions. In this way, however, the height is limited and a maximum of 10 floors can be reached.
- ***Rigid frames*** - columns and beams are rigidly connected; therefore, the horizontal actions are supported through the flexural deformation of the frame. Higher heights are possible, allowing for up to 30 floors.

- ***Rigid frames with bracing systems***: in this case the horizontal actions are supported both by frames and by shear walls (in the case of reinforced concrete structures) or by diagonal bracing systems (in the case of steel structures) . In this way, 50 floors can be conveniently reached, even using slender and spaced columns (6-9 m).
- ***Frames with ribbon trusses and/or stabilizers***: the load-bearing system is given by a frame, a core and horizontal brackets placed at appropriate points along the entire height of the building, which connect the core with the external columns. In this way, under the action of horizontal forces, the structure benefits from the stiffening contribution given by the reaction of the columns, allowing it to reach heights of up to 80 floors.
- ***External frame pipes:*** consisting of an external braced box-like structure connected to an internal frame carrying only gravitational loads. It is possible to obtain buildings from 40 to 100 floors, with the possibility of interspaces of up to 20 m for the internal pillars.
- ***Diagonalized external tubes***: consisting of an external bracing box-like structure composed of beams, pillars and megadiagonals, supporting both horizontal and gravitational actions. Thanks to this, no internal columns are needed, allowing for large free internal spaces.
- ***Spatial Truss Structures***: Consisting of a system of main trusses, usually made of steel, carrying both horizontal and vertical forces. They allow you to build very tall buildings (70-150 floors).
- ***Diagrid Systems***: With their efficiency as a varied version of tubular systems, Diagrid structures are emerging as a new aesthetic trend for tall buildings. They effectively resist lateral shear due to axial forces in the diagonal members, but the joints must be designed with care.
- ***Super Frame Structures***: These take the form of a portal which is provided on the outside of the building. The frame resists all wind forces as an external tubular structure. The portal frame consists of vertical legs in each corner of the building which are connected by horizontal elements at approximately 12-14 floors. As the vertical elements are concentrated in the corner areas of the

building, maximum efficiency is achieved in resisting wind forces. This type of systems can be used for very tall buildings, up to 160 floors.

- ***Structures with Y-shaped plan and central nucleus***: used in modern buildings, they give the possibility of obtaining reduced slenderness and internal use space.

Below is a table and a list of images to briefly summarize the various types of structural systems discussed up to now:

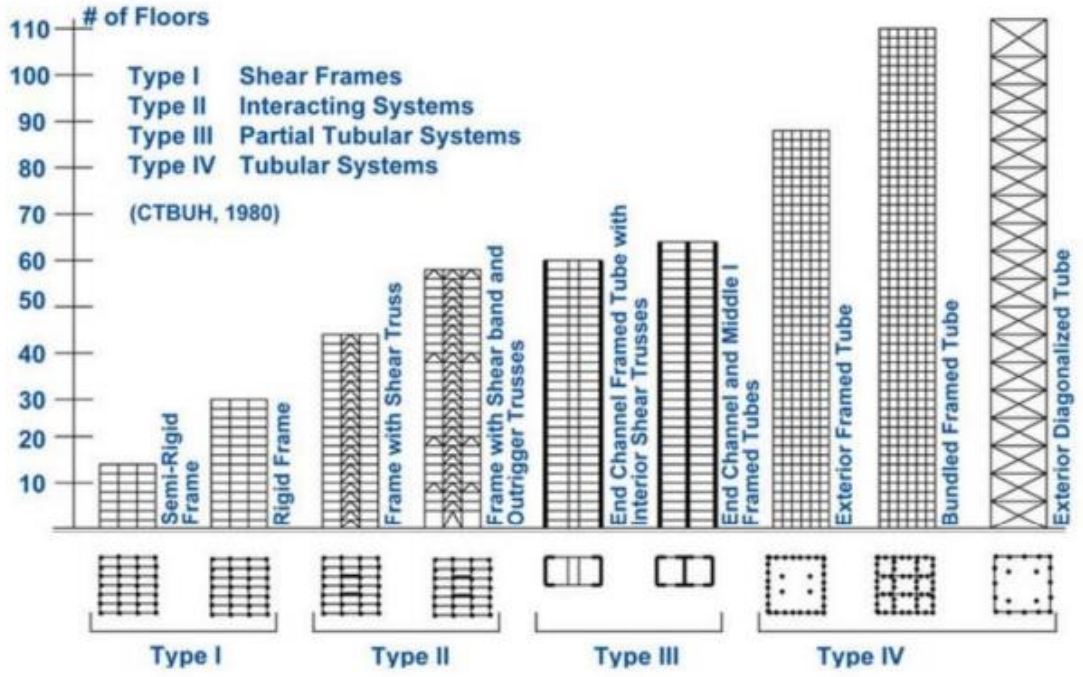

Figures 3 Skyscrapers and their evolution

Figures 2. 4Lever House (rigid frame); North Riverside (shear walls); World Trade Centre (outriggers)

Figure 2. 5Aon centre (framed tube); Hancock centre (tube trellis); Bank of China (Space Truss)

Figure 2. 6Hearst Tower (Diagrid systems); Burj Khalifa Facility (Y Footprint Structure

2.2 Introduction to Outriggers System

The ability to guarantee an efficient behaviour to lateral actions, both in the ultimate and serviceability limit states, is the fundamental characteristic of structural systems in tall buildings.

As far as the ultimate limit states are concerned, the required performances are related to the resistance, in particular to the ability to counter lateral actions in extreme situations. On the other hand, the essential requirement for a structural system in the serviceability limit state consists in its ability to adequately develop small lateral displacements when subjected to lateral forces, applied in their most unfavourable combinations.

This requirement is intrinsically connected to stiffness, which not only reduces lateral displacements, both total and relative between consecutive floors, but also makes vibrational effects acceptable, such as not to limit user comfort.

A second aspect of great importance concerns the ability to guarantee acceptable relative displacements between the load-bearing structure and the non-structural elements, without suffering significant damage. The need to guarantee reduced lateral displacements, associated with that of guaranteeing an adequate level of safety at the ultimate limit state, has always represented the fundamental problem of the structural design of tall buildings.

The solution to the problem has led to the definition of plants with known morphology, whose performances have been continuously improved, aimed at increasing the efficiency of the structural system as the height of the buildings increases. Various systems have been illustrated and discussed in detail for this purpose in the technical literature, among these the so-called "*Outrigger Systems*".

Outriggers are rigid horizontal structures designed to improve the rigidity and resistance to overturning of the building by connecting the core or backbone of the building to distant columns.

The earliest "outriggers" are horizontal beams connecting the canoe-shaped main hulls of Polynesian ocean-going boats to outrigger floats or "amas". A contemporary rustic version of this vessel type illustrates the key points about building outrigger systems.

A boat's narrow hull can capsize if tossed by unexpected waves, but a small amount of *ama* (upward drag) or *weight* (downward drag) acting through the outrigger lever is enough to prevent capsizing. Similarly, building outriggers attached to perimeter columns that can withstand top and bottom can greatly improve the building's toppling resistance.

While a boat may be weighted to resist capsizing, it can still experience uncomfortable long-term rolling, hooks attached to outriggers greatly reduce this behaviour and shorten the period of motion. Likewise, construction stabilizers can greatly reduce overall lateral drift.

Boats can have outriggers and ama on both sides or on one side (Figure 2.7). Buildings may have a centrally located core with outriggers extending to either side or a core located on one side of the building with outriggers extending to the building columns on the opposite side.

Figures 2. 7Single outrigger canoes; Double outrigger canoes

The explanation for the behaviour of building outriggers is simple: since the outriggers act as rigid arms engaging the outer columns, when a central core attempts to tilt, its rotation at the outriggers induces a tension-compression torque in the outer columns acting in opposition to this movement. The result is a type of reset moment that acts on the core at that level.

However, it is certain that joining the perimeter structural members to the core as a single lateral load resistant system will reduce the core overturning moment, but not the core horizontal plane shear forces. In fact, the shear in the core can actually increase (and change direction) at the stabilizer planes due to the horizontal force couples of the stabilizers acting upon it.

The idea of stabilizers in building structures is to couple the perimeter and internal structure as a whole to resist lateral loading. Considering the structure as shown in (Figure 2.8), both the inner core and the perimeter frame (or tube) are decoupled. Thus, the central core and perimeter frame resist lateral loading by pure cantilever action only. In theory, if the internal beams between the core and perimeter get deeper and stiffer, the core and perimeter frame can work together to resist lateral forces. However, since the typical span between the core and perimeter frame is between 9m and 15m, it is very difficult to provide girders that are rigid or deep enough to couple the core and perimeter frame, especially when the building is slender. All tall buildings have refugee floors and some buildings have mechanical floors at intermediate levels. This provides an opportunity for engineers to make full use of these spaces (sometimes one to three stories) to stiffen structures. For ease of presentation, the stabilizers are drawn as a deep beam as in (Figure 2.9) Assuming the stabilizers are strong enough to generate the supporting moment M_1 and M_2, the

moment at the base, $_0M_{base}$ will be reduced by ($M_1 + M_2$), that is, where Mi is the restrictive moment of the number i of stabilizers.

$$M_{base} = oM_{base} + M_1 + M_2 \quad (1)$$

The equation can also be written in the following form:

$$oM_{base} = M_{base} - SM_i$$

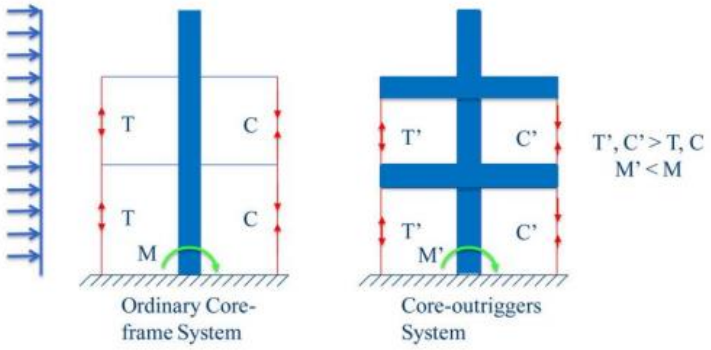

Figure 2. 8Difference between ordinary core-frame and core-outriggers system

From eq. (1), the base moment decreases by increasing the magnitude of M_i and/or the number of outriggers (i.e., i). However, if the magnitude of M_i is limited or small, even if there are many stabilizers, $_0M_{base}$ will still be close to M_{base}. In other words, it is more efficient for a stabilizer system to build with strong stabilizers than to increase the number of stabilizers with little stiffness.

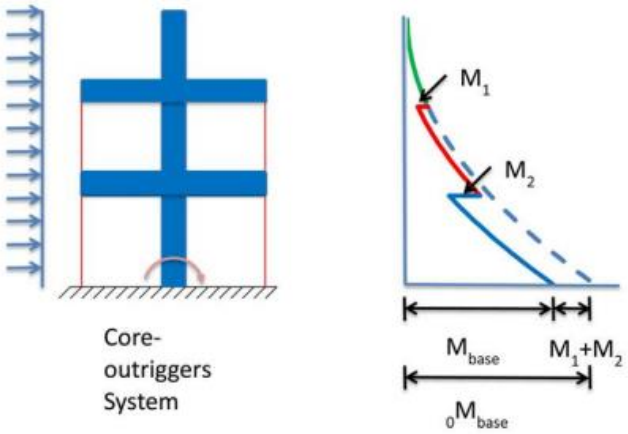

Figure 2. 9Difference of Moment Diagram between Ordinary and Outrigger Frame

Belts, such as trusses or walls surrounding the building, add further complexity. The straps can improve the efficiency of the lateral system.

- For towers with outriggers engaging individual mega columns, the straps can direct more gravity load onto the mega columns to minimize net uplift,

bracing, or column splices needed to resist the tension and stiffness reduction associated with concrete in net tension.

- For towers with external pipe systems - closely spaced perimeter columns connected by sub window beams - belting reduces the effect of external pipe shear lags, more effectively engages the axial stiffness contributions of multiple columns, and distributes more evenly across multiple columns. columns the large vertical forces applied by stabilizers.
- For both mega-column and tubular buildings, belting can further improve overall building stiffness through virtual or indirect outrigger behaviour provided by high in-plane shear stiffness, as well as increased torsional stiffness of the tower . Belts working with mega columns can also create a system that is resistant to secondary lateral loads, in seismic engineering terminology.

A core-and-outrigger system is often selected for the lateral load-resistance system of tall or slender buildings where the overturning moment is large relative to shear and where the overall flexural strains of the building are the major contributors to lateral deflections such as plane shift. In such situations, the outriggers reduce the building drift and central wind moments.

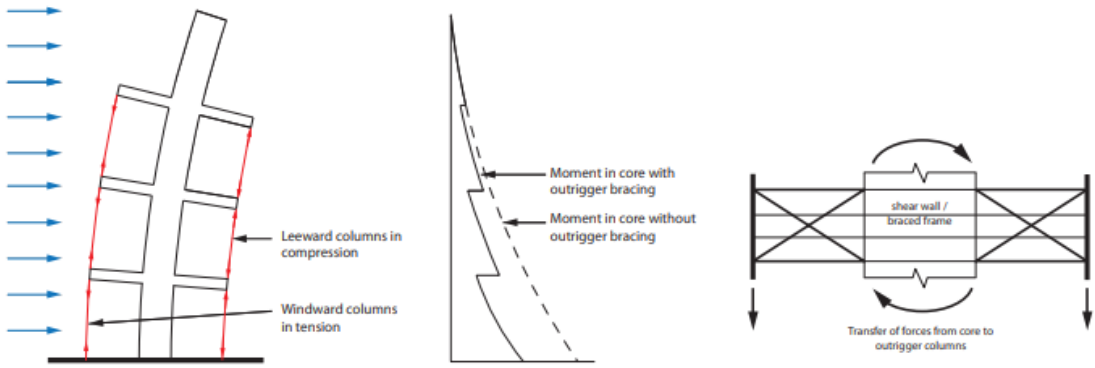

Figure 2. 10Interaction of core and outrigger

2.3 Analytical stiffness analysis

To represent in a simplified way through known static schemes the reasoning behind an outrigger system, let's make some considerations concerning the stiffness.

When the structure is subjected to a load, this produces a series of effects: displacements, tensions and deformations. In figure 2.11 we see the static scheme of a shelf, wedged at the base and subjected to a force F. Among all the effects there is one prevailing one, the one for which the force F does work.

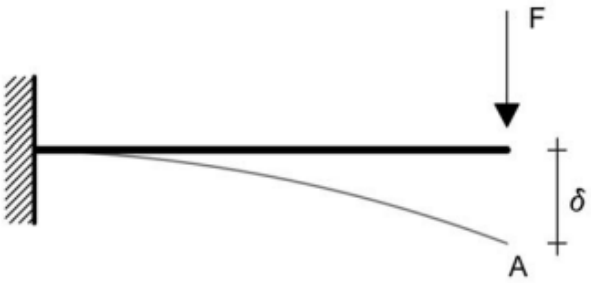

Figure 2. 11Deformed due to a shelf stuck to the base

The prevailing effect is the transverse displacement of the point of application of the force. That is (δ), which is:

$$\delta = \frac{F * l^3}{3EI}$$

The relationship between F (cause) and δ (effect) is linear (i.e.proportional) and can also be written as:

$$F = \left(\frac{3EI}{l^3}\right)\delta \qquad F = k * \delta \qquad k = \frac{3EI}{l^3}$$

Where *k* is the stiffness of the member, i.e. the force necessary to produce a unit displacement and considering the length of the element with *l :*

$$F = \frac{3EI}{l^3}(\delta = 1) = \frac{3EI}{l^3} = k$$

The greater the stiffness, the greater the force required to produce a given displacement.

Now let's refer to the frame shown in Figure 2.12, setting ourselves the goal of finding the stiffness of the frame, i.e. the coefficient of proportionality between *F* and *δ*.

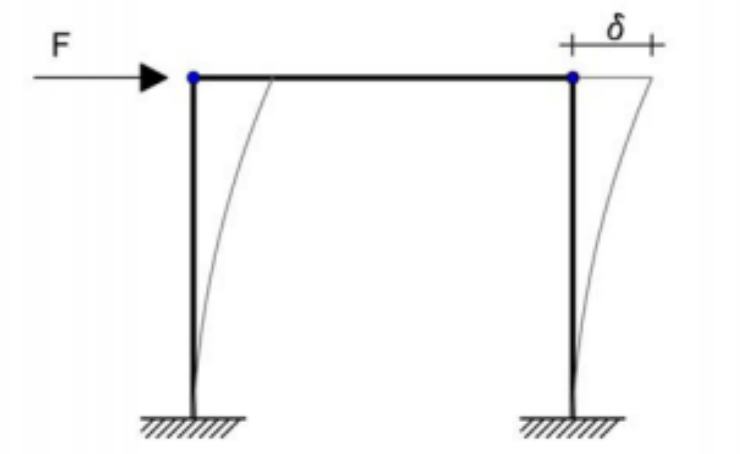

Figure 2. 12Static diagram of a portal with an applied force

We solve the once hyperstatic system, defined by two shelves connected by a pendulum. The force F is distributed between the two brackets, resulting in both being loaded by F/2, therefore the displacement will be equal to the displacement of a single bracket loaded at the top by the force F/2, i.e.:

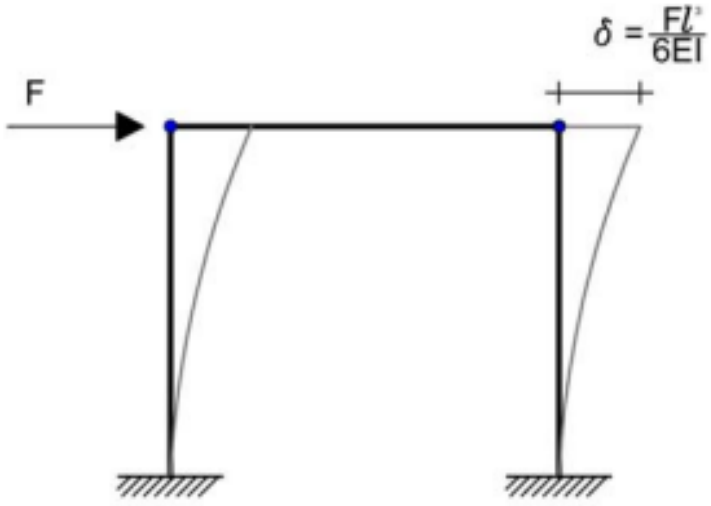

Figure 2. 13Deformed of a portal with force applied

Consequently, the translating stiffness, i.e. the one that links F and δ, of the portal in figure 2.13 is equal to:

$$k = \frac{3EI}{l^3} + \frac{3EI}{l^3} = \frac{6EI}{l^3}$$

Consequently, if we went to consider an even more complex system, which allows us to approach our case study, we will have that the stiffness will vary. For the frame in

figure 2.14, the force F will be distributed equally between the three uprights and this is equivalent to saying that the horizontal displacement will be equal to the displacement of one of the three brackets loaded with F/3.

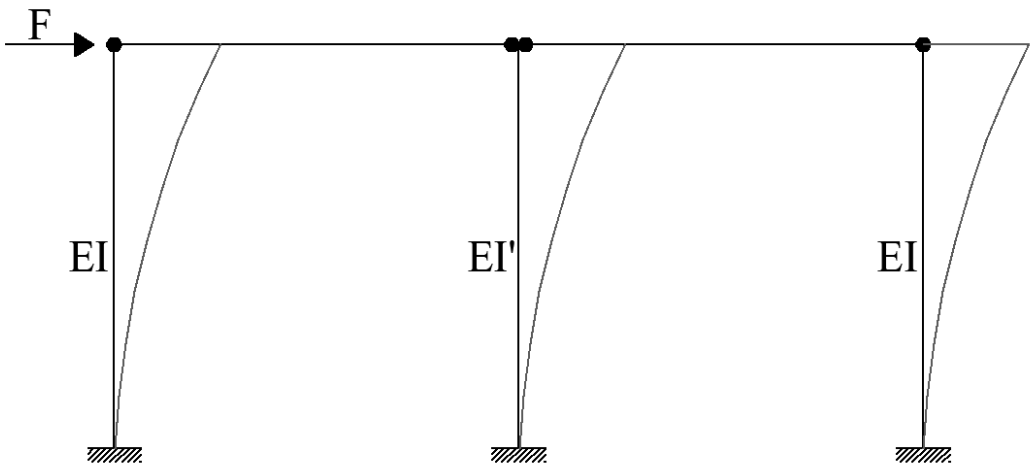

Figure 2. 14Static scheme composed of three brackets connected by two pendulums

$$\delta = \frac{F}{3} * \frac{l^3}{3EI} = \frac{F * l^3}{9EI}$$

Consequently, the total stiffness of the system will be given by:

$$k = \frac{6EI}{l^3} + \frac{3EI'}{l^3} \qquad (I)$$

The situation is different in the case of a shear-type frame, i.e. a frame with all interlocking nodes and with the beam considered infinitely rigid in bending with respect to the pillars. Studying figure 2.15:

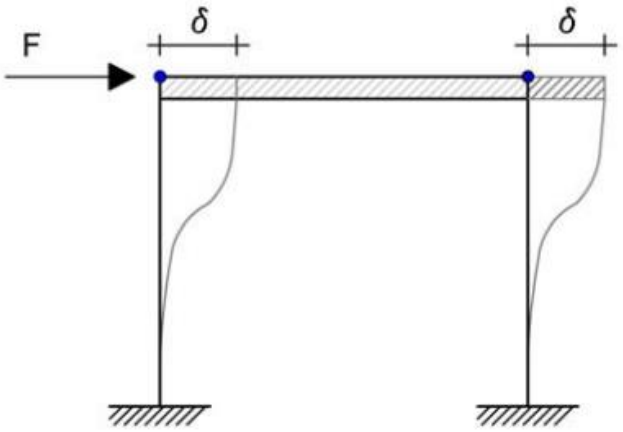

Figures 15 Shear type frame

Also, in this case the force F moves the crosspiece to the right, dragging the uprights with it, but the presence of the interlocking nodes and the hypothesis of infinite flexural stiffness of the beam imposes zero rotation on the nodes of the crosspiece.
The upright is in the condition of a doubly fixed beam and subject to a displacement imposed in a constraint. This diagram identifies the mechanical situation of the two uprights of figure 2.15 in which the two uprights and the beam which is infinitely stiff in bending define a shear-type frame. If the cross beam moves by δ , it induces a state of stress in the two uprights. In the sections where the uprights engage the crossbeam, this state of tension will act (equal but opposite) on the crossbeam and contribute to its static equilibrium. If we were to determine the equation of equilibrium at the translation of the beam we would have:

$$F = \frac{12EI}{l^3}\delta + \frac{12EI}{l^3}\delta = \frac{24EI}{l^3}\delta$$

The stiffness of the shear-type frame is therefore given by:

$$k = \frac{12EI}{l^3} + \frac{12EI}{l^3} = \frac{24EI}{l^3}$$

The situation is different in the specific case of a frame that wants to schematize the outrigger system with a central core. Let us therefore imagine that the aforementioned static diagram represents the cross section that sees the plane in which this system is defined, composed of the two external columns and a central one (representative of the central core) which allows the connection of the outrigger system to the wall, which can be schematically represented as an infinitely stiff beam is hinged on the two outer columns, while the central core will be connected directly to the infinitely stiff beam. The static scheme described is represented in figure 2.16:

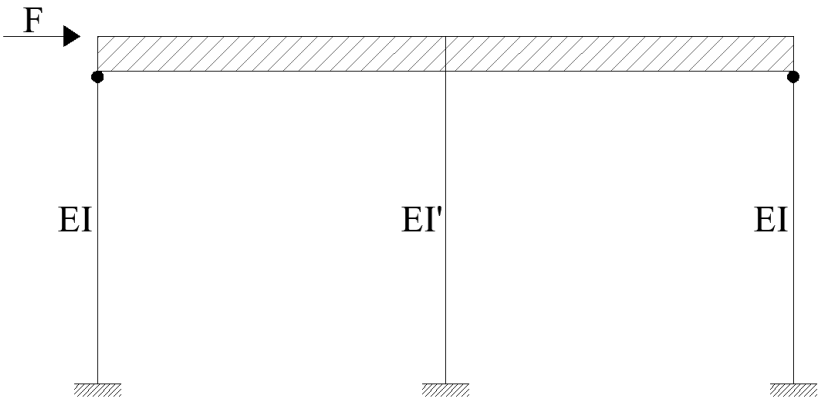

Figure 2. 16Static schematic of a system with outrigger

By applying the horizontal force to the system we will have a displacement defined as in figure 2.17:

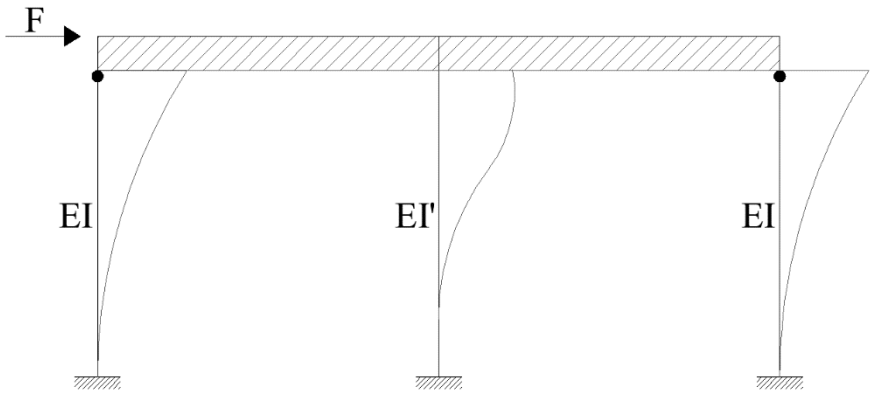

Figures 2. 17 Static scheme with deformed

If we were to determine the equation of equilibrium at the translation of the beam we would have:

$$F = \frac{3EI}{l^3}\delta + \frac{12EI'}{l^3}\delta + \frac{3EI}{l^3}\delta = \frac{6EI}{l^3}\delta + \frac{12EI'}{l^3}\delta$$

The stiffness of the frame in figure 2.17 is therefore given by:

$$k = \frac{6EI}{l^3} + \frac{12EI'}{l^3} \qquad (II)$$

Since the stiffness of the external columns is the typical stiffness of a corbel with applied force, i.e.,$\frac{3EI}{l^3}$; the central column instead being prevented from rotating at the head due to the presence of the outrigger will have a stiffness equal to $\frac{12EI}{l^3}$.

If we were to compare the static scheme in figure 2.14 and the one in figure 2.17, we would have:

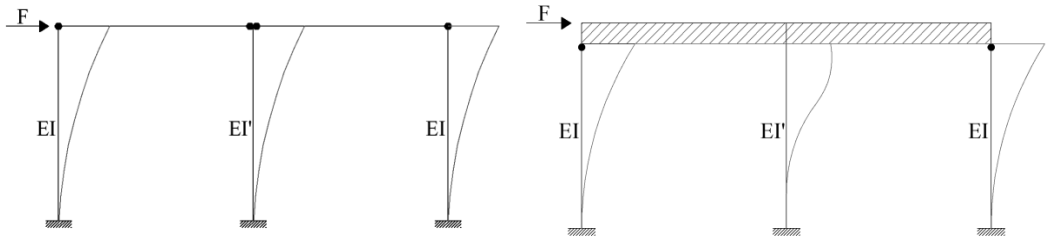

Comparing the stiffness equations (I) and (II), i.e.:

$$k = \frac{6EI}{l^3} + \frac{3EI'}{l^3} \qquad (I)$$

$$k = \frac{6EI}{l^3} + \frac{12EI'}{l^3} \qquad (II)$$

With the use of the outrigger system, we have gone from 3 to 12, therefore we have increased the stiffness of the system.

The outrigger stiffens the structure, and consequently with greater stiffnesses the displacement will decrease.

The possible addition of heat sinks, dissipating more will make me reduce the spectral ordinates due to the increase in damping. So, we will have that anyway, in any case even if the dissipator does not come into play, I have defined through the system alone an increase in stiffness beneficial for my system.

2.4 Types of outriggers systems

The use of outriggers in skyscrapers started about 5 decades ago, the first outrigger building was designed by Barbacki and was 47 story, Place Victoria Building in Montreal, Canada, completed in 1962. This braced structure serves as a single structure in a combination of stabilizers connected to the central wall and the perimeter column when subjected to lateral loads such as wind and earthquake.

Figure 2. 18Place Victoria Building , Montreal

Similarly, in cases where the core of tall buildings is unable to carry the lateral load on its own, stabilizers reduce the moment in the core by transferring some of it to the outer columns in the form of axial forces consisting of compression-tensile torques. Eventually, the core will no longer function as a shelf. A ribbon truss can be used to help distribute forces across a larger number of columns and to reduce the differential angles that can also support outriggers.

Even though the outriggers are internal structures, the contribution to the girdle trusses and megacolumns represents a large planning diffusion of the building stresses. Another benefit of a structure with outriggers is that closely spaced columns are not required, which allows for flexibility in meeting the functional requirements of the building.

With the introduction of outriggers into the structure, stiffness increases by 20 to 30%.

The introduction of them:

- increases the lateral crack resistance of the building;
- does not increase shear stiffness and the core itself will bear all lateral shear forces;
- the outer arms will decrease the lateral moment of the structure;
- the overturning moment of the core is small, which will reduce the uplift of the core, which will reduce the cost of the foundation.

Based on the different configurations of the outrigger system, it can have different structural forms.

1) From the point of view of the material:

- *Concrete outriggers*: The advantage of this type over steel is low cost and high stiffness. When sideloaded, the outrigger system must be rigid, which can easily be achieved with a concrete wall or rigid concrete deep beam. This type of stabilizer is more common in concrete rather than steel structures.
- *Steel outriggers*: These types of outriggers are employed extensively in many high-rise buildings as most high-rise buildings are a steel or composite structural system. In the conventional design, the outriggers are designed to be floor-height trusses
- *Hybrid or composite outriggers*: this type of outriggers integrates the advantages and avoids the shortcomings of steel and concrete outriggers, where those in pure concrete are very rigid, but at the same time, they are fragile. Also, steel outriggers are not as stiff as concrete ones, but have more ductility behaviour.

2) From the point of view of the system:

- *Direct or conventional outriggers*: In the conventional outrigger concept, outrigger trusses or beams are connected directly to shear walls or frame braces in the centre and to columns located outside the core. The stabilizer trusses, which are connected to the core and outboard columns of the core, restrain the rotation of the core and convert some of the momentum in the core into vertical torque at the columns.
- *Indirect or virtual outriggers (offset outriggers)* : This was proposed by Nair 1998 and also called a belt-truss system. Provides behaviour similar to the direct system but without direct connections between central walls and perimeter columns in the vertical plane.

  Eliminating a direct connection between the trusses avoids many of the problems associated with the use of stabilizers. The stabilizer concept is to use floor diaphragms, which are typically very stiff and strong in their own plane, transfer momentum from the core to the trusses or walls that are not connected directly to the core. The trusses or walls then convert the horizontal couples into vertical couples for the columns or other structural members outboard of the core. The virtual outrigger is considered the most

cost-effective type of outrigger and is employed in multi-story structures due to its many advantages over the conventional one.

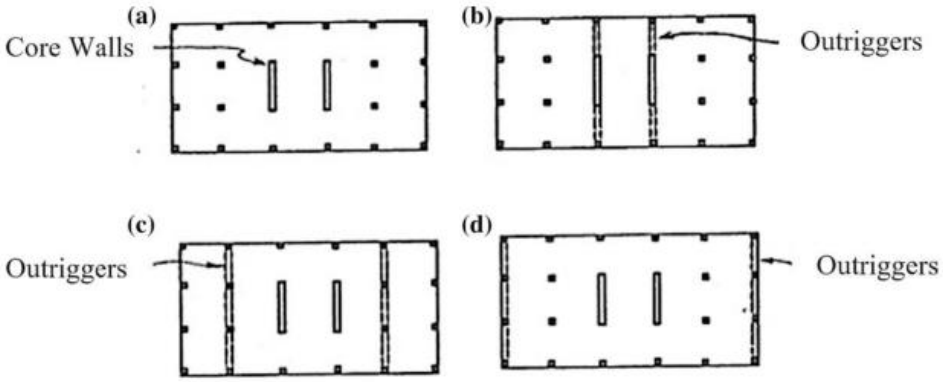

Figure 2. 19a) Plant of a typical plant of the floor, b) Conventional stabilizer, c) Offset stabilizer, d) Stabilizer staggered alternative

3) From the point of view of the response (behaviour):

- *Rigid outriggers (traditional outriggers):* This type of outrigger is intended to function as a rigid linear elastic system under wind loads, and sometimes even under seismic loads.
- *Flexible outriggers*: In this design, the stiffness of the outrigger trusses is tuned to reduce unwanted impacts such as gravity forces transferred by differential shortening.
- *Damped outriggers (Mechanically damped outriggers):* In this type, leverage provided by rigid outrigger arms protruding from the core of a structure is used to operate non-linear damping devices (DAMPEDs) (Figure 2.20). The additional or supplementary resultant is damping which can reduce the dynamic response of high-rise buildings (forces, deformations, accelerations, etc.) against crosswinds and earthquakes.

  The shock absorbers operated by the stabilizers can be:

  - Viscous dampers, such as oil-filled sealed viscous dampers and viscous pot and plate shock absorbers;

  - Viscoelastic dampers, such as the one provided by the Kinetica system;

  - Magnetorheological dampers (MR) called smart dampers, which thanks to their capacity, the damping properties can be controlled and varied efficiently and rapidly, using control methods at low electrical power;

  - Friction shock absorbers.

- *Yielding outriggers*: In this type of outriggers, yielding materials are included to establish practical maximum limits on the force demands on the connections and members, while absorbing some of the seismic energy and maintaining robustness against collapse. This is because conventional stabilizers sized for strength and stiffness under wind loads can develop massive forces in seismic events, with a high potential to damage the column, core, stabilizer elements and/or connections, which surely would not be a desirable situation. The (BRBs) Buckling Restrained Braces (Metallic Dampers) and the system of concrete stabilizers with a structural fuse (Shear Link Connections) are considered two types of compliant stabilizers. In BRBs, the major advantages are their linear-elastic behaviour under windy conditions, stable hysteretic behaviour under seismic loading conditions as well as their maximum reliable demands on adjacent connections and members. However, a BRBs system usually costs more than conventional steel stabilizers of the same stiffness, where axial stiffness is provided only by the internal steel cores of the BRBs and confinement shells are an additional cost (Figure 2.21). The element is used to connect the tip of the concrete rocker arm to the perimeter column. It is designed to remain elastic under wind loads and strong seismic events, providing the building with adequate toppling resistance and lateral stiffness. The force limit definition protects surrounding elements from damage, and stable hysteretic loops can absorb considerable seismic energy (as with the metal damper analogy). After severe seismic events, damaged shear connection elements can be replaced. Additionally, shear link connections can be installed later in the construction schedule to reduce gravity transfers from differential columns and core shortening (Figure 2.22).

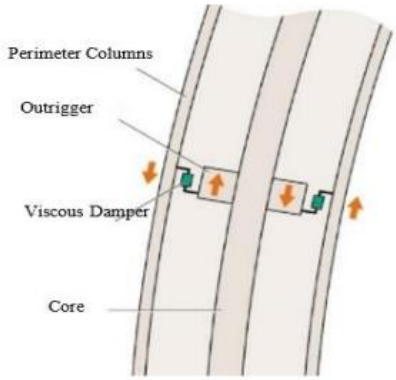

Figures 2. 20 the damped outrigger concept

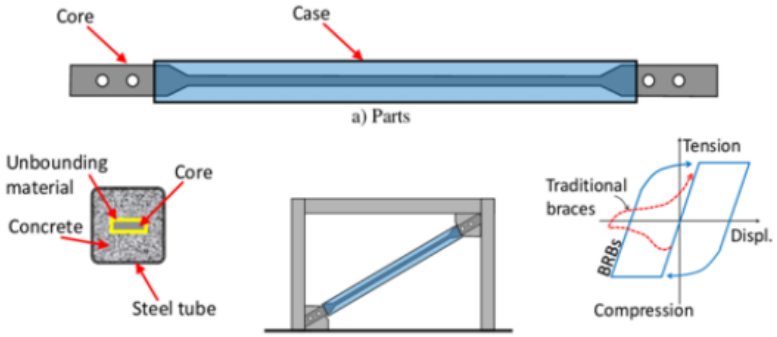

Figure 2. 21Buckling Restrained Braces (BRBs)

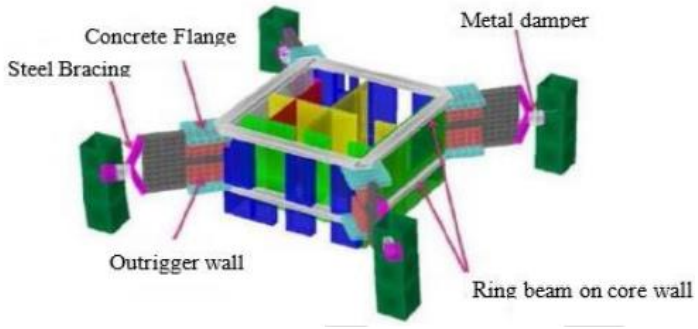

Figure 2. 22The concrete outrigger system with a structural fuse (developed by Arup)

2.5 Damped outrigger system

As the building height increases, the bracing system exhibits slow resistance to lateral loading, therefore, alternative methods are presented for tall building response control.

The structural response of the tall building is important in deciding the damping capacity of tall buildings. Initially, to increase the damping of the structure, the

passive damping system was designed, the mechanism of which depends on the structural response. A passive system does not require an external power source for its operation and is easy to maintain, making it reliable and cost-effective. Passive damping also includes dampers such as viscous dampers, tuned mass dampers, friction devices, metallic yield devices, tuned slide dampers, and tuned column dampers.

In situations that require adding additional damping to the tall building, the mechanically damped stabilization system can offer many advantages over other types of damping such as mass tuned dampers (TMDs) and tuned liquid column dampers (TLCD) due to their ability to provide similar additional damping contribution without the weight, space or tuning requirements of a TLCD and TMD (which must be tuned to a particular frequency for maximum effectiveness and perhaps lose efficiency after the event expected extreme for strength design, as building frequency changes occur when the structure achieves strength-level stresses). Additionally, the viscous dampers on the outriggers will operate at all frequencies, generating more drag as the drive speed increases. Amortized-added outriggers have been used in buildings such as Shangri-La Place in Manila and Shiba Park Tower in Tokyo. Additionally, damped stabilizers can provide multiple benefits over conventional stabilizers such as:

- Cushioned Outriggers reduce the forces induced in the components of the building's side-load resisting system by reducing the structural deformations that generate these forces. Unlike conventional stabilizers which increase the forces induced in the structural components due to increased lateral loads resisting the stiffness of the system.
- Using additional damping to reduce wind or earthquake response results in a reduction in required structural strength and stiffness, resulting in reduced structural materials and labour costs to meet occupant comfort/acceleration criteria. Smaller column dimensions lead to an increase in the clear floor area. These savings can be more than offset by the additional costs of damping, testing and installing this system.
- Damped Outriggers avoid the development of large internal element forces that can result from differential shortening in conventional

stabilizers that connect the outer columns directly to the core. This is because the damper forces vary with the speed of actuation, i.e. when the damper is actuated at a speed of inches or millimetres per second, this damper will develop large drag forces; while negligibly small forces will be developed if it is driven at a rate of inches or millimetres per year or decade.

- ❖ By using damped metal stabilizers such as BRBs, responses can be modified, such as lateral displacement demand and force distribution of central wall buildings. Thus, more plastic hinges are likely to form in the central RC wall and another plastic hinge at the base.

We will better deal with the subject in Chapters 3 and 4, in which passive dissipation systems and in particular metallic dissipators are dealt with.

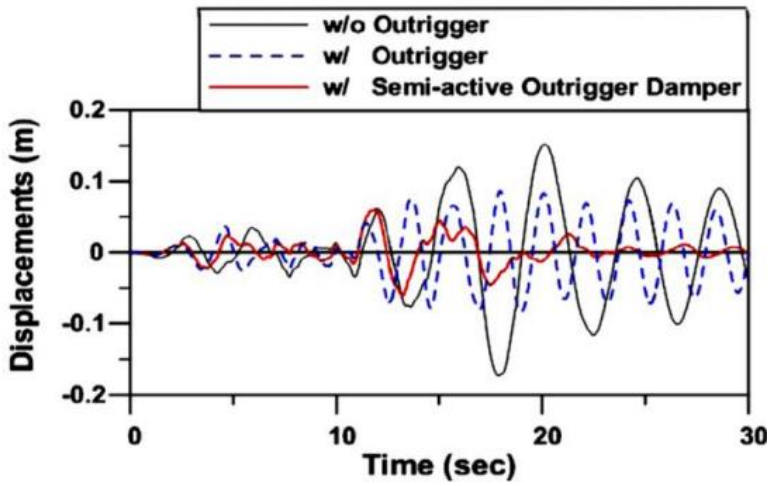

Figure 2. 23Moving the structure without and with stabilizer and stabilizer

2.6 Advantages and disadvantages of the Outrigger Systems

Given the increased stiffness they provide, outrigger systems are very efficient and cost-effective solutions to reduce building accelerations, which improves occupant comfort during high winds.

2.6.1 Advantages

Some other benefits of stabilization systems are briefly outlined below.

I. Deformation reduction

In a building with a braced central frame or shear walls, a system of stabilizers engages the perimeter columns to effectively reduce building deformations due to overturning moments and consequent lateral displacements on upper floors. A tall building structure incorporating a stabilization system can experience a reduction in core overturning moment of up to 40% compared to a free cantilever, as well as a significant reduction in drift, depending on the relative stiffnesses of the core and the stabilization system. For super-tall towers with perimeter mega columns sized for drift control, the core rollover reduction can be as much as 60%. In the case of thin-walled open cores, a stabilizer system also reduces torsional rotation and cross-sectional deformation. The system works by applying forces on the web that partially counteract the rotation due to overturning and the vertical displacements due to deformation. These forces are provided by perimeter columns and transmitted to the core through towers or walls of direct stabilizers, or the action of indirect or "virtual" stabilizers from towers and diaphragms.

II. Efficiency

For ribbon truss systems that engage all perimeter columns, those columns already sized for gravity loads may be able to withstand outrigger forces with minimal variations in dimensions or reinforcement, as different load factors are applied to the design combinations with and without side loads. Outriggers can also allow optimization of the overall building system, using techniques to identify the best location for additional material. By significantly decreasing the fraction of building overturn that the core, wall, or column must resist, the amounts of material in the core can be reduced, while the amounts of stabilizer, perimeter belt, and column are slightly increased. Lower limits for required core strength and stiffness may be defined by the amount of storey shear resisted by the core alone between stabilizer levels, special loading conditions that exist at the stabilizer floors, or short-term capacity and stability if stabilizer connections are delayed during construction.

III. Foundation Forces

A separate but related benefit is the reduction of core foundation strength. The stabilizing systems help to effectively distribute the overturning loads on the foundations. Even when a foundation pad is extended over the entire tower surface, a central-only lateral system applying large local forces due to overturning can generate such large pad shear and bending stresses, as well as net stress in the piles or loss of footing, that the project becomes uneconomical or impractical. Another potential benefit related to the force transfer capability is the progressive resistance to disproportionate collapse. In designs that require consideration of the sudden loss of local members or connection capabilities, stabilizers can provide alternative load paths. Reducing lateral load variations in subgrade stresses or pile loads below the core will reduce foundation rotations that can contribute to overall and inter-story displacements. Having a stabilizer system may or may not change other aspects of foundation design, such as regulating pile loads and footing or bearing pressures.

IV. Gravity Transfer

Stabilizers and belt trusses can help reduce differential vertical shortening between columns or between a column and the core. This can reduce floor slopes between those elements which can occur due to creep, shrinkage or thermal variations. Reduction is achieved by force transfers between adjacent columns via ribbon trusses or between columns and core via stabilizers. This is at best a secondary benefit and is a double-edged sword: force transfers can get quite large and expensive to obtain. Balancing potential benefits and costs requires a solid understanding of the phenomenon, as well as an adequate application of the details and building strategies to manage its effects.

V. Torsional Stiffness

Ribbon trusses can provide a different secondary benefit: improved torsional stiffness. A core-only tower can have low torsional stiffness compared to a perimeter frame tower, due to the much smaller spacing between resisting members. A core and stabilizer building can have similarly low torsional stiffness. Ribbon trusses can force the perimeter columns to act like fibres of

a perimeter pipe which, while not as stiff as continuous frame pipe, still provides significant additional torsional stiffness.

VI. Disproportionate collapse resistance

Another potential benefit related to force transfer capability is the progressive resistance to disproportionate collapse. For example, where perimeter columns are engaged by belt trusses, loads from floors above a damaged perimeter column could "hang" from the upper column, acting in tension, and thus be transferred through the upper belt trusses to the adjacent undamaged columns. Where outriggers without trusses are present, it may be possible to suspend upper deck loads from the outriggers loading the core, but the massive outrigger columns may be too heavily loaded for this load path to be practical. In a braced frame building, loads from floors above a collapsed column may be shared by the perimeter members through the stabilizers.

VII. Architectural Flexibility

Core-and-outrigger systems allow for design variations in external column spacing to meet specific aesthetic goals and, in some cases, functional requirements. Internal or direct stabilizers must not affect the framing or perimeter aspect of buildings relative to other floors. Super-tall buildings with outriggers can have a few exterior mega columns on each face, opening up the facade system for flexible architectural and aesthetic expression. This overcomes a primary disadvantage of closed form tubular systems used in tall buildings. The amount and location of mega columns have an impact on the typical floor framing. Floors featuring widely separated columns and column-free corners may require deep and heavy spandrels for the strength, deflection control, and vibration control requirements of long spans and cantilevered beams. The core-and-outrigger approach is scalable, with potential applicability to buildings 150 stories tall or more.

2.6.2 Disadvantages

I. Usable space

The space occupied by the stabilizer trusses (especially the diagonals) places constraints on the use of the floors where the stabilizers are located.

A solution can be:

- interstitial and mechanical outrigger localization;
- the localization in the natural inclined lines of the profile of the structure;
- use multilevel single diagonal outriggers to minimize member interference on each level;
- use virtual outriggers;

II. Installation to Building Process

In traditional construction, the speed of construction of the core wall will be on the order of three to four days per floor, but it becomes almost a month for outriggers due to the lifting, welding and installation of the various components. Then, to allow for the construction of bus lanes and not to postpone the construction of the central wall, the tiered core where the outriggers are located is partially blocked during construction, as shown in Figure 2.24. This makes the construction of the centre wall separate from the installation of the stabilizers. Then, after the stabilizers have been installed, the core will need to be filled with concrete to form a monolithic element. This method is called the *back fusion technique* .

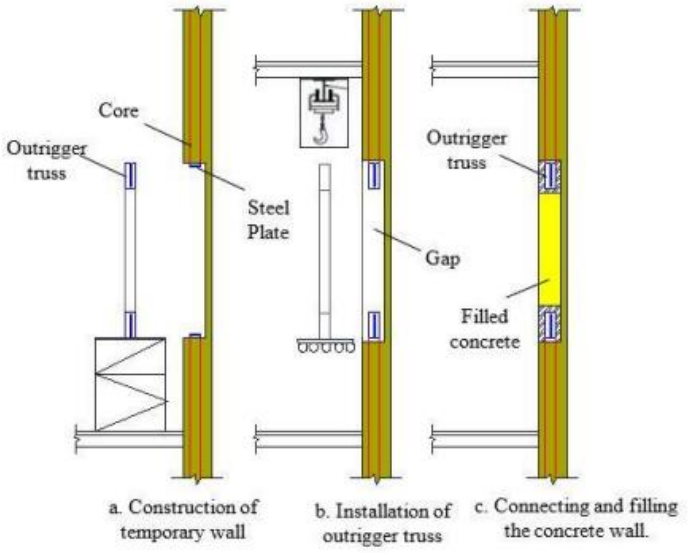

Figure 2. 24Retro-Casting Construction Sequence of the Outrigger

III. Shrinkage, elastic deformation and sudden changes in temperature

These are the main causes of the shortening of the perimeter frame and of the core. The stiffness of the stabilizers is usually very high, a small vertical deflection will induce very high axial forces in the outriggers. Thus, the gravitational forces transferred through the outriggers due to differential shortening could be of a magnitude comparable to the lateral forces. In other words, the size of the stabilizers would be doubled if the axial forces due to the shortening could not be released. This effect can be mitigated by:

- Delay the final connection of the outriggers until the building out is complete; this method will recover almost 95% of the shortening resulting from elastic deformation. But another drawback could be that the outrigger system is not active, so the stiffness and strength will not be sufficient to withstand the loads during the construction period; however, this inconvenience can be compensated by using the adjustable stabilizers.
- Using Adjustable Outriggers; are special type connections that allow adjustment during the construction period and sometimes even after, these can be:

  - Jack Cross-Connected system, it is adjustable only on site, it eliminates the effects of elastic shortening, but not the effects of shortening due to creep and shrinkage;

  - Shim-Plate correction method and Oil- Jack joining systems; they are adjustable during and after construction, they can eliminate shortening from elastic deformation, sliding, shrinkage and thermal shock;

  - Outrigger mechanically cushioned with viscous or other types of dampers;

IV. Limits imposed by Eurocode 8 and IBC

The Outriggers system used in buildings usually exceeds the limit and provisions of Eurocode 8 and IBCM which have not been developed for application to high-rise buildings. In tall buildings, the minimum base shear is typically greater than the shear determined by response spectrum and

construction period. Consequently, the effective value of the response of the modification factor R in the prescriptive design is reduced by the value specified in the building code for that framing system lower value dependent on the construction period and other factors. These prescriptive procedures may underestimate shear demand and may not provide the necessary flexural ductility underpinning the core. Therefore, to solve this problem, it is recommended by the Council on Tall Buildings and Urban Habitat (CTBUH) to conduct performance-based design PBD approach rather than prescriptive design to design the structure with stabilizing system. The stabilizer members can be designed to remain elastic under Design Basis Earthquake or Maximum Considered Earthquake, or can be "melted" to limit forces and members absorb seismic energy.

V. Asymmetrical System

An asymmetrical system can have stabilizing force pairs involving axial forces in the core, complicating core analysis and design. Gravity transfers in an asymmetrical system can cause an overturning moment inserted into the building, resulting in lateral displacements under gravity loads. However, this does not mean that asymmetrical systems cannot be used.

VI. Column Sizes

Effective stabilizers often require the ability to adjust the stiffness of the column. This can result in increasing column sizes, especially for stabilizers located high up in a building, as more stiffness from a larger area offsets the softening effect of the column length. If the dimensions of the columns are strictly limited, this could limit their usefulness in a stabilizing system.

2.7 Optimal position

There is no specific code or design guideline for reducing the seismic response by the outrigger system.

When an outrigger is introduced into a structure, it reduces the structural response, but when this stabilizer position is in the optimal position, the structural response is

reduced to the maximum. Therefore, different approaches are used to find the optimal placement, with reduced response of the structure.

Once the optimal position of the outrigger has been found, the lightness of the structural system and the construction cost can be calculated. Consequently, Mousleh and Batikha found the optimum position of the stabilizer in a structure, and therefore, the weight of the steel and the volume of the reinforced concrete are calculated according to the model without the stabilizer and the stabilizer in a different position. The authors have found that a stabilizer placed in an optimal position gives less weight to the structural element and therefore the cost of the material decreases; therefore, economy is responsible for the structure of the stabilizers.

A graphical method is proposed to find the optimal positioning of the stabilizer as shown in Figure 2.25 knowing two characteristic non-dimensional parameters of the structure as ω and x/H, considering the bending stiffness and flexibility of the shear wall, the stabilizer and the external column.

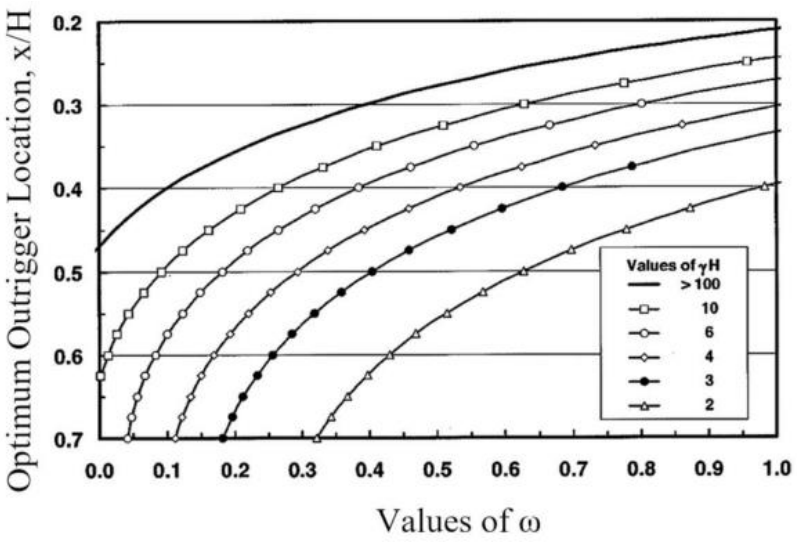

Figure 2. 25Optimal position of the Outrigger

It should be noted that most of the time the graphical method does not interpret the exact result, for this reason in this thesis project, and in particular in Chapter 5, an experimental method is defined to find the optimal position of the outriggers in the structure. The positioning of the outriggers will be simulated, applying 2 or 3 of them in different positions along the height of the building in order to obtain a higher maximum displacement, a reduced drift and acceleration compared to the response of the bare structure, i.e. without the application of the outrigger system. A study is

undertaken, using the ETABS software for the calculation of a regular structure with a linear and non-linear analysis and a temporal analysis to observe the behaviour under earthquake load or wind load. There are many studies undertaken using ETABS and SAP 2000 software for regular and irregular structures with a linear and non-linear pushover analysis and time analysis to observe the behaviour under earthquake load or wind load.

The study was further advanced with the addition of a metal damper connected between the column and the outrigger excited primarily by seismic forces.

By finding the optimal position of the stabilizer, the response of the structure can be reduced to a considerable radius compared to a stabilizer placed elsewhere as shown by several studies in the literature.

Height and no. of stories in structure	Type of structure	Type of loading	Structural response parameter for optimum position		Optimum position (single outrigger)
87 m (27 stories)	Outrigger braced shear wall	Wind load	Horizontal deflection and displacement		0.33 times its height from the top
187.5 m (50 stories)	Outrigger with shear core	Earthquake load	Story drift index		0.44–0.48 times its height from bottom
240 m (60 stories)	Outrigger with shear core	Wind and Earthquake load	Inter-story drift		0.63 and 0.67 times its height from the bottom
400 m (100 stories)	Outrigger with shear wall	Wind load	Top displacement		0.39 times its height from the bottom
280 m (80 stories)	Outrigger with shear core	Wind load	Drift at top		0.375 times its height from top
201 m (67 stories)	Outrigger and belt truss with shear core	Wind load	Top displacement		0.31 times its height from the bottom
					More than one outrigger
a) 70 m (20 stories)	Outrigger with shear wall with belt truss	Earthquake load	a)	Drift	6, 12, 16 floor
				Weight	12 floor
b) 105 m (30 stories)			b)	Drift	6, 12, 18, 24 floor
				Weight	8, 15, 24 floor
c) 140 m (40 stories)			c)	Drift	12, 20, 26, 34 floor
				Weight	12, 20, 32 floor
d) 175 m (50 stories)			d)	Drift	12, 26, 34, 42 floor
				Weight	12,18, 30, 42 floor

Figure 2. 26Optimum position of outrigger for different buildings

3. PASSIVE ENERGY DISSIPATION SYSTEM

3.1 Basic principles

In conventional seismic design, the acceptable performance of a structure during earthquake shaking relies on the lateral force resistance system which is able to absorb and dissipate energy stably over a large number of cycles.

According to the capacity design, energy dissipation occurs in particularly detailed ductile plastic hinge regions of beams and column bases. This design approach aims to prevent structural collapse and ensure the safety of life.

The equation of motion of a system of one elastic degree of freedom with linear viscous damping, subject to ground motion, is given by the following expression:

$$M\ddot{u}(t) + C\dot{u}(t) + Ku(t) = -Mu_g\ddot{}(t)$$

Where M, C, K are the mass, stiffness and damping, respectively, while u is the mass displacement with respect to the ground.

Displacement dependent dissipative devices involve or act on the term $Ku(t)$while those dependent on the velocity (or dampers themselves) on the term $C\dot{u}(t)$. There are several significant differences between the two groups, among which:

- velocity dependent devices require a high global damping or at a high speed of the structure;
- displacement dependent heat sinks may, depending on the system, start dissipating energy from very low displacement values and, in particular, change the global structural period by lengthening it, after its plasticization.

Displacement-dependent devices represent an improvement or advancement of the classical seismic design of structures based on ductility and structural redundancy, and allow to significantly reduce the forces induced by a strong earthquake.

The reduction of forces in the design is based on the implicit acceptance that the structure will present damages when a strong earthquake occurs, since the real induced forces if the structure has remained elastic, will be greater than those considered in the design. This factor (called R, q etc. according to the different standards) can vary between 2 and 12, approximately, depending on the country, and represents the overall ductility of the structural system and overstrength. Thus, the structure will operate in the non-linear range with its total or partial plasticization,

causing permanent deformations and usually generating damage to structural and non-structural elements (such as masonry partition walls, false ceilings, mechanical equipment, fixtures, among others).

Displacement-dependent energy dissipation systems, unlike the classic design previously described, allow to concentrate the damages that may occur present from the action of a strong earthquake in some elements or connections industrially produced with high quality controls. They may eventually be replaced and it should be easy to inspect. On the other hand, its inability to be ductile does not jeopardize the overall safety of the structures, being able to control damage to non-structural elements with a rigid plane displacement limit.

These characteristics of displacement-dependent energy dampers allow to significantly improve the resilience of structures. Recent severe earthquakes such as the one in New Zealand (Christchurch 2010-2011) have provoked a demonstration describing those structures designed by applying conventional "design for capacity" criteria, even if they have adequately dissipated energy in the intended areas (hinges plastics), were excessively damaged. As a result, in many cases, it was cheaper to rebuild than to repair. This involves very high costs due to both demolition and reconstruction, for example due to disruption of the building's function which causes serious economic expenses.

Therefore, the implementation of energy dissipation systems in a structure allow to modify the hierarchy of resistances, making the dampers the "weak elements" where the energy is dissipated and the damage is concentrated. A structure equipped with displacement-dependent energy absorbers can be considered as a mixed system formed by a flexible part, given by the structure deriving from the elimination of the energy absorbers, and by a rigid part, formed by the absorbers, which work inside in parallel. Consequently, the resulting dynamic equation for a single degree of freedom system would be:

$$M\ddot{u}(t) + C\dot{u}(t) + Ku(t) + R(t) = -Mu_g\ddot{}(t)$$

where the linear term Ku refers to the flexible system assumed to be elastic, and the term R refers to the displacement-dependent contribution of the heat sinks. On the other hand, since the coupling or interaction between both systems consists of ductile

connections what we have is a mixed "rigid flexible-ductile" system. This system is all the more effective the greater the difference between the vibration periods of the flexible part and the rigid part, given that in the event of a strong earthquake, the devices plasticize and the structural period of the mixed system is on that of the flexible part. Many classic seismic design systems such as reinforced concrete coupled walls, eccentric frames and even dual systems can be redesigned or redesigned using these devices.

The effects of these systems can also be defined in energy terms. During a seismic event, a finite amount of energy is released into a structure. This input energy is transformed into kinetic and potential energy (strain), which must be absorbed or dissipated through heat. If there were no damping, vibrations would exist forever. However, there is always an intrinsic level of damping that draws energy from the system and then reduces the amplitude of the vibration until motion ceases. However, structural performance can be improved if some of the input energy can be absorbed, not by the structure itself, but by some type of supplement, i.e., some "device".

This is clarified by considering the conservation of the energy relation (Uang and Bertero, 1988):

$$E = E_k + E_s + E_h + E_d$$

Where:

- E is the absolute input energy from the earthquake motion;
- E_k is the absolute kinetic energy;
- E_s is the recoverable elastic strain energy;
- E_h is the unrecoverable energy dissipated by the structural system through inelastics or other forms of action;
- E_d is the energy dissipated by the supplementary damping devices;

The absolute energy input, ***E,*** represents the work done by the total shear force at the base of the structure. Therefore, it contains the effect of the inertial forces of the structure. In the conventional design approach, acceptable structural performance is achieved by the occurrence of inelastic deformations. This hypothesis defines two different effects:

- direct effect, consists in the increase of the energy $\boldsymbol{E_h}$;

- indirect effect, the inelastic deformations that occur translate into a softening of the structural system, which in turn modifies the absolute input energy from the motion of the earthquake, i.e. if E_h increases, E consequently increases.

In effect, the increased flexibility acts as a filter that reflects some of the earthquake's energy. The significant result is that it leads to reduced accelerations and reduced stresses in regions away from the plastic hinges.

Another approach to improve earthquake response performance is to use seismic protection devices, so there will be direct effects of increasing energy E_d.

Mechanical devices are usually embedded within the frame of the structure and dissipate energy throughout the height of the structure. In addition to increasing the energy dissipation capacity of the structure, some energy dissipation systems also increase strength and stiffness.

These systems include the following types of energy dissipation devices: metallic, frictional, and viscoelastic yield. Viscous fluid damping devices generally do not increase the strength or stiffness of the structure unless the excitation frequency is high. In general, all these systems provide for a reduction of the drift and, therefore, a reduction of structural damage, thanks to the dissipation of energy, and an increase in the total lateral forces, thanks to the greater resistance and/or stiffness.

Figure 3.1 shows the force-strain curves of a simple one-story structure with e without energy dissipation systems (EDS).

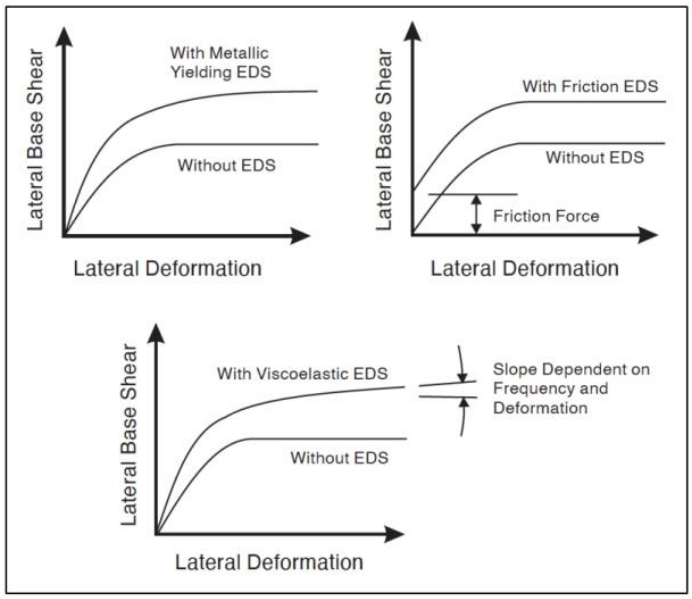

Figure 3. 1Effect of Energy Dissipation Systems on Force-Deformation curves of a structure

3.2 Passive structural control system

Energy dissipation systems are classified as anti-seismic protection systems as their function is to mitigate seismic risk; however, these devices are also useful by reducing the dynamic response under horizontal wind loads. Figure 3.2 illustrates the elements of a passive control system (Symans and Constantinou, 1995).

It is important to understand that its functioning is activated by the movement of the structure during dynamic excitation and does not require an external source of energy to activate it, while the active or semi-active system does.

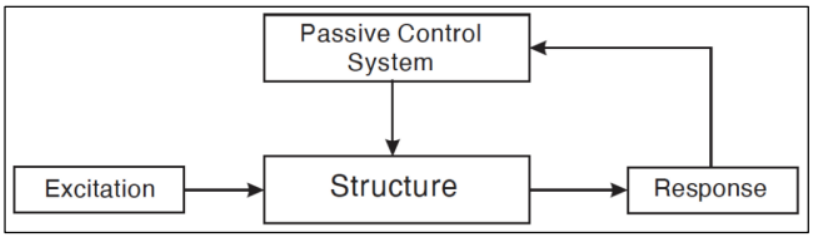

Figure 3. 2Scheme of a Passive Control System (Symans and Constantinou, 1995

According to the US FEMA 273 (Federal Emergency Management Agency) "NEHRP Guidelines for Seismic Rehabilitation of Buildings", energy dissipating devices are classified as displacement dependent, velocity dependent, or others.

- *Displacement-dependent devices* can exhibit either rigid plasticity (friction devices), bilinear hysteresis (metallic yield devices), or trilinear. The

response of displacement dependent devices is independent of excitation speed and/or frequency. The simplest model of hysteretic behaviour involves algebraic relationships between force and displacement. Figure 3.3 shows typical force-displacement loops of hysteretic energy dissipation systems.

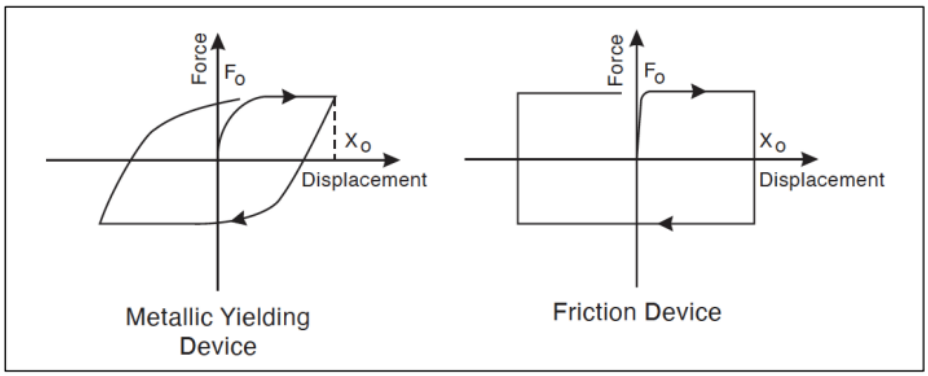

Figure 3. 3Idealized force-displacement loops of hysteretic energy dissipation devices

- *Velocity-dependent devices* include solid and fluid viscoelastic devices and fluid viscous devices. Figure 3.4 shows the force-displacement loops of these devices. Typically, these devices exhibit stiffness and damping coefficients that are frequency dependent; the damping force in them is proportional to the speed due to their viscous behaviour. These devices are classified as viscoelastic devices;

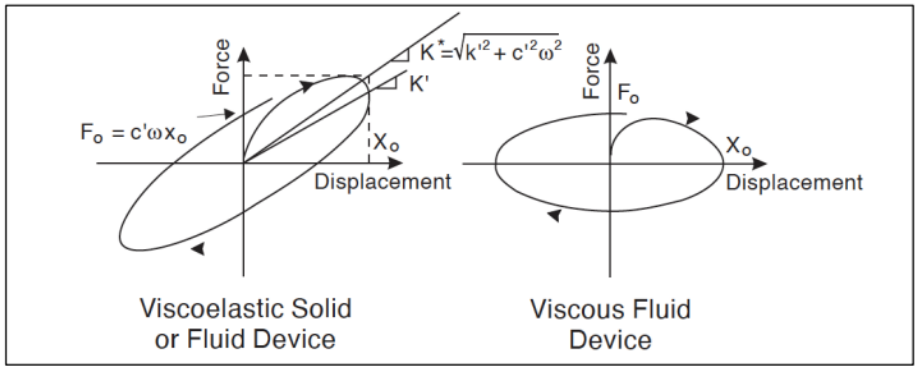

Figure 3. 4Idealized force-displacement loops of viscoelastic energy dissipation devices

- Energy dissipating devices that cannot be classified as displacement or velocity dependent are classified as other systems. Examples of other devices include friction spring devices with re-centring capabilities, fluid restoring force damping devices. Figure 3.5 illustrates the behavior of these devices.

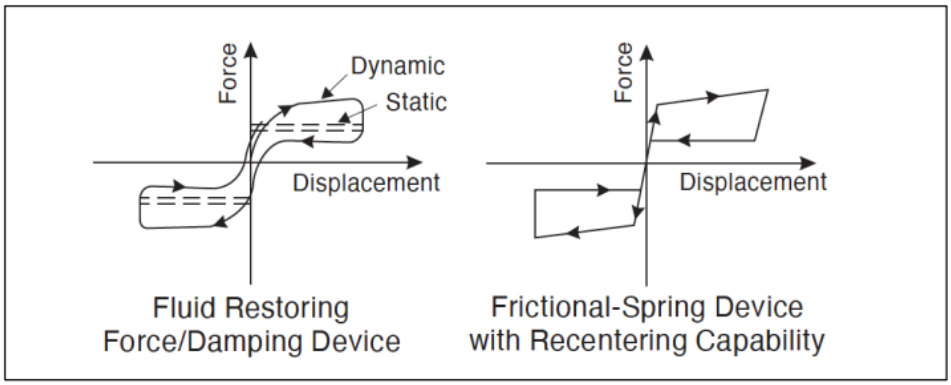

Figure 3. 5Idealized force-displacement loops of other energy dissipating devices

The following Table 3.1 summarizes the main aspects of the most common energy dissipation devices used in North America.

	Viscous Fluid Damper	Viscoelastic Solid Damper	Metallic Damper	Friction Damper
Basic Construction			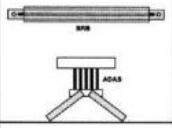	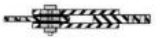
Idealized Hysteretic Behavior	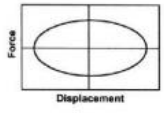	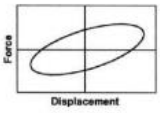	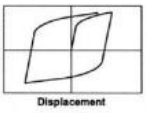	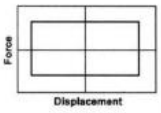
Idealized Physical Model	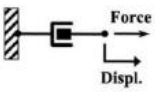	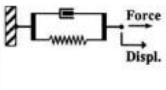	Idealized Model Not Available	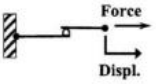
Advantages	- Activated at low displacements - Minimal restoring force - For linear damper, modeling of damper is simplified. - Properties largely frequency and temperature-independent - Proven record of performance in military applications	- Activated at low displacements - Provides restoring force - Linear behavior, therefore simplified modeling of damper	- Stable hysteretic behavior - Long-term reliability - Insensitivity to ambient temperature - Materials and behavior familiar to practicing engineers	- Large energy dissipation per cycle - Insensitivity to ambient temperature
Disadvantages	- Possible fluid seal leakage (reliability concern)	- Limited deformation capacity - Properties are frequency and temperature-dependent - Possible debonding and tearing of VE material (reliability concern)	- Device damaged after earthquake; may require replacement - Nonlinear behavior; may require nonlinear analysis	- Sliding interface conditions may change with time (reliability concern) - Strongly nonlinear behavior; may excite higher modes and require nonlinear analysis - Permanent displacements if no restoring force mechanism provided

Table 3. 1Summary of the main aspects of Passive Energy Dissipation systems

3.3 Metallic dampers

Metallic hysteretic buffers can provide energy dissipation under seismic action due to the inelastic deformation of the material, usually mild steel, but also lead or other metal alloys. The typical constitutive law of a metallic specimen is shown in Figure 3.6 where the conventional strain ε and the nominal stress σ_n , on the abscissa and ordinate axes, respectively, are given by the following equations:

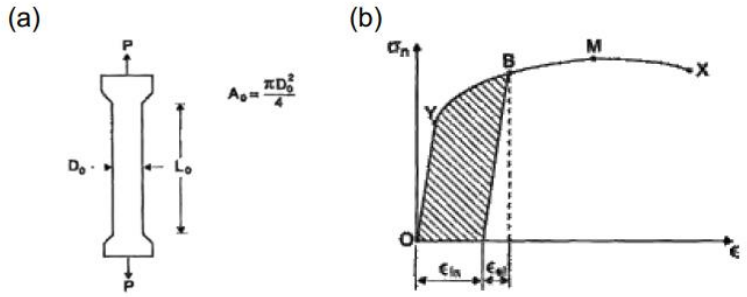

Figure 3. 6(a) Sample for simple tensile test, (b) Stress-strain curve

$$\varepsilon = \frac{L - L_0}{L}\sigma_n = \frac{P}{A_0}$$

where L is the length of the bar after elongation, Lo is the initial length of the specimen, P the applied load, and the nominal cross-sectional area. For loads originating nominal stress values lower than the yield stress σy, the material behaves elastically, i.e. essentially with σn proportional to ε through the Young's modulus and with recoverable initial conditions when the applied load is removed (linear elastic material) . Conversely, irreversible or permanent plastic deformations occur when the elastic limit is exceeded. This means that by removing the applied load, only a part of the deformation is recovered (corresponding to the elastic part), while the inelastic deformation is permanent and contributes to energy dissipation. Referring to the previous figure, the shaded area represents dissipated energy, most of which is converted into heat. The following expression provides a more appropriate definition for strains and stresses:

$$\varepsilon = \ln\frac{L_0}{L}\sigma_n = \frac{P}{A}$$

where A is the reduced cross-sectional area.

There are various mathematical models to represent stress-strain curves, and they are: perfectly elastic plastic, elastoplastic or Ramberg-Osgood model which are illustrated in Figure 3.7.

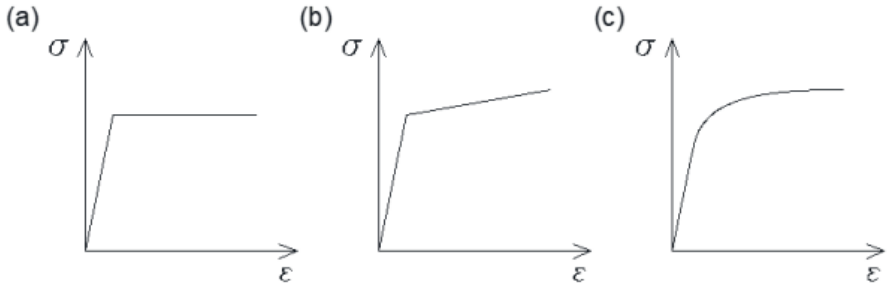

Figure 3. 7Tensión deformación para modelos matemáticos: (a) curva elasto plastic ; (b) bi-lineal curve with hardening; (c) Ramberg-Osgood

However it is important to define their stress-strain response under alternating loads. Figure 3.8.

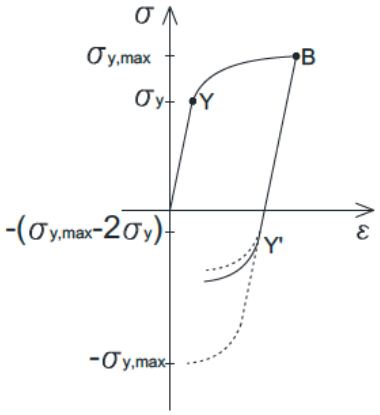

Figure 3. 8Steel Strain Stress Ratio

To do this, in the image above, the sample is first loaded up to yield point "Y" and then to a point B in the work hardening range. Gradually unloading the curve, it is seen that it is parallel to the initial charge curve, thus indicating an elastic response. However, if the unloading phase continues long enough within the compression range, creep or plasticization will again take place at the point denoted as Y' for a stress σ'_y. The stress associated with point Y' depends on the amount before strain hardening and this behaviour is known as the "*Bauschinger effect* ". As a useful simplification, isotropic hardening theory defines that:

$$\sigma'_y = -\sigma_{y,max}$$

While the kinematic hardening theory establishes that:

$$\sigma'_y = -(\sigma_{y,max} - 2\sigma_y)$$

The experimental results indicate that Y' is somewhere in between, suggesting a combination of the isotropic and kinematic theories. Thus, it can be stated that knowledge of metallic constitutive models is an important step to correctly define the force-displacement relationship of metallic devices and to reliably predict the nonlinear response of structures under seismic loads.

Many different steel dampers have been proposed and studied in the literature, exploring different materials, geometric shapes, manufacturing processes and connection configurations to the structure. These devices dissipate seismic input through inelastic deformation of the metal. They are usually made of mild steel plates with triangular or X shapes so that the sagging is almost evenly distributed throughout the material. Metallic devices generally exhibit stable hysteretic behaviour, low cycle fatigue properties, long-term reliability, and relative insensitivity to ambient temperature. Different metal devices are analyzed below.

3.3.1 ADAS damper

The ADAS (Adding Damping And Stiffness) device was first studied by Bergmann et al. and Whittaker. This device is made of X-shaped metal sheets arranged in parallel. Each plate has the dimensions indicated in the figure, but their number may vary with each connection. The lamination takes place simultaneously on all the sheets and the variation in height of the number of sheets used makes it possible to optimize the structural response. Each plate is bi-interlocked and its X shape causes the plasticization of its entire volume.

Various experimental tests have demonstrated its ability to sustain many deformation cycles with stable performance before reaching failure, resulting in a high dissipation capacity based on the flexural deformation of the individual plates. The "X" shape implies constant variation of deformation over the height of the shock absorber, thus ensuring that the failure occurs simultaneously and uniformly over the entire height of the heatsink. The consequence of metallic hysteretic dampers is that, in addition to increasing the damping, they significantly modify the dynamic characteristics of the structure. In most cases, the introduction of the devices has led to a stiffer structure, because they reduce the fundamental period, and this leads to an increase in the base shear.

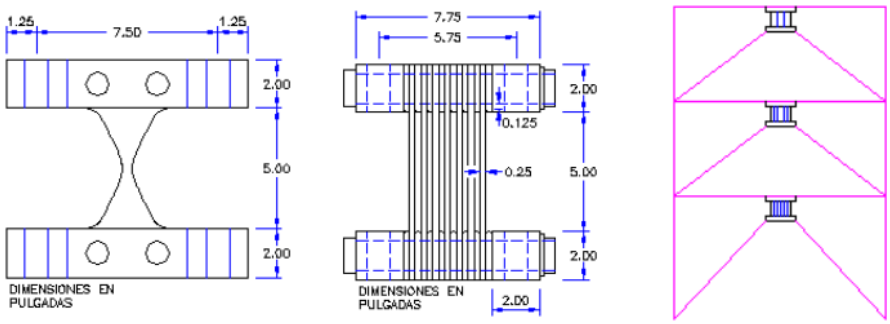

Figure 3. 9ADAS system; dimensions; typical connection of sheets

The preferred location of these connections is shown in Figure 3.9. Alternatively, they can be placed in coupled reinforced concrete walls, as shown in Figure 3.10.

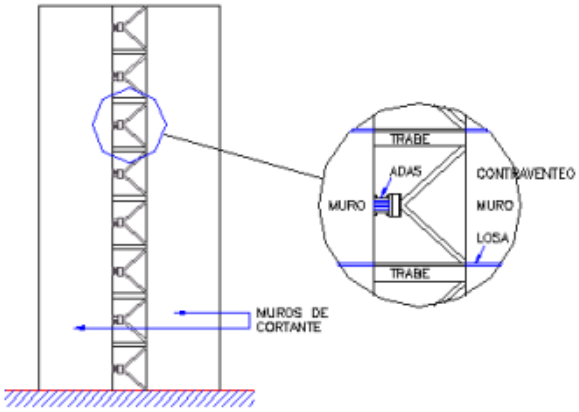

Figure 3. 10Alternative wall-chevron braces configuration for ADAS devices installation

The typical hysteretic response of these connections is stable with no significant degradation after many recharging cycles. Figure 3.11 presents typical hysteretic curve results for this connection, after one charge cycle and one hundred low amplitude cycles.

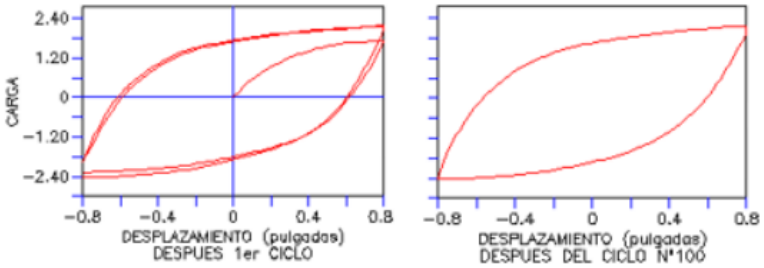

Figure 3. 11Force-displacement behavior of ADAS

3.3.2 TADAS damper

Another example of a heat sink is known as a TADAS (Triangular Added Damping and Stiffness) system. These devices consist of a set of metal plates, of constant thickness and trapezoidal section, parallel to each other, which are welded to a common base plate and the acting forces are perpendicular to the plane shown.

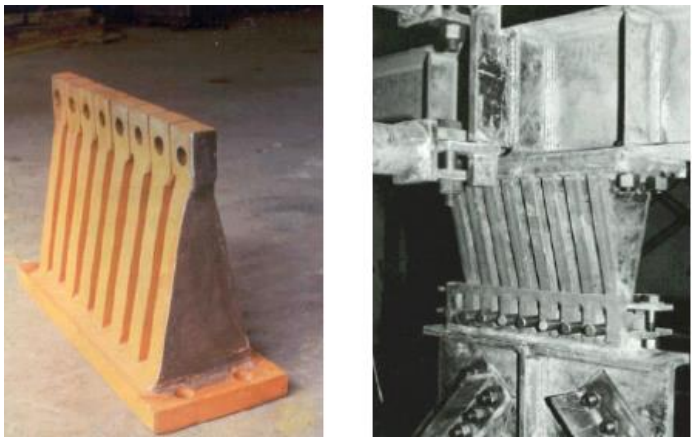

Figure 3. 12TADAS devices

The TADAS system is recessed at the top and hinged at the bottom, so that the slabs deform by bending into a simple curvature. Furthermore, the curvature is uniformly distributed and, therefore, plasticization can occur simultaneously over the entire height of the sheets without concentration of the curvature.

Figure 3.23 shows the hysteresis loops of the heat sink which, as we can see, are approximately rectangular, which makes it very efficient since the energy dissipated is the enclosed area and is maximum if it is rectangular.

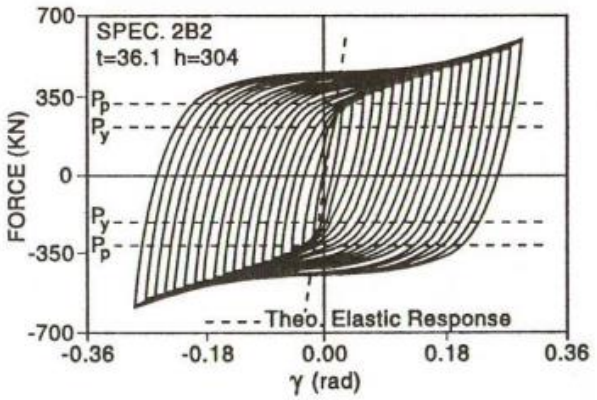

Figure 3. 13Force-displacement curves TADAS service

3.3.3 Honeycomb steel damper

The honeycomb steel damper (or "panel system") was first developed by Kobori et al. 1992. with the aim of increasing energy absorption in high-rise buildings. It consists of a steel plate characterized by a honeycomb shape with an opening in the central part (see Figure 3.14) which is subjected to loads acting in its own plane.

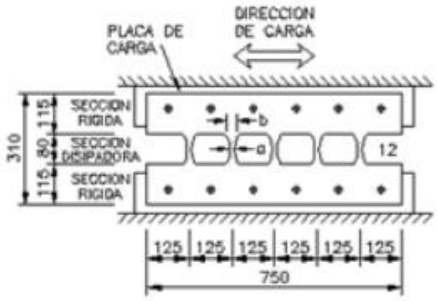

Figure 3. 14Honeycomb damper geometry

It exhibits quite stable hysteretic behaviour, as shown in Figure 3.15.

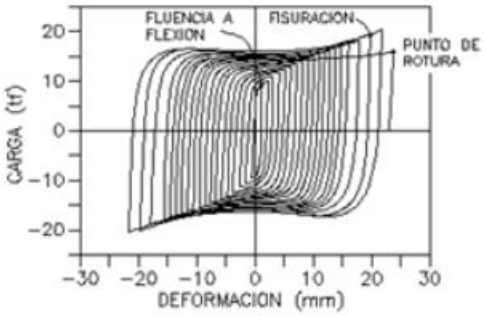

Figures 15 Honeycombs damper hysteretic loops

3.3.4 BRB damper

Developed by Clark et al., Buckling Restrained Braces belong to the family of dampers that dissipate load input cyclic energy through axial strain. BRBs are devices to be attached to steel or concrete frames as ordinary concentric braces. They are composed of a thin steel whose core is surrounded by a steel tube filled with concrete, as shown in Figure 3.16. The inner steel core yields under tension, as it sags and the outer shell is avoided.

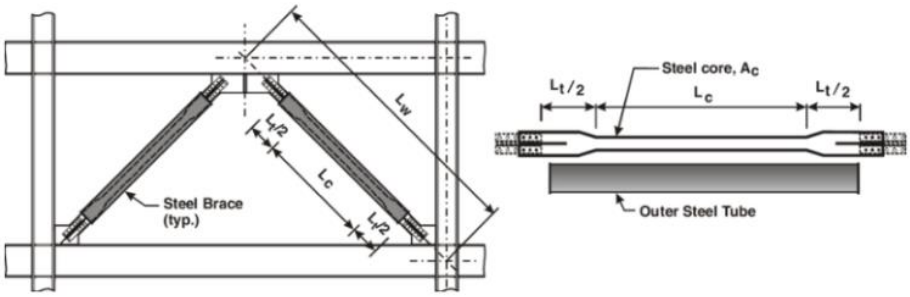

Figure 3. 16Typical buckling restrained frame and buckling restrained brace

For BRBs, three types of connections are generally used:

- Welded connection: the BRB is welded to the gusset on site. While this procedure involves additional hours on site, it can improve the energy transfer mechanism and potentially require smaller BRBs.
- Bolted connection: the BRB is bolted directly on site. It doesn't require a lot of time or skilled personnel to do this, which makes the connection much easier.
- Stud Connection: Both the arm and dowel are designed to accept a stud. This pin connects them together and allows the connection to rotate freely.
The BRB device can generally be divided into three different parts: an elastic unconstrained zone, an elastic contained and a plastic contained: -
The elastic unconstrained zone is designed to provide a connection between the BRB and the plate and is also capable of resist axial stress without deformation.
- The contained elastic zone is a transitional part of the central plate between elastic and plastic behaviour. Although this area is characterized by an elastic behaviour under tension and compression, the casing element prevents it from buckling.
- The retained plastic zone carries the forces of tension and compression elastically and plastically.

Furthermore, the material interposed between the steel core and the concrete is the mortar which allows the core to slide inside the casing, preventing the transfer of shear stress.

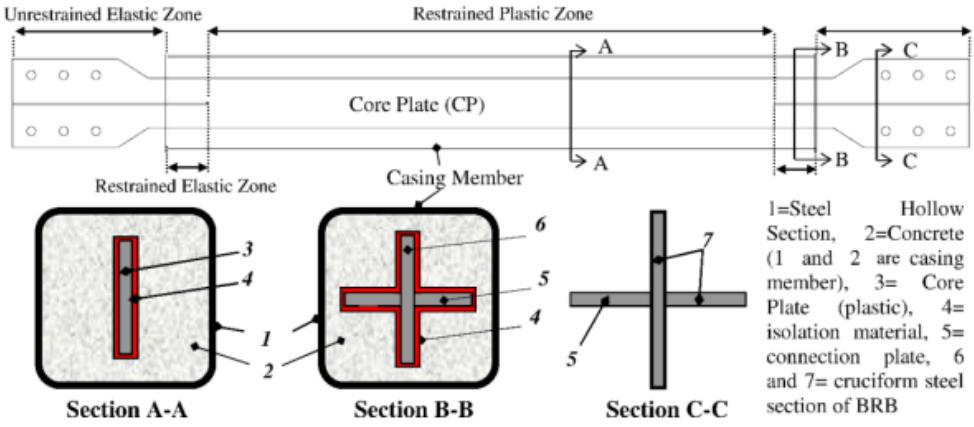

Figure 3. 17Details of BRB (from Ozcelik et al., 2016)

Finally, the typical hysteretic cycle of BRB is shown in Figure 3.18, also highlighting the main differences in behaviour between conventional braces and stiffeners constrained to buckling under cyclic loading. During the initial elastic response of the BRB shock absorber, the device only provides stiffness to the structure. As the BRB begins to fail, the stiffness reduces and energy dissipation occurs due to the inelastic hysteretic response.

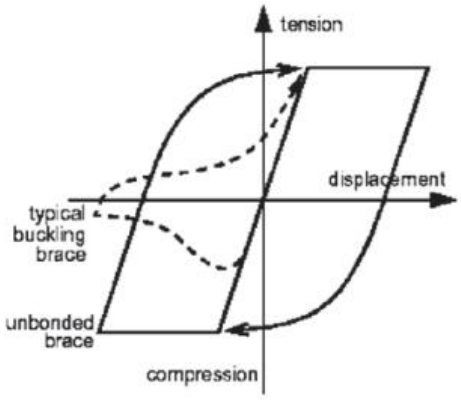

Figure 3. 18Force-displacement relationship of the BRB device

3.3.5 Shear Link Device

The shear connection device represents a more recent application in the field of metal shock absorbers. The classic application of the shear link device is a device connected to diagonal braces or chevrons, such as for ADAS and TADAS devices. A particular shear link device is the SLB (Shear Link Bozzo), which is a low-cost metallic hysteretic device obtained from a hot-cast laminated steel sheet, made thinner by a milling process. SLB heat sinks are devices that act by displacement.

The energy dissipation is produced by the shear force and by the lateral displacement action starting from 0.5 mm from the start of deformation. SLBs are characterized by having a high initial stiffness (Rigid) and a large deformation capacity more than 25 times the creep deformation (ductile).

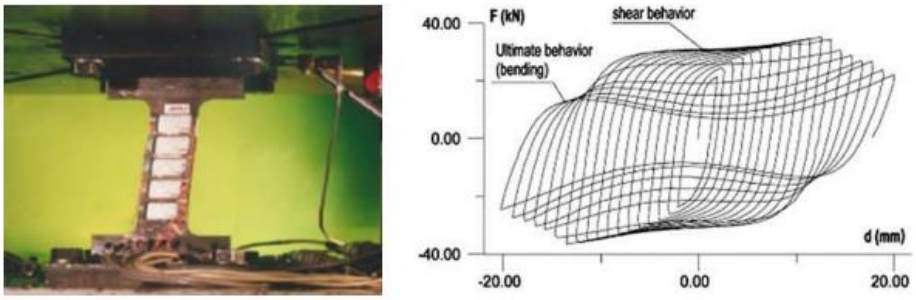

Figure 3. 19Shear link device (left) and force-displacement relationship (right)

The Shear Link Bozzo device is described in more detail in the following paragraph dedicated to chapter 4, as its study represents one of the fundamental topics of this thesis.

4. SHEAR LINK BOZZO DEVICE

4.1 Description of the Shear Link Bozzo (SLB) device

This chapter describes the main aspects of the Shear Link Bozzo device, i.e. an energy dissipation device suitable for seismic protection. It consists of a metal device first developed at the University of Girona, Spain in 1997. This device is particularly advantageous due to its flexibility to cover a wide range of force capabilities, which makes it adaptable to different levels of request. The basic idea behind the SLB device is that it provides local ductility, avoiding local buckling in a simple, controlled and cost-effective manner. The simplicity of the geometry of the SLB devices makes them particularly suitable for being adapted within the structure. Figure 4.1(a) shows the classic application with steel tie rods, which limit the force transferred to the diagonal, and heat sinks. Figure 4.1(b) shows an alternative application by decoupling concrete walls characterized by a thickness of 15-30 cm and with SLB connections.

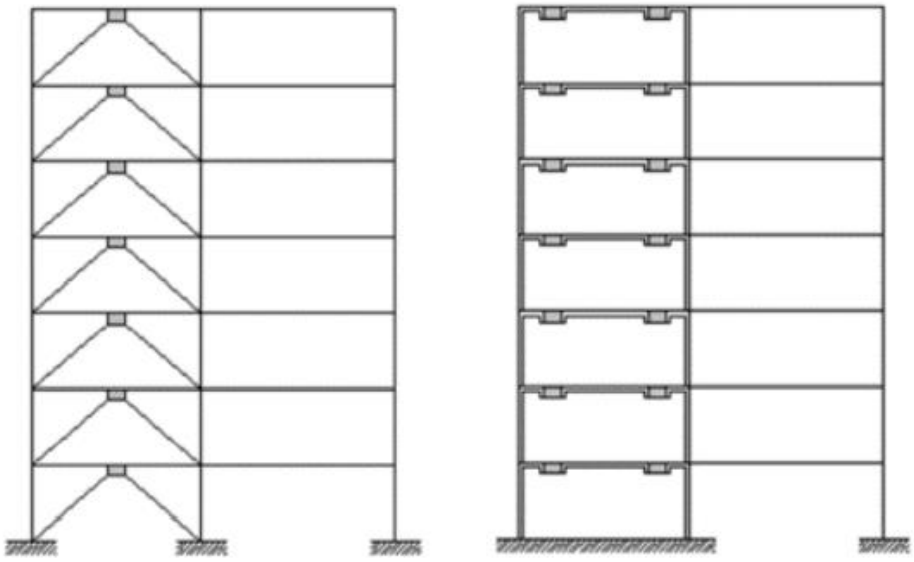

(a) (b)

Figure 4. 1Location of SLB energy dissipators: (a) Steel braces that limit the force transferred to diagonals and dissipators. (b) SLB connections through decoupled reinforced concrete walls.

It is important to highlight another peculiarity of the SLB device, which consists in the fact that these devices do not need to be aligned vertically from the current connection as the new generations do not transfer the axial load. The main shape is obtained from a hot-rolled rectangular element, which is partially reduced by a milling machine. In this way, without any soldered parts, it is possible to obtain “windows” of thinner thickness along the mesh of the device. The flanges of the device represent the most rigid parts and are used to make the connection with structural elements.Figure 3.2 shows the general geometry of the SLB energy absorber and the connection system called crenelation (or “toothed”), which do not transmit the axial load.

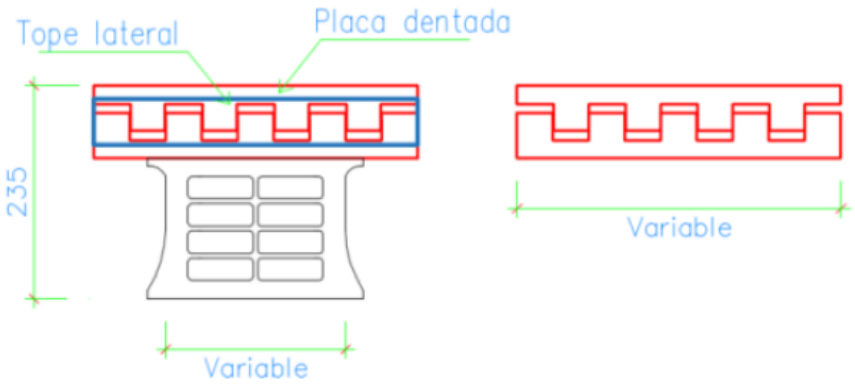

Figure 4. 2SLB energy dissipator

The dissipation capacity of the SLB depends on the height, width and thickness of the dissipative windows and web stiffeners. A correct design of the SLB guarantees the device two working phases: before the yielding of the milled parts, it works according to a "shear mode", therefore characterized by an approximate linearity of the deformation of the element, uniform distribution of the cut and "windows" that plasticize uniformly (Figure 4.3).

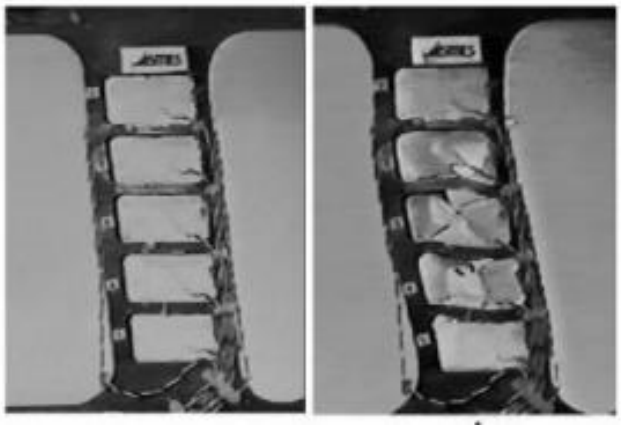

Figure 4. 3Working modes of SLB device: (a) shear and (b) bending

After yielding and buckling of the tape, the thinnest parts of the device are subjected to degradation, however the device continues to dissipate energy through a "bending mode" with a reduced stiffness, when compared to the "shear mode" stiffness, such as shown in Figure 4.4.

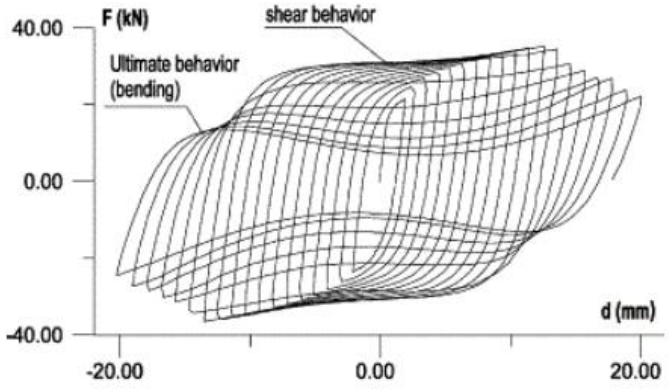

Figure 4. 4Shear Link Bozzo typical hysteretic curves

Stable hysteretic curves imply that the SLB energy dissipation device must be designed so that failure is reached before failure of the thinnest “windows”, since buckling causes a significant reduction in dissipative capacity. For this reason, these devices feature horizontal and vertical stiffeners between milled areas. Designing a shear connection energy dissipation device means defining several parameters, the most important being: material steel grade, total height, dissipative height, width,

thicknesses, position and size of the stiffeners. For this reason, several generations of SLBs, described in the following paragraphs, have been proposed and studied both numerically and experimentally during the last 20 years (Figure 4.5) with the aim of optimizing their mechanical behaviour.

Figure 4. 5Fourth generations of SLB devices

- The first device was characterized by two columns of dissipative windows in the web and a bolted connection, the role of tolerance between holes and bolts was analysed through a parametric analysis;
- The second-generation SL, characterized by heights, as well as stiffening of the thickness, substantially unchanged compared to the previous geometry. The connection is totally bolted, in order to avoid welding and to make the installation and replacement process easier during the life of the building. As a difference from the previous generation, the number of dissipative windows, always distributed in two columns, is increased from 2 to 4, reducing their height but significantly increasing their width, in order to increase the ductility as well as improve the film resistance to instability. A further innovation is the adoption of slotted holes for connection on one side, with the aim of avoiding the axial load transferred from the upper beam to the device and the other way around.
- flanged connections which prevent the axial transfer of the load to the heat sink, allowing the devices to be incorporated freely into the structure both in plan and in height. However, fixing the device at one end, while providing a

number of benefits, reduces the total energy dissipated compared to a system fixed at both ends.

- The fourth-generation prototype aims to increase the deformation capacity of the devices, to achieve this, a first option is to increase their height and a second option is to increase the height of the dissipative windows. The height of the SLB3 devices is 155mm, so to increase the deformation capacity without compromising stability, a height of 270mm has been set and the windows have been enlarged from 25mm to 50mm. It is important to underline that the fourth generation SLB also has a "toothed" attachment to avoid axial load transfer.

4.2 Experimental campaign of SLB Device

In the last 20 years a large experimental campaign has been conducted to investigate and improve the behaviour of the SLB device. Each generation was tested leading to the calibration of the analytical and numerical models on the basis of the results obtained from the tests.

4.2.1 First generation

The first experimental studies were performed at ISMES Spa, in Bergamo (Italy) in 1997, where the prototype (Figure 4.6) of the first generation of tested SLB devices was located.

Figure 4. 6Prototype of the SLB 1st generation

The flanges of the devices have been welded to thick horizontal plates, constituting connection elements to the machine, using high-strength bolts. The fabric was defined by a single column of dissipative windows ranging in thickness from 1.5 to 2.0 mm, while the flanges and other reinforcements were 15 mm thick. Four devices with different transition zones between web and stiffeners were cyclically tested performing stable hysteretic behaviour with significant work hardening. It is important to note that after the severe damage of the dissipative windows, the SLB devices exhibit a stable behaviour even with lower hysteretic curves corresponding to a dissipative bending behaviour as shown in Figure 4.7.

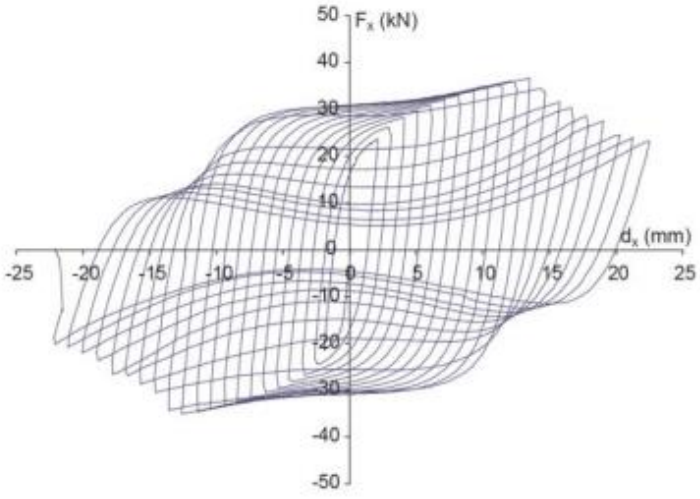

Figure 4. 7Experimental force-displacement hysteretic curve (ISMES, 1997)

A further device belonging to the first-generation SL (see Figure 4.8) was tested again at ISMES Spa in 2001 with the aim of generalizing its mechanical properties for many different levels of yield strength.

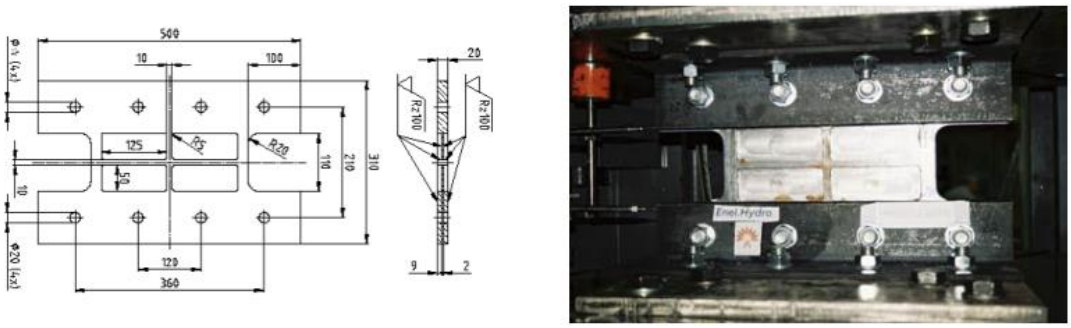

Figure 4. 8Dimensions of the SLB device and SL tested at ISMES, Italy (2001)

To define the optimal shape and characteristics of the heatsink, four basic devices were compared. All are characterized by two columns of dissipative windows; all the devices have in common two vertical reinforcements (20 mm wide) at the two lateral ends, the width is 300 mm, the thickness of the core is 2 mm and the initial thickness of the plate is 20 mm. The connection to the equipment is bolted only and the role of the tolerance between holes and bolts was investigated through a parametric analysis. In the case of tolerances of 2 or 4 mm, the tests were not successful because the creep was too high. In contrast, specimens with a hole tolerance of 1 mm showed stable hysteretic curves with hardening, shear and bending behaviour, similar to what is shown in Figure 4.7. However, also in this case significant slips were recorded, observing the collapse in correspondence of the vertical bolted connection. In this case the nonlinear plastic analysis was performed using the ANSYS computer program. The model for all cases corresponds to that of isotropic hardening which gives the complete material stress-strain relationship. Figure 4.9 shows the von Mises stresses for a given imposed relative displacement of 20mm for two of the four preliminary fixtures.

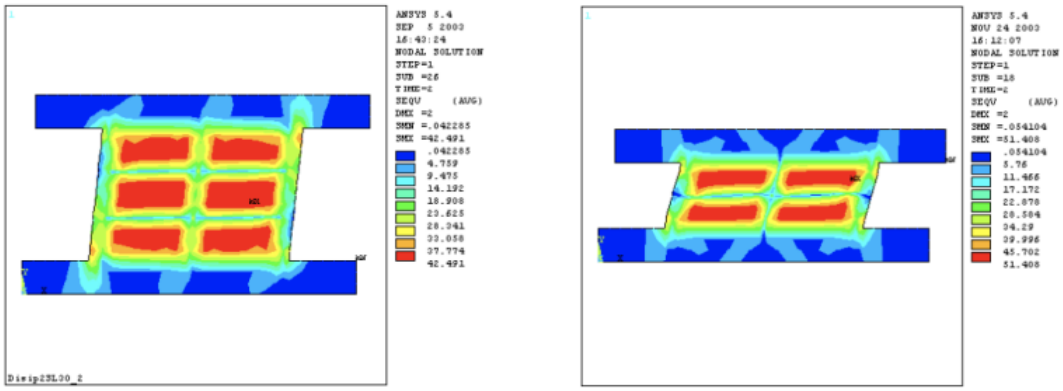

Figure 4. 9Von Mises stresses for the Dissip3SL30_2 and Disip4SL30_2 devices

These stresses are uniformly distributed across all dissipative windows, indicating maximum material gain. Furthermore, this indicates that the stiffeners do not significantly affect the dissipation. Figure 4.10 shows the force-displacement relationship for the proposed devices with a preliminary vertical height of 200 mm. In this phase, the main objective was to study the influence of the stiffeners on the yield strength and post-yield slope. Increasing stiffeners results in a small increase in yield strength, although the post-yield slope is kept constant in all cases. Thus, the total energy dissipated increases as the number of stiffeners increases, although the milled area is reduced by them. This result is explained by the increase in stiffness. For design purposes, however, all tested devices performed very similarly in the force-displacement relationship.

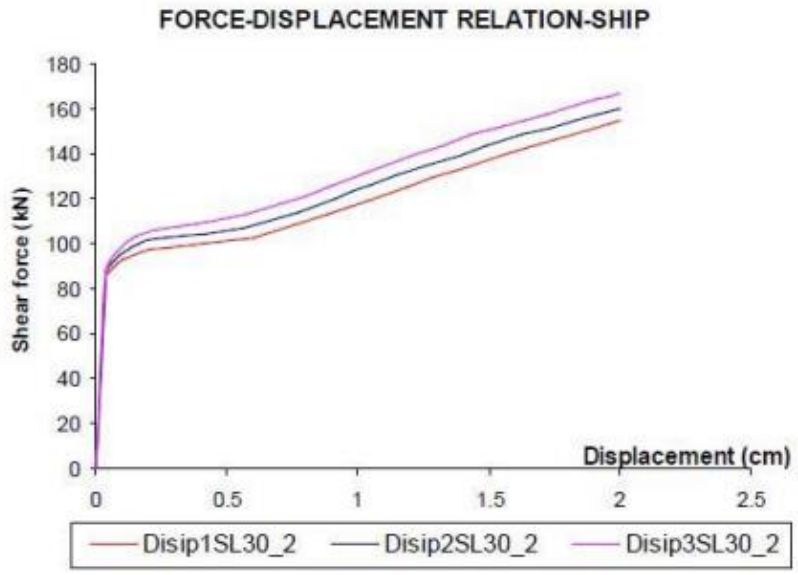

Figure 4. 10Nonlinear monotonic force-displacement relationship

The device, referred to as SL30_2, was compared with the first tested in 1997 (prototype) and is characterized by two columns of dissipative windows. The connection to the equipment was bolted and the role of the tolerance between holes and bolts was investigated through a parametric analysis. In the case of tolerances of 2 or 4 mm, the tests were not successful because the creep was too high. In contrast, specimens with a hole tolerance of 1 mm showed stable hysteretic curves with hardening, shear and bending behaviour, similar to what is shown in Figure 4.7. However, significant creep was also observed here, with collapse observed at the vertical bolted connection. In any case, slippage has not been considered a good response characteristic since, in general, it is difficult to consider its influence. For this reason, the tolerance has been reduced as much as possible to avoid this problem. In order to develop a design table for SLB devices, a numerical-experimental calibration test was performed. Figure 4.10 summarizes this calibration by showing that a good correlation can be obtained using a relatively simple isotropic hardening plasticity model. This aspect represents an advantage of the device over others based on friction or viscos-elastic response which require more difficult modelling.

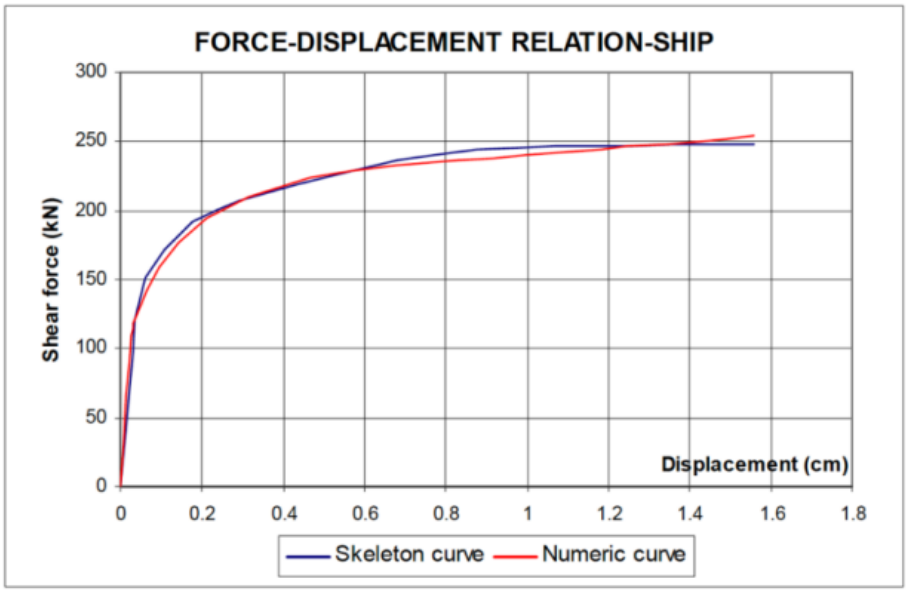

Figure 4. 11Experimental vs numerical monotonic force-displacement relationship

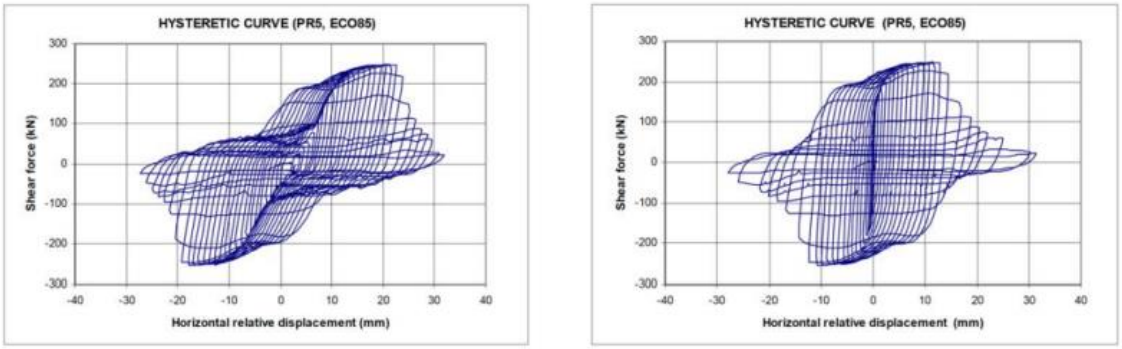

Figure 4. 12Hysteretic curve for device with (left) and without (right) slippage of the bolts

A further device belonging to this generation was tested at the laboratory of the Pontificia Universidad Católica del Perú in Lima, in 2015. The geometry was similar to the SL30_2, but smaller, with a total width of the tape L of 25 cm, therefore reason is listed as SL25_2. A horizontal actuator was used to apply a quasi-static load history to the device through the interposition of an underlying hollow square member with controlled displacement. During the test, the sample experienced an out-of-plane failure mechanism, which caused the experiment to terminate prematurely.

4.2.2 Second generation

The performance of the second generation of SLBs was tested at the laboratory of the University of Naples Federico II in collaboration with the University of Naples Parthenope, in 2016. A total of 10 devices of 5 different geometries were tested, having 2 samples for each type. Each device is generally referred to as SL X_Y, where X is the width of the tape in cm and Y is the thickness of the dissipative windows in mm. The total height (310 mm), the tape height (110 mm) and the plate thickness (19 mm) are the same for all devices. The thickness of the dissipative windows is 3 or 5 mm, while the width of the core is 300, 400 or 500 mm. Seven devices were tested under cyclic loads, the remaining three were subjected to monotonic loading.

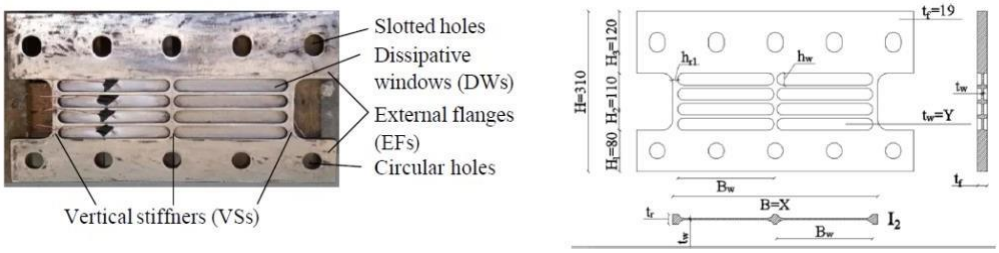

Figure 4. 13Geometry of the tested 2nd generation SLB device

The connection of the tested devices is made using high strength M30 bolts. On one side there are 30.5 mm round holes, while on the other side there are 30.5 x 38 mm slotted holes. The bolts in the round holes have always been fully tightened to achieve a fixed setup with no slippage. To understand the role of boundary conditions in the mechanical response of the device, the bolts in the slotted holes were fully tightened in some configurations, denoted as FF (fixed-fixed), and in other cases were not tightened at all, obtained a configuration FNF (fixed-unfixed). In particular, the slotted holes were designed to avoid axial stress in the device due to bending of the beam under gravity loads. In conclusion, due to the free or constrained rotations at the slotted holes, the device can be roughly studied as a cantilever in the FNF configuration and as fixed at both ends in the FF configuration, as illustrated in Figure 4.14.

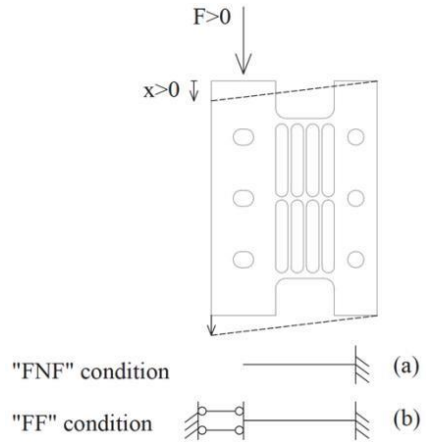

Figure 4. 14Boundary condition for SLB devices

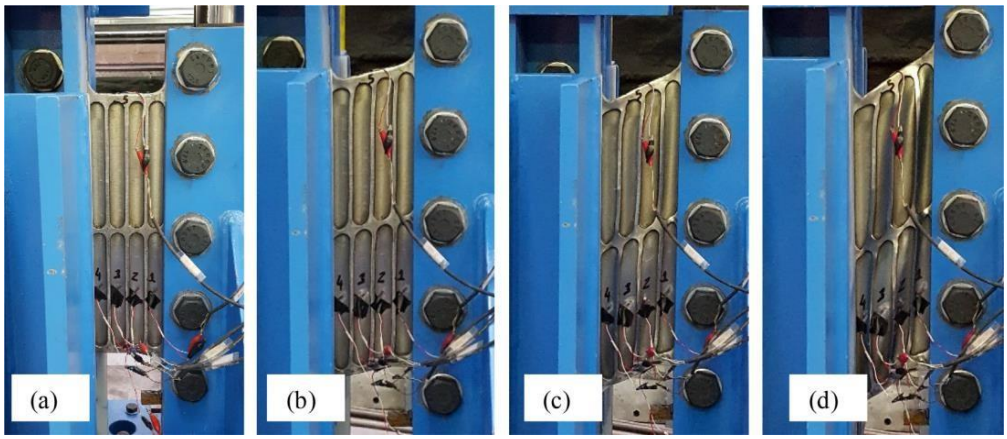

Figure 4. 15Monotonic test #4 damage scenario: (a) initial condition, (b) yielded phase, (c) onset of buckling, (d) global buckling

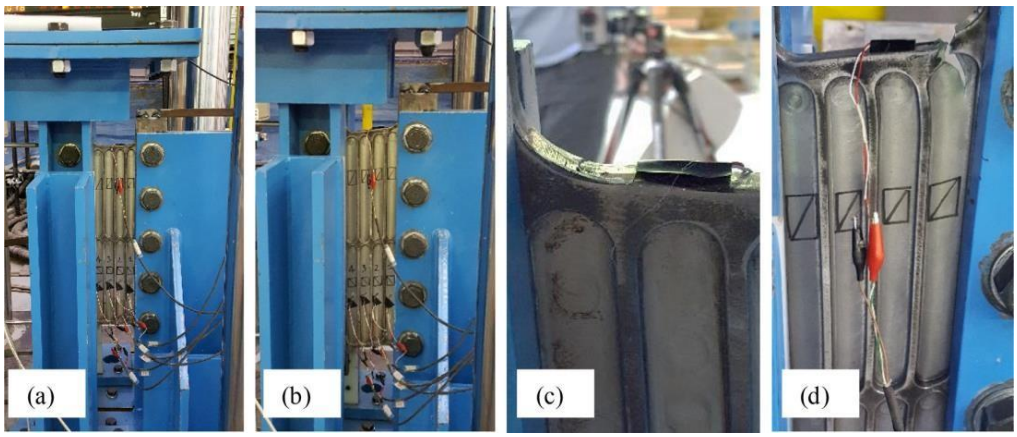

Figure 4. 16Cyclic test #10 damage scenario: (a) initial condition, (b) yielded phase, (c) onset of tearing, (d) distribution of tearing

The force-displacement response test results showed smoother curves for devices in the FF configuration, as expected, while those in the FNF configuration are more erratic due to the sliding of the bolts within the slotted holes.

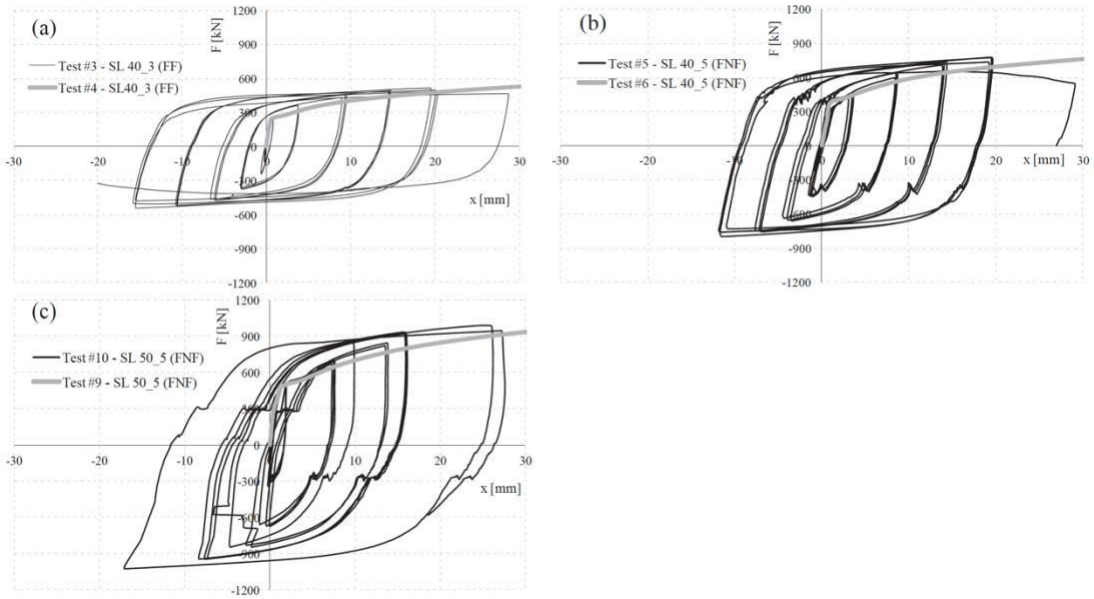

Figure 4. 17Example of cyclic and monotonic Fx curves obtained from tests

Due to the different boundary conditions, it can be observed that SL devices in FF configuration usually provide higher values of initial stiffness and yield strength than in the FNF case, although without significant discrepancies. The same SL device delivered nearly the same maximum peak force for both cyclic and monotonic tests. However, they have occurred for different amounts of displacement. Indeed, the envelope of the coils recorded for the cyclic tests gave higher force values than the active monotonic test for the same device. In conclusion, the collapse phenomenon in the cyclic tests was due to the tearing of the external stiffeners, while in the monotonic tests the samples suffered from core instability. In terms of the grip configuration for the same fixture, the primary difference between FF and FNF specimens comes from the slip at the ports due to the slotted holes. Also, due to slippage of the connections, non-symmetrical hysteretic loops have been obtained, especially in the FNF configuration. Finally, the finite element analysis of the SLB device was performed using ABAQUS and analysing both FF and FNF

configurations under monotonic and cyclic loading conditions. For the monotonic analysis, the plastic behaviour was defined through an isotropic hardening model, while for the cyclic analysis the plastic behaviour was characterized through the Chaboche model, also known as “combined hardening model” implemented in ABAQUS. The assumption of this model is justified by the experimental hysteretic behaviour of the device, which is affected by both kinematic and isotropic hardening, respectively responsible for the translation and expansion of the yielding surface. An example of ABAQUS analysis of the distribution of stresses to failure for one of the specimens is presented in Figure 4.18. The results demonstrate that the windows are characterized by a uniform shear stress distribution, confirming a global mechanism of energy dissipation through the windows.

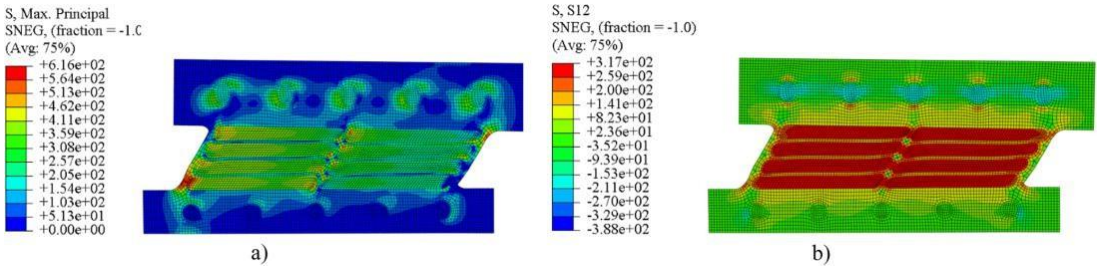

Figure 4. 18Stress distribution in FNF configuration: (a) principal maximum normal stress;

Figure 4.19 shows the distribution of strain at failure. In the FNF configuration (Figure 4.19, left) the maximum strain occurs in the stiffeners, while in the FF configuration (Figure 4.19, right) it is concentrated in the windows, demonstrating a great consistency with the experimentally observed failure mechanisms.

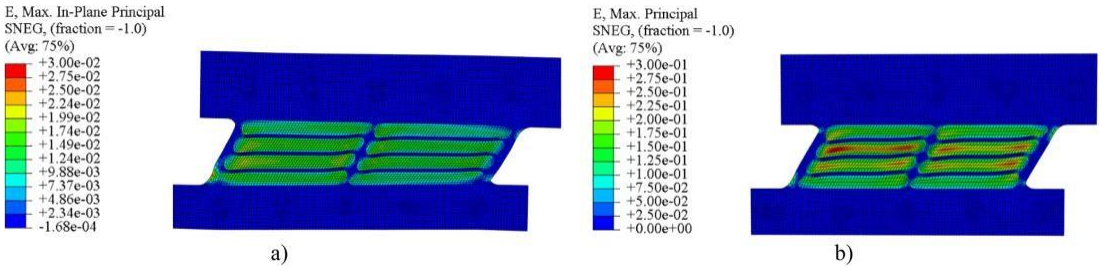

Figure 4. 19Strain distribution at failure for FNF (left) and FF (right) configuration

4.2.3 Third generation

The third generation of Shear Link Bozzo was tested at the UNAM laboratory, Mexico, 2018. The main objective of the work was to study the structural behaviour of the SLB connections for a cyclic load test, in order to compare an experimental and a numerical test model of uncoupled reinforced concrete walls equipped with the SLB devices.

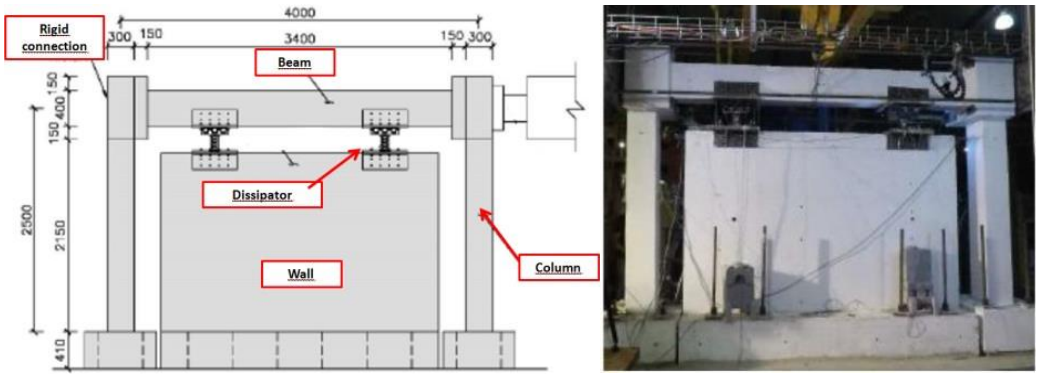

Figure 4. 20Geometry of the reinforced concrete frame, UNAM laboratory

The main significant feature of this generation of the device is the crenelated attachment, which avoids transferring axial force to the heat sink. Since these devices do not transfer axial load, this solution is called "decoupled" concrete walls. The combination of reinforced concrete frames and decoupled walls with heat sinks increases stiffness and ductility, but above all it allows not necessarily aligning the walls in height, with important architectural advantages.

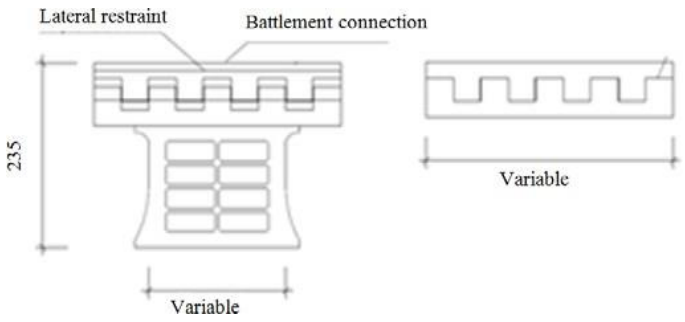

Figure 4. 21Geometry of 3rd generation SLB device

To understand the structural behaviour of the SLB connections, three 1:1 scale tests were performed: an exposed reinforced concrete frame, a reinforced concrete frame with 50 kN SLB devices (Type 1, see Figure 4.22) on non-coupled and a reinforced concrete frame with 100 kN SLB devices (Type 2, Figure 4.23) on the same wall support system. The test results were used to validate numerical simulations of the system using ABAQUS CAE, a finite element analysis (FEM) software. SLB connection type 1 has an initial yield strength of 125 kN, while type 2 has an initial yield strength of 250 kN. The material of the steel connections is ASTM 36 structural steel, with a nominal strength of 250 MPa.

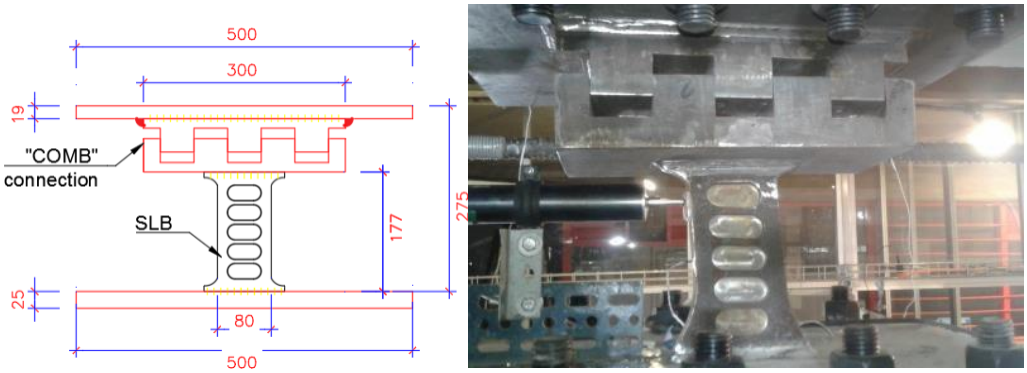

Figure 4. 22Dimensions in mm (left) and SLB connection type 1 (right)

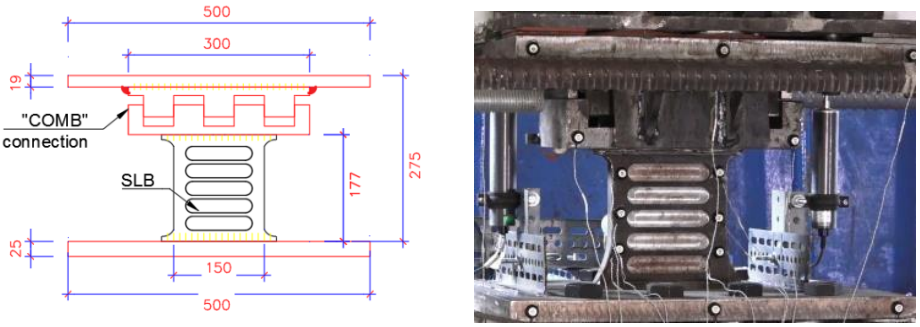

Figure 4. 23Dimensions in mm (left) and SLB connection type 2 (right)

The bare frame experimental results show an approximately linear elastic behaviour without significant energy dissipation by the plasticity of the concrete frame, as shown in Figure 4.24.

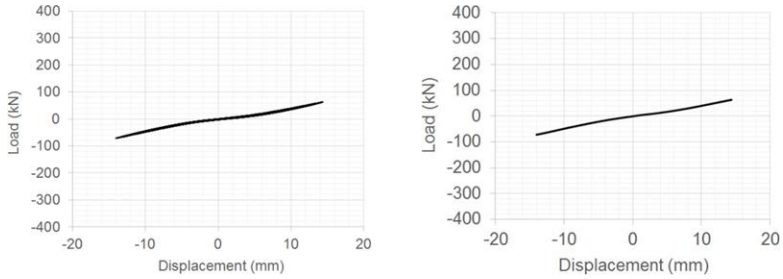

Figure 4. 24Bare concrete frame, hysteresis curve (left) and skeleton curve (right)

Figure 4.25 and Figure 4.26 show the hysteresis and skeleton curves for the concrete frame with type 1 (Figure 4.25) and type 2 (Figure 4.26) SLB connections.

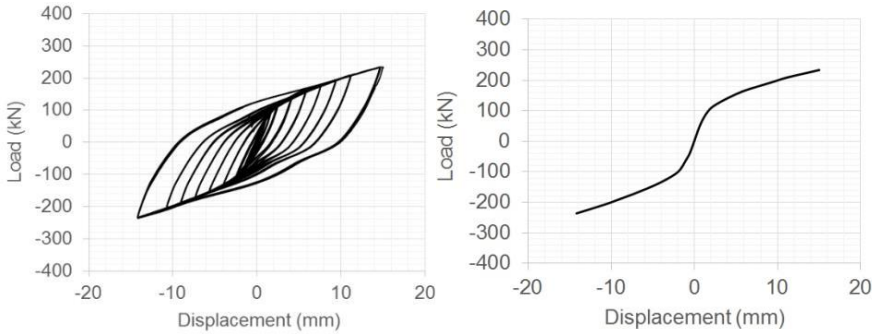

Figure 4. 25Concrete frame with SLB connections type 1, hysteresis curve (left) and skeleton curve (right)

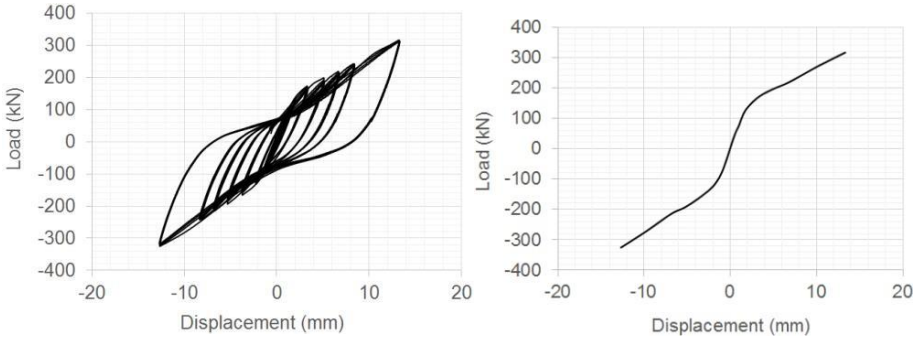

Figure 4. 26Concrete frame with SLB connections type 2, hysteresis curve (left) and skeleton curve (right)

The hysteresis curve shows that the structural behaviour of the concrete frame with type 1 SLB connections shows constant hysteresis loops without strength loss and stiffness degradation, while type 2 SLB connections show hysteresis loops without strength loss, but with some degradation of stiffness.

The finite element analysis software ABAQUS CAE was used to simulate the

experimental results of the tests through the modelling, analysis, assembly and visualization of the structural components considering only the frame without SLB connections and the frame with SLB connections Type 1, since the one with SLB connections the Type 2 connections showed an unexpected behaviour due to the excessive displacements of the connection plates.

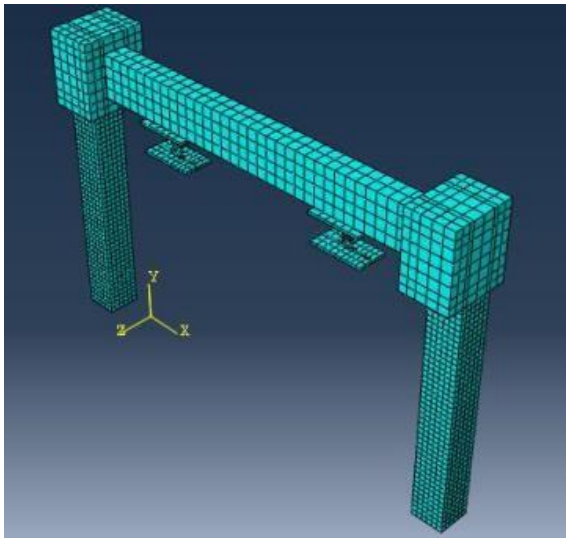

Figure 4. 27Mesh configuration of FE model of the test

First, the exposed concrete frame was modelled to calibrate the model, then the decoupled frame with type 1 SLB connections was modelled until the correct behaviour of the SLB connections was obtained.

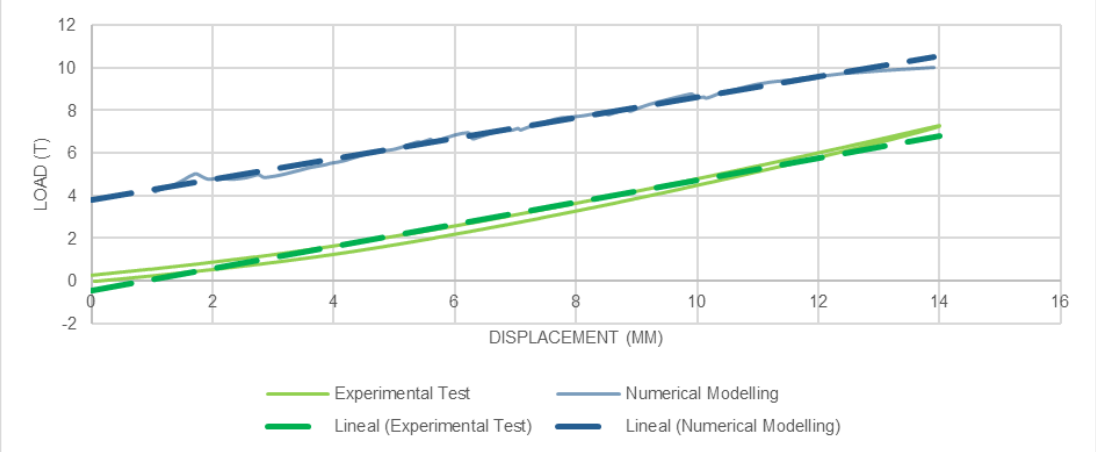

Figure 4. 28Load-displacement relationship of bare concrete frame - Experimental test vs numerical modelling

Concerning the decoupled frame with type 1 SLB connections, through several iterations it was possible to obtain a numerical model that shows a behaviour similar to the experimental test. Figure 4.29 shows comparisons between experimental and numerical hysteresis loops.

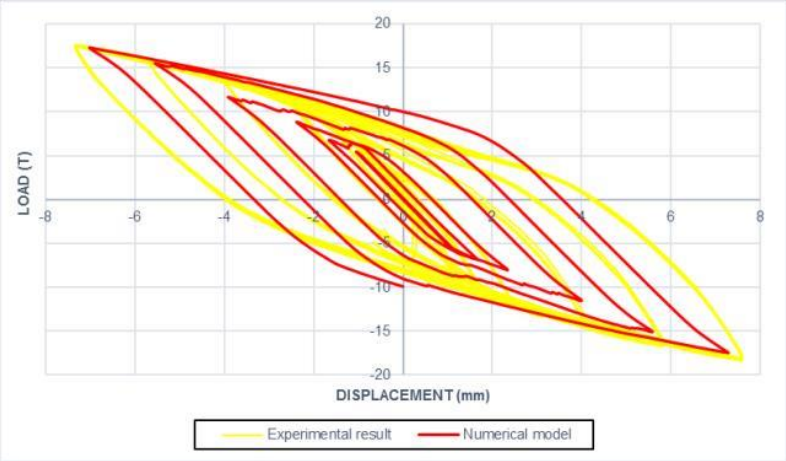

Figure 4. 29Comparison between experimental and numerical hysteresis loop of SLB connections type1

Figure 4.30 shows that the stress distribution in the type 1 SLB connection is mainly distributed in the "windows" which are the thinnest sections; however, it is important to consider that the upper part of the frames also has high levels of stress. Furthermore, the welded sections are subjected to minimal levels of stress. On the other hand, sections such as the steel plate and steel teeth (located above the SLB connection) do not show significant stress distribution.

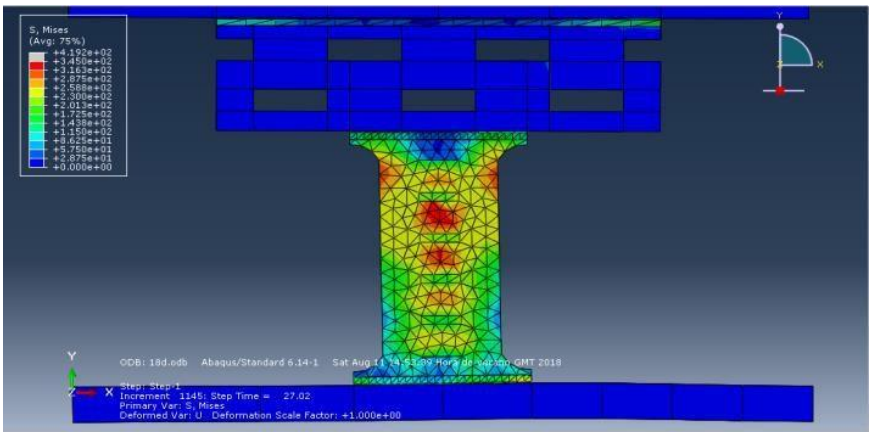

Figure 4. 30Von Mises stresses for the SLB connection type 1

Finally, a model using fixed supports has been implemented and shows that by using good connections between the reaction wall and the SLB devices, the behaviour of the SLB connections is significantly improved, reaching values of 140% of the model load capacity using supports spring. For this reason, the stiffness of the connection was a significant parameter for future tests.

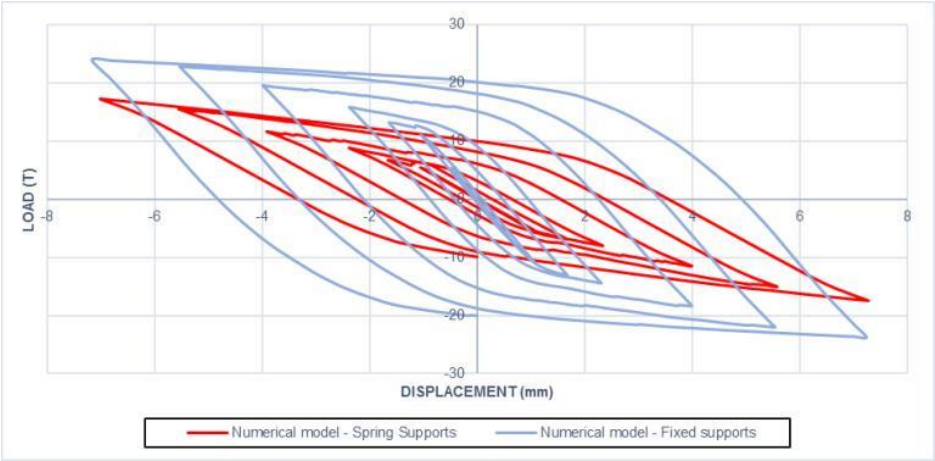

Figure 4. 31Comparison between spring supports and fixed supports in numerical model

4.2.4 Fourth generation

Tests of the 4th generation of SLB devices were performed at the University of Cantabria, Spain in November 2020. The main objective of the 4th generation was to increase the deformation capacity of the device. For this reason, the height of the

device has been increased from 155 mm of the previous generation to 270 mm and the width of the dissipative windows from 25 mm to 50 mm, in order to avoid buckling problems. The two geometries of the devices proposed for testing are shown in Figure 4.32.

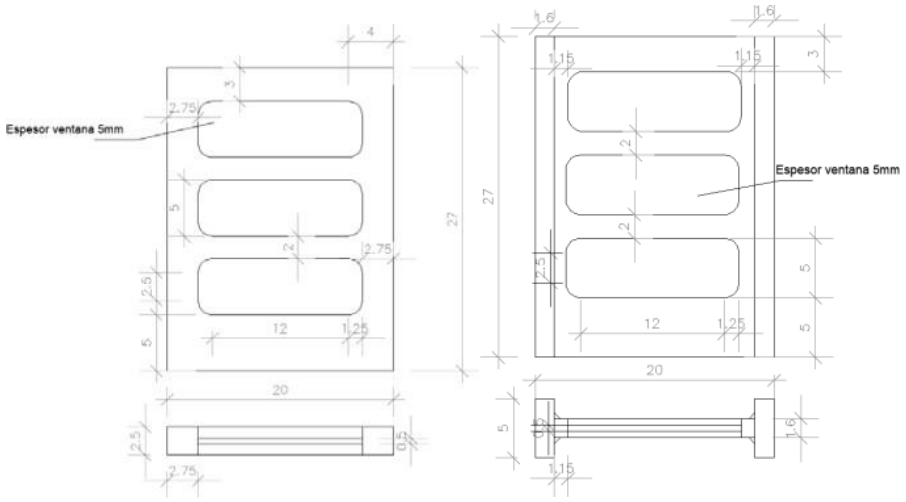

Figure 4. 32Geometries of the devices proposed for the tests

The test configuration of the device consisted of a heat sink connected to a concrete wall and subjected to cyclic loads applied to the free end of it. The device is welded to a steel plate anchored to the wall by means of steel rods, designed according to the ACI 318-19 standard.

Figure 4. 33Steel reinforcement details in the concrete wall

A total of four experimental tests were performed, involving the two SLB alternatives in Figure 4.32. The results obtained were used for the calibration of the

finite element model defined in the Diana FEA software in order to study the behaviour of the devices.

Figures 4. 34Experimental tests

Although four trials were carried out, the numerical-experimental correlation was obtained using only the results of the second and third trials, which were the most representative of the two geometrical alternatives proposed. Figure 4.35 compares the hysteretic behaviour of the sample with the finite element model results showing good agreement. In particular, the comparison shows that a simple Von Mises isotropic hardening model is sufficient to model the behaviour of the device.

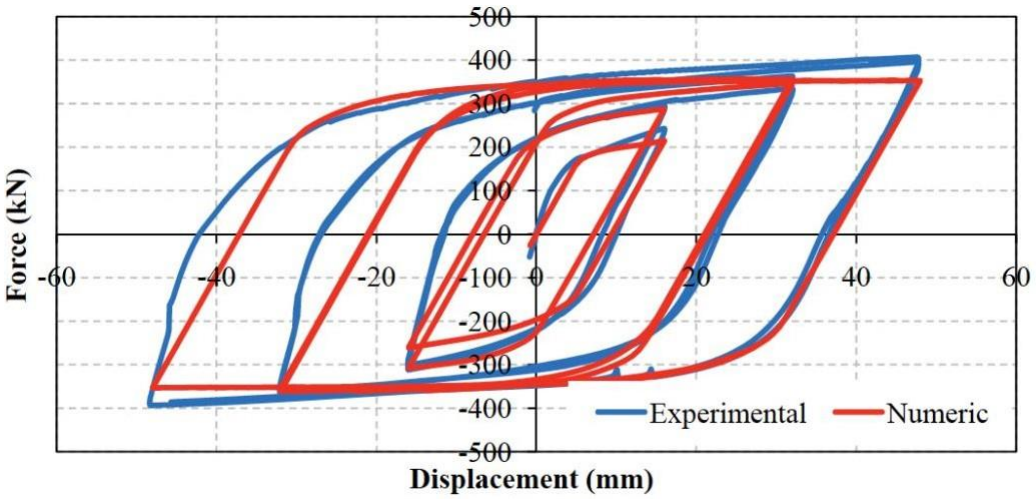

Figure 4. 35Force-displacement relationship for SLB device

The experimental campaign led to the definition of a design table for each generation of the device. The following Table 4.1 reports the geometrical and mechanical properties of the 4th generation heat sink, where K1 is the initial elastic stiffness, K2 is the post-elastic stiffness after yield, Dy is the yield displacement of the device, Fy us the corresponding force of yield strength and Fmax is the maximum force acting in the SLB.

Device	K_1 (KN/cm)	K_2 (KN/cm)	D_y (mm)	F_y (KN)	F_{max} (KN)
SLB4_10_5	2026.65	21.62	0.749	151.79	250.00
SLB4_10_6	2163.53	22.90	0.742	160.54	265.78
SLB4_15_5	2472.60	24.85	0.720	177.92	293.72
SLB4_15_6	2761.73	26.96	0.706	195.09	320.62
SLB4_15_7	3021.88	28.76	0.697	210.76	345.09
SLB4_20_6	3361.00	33.09	0.687	230.93	381.61
SLB4_20_7	3700.15	35.28	0.673	248.98	410.70
SLB4_25_6	4260.80	42.53	0.654	278.74	468.96
SLB4_25_7	4767.68	46.51	0.638	304.31	512.31
SLB4_25_8	5238.65	50.43	0.626	327.73	552.76
SLB4_30_7	5785.96	57.25	0.619	358.28	611.14
SLB4_30_8	6419.52	62.36	0.608	390.28	665.17
SLB4_30_9	6994.22	66.79	0.601	420.37	716.61
SLB4_30_10	7535.22	70.90	0.596	449.29	764.52
SLB4_40_7	7797.49	78.07	0.596	464.68	807.56
SLB4_40_8	8718.88	86.41	0.588	512.48	890.20
SLB4_40_9	9580.18	93.66	0.582	557.71	966.06
SLB4_40_10	10439.63	101.20	0.576	601.31	1043.20
SLB4_40_11	11253.53	109.93	0.571	643.06	1117.73
SLB4_40_12	12033.64	115.64	0.570	685.73	1191.30
SLB4_50_9	12289.99	120.57	0.578	709.95	1236.23
SLB4_50_10	13421.60	130.96	0.572	768.20	1340.09
SLB4_50_11	14537.41	141.39	0.569	827.48	1443.52
SLB4_50_12	15599.37	150.54	0.567	884.08	1540.02
SLB4_60_5	8891.13	91.74	0.598	531.45	932.94
SLB4_60_6	10457.28	106.25	0.586	613.19	1078.09
SLB4_60_11	17684.45	174.36	0.562	993.08	1746.50
SLB4_60_12	19029.62	185.88	0.560	1065.32	1868.98
SLB4_65_11	19829.08	194.60	0.562	1113.76	1957.04
SLB4_65_12	21326.70	209.74	0.560	1194.73	2103.54
SLB4_65_13	22872.65	223.05	0.558	1276.57	2245.62
SLB4_65_14	24379.36	235.06	0.556	1356.52	2382.04
SLB4_65_15	25869.86	249.17	0.554	1433.77	2519.93
SLB4_65_16	27331.55	261.77	0.553	1511.96	2654.85
SLB4_65_18	30180.37	286.67	0.554	1671.12	2912.47
SLB4_65_20	32951.18	306.56	0.553	1822.60	3157.88

Table 4. 1Design Table for 4th generation of Shear Link Bozzo devices

4.3 Modelling and design of SLB devices

4.3.1 SLB device mathematical modelling

The Bozzo Shear Link device features high initial spring stiffness and high plastic deformation capacity. Thus, the device exhibits ductile behaviour, as illustrated in the force-displacement relationship in Figure 4.36.

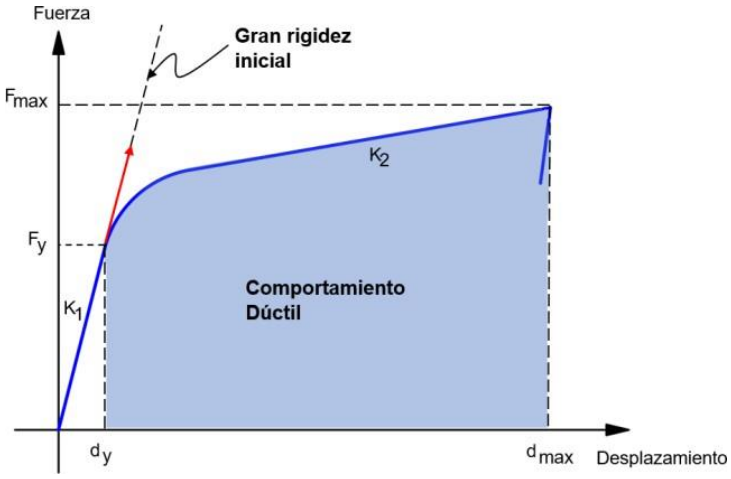

Figure 4. 36Force-displacement relationship of the SLB device

Due to its mathematical modelling, the SLB device can be easily modelled as an elastic-plastic element through the definition of an elastic K1 and post-elastic K2 stiffness after yielding, as shown in Figure 4.37.

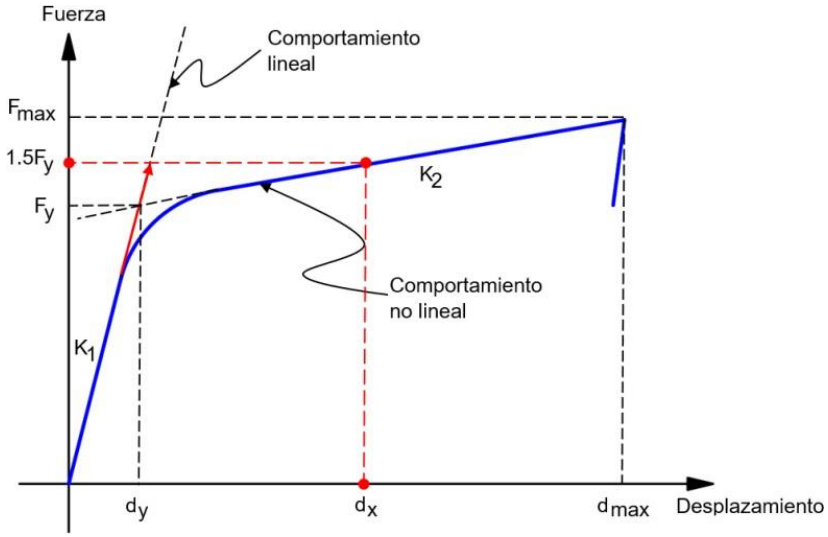

Figures 4. 37Elasto -plastic force-displacement relationship

Considering the force-displacement relationship in Figure 4.37, the SLB device can be represented as two springs in parallel, respectively of stiffness Ksec and (K1-Ksec), where the second spring works in series with a rigid-plastic device characterized by a yielding force Fy.

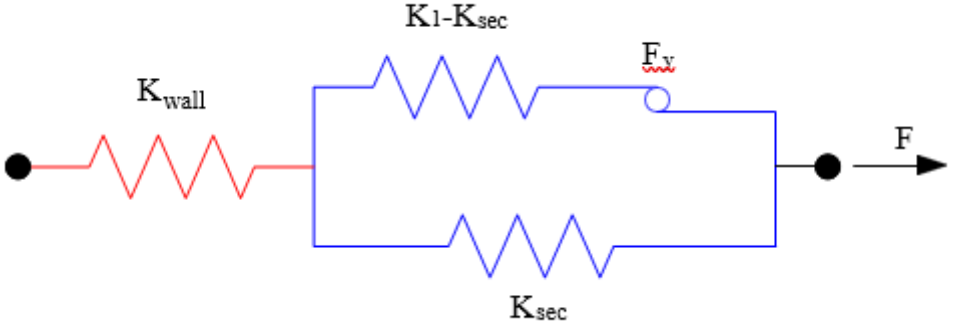

Figure 4. 38SLB device mathematical modelling

Therefore, the equivalent stiffness of the device is equal to:

$$K_{eq,\,SLB} = K_1 \qquad for F \leq F_y$$

$$K_{eq,\,SLB} = K_{sec} \qquad for F > F_y$$

where K_{sec} is the secant stiffness, which depends on the displacement of the device, and can be calculated according to the following expression:

$$K_{sec} = K_2 + (K_1 - K_2) * \frac{d_y}{d}$$

The outrigger can be considered as a spring working in series with the SLB device. Therefore, the equivalent stiffness of the bearing wall of the system can be calculated with the following expression:

$$k_{eq} = \frac{k_{wall} * k_{eq,SLB}}{k_{wall} + k_{eq,SLB}} \;;$$

The stiffness of the wall can be calculated with the following expression:

$$k_{wall} = n * k_{eq,SLB}$$

Ai then compares the equivalent stiffness with the stiffness of the device:

$$k_{eq} = \left(\frac{n}{1+n}\right) k_{eq,SLB}$$

Where:

- k_e is the elastic stiffness;
- k_m is the stiffness of the wall and is equal to $k_m = \frac{12EI}{h^3}$;
- k_d is the stiffness of the device which can be seen in table 4.1;

4.3.2 SLB extension device finished element modelling

The behaviour of the SLB device can be characterized numerically using FRAME or NLINK elements. Usually, the first analysis with these devices is a linear modal spectral analysis, so both items are correct to start with. NLINK elements provide similar results to FRAME elements and also leave the model prepared for later non-linear history analysis. Programs like SAP2000 or ETABS offer different types of NLINK models. To represent steel failure heat sinks such as SLBs, the plasticity model used is based on a hysteretic behaviour proposed by Wen, which simulates the behaviour of such devices with great precision. In this thesis, the analyses are performed using the ETABS software, in particular considering the SLB application to the Outrigger structure. For this reason, the modelling and design of SLB heat sinks is described in the following paragraphs with particular reference to this application.

4.3.2.1 Wen plasticity model

The plasticity model is based on the hysteretic behaviour proposed by Wen (1976) and is represented in Figure 4.39.

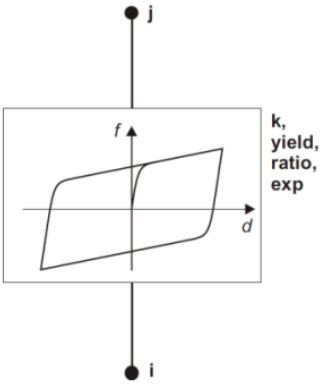

Figure 4. 39Wen Plasticity Property Type for Uniaxial Deformation

For each deformation degree of freedom, it is possible to specify independent uniaxial plasticity properties. All internal strains are independent, so the single degree of freedom failure does not affect the behaviour of the other strains. When nonlinear properties for a degree of freedom are not specified, that degree of freedom is assumed to be linear using the effective stiffness.

The nonlinear force-strain relationship in Wen's plasticity model is given by the following expression:

$$f = \alpha * k * d + (1 - \alpha) * f_y * z$$

where k is the spring constant, f_y is the yield strength, α is the specified ratio of post-yield stiffness to elastic stiffness (k), and z is an internal hysteretic variable that has a range of $|z| \leq 1$, with the yield surface represented by $|z| = 1$. The initial value of z is zero, and evolves according to the following differential equation:

$$\dot{z} = \frac{k}{f_y} * \dot{d}(1 - |z|^n) \qquad \text{if} \quad \dot{d} * z > 0$$

$$\dot{z} = \frac{k}{f_y} * \dot{d} \qquad \text{otherwise}$$

where n is an exponent greater than or equal to unity. Greater values of this exponent increase the sharpness of the yield, as shown in Figure 4.40. The practical limit for this exponent is about 20, but for the particular case of the SLB heatsink it is recommended to use an exp value equal to 2

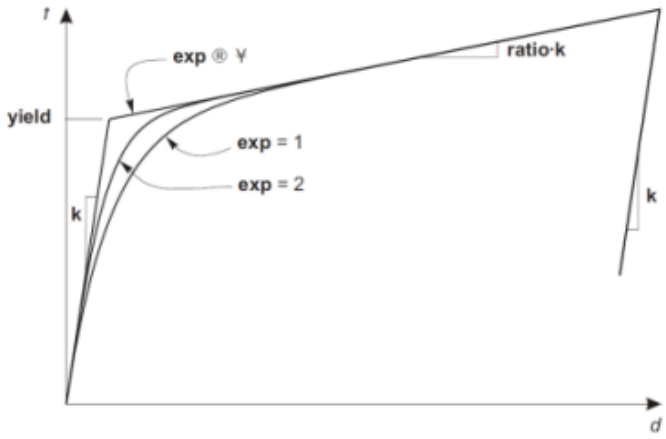

Figure 4. 40Definition of parameters for the Wen Plasticity Property

4.3.2.2 Link properties

The most useful methodology to define the SLB device in a FEM software (e.g. ETABS) consists in the use of a link. In particular, ETABS allows to define the device as an NLINK element, using the elastic properties of the element for linear analyses and the Wen plasticity model introduced in section 4.3.2.1 for non-linear analyses. Concerning the definition of the NLINK element, an important parameter is the so-called "position of the shear strain" or "zero moment point". It is defined in ETABS, as shown in Figure 4.41, as the distance from the inflection point or where the moment due to shear on the link is zero. This distance must be measured from the end point of the link. It is important to highlight that in the case of the SLB device, the "point of zero moment" corresponds to the connection of the battlements, therefore this distance is equal to zero or to the height of the device, depending on how the connection is defined or entered. Thus, depending on the connection of the battlements, the NLINK must be directed up or down. In particular, in the case applied to the project developed in Chapter 6, i.e. the case of outriggers, the SLB devices are modelled as a link with properties on the local axis 2 and their insertion point, or joint i, of the NLINK corresponds to the middle of the column and the joint on the left corresponds to the point of intersection of the diagonals, where there is the point of null moment of the connection.

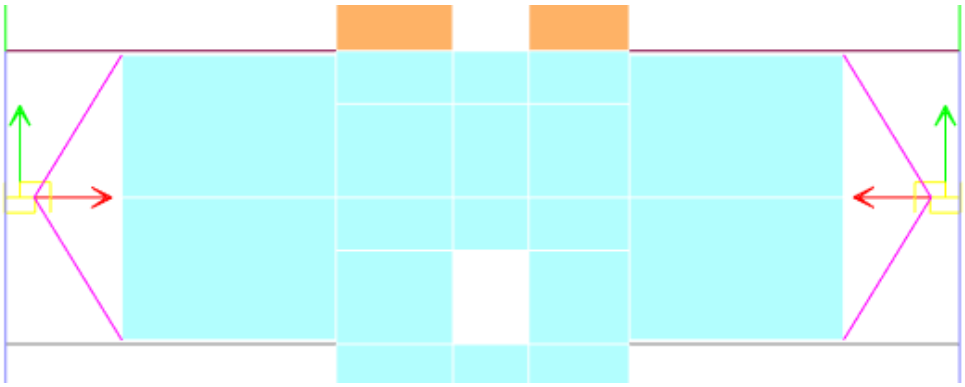

Figure 4. 41SLB modelling as Link element in ETABS

In local directions, the displacement of the link could be limited by using the "fixed" sections, but it is recommended to assign a stiffness low enough to limit the displacement (for example, 10 kN/cm) or better yet calculate it based on the connection plates without compromising the overall result.

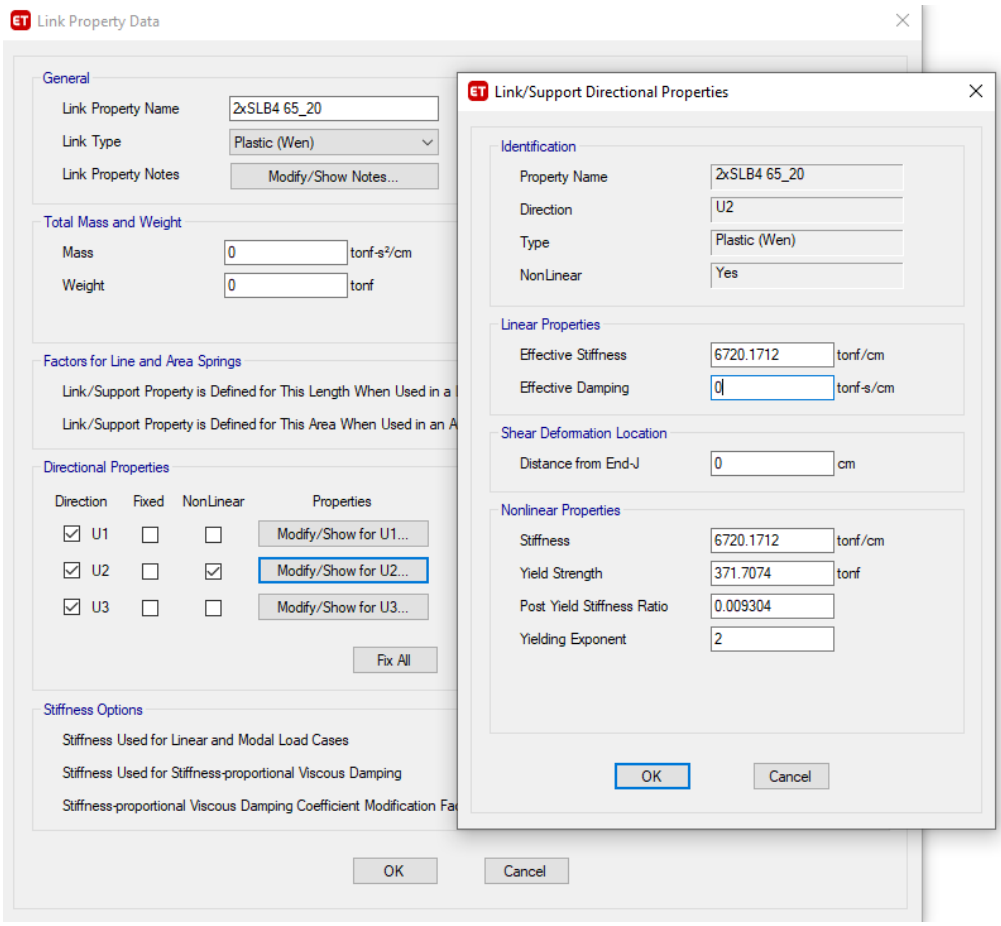

Figure 4. 42Assignment of the lateral stiffness of the Nlink for the local axis - ETABS

In the “DISSIPA-SLB” plugin the lateral stiffness values are incorporated in the load tables and are calculated based on the upper connection plates.

4.4 Iterative design methodology

The following paragraphs present two different design methods, the forward iteration method and the reverse iteration method, of SLB devices. These procedures have also been implemented in the ETABS software through the “DISSIPA-SLB” plugin. Both are based on elastic modal analyses, which replace the procedures that make use of non-linear history analyses, thus obtaining a considerable saving of computational time for the solution. This is especially useful in preliminary design, where the most important decisions are made.

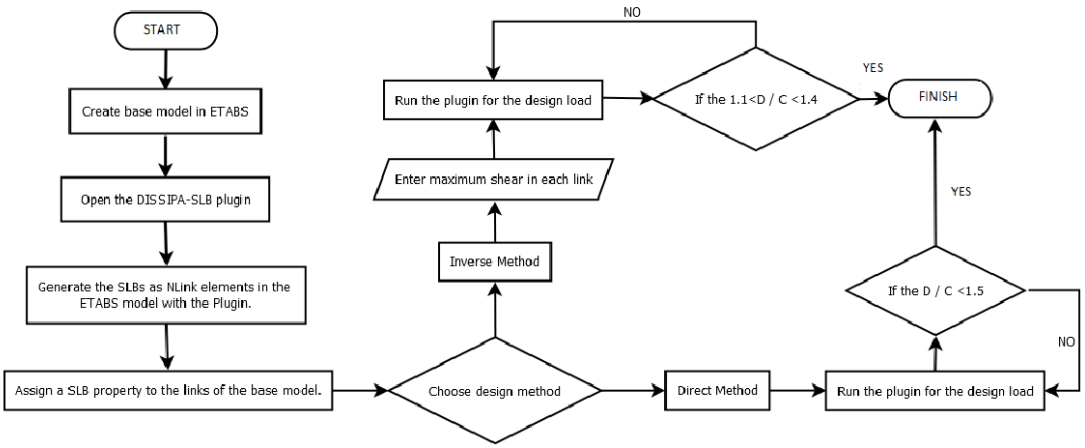

Figure 4. 43Flowchart for the design of SLB dissipators using DISSIPA SLB plugin for ETABS

4.4.1 Direct iteration method

The direct method consists in iterating a group of devices, previously defined, through a series of seismic analyses of linear modal spectral analysis, until a shear demand ratio compatible with the device capacity is reached. More specifically, the ratio between the acting shear and the yield strength of the device is required to be less than or equal to a certain demand/capacity ratio typically assumed to be equal to 1.5. This value is considered to be corrected by various cumulative factors such as the kinematic hardening of the steel or its greater resistance to dynamic loads; these factors can only be considered through non-linear history analysis, which is strongly recommended to be performed at the end of the design procedure to verify the structural behaviour of the building.

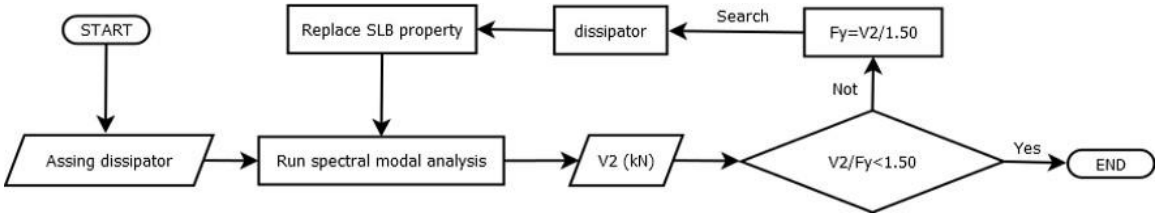

Figure 4. 44 Flow chart of direct iteration method

The design process is iterative because the modification of the devices involves a variation of the stiffness of the structure and implies the need to recalculate the seismic forces on the structure to verify again the demand/capacity ratio.

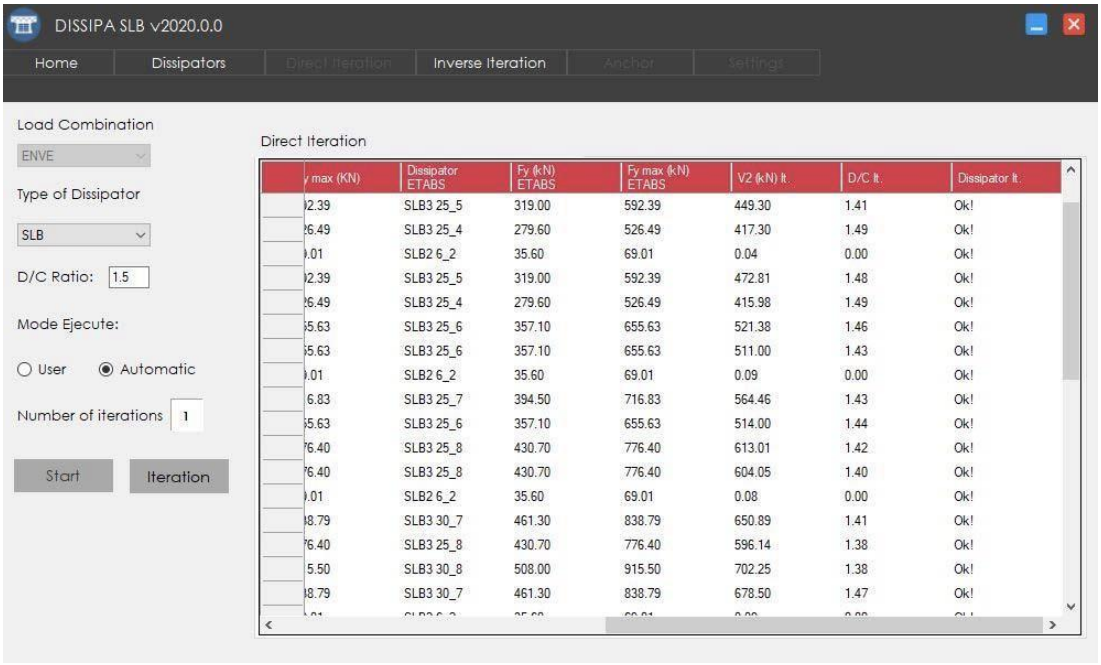

Figure 4. 45 Direct iteration method - Dissipa plug-in for ETABS

Once the dimensions of the SLB devices have been defined, it is possible to design the walls considering the maximum force value that can act on them. The shear capacity of a structural concrete wall according to the ACI code can be calculated with the following expression (units in MPa):

$$V_d = 0.75 \cdot 0.83 \cdot \sqrt{f_{ck}} \cdot L \cdot t$$

Where:

- fck is the compressive strength of the concrete;
- L is the length of the wall;
- t is the thickness of the wall.

The shear capacity of each concrete wall, calculated with the previous equation, must be greater than the maximum force that can act on the devices. The iterative iteration procedure usually increases the size of the sink at each iteration, for this reason the reverse iteration procedure, described in the next paragraph, has been developed.

4.4.2 Inverse iteration method

The "fixed force" or "reverse" iterative procedure is an alternative to the "direct iteration" one to limit the thickness of the walls and the dimensions of the devices since the direct procedure increases their dimensions consecutively. According to the ACI code, as shown in the equation in paragraph 4.4.1, the shear capacity of a concrete wall, considering a certain value of fck, length and thickness, is fixed and, according to this capacity, it is also fixed the maximum force that can act on the devices. It is important to highlight that since the special connection of the battlements does not transfer axial force, there is a direct isostatic equilibrium relationship between the shear force of the heat sinks and the shear to the concrete support wall. Unlike the forward iteration procedure, which usually increases the size of the heat sink with each iteration, as well as its shear force, in the reverse iterative procedure, the value of the shear force in the heat sink is set and, therefore, the method consists in reducing the size of the device in the numerical model, but not in reality, to calibrate that transferred shear force.

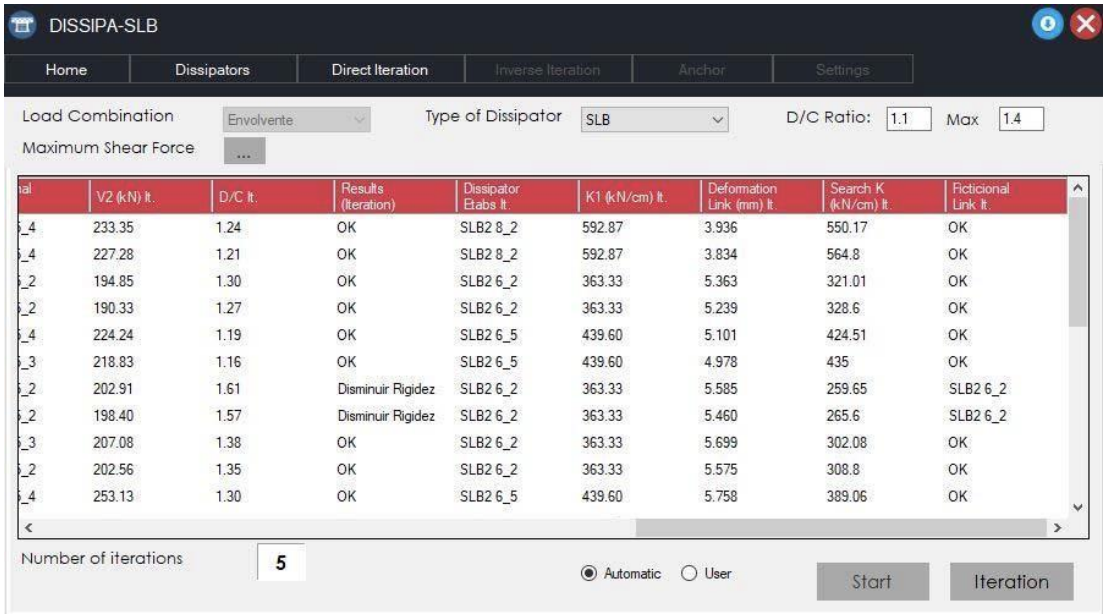

Figure 4. 46Inverse iteration method - Dissipate plug-in for ETABS

The selection procedure of the SLB devices is always performed by means of a linear modal spectral analysis which allows for a reduced calculation time and can be summarized in the following steps:

1. Definition of a SLB device type (for example, SLB 30_3) and a preliminary wall thickness (for example, 150 mm).
2. A direct iteration procedure is initially implemented to verify the design parameters to be controlled, usually the interstudy drift. If necessary, it is possible to increase the number of devices or the thickness of the decoupled walls in order to reduce the inter-floor drift to verify local design needs; in other cases it may be necessary to increase the number of decoupled walls. Also, it is necessary to check the limits of the capacity ratio in the range 1.1-1.4 to proceed with the modification of the selected devices in the analysis.
3. The total shear force in the decoupled wall should be checked at each step according to the expression:

$$V_d = 1.5 \cdot F_y \cdot n_{SLB}$$

where Fy is the yield strength of each device, 1.5 is an additional safety factor with respect to those corresponding to the ELUs and $nSLB$ is the number of devices on the wall.

4. The maximum shear force in the decoupled wall must respect its shear capacity, which can be evaluated according to the ACI code and which depends on the length and thickness of the wall and the strength of the concrete (units in MPa):

$$V_d = 0.75 \cdot 0.83 \cdot \sqrt{f_{ck}} \cdot L \cdot t$$

For steel bracing the expression is similar, but depends on the resistance to buckling of the diagonals, so the system is similar to the BRB or "Buckle Restrained Braces".

5. In case the wall thickness cannot be increased, as in the second case the concrete strength of the wall, it is necessary to proceed with the reverse iteration procedure in order to limit the force on the decoupled wall.

6. The shear capacity of the wall is fixed as previously established by the equation in step 4 and considering this the following expression is developed to calculate the maximum force in each wall device:

$$F_{max,SLB} = \frac{0.75 * 0.83 * \sqrt{f_{ck} * (L * t)_{wall}}}{1.5 * \eta_{SLB}}$$

   This is the maximum target force that corresponds to a specific type of device and that would ultimately be employed in the design.

7. Thus, the device is selected using the SLB device table such that its $Fy$is the one immediately below FmForce,SLB. There is usually more than one option for this selection, which is why it is recommended to choose the fixture with the highest window thickness due to its lower cost. At this point the interstudy drift has to be checked again because it could be that the force is too low and the drift limit of the design code is not respected.

8. Since the modal spectral analysis is linear, the force acting in each device has no limit, so when the device is selected in step 7 and the analysis is repeated, the acting shear will change and will most likely exceed the established demand/capacity limit from 1.1-1.4. One solution is to "fictitiously" reduce the device size in the RSA numerical model and repeat the analysis until obtaining a shear force within the established range.

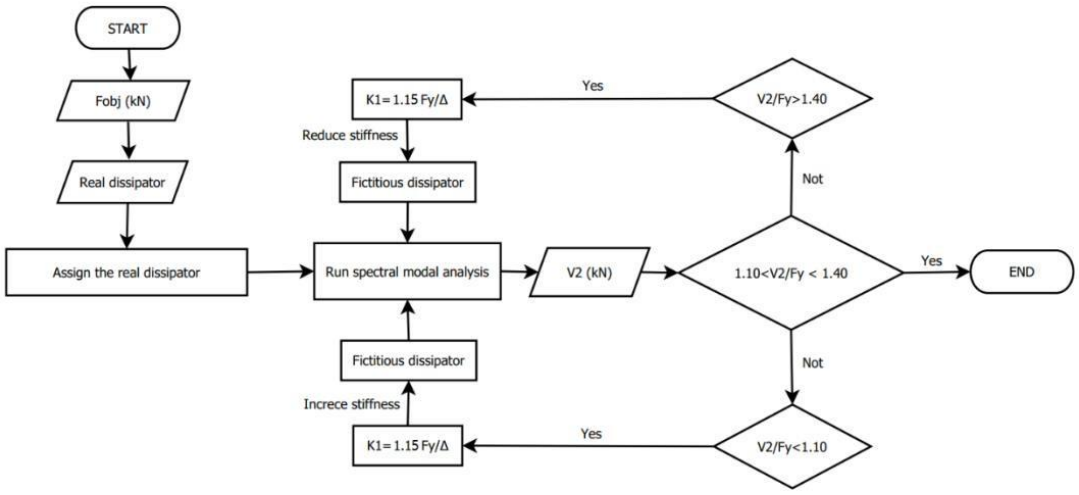

Figure 4. 47Flow chart of inverse iteration method

Actually, the reverse iteration procedure has two important steps: first, the target force is fixed on each device and through linear spectral modal analysis it is iterated with "dummy" dimensions up to a demand capacity cut ratio between 1.1 and 1.4. The force in the device must be greater than its Fy to ensure its influence in a seismic event. Furthermore, the upper bound on the capacity-demand ratio of 1.4 is set because the analysis used is linear elastic, so the shear difference between that obtained with the modal spectral analysis and the shear capacity transferred from the devices is equivalent to less effective stress in the rest of the structure. This result is incorrect because each device transfers a cut-off limit that is not counted by a linear spectral modal analysis. The procedure is iterative because the shear force in the device largely depends on its stiffness. Thus, the change of the device implies a change in the shear force acting in it. The iteration will repeat until a convergence condition is reached, which usually takes only 3 or 4 iterations. This procedure has been implemented in ETABS through the DISSIPA-SLB plugin. The second step in this procedure is to verify the results using a non-linear history analysis. As indicated, it is always important to remember that the modal spectral analysis, which is used in the first phase of the project, is a linear analysis, therefore it is not possible to consider the maximum shear force that the device can transfer to the wall support. Therefore, the difference between the shear stress acting in the device according to the modal analysis and its maximum capacity will be absorbed by the structure

resulting in a non-conservative situation. For this reason, it is important to verify a maximum force factor of 1.4 between the actual capacitance of the device and the shear force acting on it when performing linear response spectrum analysis. In order to evaluate the actual seismic performance of structures equipped with SLB devices in severe seismic events and validate the design procedure mentioned in the first stage, a non-linear historical analysis (second stage), but with real devices based on the cutting target adopted .

5. CASE STUDY: PASEO DE GRACIA

This chapter describes the main results obtained for the case study considered in this thesis, which concerns a new building located in the city of Nuevo Vallarta, Nayarit (Mexico)whose architectural design was carried out by another engineering company. The purpose of the study is to demonstrate that combination an Outrigger system and a shear Link Bozzo increases the rigidity of the structure, reducing interstory drift to both Service Level Earthquake (SLE) and Maximum Considered Earthquake (MCE) and providing an additional source of dissipation, which leads to a reduction of damage in structural elements (e.g. beams and pillars) and non-structural components. As a first step, a bare frame structure is defined, therefore without Outrigger and SLB system, as a second step two other models are defined in which the new system is inserted. We want to compare the structure in the three different models, in order to highlight the pros and cons of using such a system, as well as define the most appropriate position of Outrigger within the structure being studied. The analyses are carried out using the ETABS software.

5.1 Description of the building

The case study concerns a new reinforced concrete structure located in the city of Nuevo Vallarta, Nayarit (Mexico). Paseo de Gracia is a project that sees the construction of 4 towers for residential use:

- Tower 1, 38 levels, 709 m^2 for levels;
- Tower 2, 5 levels,729m^2 for levels;
- Tower 3, 56 levels, 709 m^2 for levels;
- Tower 4, 20 levels, 709 m^2 for levels;

At the base of these towers we find a base consisting of 4 levels, in which the first has a double height and is used for commercial use, the other three levels instead will be intended for the construction of a hotel, as in Figure 5.1.

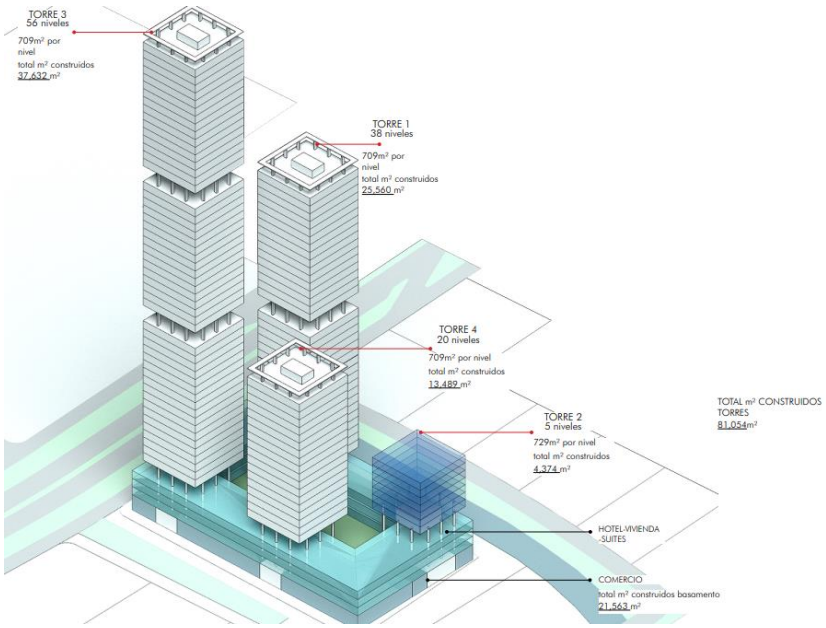

Figure 5. 1 Representation of the four towers of the Paseo de Gracia project

The thesis project is aimed at the realization of Torre 3, the highest of the Paseo de Gracia project with a total of 60 levels, for a height of 222.60m. The plan has a square and doubly symmetrical geometric shape, with a central core consisting of stairs and elevators, regular along the entire height of the building, with 4 levels in double height.

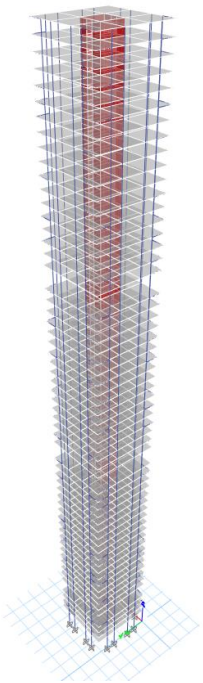

Figure 5. 2 Bare frame 3D model on Etabs

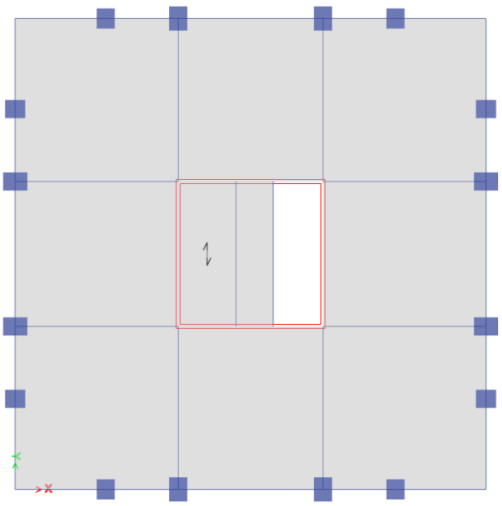

Figure 5. 3 Plan of the building

The cross-sections of reinforced concrete beams, columns and walls and the mechanical properties of the materials are defined in Table 5.1:

Table 5. 1 Geometric and mechanical proprieties of structural element

Beam Section	**b**	**h**	**A_c**	**Concrete**	**f_{ck}**
[-]	**[cm]**	**[cm]**	**[cm^2]**	**[-]**	**[Mpa]**
T 50X120	50	120	6000	C35	35
T 50X90	50	90	4500	C35	35
T 30X70	30	70	2100	C35	35
ColumnSection	**b**	**h**	**A_c**	**Concrete**	**f_{ck}**
[-]	**[cm]**	**[cm]**	**[cm^2]**	**[-]**	**[Mpa]**
C 90X160	90	160	14400	C65	65
C 90X140	90	140	12600	C55	55
C 90X120	90	120	10800	C45	45
C90X140	90	140	12600	C65	65
C 90X120	90	120	10800	C55	55
C 90X100	90	100	9000	C45	45
Level	**Wall Section**	**s**	**Concrete**	**f_{ck}**	**Level**
[-]	**[-]**	**[cm]**	**[-]**	**[Mpa]**	**[-]**
Story60	M 20	20	C45	45	Story60
Story59	M 20	20	C45	45	Story59
Story58	M 20	20	C45	45	Story58
Story57	M 20	20	C45	45	Story57
Story56	M 20	20	C45	45	Story56
Story55	M 20	20	C45	45	Story55

5.2 Reference code

The following reference codes are considered for this case study:

- MOC-CFE (2015) – Mexican building code for the design and verification of the structure for seismic loads;
- ASCE 41-13 – Reference code used for modelling parameters and numerical acceptance criteria for reinforced concrete elements (e.g., columns);
- ACI 318-19 – Building regulations used for structural design and verification of reinforced concrete elements;

- TBI – Guidelines for Performance Based Seismic Design of Tall Buildings, 2017 – Guidelines developed by the Pacific Earthquake Engineering Research Center (PEER), to define the actual stiffness of the reinforced concrete elements;
- Manual de diseño de obras civiles, diseño por viento.

5.3 Load combination

The following load combinations were used for the structural design of the building:

- $1,4\ G_1 + 1,4\ G_2$
- $1,2\ G_1 + 1,2\ G_2 + 1,6\ L$
- $1,2\ G_1 + 1,2\ G_2 + L + B$
- $G_1 + G_2 + 0,5\ L \pm Ex \pm 0,3\ Ey$
- $G_1 + G_2 + 0,5\ L \pm 0,3\ Ex \pm Ey$
- $G_1 + G_2 + 0,5\ L + TH$

where G1 and G2 represent the permanent structural loads and the non-structural permanent loads respectively; L indicates the load in motion, W the wind load, E represents the equivalent static seismic load (seismic response analysis, RSA), TH corresponds to the time history considered in the case of linear or non-linear chronological analysis. The first three load combinations are related to the limit state assessments of the structure, while the others are related to the seismic assessment of the building Service Level Earthquake and Maximum Considered Earthquake.

5.3.1 Gravity loads

Gravitational loads are defined as static loads. According to the code, dead loads were defined, consisting of the weight of all construction materials incorporated in the structural elements of the building, the permanent non-structural load, consisting of the weight of the non-structural elements of the building, and live loads, consisting of the load produced by the use and occupation of the building or by environmental loads, such as wind load, snow load, rain load, earthquake load.
For the case study representing a residential building was considered:

Dead load (DL): automatically calculated by ETABS

Permanent non-structural loads (SCM): 200 kg/m2

Dynamic loads (LL): 190 kg/m2

5.3.2 Seismic Load

5.3.2.1 Site response spectra

The intensity of the earthquake and its periocolosity vary continuously in the Mexican territory, both the reference values, as well as those associated with the periods of return. Four zones are considered: two of low seismicity and two of high seismicity. To determine the seismic zone a simple criterion based on the value of the maximum acceleration in rock is provided, a_0^r for the reference level given, obtained with the programme PRODISIS (Figura 5.4)

Figure 5. 4 Sismic map of Mexixo

It is considered the site of Nuevo Vallarta in the state of Nayarit that coincides with the zone D with high seismicity with maximum acceleration greater than 200 cm/s^2 as can be seen in Table 5.2.

Aceleración máxima en roca, a_0^r (cm/s^2), correspondiente al nivel de referencia ER	Zona	Intensidad sísmica
$a_0^r \geq 200$	D	Muy Alta
$100 \leq a_0^r < 200$	C	Alta
$50 \leq a_0^r < 100$	B	Moderada
$a_0^r < 50$	A	Baja

Table 5. 2 Bedrock Acceleration

The soil type is determined by considering the dynamic parameters of the soil, modelled as a stratified medium. The parameters to be taken into account are the depth of the soil and the propagation speed of the shear waves through the ground. The code provides the classification of the soil type by considering three different types. The requirements are shown in Table 5.3. Paseo de Gracia corresponds to soil type II.

TYPE	Description
I	Firm or rocky ground where there are no dynamic amplifications: Deposit of ground with $v_s \geq 720$ m/s and $H_s \leq 2$m
II	Terrain formed by soils in which intermediate dynamic amplifications occur: Soil deposit with $v_c \leq v_s < 720$ m/s and $H_s > 2$m, or $H_s > H_c$ and $v_s < 720$m/s
III	Terrain formed by soils in which great dynamic amplifications occur: Soil deposit with $v_s < v_c$ m/s and $2 < H_s \leq H_c$ m

Table 5. 3 Type of soil

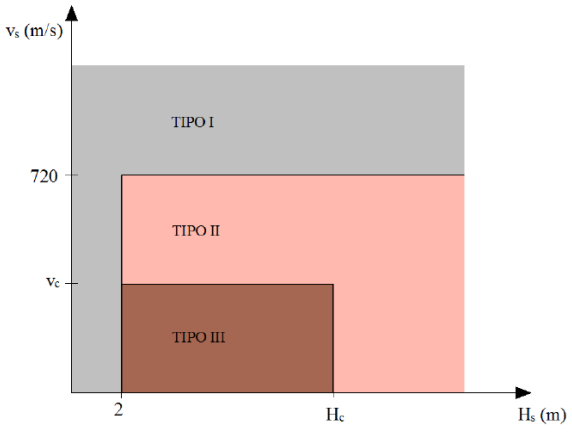

Figure 5. 5 Type of soil

The spectrum of the initial site is adjusted to obtain an elastic design spectrum, which will be used for the design of the steel armature of the bare frame structure, in accordance with the MOC-CFE building regulations. The elastic design spectrum for the earthquake design level is shown in Figure 5.6 and is characterized by:

• a first linear segment starting from the ground peak acceleration (PGA), a_0, at maximum spectral acceleration, c;

• a second segment, the plateau, defined by the interval of periods between T_a e T_b, characterized by a constant spectral acceleration value equal to c;

• a third exponential tract defined by the parameter p.

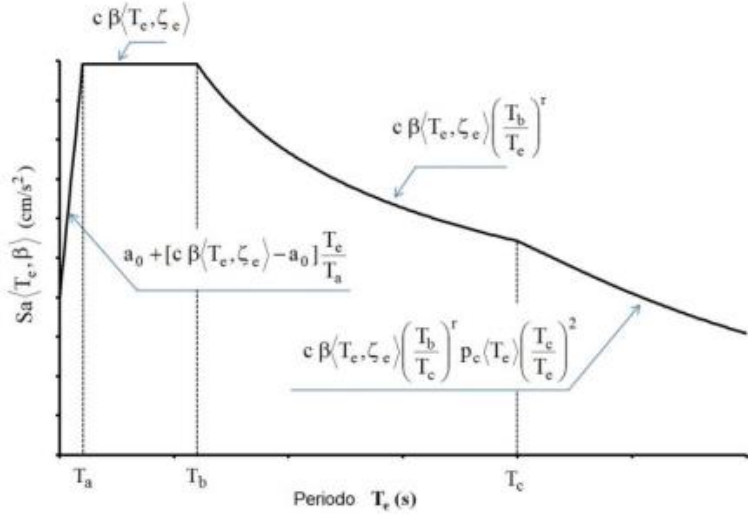

Figure 5. 6 Seismic design spectrum

Mathematical expressions describing the elastic design spectrum are shown below:

$$S_a = a_0 + (c\ \beta\langle T, \zeta_e\rangle - a_0) * \frac{T}{T_a} \qquad 0 \le T < T_a$$

$$S_a = c\ \beta\langle T, \zeta_e\rangle \qquad T_a \le T < T_b \qquad (5.1)$$

$$S_a = c\ \beta\langle T, \zeta_e\rangle \left(\frac{T_b}{T}\right)^2 \qquad T_b \le T < T_c$$

$$S_a = c\ \beta\langle T, \zeta_e\rangle \left(\frac{T_b}{T}\right)^2 p\langle T\rangle \left(\frac{T_c}{T}\right)^2 \qquad T \ge T_c$$

where :

- ***a₀*** is the maximum ground acceleration (cm/s^2);
- ***c*** is the maximum spectral acceleration (cm/s^2);
- ***Ta*** is the lower limit of the design spectrum plateau;
- ***Tb*** is the upper limit of the design spectrum plateau (s);

- ***Tc*** is the initial period of the descending branch in which the displacement of the spectrum tends to the displacement/i to the ground;
- ***T*** is the structural period in the direction of the analysis (s);
- $\boldsymbol{\beta\langle T, \zeta_e \rangle}$ is the damping factor. For structural damping $\zeta_e = 5\%$, the value of $\beta\langle T, 0{,}05\rangle$=1;
- ***r*** is the parameter that controls the decay of the spectral ordinates for Tb ≤ Te < Tc;
- $\boldsymbol{p\langle T \rangle}$ is a coefficient calculated using the following expression:

$$p\langle T\rangle = k + (1-k) * \left(\frac{T_b}{T}\right)^2 \qquad (5.2)$$

The seismic parameters used in equations (5.1) and (5.2) for the calculation of the elastic spectrum are given in Table 5.4.

Seismic parameters values - Elastic design response spectrum					
T_R [years]	**a_0 [g]**	**c [g]**	**T_a [s]**	**T_b [s]**	**k [-]**
475	0.55	1.25	0.1	0.9	1.5

Table 5. 4 Seismic parameters values for the elastic design response spectrum

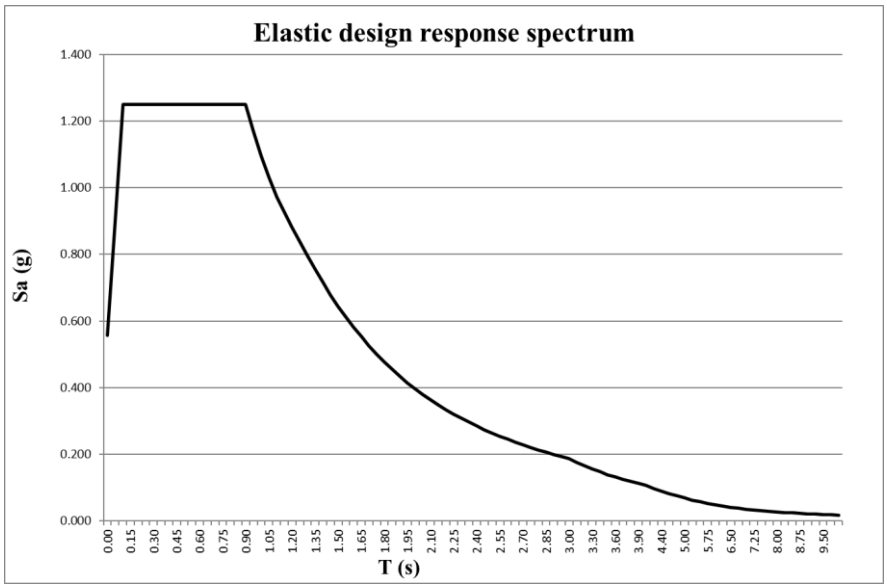

Figure 5. 7 Elastic design response spectrum

The inelastic drawing spectrum (CFE, 2015) is obtained by dividing the ordinates of the elastic drawing spectrum by values that in the aforementioned case are (Figure 5.8):

- ***Q*** is the seismic behaviour factor, taken as 3;

- R_0 is the excess resistance factor, and is taken equal to 2;
- ρ is the redundancy factor, is taken equal to 1;
- α takes into account the irregularity of the structure and is taken equal to 0.7;

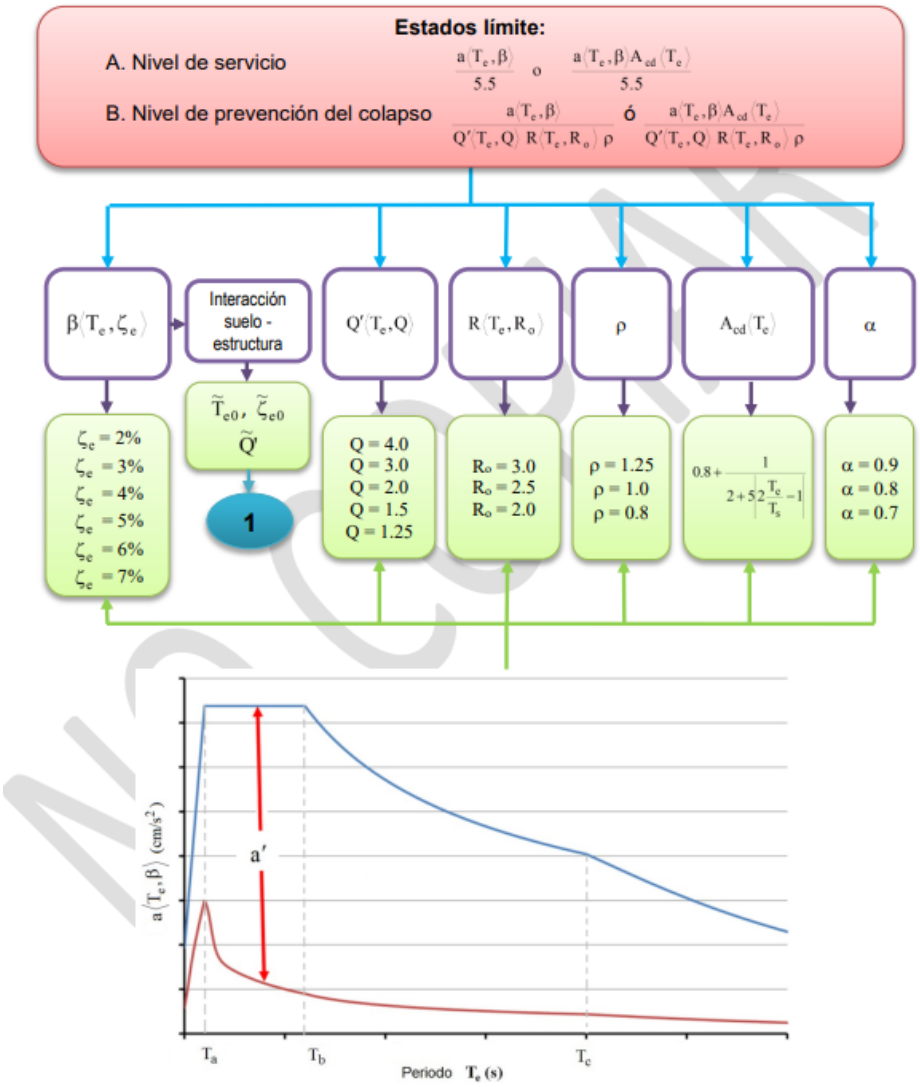

Figure 5. 8 Correction factors of the elastic spectrum

As a result, a representative spectrum of the study site is obtained in which, in figure 5.9, the spectrum is observed in the case of Collapse Level Earthquake (green) and the spectrum in the case of Service Level Earthquake.

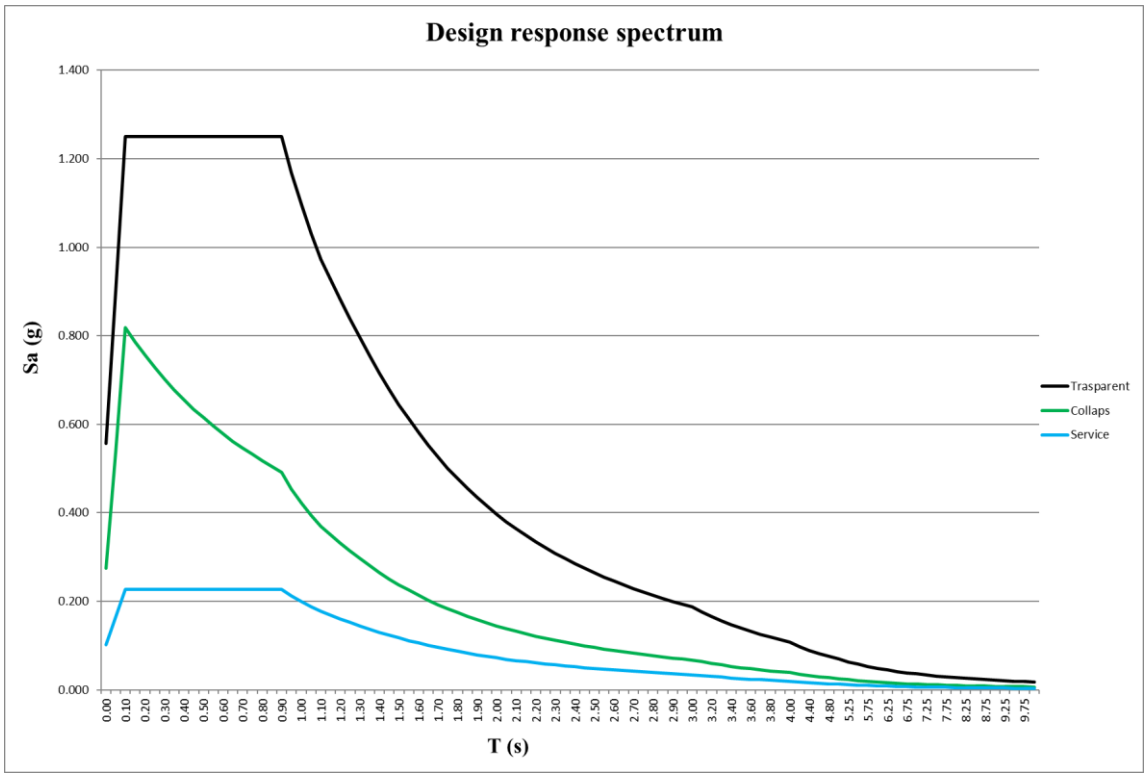

Figure 5. 9 Design Response Spectra

5.3.2.2 Seismic Signals

According to the ASCE/SEI 7 code, approximately 11 ground motion signals must be used to identify the mean value of drift.

The signals considered are 10 and are representative of the site of Nueva Vellarta, provided by another engineering company.

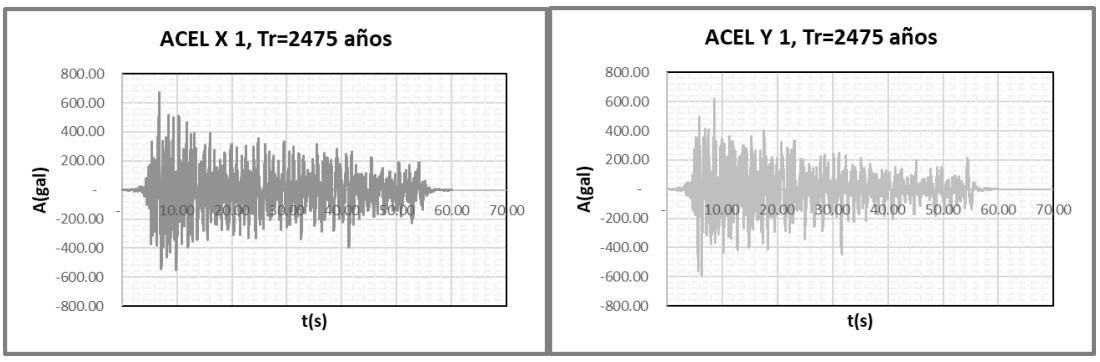

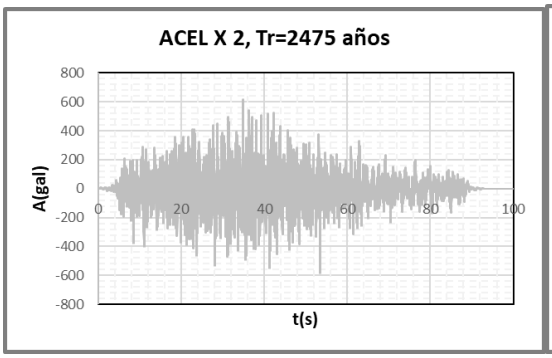
ACEL X 2, Tr=2475 años
A(gal)
t(s)

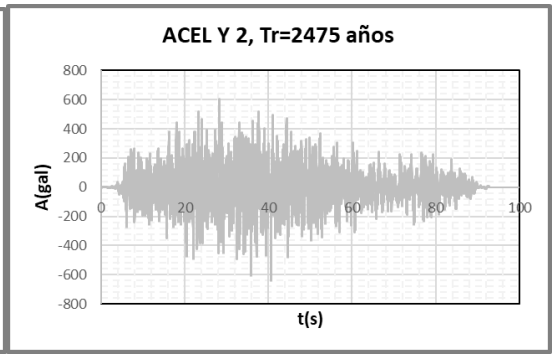
ACEL Y 2, Tr=2475 años
A(gal)
t(s)

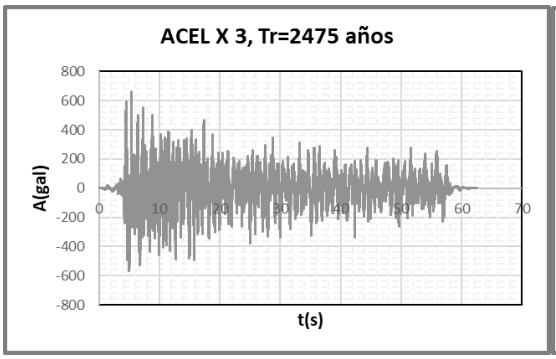
ACEL X 3, Tr=2475 años
A(gal)
t(s)

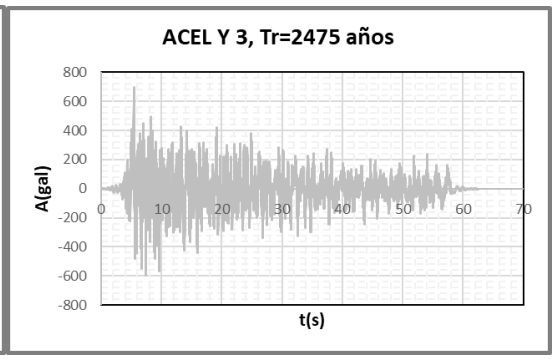
ACEL Y 3, Tr=2475 años
A(gal)
t(s)

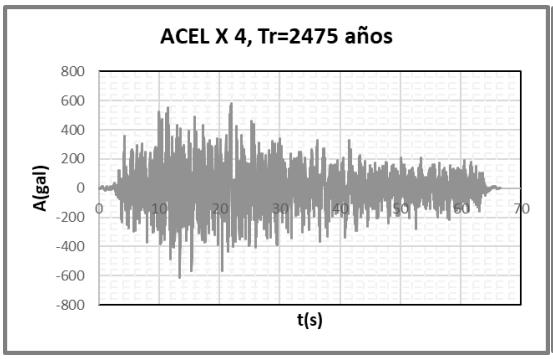
ACEL X 4, Tr=2475 años
A(gal)
t(s)

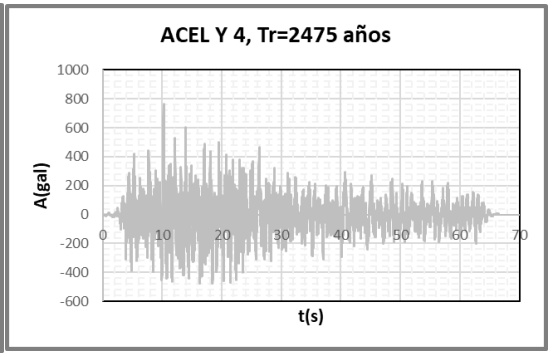
ACEL Y 4, Tr=2475 años
A(gal)
t(s)

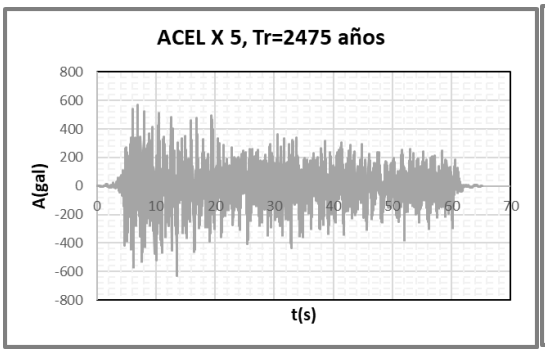
ACEL X 5, Tr=2475 años
A(gal)
t(s)

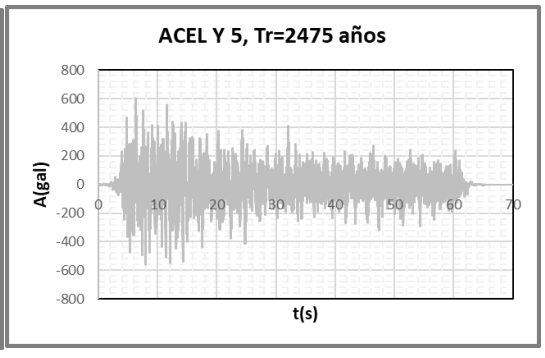
ACEL Y 5, Tr=2475 años
A(gal)
t(s)

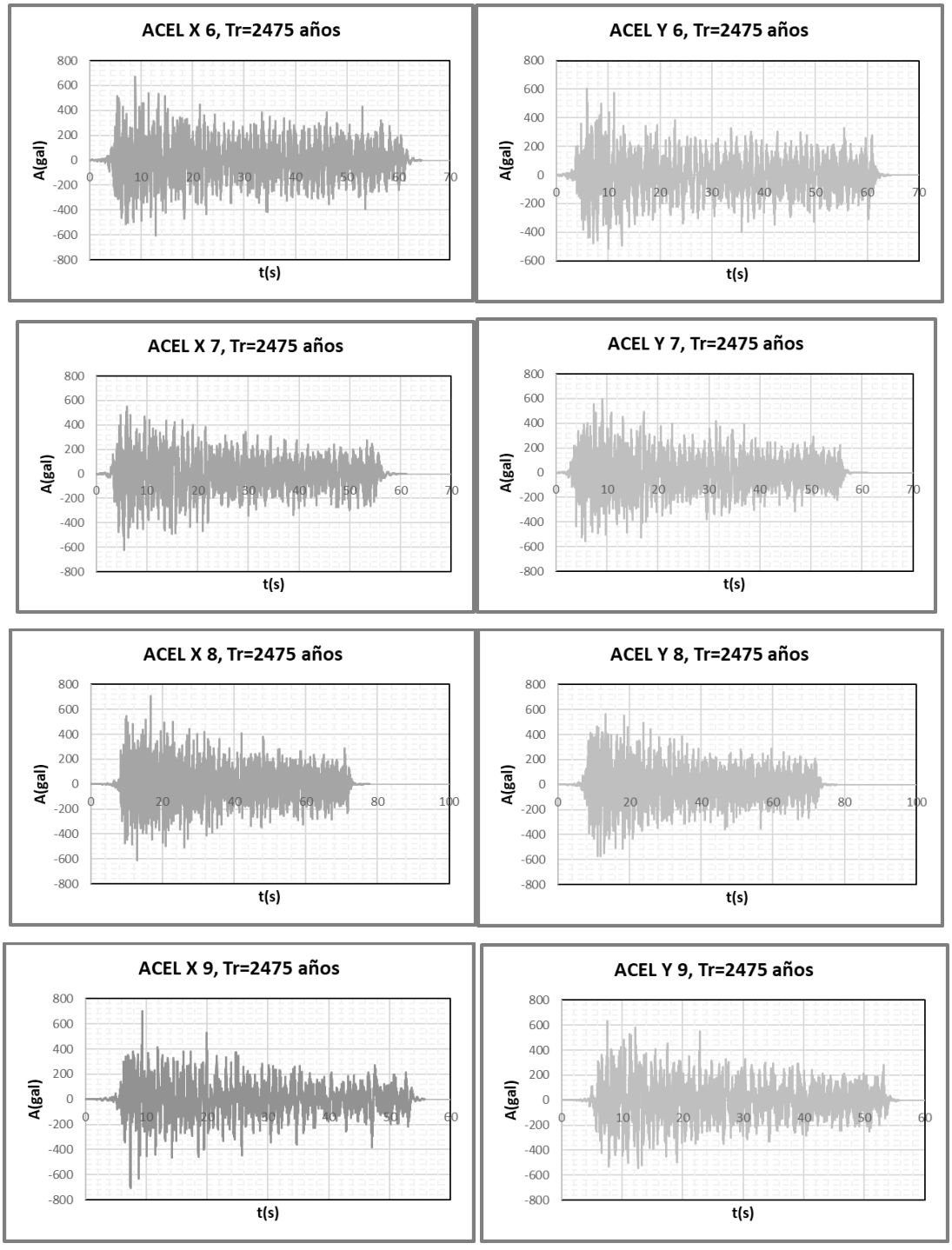
ACEL X 6, Tr=2475 años
ACEL Y 6, Tr=2475 años
ACEL X 7, Tr=2475 años
ACEL Y 7, Tr=2475 años
ACEL X 8, Tr=2475 años
ACEL Y 8, Tr=2475 años
ACEL X 9, Tr=2475 años
ACEL Y 9, Tr=2475 años
A(gal)
t(s)

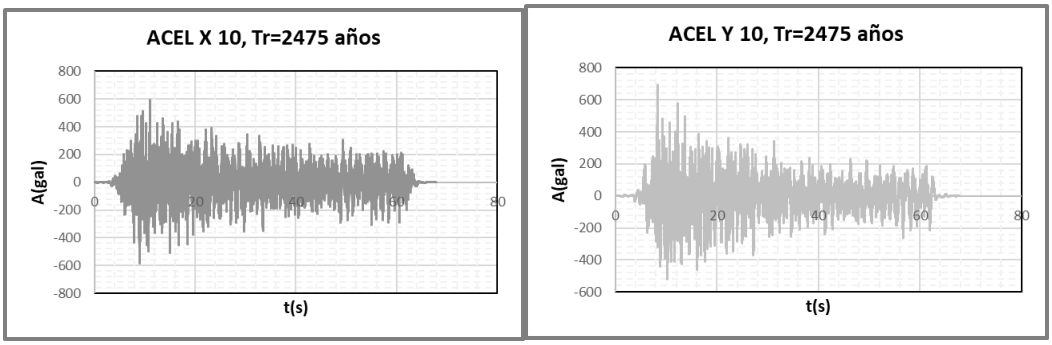

Figure 5. 10 All seismic signal

Figure 5.11 shows the response spectra to the acceleration of the matched seismic signals (in grey), their average spectrum (in red), and their envelope (in green).

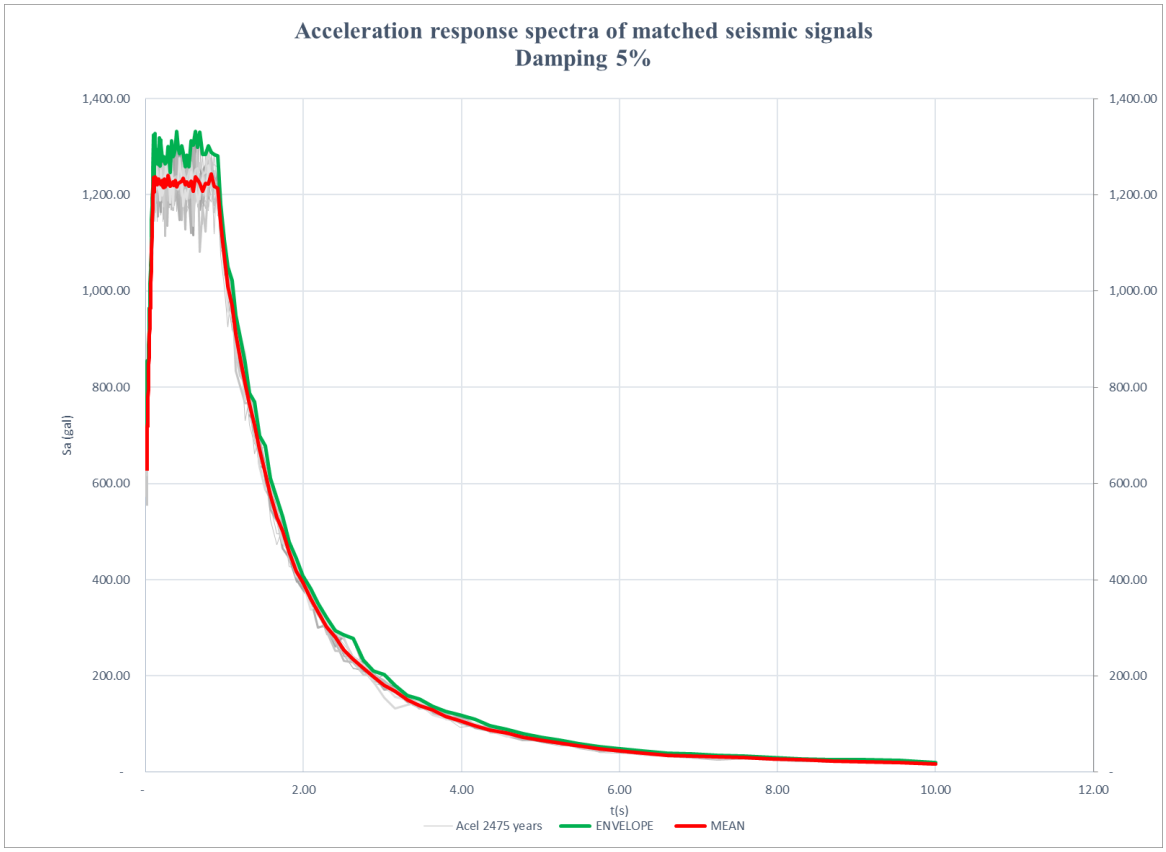

Figure 5. 11 Acceleration response spectra of matched seismic signals (Damping 5%)

5.4 Modelling assumptions for the analyses

5.4.1 Identified Damping Ratios

The damping ratios for the fundamental mode were initially studied and analyzed. Figure 5.12 shows the damping ratios identified for the first mode and for both directions of each building, and its variation with the height of the building. It can be seen that, as noted earlier by other researchers (Suda et al. 1996; Smith and Willford 2007; Bernal et al. 2015) the damping coefficient decreases as the height of the building increases. Unlike the first two studies, which mainly included damping ratios from buildings subject to wind and other low amplitude vibrations, the study by Bernal et al. (2015) is based entirely on instrumented buildings subjected to seismic load. This study significantly expands Bernal's study for tall buildings by including almost three times more buildings with more than 20 floors. Except for one point (a building in one direction), all damping ratios are obtained for buildings taller than 150 m have values lower than 2.5%, that is the damping value commonly recommended for seismic design of tall buildings in the United States (LATBSDC 2006; TBI 2010). The resulting coefficients can be seen in Table 5.5. Figure 5.12 also compares the data with damping recommendations from four different studies: Satake et al. (2003), Friz et al. (2009), PEER/ATC-72- (2010) and Bernal et al. (2015).

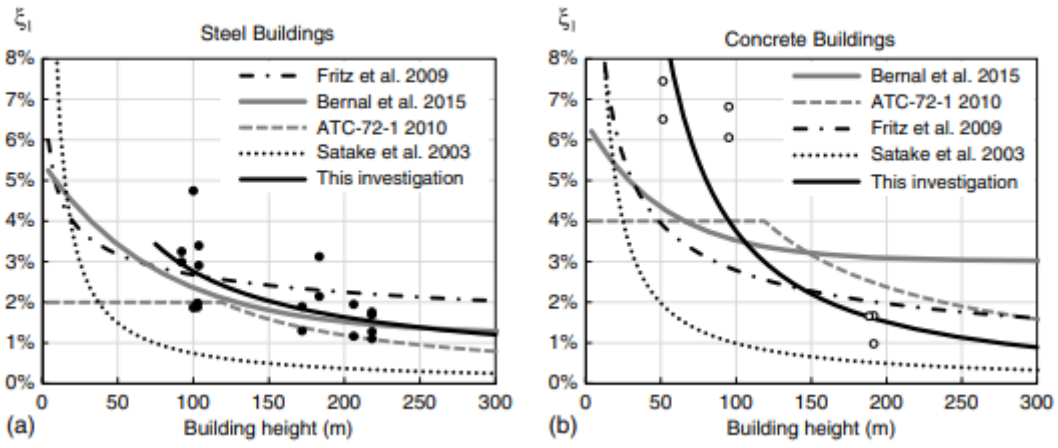

Figure 5. 12 Identified damping ratios for the fundamental mode versus building height, compared to some proposed recommendations: (a) steel buildings (b) reinforced concrete buildings;

Material	A	B	R^2	Function form
Steel	0.90	−0.76	0.45	$\xi_1 = A \cdot H^B$
Concrete	15.60	−1.31	0.81	

Table 5. 5 Coefficients for Power Regression

Care should be taken when comparing these regressions because they were calculated from damping ratios that were collected from different load conditions, using different methods and system identification assumptions. However, they all show a similar downward trend with height. For steel buildings [Figure 5.12 (a)], it can be seen that the Bernal curve agrees with the full height data. The equation proposed by Satake et al. (2003) underestimates the damping ratios inferred in this study. This is probably due to the fact that most of the data used by Satake is based on vibrations with very small amplitudes. For buildings over 150 m, the suggested equation of Fritz et al. (2009) slightly overstates the data. For concrete buildings [Figure 5.12(b)] the data are very scarce. However, it is worrying that, with the exception of Satake et al. (2003), all recommendations overestimate the data for buildings over 150 m high. The constant value of 2%, recommended in the PEER performance-based guidelines, seems to be high even for buildings taller than 180 m. Damping values with ratios below 2%, deduced from this survey, are consistent with those reported by Smith and Willford (2007) or by Spence and Karem (2013).

Paseo de Gracia has a height of 222,60m, so going to calculate the expected damping with the formula defined in Table 5.5 using the coefficients provided for concrete buildings we get:

$$\xi_1 = A * H^B = 15{,}60 * 222{,}60^{-1{,}31} = 0{,}013 = 1{,}3\%$$

This results in 1.3% damping. Consequently the spectrum of response to the acceleration of seismic signals will have the course defined in figure 5.13.

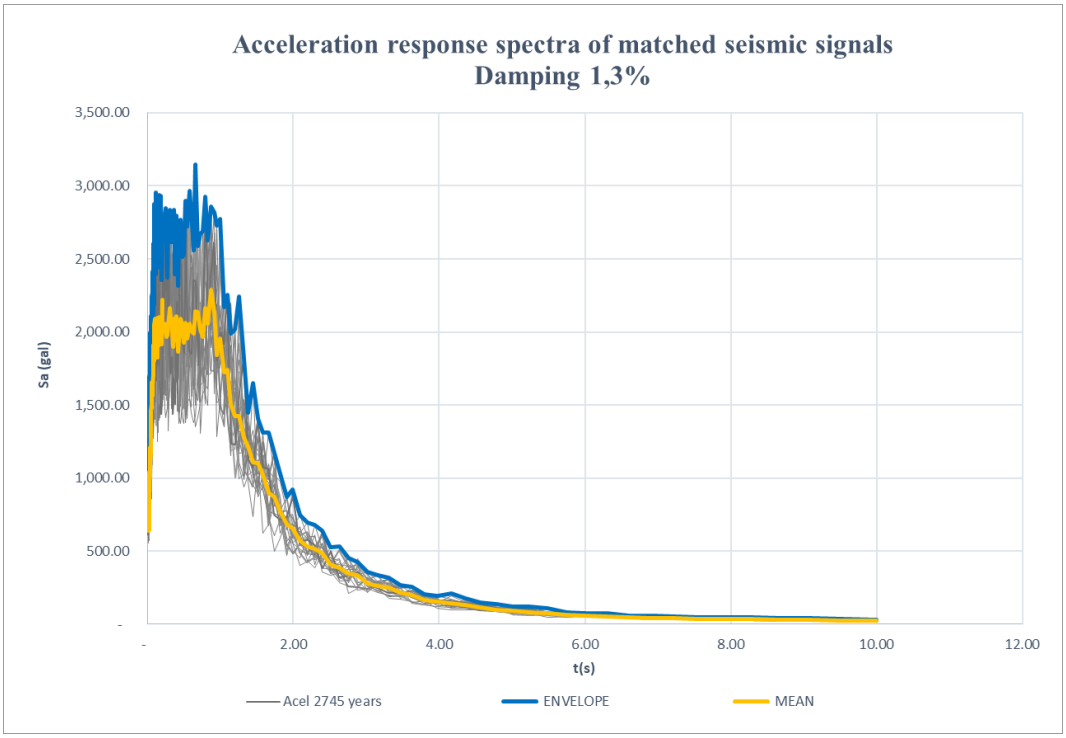

Figure 5. 13 Acceleration response spectra of matched seismic signals Damping 1,3%

Figure 5.14 shows a comparison of the seismic response spectrum for all signals with a different applied damping.

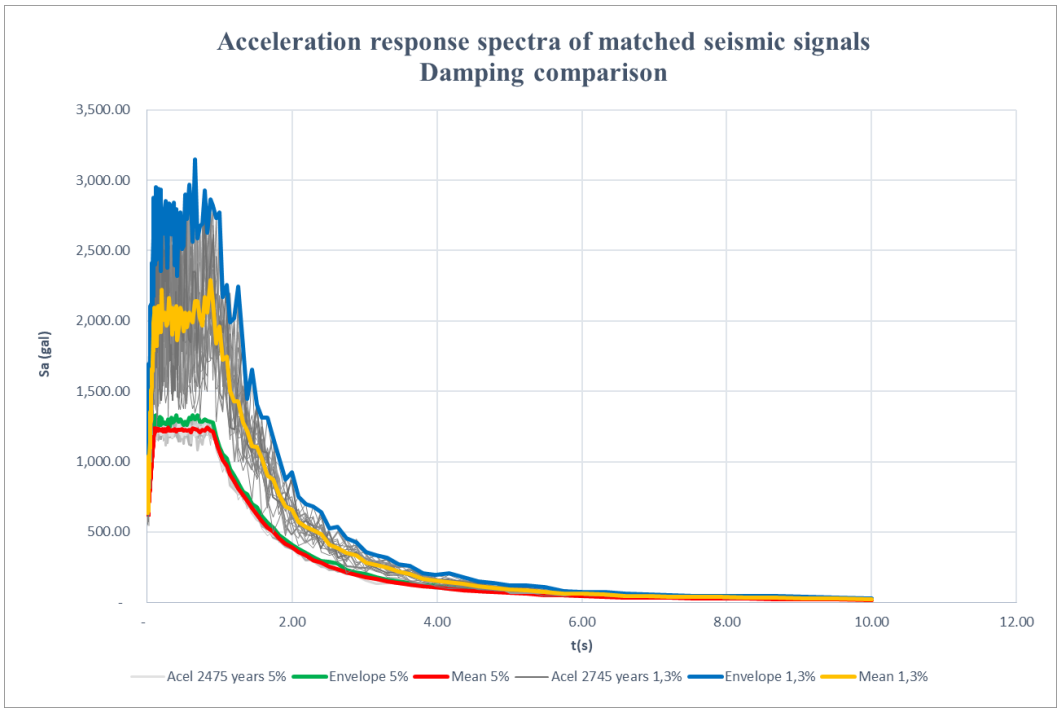

Figure 5. 14 Acceleration response spectra of matched seismic signals

5.4.2 Reinforced concrete stiffness values

This paragraph describes the modelling hypotheses formulated for the analysis of the bare frame structure and the structure equipped with a system with Outrigger plus SLB heatsinks. The approach used is PBSD, which suggests to reduce the properties of the section to take into account the cracking of the concrete and the damage to the structural elements through property modifiers, whose values are defined according to the *"TBI – Guidelines for Performance-Based Seismic Design of Tall Buildings"* in table 5.6.

Component	Service-Level Linear Models			MCE$_R$-Level Nonlinear Models		
	Axial	Flexural	Shear	Axial	Flexural	Shear
Structural walls[1] (in-plane)	$1.0E_cA_g$	$0.75E_cI_g$	$0.4E_cA_g$	$1.0E_cA_g$	$0.35E_cI_g$	$0.2E_cA_g$
Structural walls (out-of-plane)	--	$0.25E_cI_g$	--	--	$0.25E_cI_g$	--
Basement walls (in-plane)	$1.0E_cA_g$	$1.0E_cI_g$	$0.4E_cA_g$	$1.0E_cA_g$	$0.8E_cI_g$	$0.2E_cA_g$
Basement walls (out-of-plane)	--	$0.25E_cI_g$	--	--	$0.25E_cI_g$	--
Coupling beams with conventional or diagonal reinforcement	$1.0E_cA_g$	$0.07\left(\frac{\ell}{h}\right)E_cI_g \le 0.3E_cI_g$	$0.4E_cA_g$	$1.0E_cA_g$	$0.07\left(\frac{\ell}{h}\right)E_cI_g \le 0.3E_cI_g$	$0.4E_cA_g$
Composite steel / reinforced concrete coupling beams	$1.0(EA)_{trans}$	$0.07\left(\frac{\ell}{h}\right)(EI)_{trans}$	$1.0E_sA_{sw}$	$1.0(EA)_{trans}$	$0.07\left(\frac{\ell}{h}\right)(EI)_{trans}$	$1.0E_sA_{sw}$
Non-PT transfer diaphragms (in-plane only)[3]	$0.5E_cA_g$	$0.5E_cI_g$	$0.4\ E_cA_g$	$0.25E_cA_g$	$0.25E_cI_g$	$0.1E_cA_g$
PT transfer diaphragms (in-plane only)[3]	$0.8E_cA_g$	$0.8E_cI_g$	$0.4E_cA_g$	$0.5E_cA_g$	$0.5\ E_cI_g$	$0.2E_cA_g$
Beams	$1.0E_cA_g$	$0.5E_cI_g$	$0.4E_cA_g$	$1.0E_cA_g$	$0.3E_cI_g$	$0.4E_cA_g$
Columns	$1.0E_cA_g$	$0.7\ E_cI_g$	$0.4E_cA_g$	$1.0E_cA_g$	$0.7\ E_cI_g$	$0.4E_cA_g$
Mat (in-plane)	$0.8E_cA_g$	$0.8E_cI_g$	$0.8E_cA_g$	$0.5E_cA_g$	$0.5\ E_cI_g$	$0.5E_cA_g$
Mat[4] (out-of-plane)	--	$0.8E_cI_g$	--	--	$0.5E_cI_g$	--

Table 5. 6 Reinforced concrete effective stiffness values

This means that for each structure two different structural models must be made, one for linear analysis and one for non-linear analysis.

5.4.3 Hilber-Hughes-Taylor alfametod

The results of the analysis are extremely sensitive to the size of the time step, Therefore it is important to perform direct integration analysis with decreasing time step sizes until the step size is small enough to no longer be affected by the results. A

variety of common methods are available to perform direct integration chronological analysis, but it is commonly recommended to use the *"Hilber-Hughes-Taylor alfa"* (HHT) method. This method uses a single parameter called alpha that may require values between 0 and -1/3. The *"Hilber-Hughes-Taylor alfa"* method was used to perform direct integration chronological analysis using alpha = -1/3.

5.4.4 Plastic hinge modelling approach

Structures are not normally designed to remain in the elastic field under horizontal forces induced by the earthquake. As a result of a consistent application of horizontal load, they are damaged and respond outside the elastic regime. With reference to Figure 5.15, imagine to apply in increments (or decrements) the horizontal force applied on a structure, proceed by step. This curve, known as the Force-Shift diagram, if we monitor the force at the foot (overall cut) and the displacement of a summit point (control point) takes the common name of Capacity curve. In the first steps of application, of this force, the structure, remains in the elastic field, the slope of this first stretch is defined as initial stiffness or elastic stiffness. Such rigidity is that which occurs in the absence of damage. By increasing the external forces, some elements begin to stretch, the first yield is reached. The stiffness, that is, the slope of this curve, begins to be reduced, although it remains a hardening (displacements increase, also increasing the magnitude of the forces applied).

Continuing to increase, you get to a level of damage, for which, the curve assumes a pseudo-horizontal tangency, you are in other words reached the maximum possible action, that is, the maximum strength resistance. It is still pushing, but by definition, having reached the maximum possible action, the external forces begin to shrink. The shift increases. The focus here is on this shift. You will come to a certain point where you reach the deformation limits. The summit displacement of the structure, caused the achievement, in one or more membranes of the same of displacements and/or rotations limit. These limit strains are called ductility limits. These membranes fail, local collapses or local ruptures occur, one enters that phase known as loss of resistance. The overall resistance to horizontal forces is now much reduced, but the structure is still capable of carrying vertical loads. It continues to push, with an even lower force, until the actual collapse.

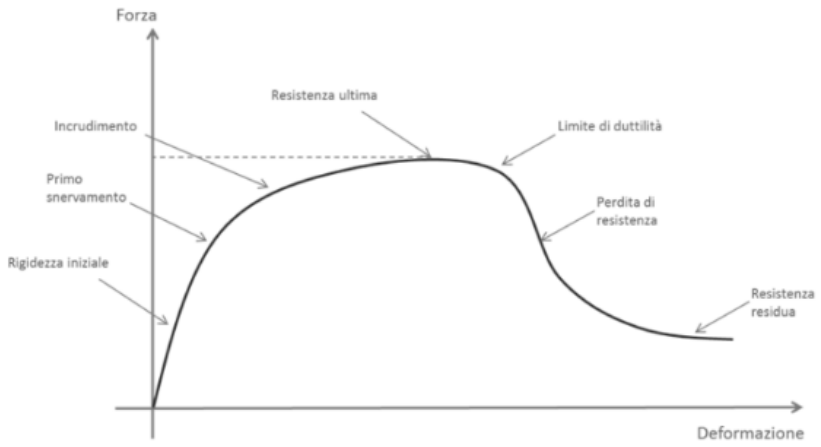

Figure 5. 15 Force displacement curve, capacity curve

The FEM model of the structure must contain all the constitutive laws of the members in order to keep track of the state of deformation and damage of the same. Inside the structure there will be plastic hinges in which you will control the deformation, for all ductile mechanisms and plastic hinges in which you will control the force for fragile ones.

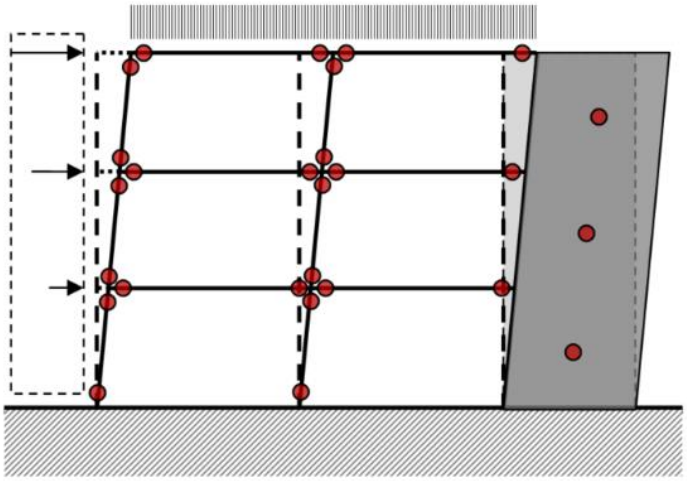

Figure 5. 16 Possible formations of plastic hinge

he possible positions normally correspond to the ends of each structural element as shown in Figure 5.16. Assuming a shear type behavior for the frame, one can imagine that they are the beginning and end of each beam and column. Also for the septa it is possible to reason in a similar way, assuming the formation of a plastic hinge at the base of the same, deformation of pure shelf, or, with the hypothesis of possible structural interaction, extending this control to the whole wall.

The red circles show the potential position of inelastic actions in which structural damage is expected, so in the model the hinges with concentrated plasticity are placed in those positions. Each plastic hinge is shaped like a discrete point hinge. All plastic deformations, be it displacement or rotation, occur within the pivot point. For each degree of freedom of force or momentum, a force-displacement (moment-rotation) curve must be defined which gives the yield strength and plastic deformation after yield strength. For the seismic evaluation based on the performance of the components, there are different levels of performance (Immediate Occupancy, Life Safety and Collapse Prevention) are defined and marked on the non-linear force-strain relationships assigned to the plastic hinges.

This is done through a curve with values represented in five points, A-B-C-D-E, which are normally called plastic hinge model parameters, they represent the real input data of the plastic hinge: they fix the behavioral law (backbone curves) as shown in Figure 5.17.

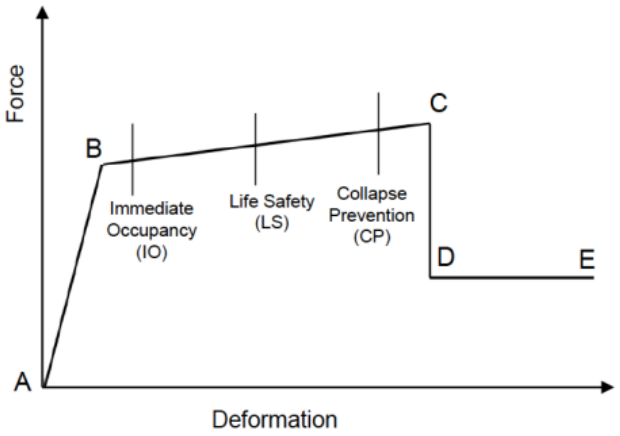

Figure 5. 17 Force vs. Deformation curve for the plastic hinge definition – Acceptance

n the Immediate Occupancy (IO) level, only a small amount of inelastic behavior is allowed, so elastic analysis should be sufficient. In the Life Safety (LS) level, a greater amount of inelastic behavior is allowed, so it is necessary to use an inelastic model of the structure, which should consider the subsidence and the ultimate resistances of the structural components. Hysteresis cycles can be expected to be fairly simple at this level of deformation, with a modest degradation of stiffness and strength. In Collapse Prevention (CP), the permissible amount of inelastic behavior is even greater than the LS level, so in this case it is reasonable to expect more complex hysteresis cycles with substantial degradation in stiffness and strength.

Referring to figure 5.17:

• Point A is always the origin.

• Point B represents failure. No deformation occurs in the hinge up to point B. The displacement at this point will be subtracted from the deformations at points C, D, E to consider only the plastic deformation exhibited by the hinge.

• Point C is the ultimate capacity for pushover analysis.

• Point D represents a residual force for pushover analysis.

• Point E represents the total collapse of the hinge.

Before reaching point B, all deformations are linear and occur in the frame element and not in the hinge. The plastic deformation beyond the point B also occurs in the

hinge in addition to the elastic deformation that occurs in the frame element. One way to obtain such properties, when experimental results are not available, is to refer to guidelines, such as ASCE 41, in which modeling parameters are prescribed.

ASCE 41 is a standard for the seismic rehabilitation of existing buildings, but could also be used in the design of new ones. Among many other things, ASCE 41 provides modeling guidelines for inelastic analysis and performance evaluation of different structural components.

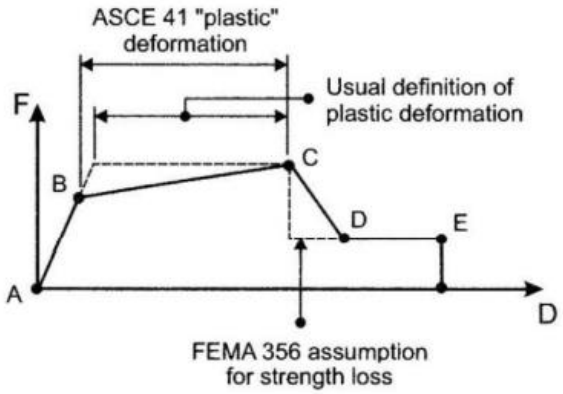

Figure 5. 18 ASCE 41 force-deformation relationship

In addition to behavioural parameters, rotational limits of acceptance are defined. At each limit state: limited damage, severe damage and collapse, limit rotations are associated, after which the relative limit states are exceeded. These values depend on the same discriminators and are automatically deductible as the behavioural parameters. To better understand these aspects, we report the definition tables taken in accordance with ASCE 41:2010 which defines the modeling parameters and numerical acceptance criteria for reinforced concrete beams and pillars.

Table 6-7 Modeling Parameters and Numerical Acceptance Criteria for Nonlinear Procedures—Reinforced Concrete Beams

			Modeling Parameters[3]			Acceptance Criteria[3]				
						Plastic Rotation Angle, radians				
						Performance Level				
			Plastic Rotation Angle, radians		Residual Strength Ratio		Component Type			
							Primary		Secondary	
Conditions			a	b	c	IO	LS	CP	LS	CP
i. Beams controlled by flexure[1]										
$\frac{\rho-\rho'}{\rho_{bal}}$	Trans. Reinf.[2]	$\frac{V}{b_w d \sqrt{f'_c}}$								
≤ 0.0	C	≤ 3	0.025	0.05	0.2	0.010	0.02	0.025	0.02	0.05
≤ 0.0	C	≥ 6	0.02	0.04	0.2	0.005	0.01	0.02	0.02	0.04
≥ 0.5	C	≤ 3	0.02	0.03	0.2	0.005	0.01	0.02	0.02	0.03
≥ 0.5	C	≥ 6	0.015	0.02	0.2	0.005	0.005	0.015	0.015	0.02
≤ 0.0	NC	≤ 3	0.02	0.03	0.2	0.005	0.01	0.02	0.02	0.03
≤ 0.0	NC	≥ 6	0.01	0.015	0.2	0.0015	0.005	0.01	0.01	0.015
≥ 0.5	NC	≤ 3	0.01	0.015	0.2	0.005	0.01	0.01	0.01	0.015
≥ 0.5	NC	≥ 6	0.005	0.01	0.2	0.0015	0.005	0.005	0.005	0.01
ii. Beams controlled by shear[1]										
Stirrup spacing ≤ d/2			0.0030	0.02	0.2	0.0015	0.0020	0.0030	0.01	0.02
Stirrup spacing > d/2			0.0030	0.01	0.2	0.0015	0.0020	0.0030	0.005	0.01
iii. Beams controlled by inadequate development or splicing along the span[1]										
Stirrup spacing ≤ d/2			0.0030	0.02	0.0	0.0015	0.0020	0.0030	0.01	0.02
Stirrup spacing > d/2			0.0030	0.01	0.0	0.0015	0.0020	0.0030	0.005	0.01
iv. Beams controlled by inadequate embedment into beam-column joint[1]										
			0.015	0.03	0.2	0.01	0.01	0.015	0.02	0.03

1. When more than one of the conditions i, ii, iii, and iv occurs for a given component, use the minimum appropriate numerical value from the table.
2. "C" and "NC" are abbreviations for conforming and nonconforming transverse reinforcement. A component is conforming if, within the flexural plastic hinge region, hoops are spaced at ≤ d/3, and if, for components of moderate and high ductility demand, the strength provided by the hoops (V_s) is at least three-fourths of the design shear. Otherwise, the component is considered nonconforming.
3. Linear interpolation between values listed in the table shall be permitted.

Table 5. 7 Behavior and verification parameters of plastic hinges of reinforced concrete beams

Table 6-8 Modeling Parameters and Numerical Acceptance Criteria for Nonlinear Procedures—Reinforced Concrete Columns

			Modeling Parameters[4]			Acceptance Criteria[4]				
						Plastic Rotation Angle, radians				
						Performance Level				
			Plastic Rotation Angle, radians		Residual Strength Ratio		Component Type			
							Primary		Secondary	
Conditions			a	b	c	IO	LS	CP	LS	CP
i. Columns controlled by flexure[1]										
$\frac{P}{A_g f'_c}$	Trans. Reinf.[2]	$\frac{V}{b_w d \sqrt{f'_c}}$								
≤ 0.1	C	≤ 3	0.02	0.03	0.2	0.005	0.015	0.02	0.02	0.03
≤ 0.1	C	≥ 6	0.016	0.024	0.2	0.005	0.012	0.016	0.016	0.024
≥ 0.4	C	≤ 3	0.015	0.025	0.2	0.003	0.012	0.015	0.018	0.025
≥ 0.4	C	≥ 6	0.012	0.02	0.2	0.003	0.01	0.012	0.013	0.02
≤ 0.1	NC	≤ 3	0.006	0.015	0.2	0.005	0.005	0.006	0.01	0.015
≤ 0.1	NC	≥ 6	0.005	0.012	0.2	0.005	0.004	0.005	0.008	0.012
≥ 0.4	NC	≤ 3	0.003	0.01	0.2	0.002	0.002	0.003	0.006	0.01
≥ 0.4	NC	≥ 6	0.002	0.008	0.2	0.002	0.002	0.002	0.005	0.008
ii. Columns controlled by shear[1, 3]										
All cases[5]			—	—	—	—	—	—	.0030	.0040
iii. Columns controlled by inadequate development or splicing along the clear height[1,3]										
Hoop spacing ≤ d/2			0.01	0.02	0.4	0.005	0.005	0.01	0.01	0.02
Hoop spacing > d/2			0.0	0.01	0.2	0.0	0.0	0.0	0.005	0.01
iv. Columns with axial loads exceeding $0.70P_o$[1, 3]										
Conforming hoops over the entire length			0.015	0.025	0.02	0.0	0.005	0.01	0.01	0.02
All other cases			0.0	0.0	0.0	0.0	0.0	0.0	0.0	0.0

1. When more than one of the conditions i, ii, iii, and iv occurs for a given component, use the minimum appropriate numerical value from the table.
2. "C" and "NC" are abbreviations for conforming and nonconforming transverse reinforcement. A component is conforming if, within the flexural plastic hinge region, hoops are spaced at ≤ d/3, and if, for components of moderate and high ductility demand, the strength provided by the hoops (V_s) is at least three-fourths of the design shear. Otherwise, the component is considered nonconforming.
3. To qualify, columns must have transverse reinforcement consisting of hoops. Otherwise, actions shall be treated as force-controlled.
4. Linear interpolation between values listed in the table shall be permitted.
5. For columns controlled by shear, see Section 6.5.2.4.2 for acceptance criteria.

Table 5. 8 Behavior and verification parameters of reinforced concrete columns

ETABS integrates the automatic calibration procedure of plastic hinges based on these tables. For the concrete beams were generated hinges in plastic type M2 or M3, for the concrete columns were generated in plastic hinges type P-M2 or P-M3, as it is a two-dimensional case. To assign the plastic hinges it is necessary to define the relative distance that is a defined point where the plastic hinge focuses. This value is the ratio of the height of the plastic hinge to the total height of the column. The length of the plastic hinge was calculated, according to ACI 318-14, as $L_{col} = \max\{h_{col}, \frac{L_{col}}{6}, 450mm\}$. The parameters of the hinges with respect to the reference table, the degree of freedom and the condition of failure were then set.

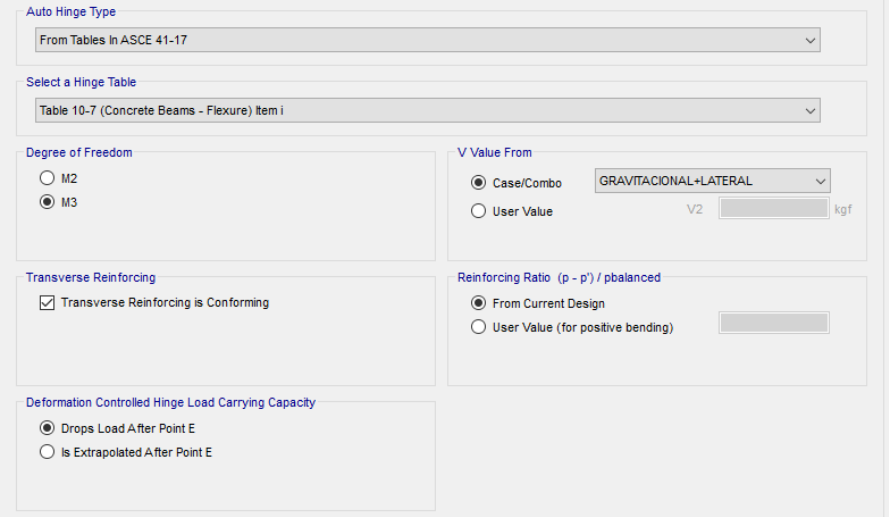

Figure 5. 19 Plastic Hinge proprieties setting of beam - ETABS

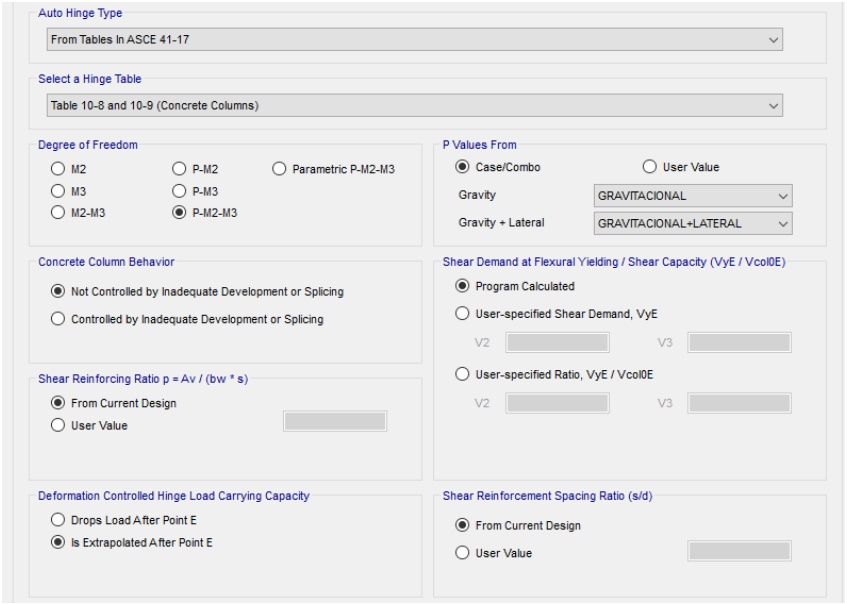

Figure 5. 20 Plastic Hinge proprieties setting of columns- ETABS

Fibre plastic hinges have been defined for reinforced concrete walls. In ETABS the treatment of non-linear walls is managed by means of a fiber modelling represented in Figure 5.21. The wall, composed of a portion of cls confined at the end of the same, of a portion of cls not confined and of the reinforcements is automatically schematized by the program, passing the reinforcements inserted in the wall, using three layers of fibers.

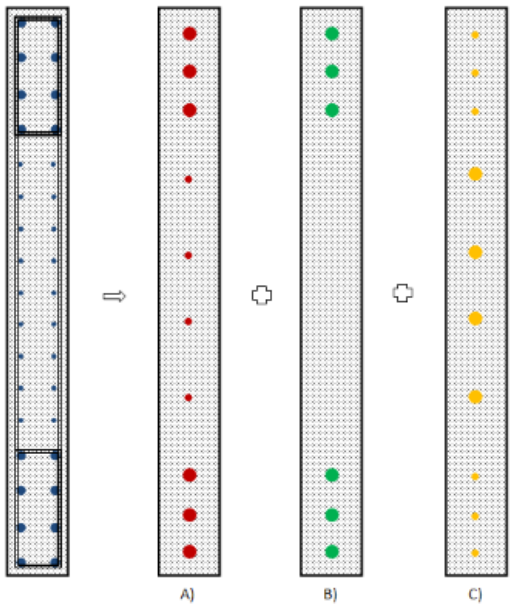

Figure 5. 21 Automatic fiber tracking

The first layer, indicated with A in the figure, represents the fibers of the reinforcements inserted in the wall. The reinforcements are bundled and then divided into a number of fibers. The area corresponding to the individual fibers is the sum of the reinforcements efferent to it, the constitutive law is that of the material used. The second layer, the letter B, represents the confined cls. Present only in the case of the confined area at the end of the wall, normally extended the 20% of the length of the wall, but in any case since it is required in the definition and therefore modifiable, also in this case the area of the individual fibers of cls, represents the efferent area of cls. The last layer, the letter C, represents the unconfined cls: the one outside the brackets in the end zone and the remaining part of cls inside the wall. All required geometric and reinforcement information is passed through a parametric window, the fibers are then drawn automatically and can be displayed.

Fiber plastic hinges are PMM interaction plastic hinges, that is, they work simultaneously in interaction between normal stress and bending moments, whether simple or deviated. They are based on the assumption that the moment-rotation law can be determined by treating the section as an aggregate of fibers.

With reference to Figure 5.22, any section in c.a., is automatically broken down into an aggregate of fibres of cls, each of which having an area equal to its due portion, position of its centre of gravity and with the constitutive law of unconfined or

confined concrete using the common definition and parameterisation of the Mander model, which takes into account the reinforcement and confinement induced by it, and one fibre for each reinforcement, having an area equal to the armature itself and constitutive law of the material used for the armatures.

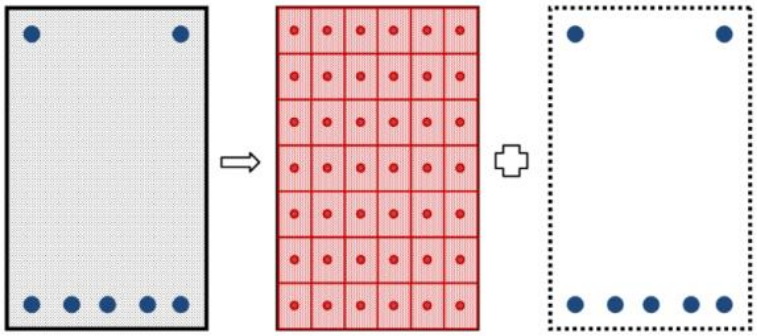

Figure 5. 22 composition of a fiber hinge

With this schematization it is possible to parameterize any section automatically, without form or reinforcement limit. The backbone is directly the moment-rotation of this aggregate of fibers and the rotation limits, used as rotational capacities of the hinge, are deductible from the state of damage of individual fibers. In this case, the acceptance criteria (IO, LS, CP) are specified directly on the stress-strain relationship of the material. We start by defining the constitutive law of the material cls base, or excluding the correction that takes into account, according to the model of Mander confinement.

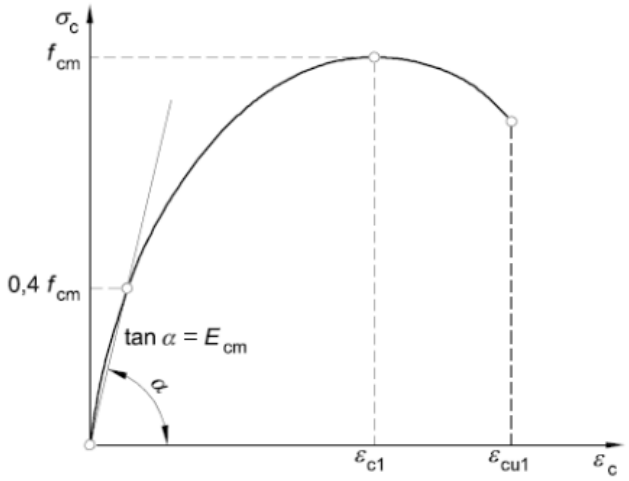

Figure 5. 23 Constitutive law of the basic material

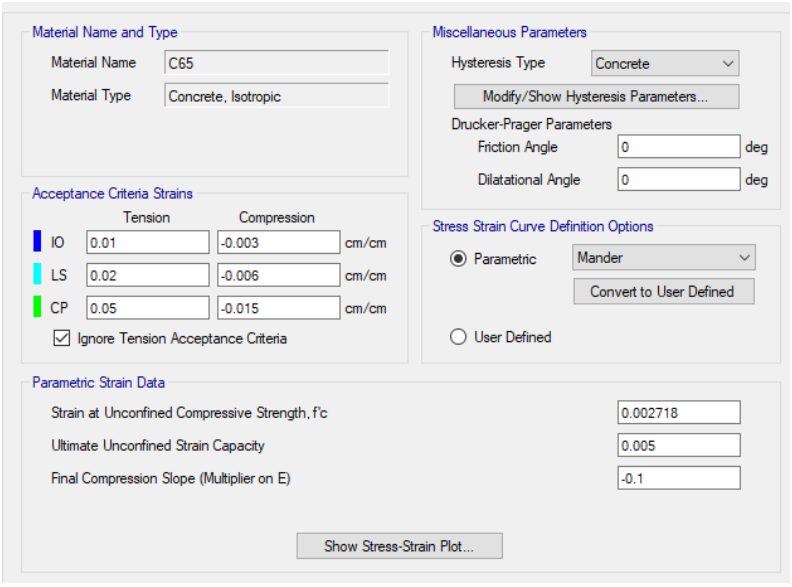

Figure 5. 24 Parameterization of the material according to the Mander model

The values of the materials used in the project are defined below with the constitutive law of the material automatically defined in ETABS:

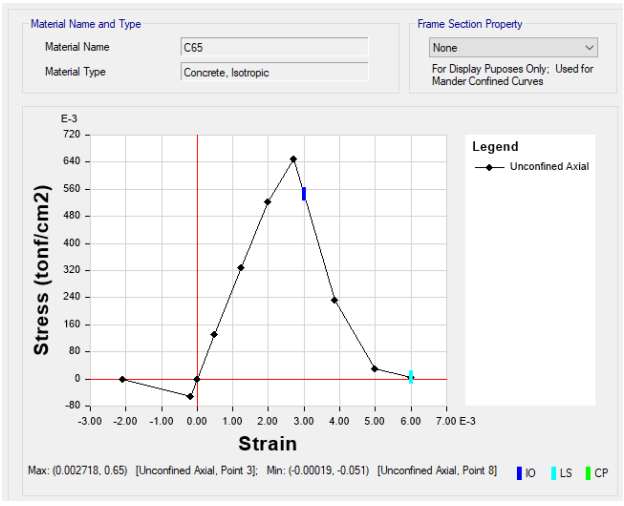

Figure 5. 25 Concrete C65 - Material stress-strain relationship

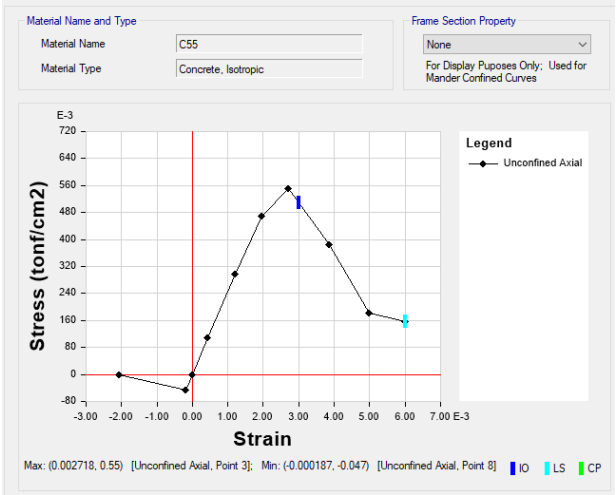

Figure 5. 26 Concrete C55 - Material stress-strain relationship

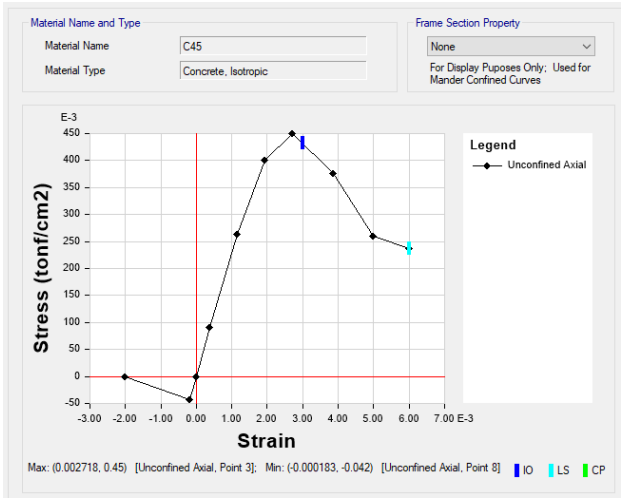

Figure 5. 27 Concrete C45 - Material stress-strain relationship

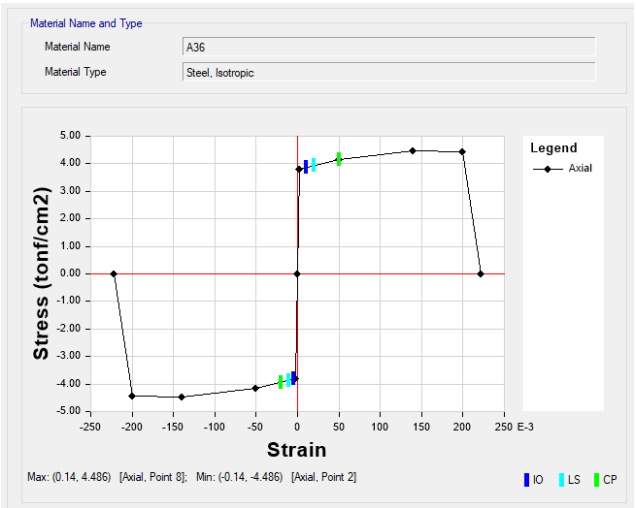

Figure 5. 28 Steel A36 - Material stress-strain relationship

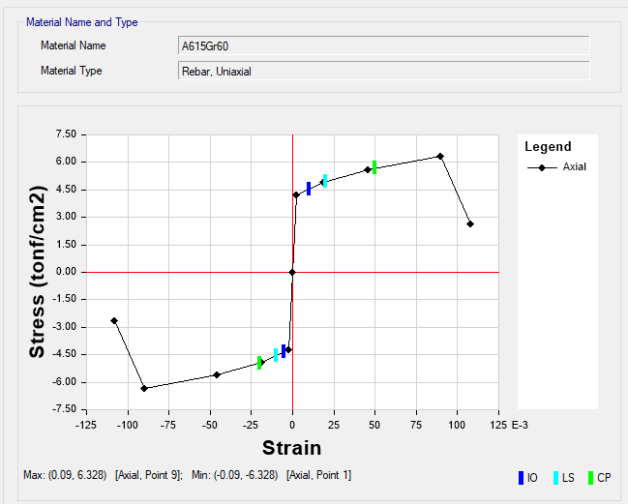

Figure 5. 29 Steel A615Gr60 - Material stress-strain relationship

The use of concrete in skyscrapers has largely increased for many reasons. First, it is much cheaper than other structural materials, such as steel, so it allows you to significantly reduce construction costs. Then, thanks to modern construction technologies, based on industrial formwork that can be moved quickly after casting concrete, it is possible to reduce construction times, also reducing the costs directly related to them. For high-rise buildings, high-strength concrete is required to reduce the size of the cross-section of vertical elements, so as to have more surface available. For this type of structures, the demand for high strength is often associated with other requirements related to mechanical and physical characteristics. For example, in the case of the Burj Khalifa Tower it was necessary to use a self compacting and self-leveling concrete with 60 MPa force pumped up to 600 m high. In this case, it is necessary to satisfy not only demands for strength, but also special needs such as workability at height. It is necessary to use high-quality, superfluidificant cements to reduce the water/cement ratio, fine materials with pozzolanic characteristics, and carefully select the particle size curve. This allows to reduce the total porosity, increasing the quality of the products of the hydration process, also obtaining a greater durability. Finally, the installation of concrete is guaranteed thanks to self-contained materials that do not require vibrations and flow easily even through very congested reinforcement configurations, without segregation phenomena.

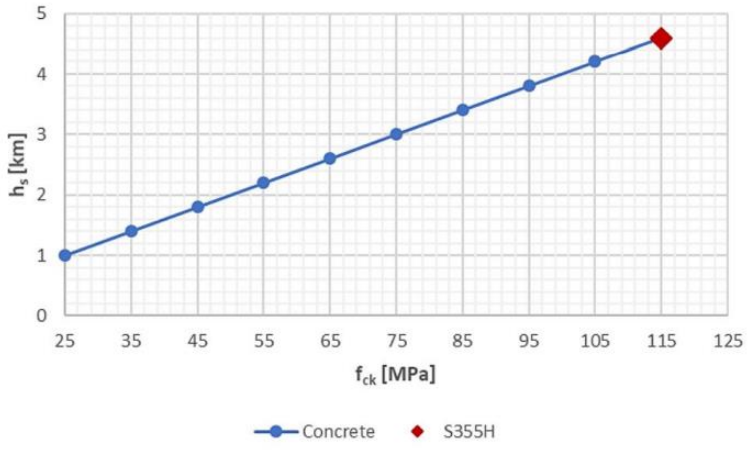

Figure 5. 30 Concrete static efficiency

For ordinary concrete (= 55 MPa) the static efficiency is almost 2.2 km, much lower than that of steel (red sign). Therefore, comparing these two materials, steel is the

only suitable for skyscrapers. On the contrary, if we consider high-strength concrete (= 90 MPa), the static yield increases up to 3.6 km, almost like the 4.5 of structural steel. Considering that the steel sections are also subject to instability phenomena and in real cases the static efficiency is never reached completely, cement materials with compressive strengths of the order of 75-80 MPa are sufficient for super high buildings, such as the Burj Khalifa in Dubai.

5.5 MODEL 1: Bare frame structure design

5.5.1 Modal analysis

The first step to follow is to define a modal analysis with the aim of studying the dynamic behavior of the bare frame structure. Table 5.9 shows the periods and the participating mass of the first three natural modes of vibration of the structure, as well as the way it presents 90% participating mass The results are obtained by considering the actual stiffness values seen in paragraph 5.4.2.

Mode	**Period**	**U_X**	**U_Y**	**R_Z**	**SumU_X**	**SumU_Y**	**SumR_Z**
[-]	sec	[-]	[-]	[-]	[-]	[-]	[-]
1	9.133	0%	66%	0%	0%	66%	0%
2	9.045	66%	0%	0%	66%	66%	0%
3	3.267	0%	0%	79%	66%	66%	79%
10	0.683	3.00%	0.00%	0.00%	91.00%	91.00%	89.00%

Table 5. 9 Modal analysis results for Bare frame structure

It is possible to observe that the first two modes are translational, while the third mode is rotational, to be precise, the first is translational along Y with 66% of participating mass, the second along X with 66% of participating mass, finally the third rotational around Z, with 79% participating mass.

Figure 5. 31 1st mode

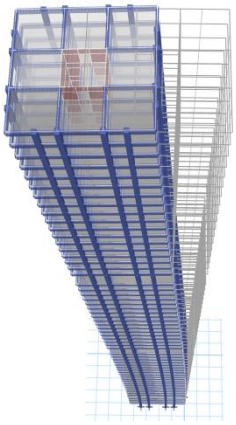

Figure 5. 32 2st mode

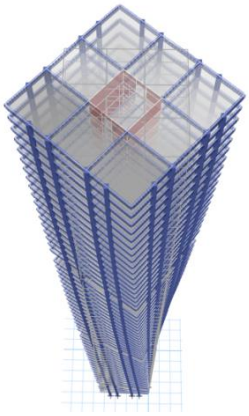

Figure 5. 33 3st mode

The fundamental period is 9.13 seconds, an acceptable value for 60 floors of a reinforced concrete building, while 90% of the participating mass ratio is achieved in all directions considering the first 10 natural modes of vibration of the structure.

5.5.2 Response spectrum analysis

The next step is to verify the structure at the Earthquake Collapse Level according to the requirements of the CFE, ie defining a limit to 0.015 as required by the standard and reported in Table 5.10.

SISTEMA ESTRUCTURAL	Q	DISTORSIÓN
Marcos dúctiles de concreto reforzado	4	0.030
	3	0.025
Marcos dúctiles de acero	4	0.030
	3	0.025
Marcos dúctiles de sección compuesta de acero y concreto reforzado	4	0.030
	3	0.020
Marcos de acero, de concreto reforzado o compuestos de ambos materiales con ductilidad intermedia	1.25	0.008
Marcos de acero, de concreto reforzado o compuestos de ambos materiales con ductilidad limitada	2	0.015
Marcos con losas planas sin muros o contravientos	2	0.015
Marcos de acero con contravientos excéntricos	4	0.020
Marcos de acero, de concreto reforzado o compuestos de ambos materiales con contravientos concéntricos	3	0.015
Muros combinados con marcos dúctiles de concreto reforzado, o de placa de acero, o compuestos con los dos materiales o muros de madera contrachapada	3	0.015
Muros de carga de mampostería confinada de piezas macizas con refuerzo horizontal o malla	2	0.008
Muros de carga de mampostería confinada de piezas macizas; mampostería de piezas huecas confinada y reforzada horizontalmente o mampostería de piezas huecas confinada y reforzada con malla	2	0.006
Muros diafragma	2	0.006
Muros de carga de mampostería combinada y confinada	2	0.004
Muros de carga de mampostería de piezas huecas con refuerzo interior, o muros de madera de duela	1.5	0.004
Muros combinados con marcos de concreto reforzado con ductilidad limitada	1.5	0.010
Muros de carga de mampostería confinada de bloques huecos de concreto	1.25	0.003
Muros de carga de mampostería que no cumplan las especificaciones para mampostería confinada ni para mampostería reforzada interiormente	1.25	0.002

Table 5. 10 Limit of interstory drift

The interstory-drift results for the collapse condition, in the X and Y direction are given in Figure 5.34.

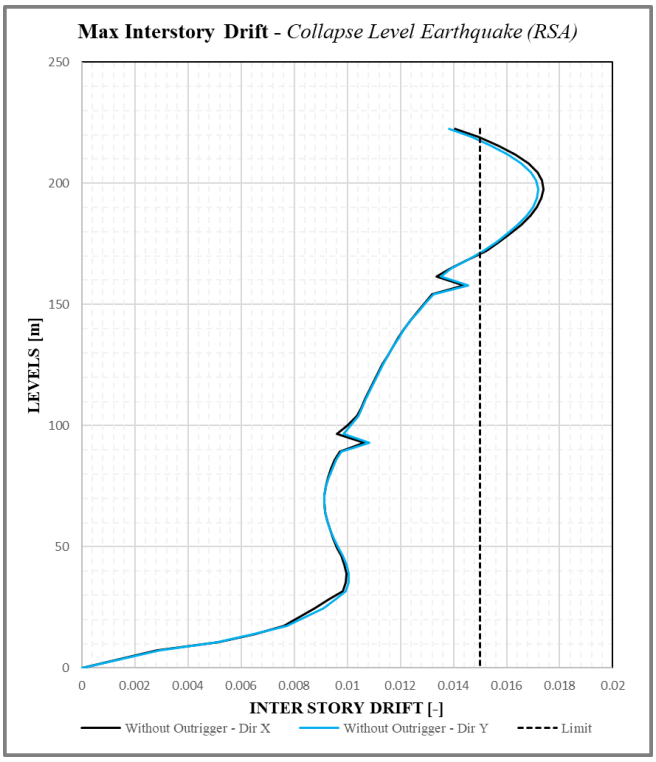

Figure 5. 34 Max Interstory Drift at Collapse Level Earthquake (RSA)

The maximum values in the X and Y direction for drift in the collapse condition are given in Table 5.11:

MAX X	DRIFT	MAX Y	DRIFT
w/o OUTRIGGER	0.017	w/o OUTRIGGER	0.017

Table 5. 11 Maximum drift values (Collapse-RSA)

The interstory-drift results are also analyzed for the condition of Service Level Earthquake that, according to the requirements of the CFE in paragraph 3.3.7 that defines: "The spectra of the operational limit state shall not exceed 0,002, except that there are no elements which are incapable of withstanding appreciable deformations, such as brick walls, or separating the main structure so that it is not damaged by its deformations. In this case, the limit will be 0.004." Below in Figure 5.35 are the values obtained for the service condition, in direction X and Y .

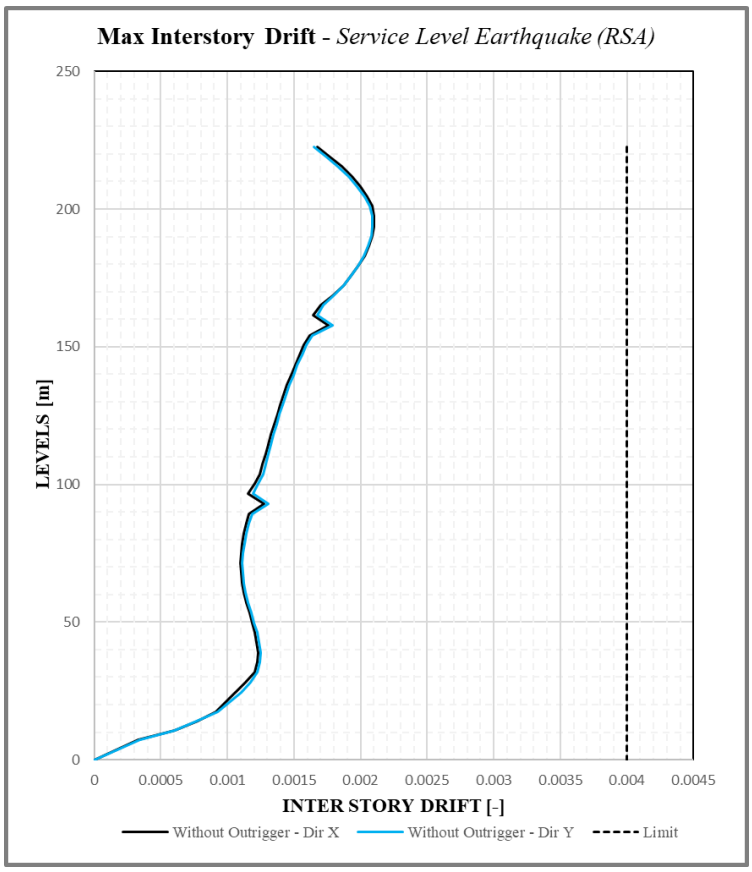

Figure 5. 35 Max Interstory Drift at Service Level Earthquake (RSA)

Table 5.12 shows the maximum values in X and Y direction for drift in Service condition:

MAX X	DRIFT	MAX Y	DRIFT

w/o OUTRIGGER	0.002	w/o OUTRIGGER	0.002

Table 5. 12 Maximum drift values (Service-RSA)

It is possible to note that with linear analysis the response in terms of drift in collapse conditions exceeds the limit defined by the legislation, while in the service condition is within the limit prescribed by the legislation; Moreover, the answer is similar in both X and Y direction. This is easily deduced because the structure is doubly symmetrical, so the structural response in both directions is the same.

The results for displacement in the collapse condition in the X and Y direction are shown in Figure 5.36.

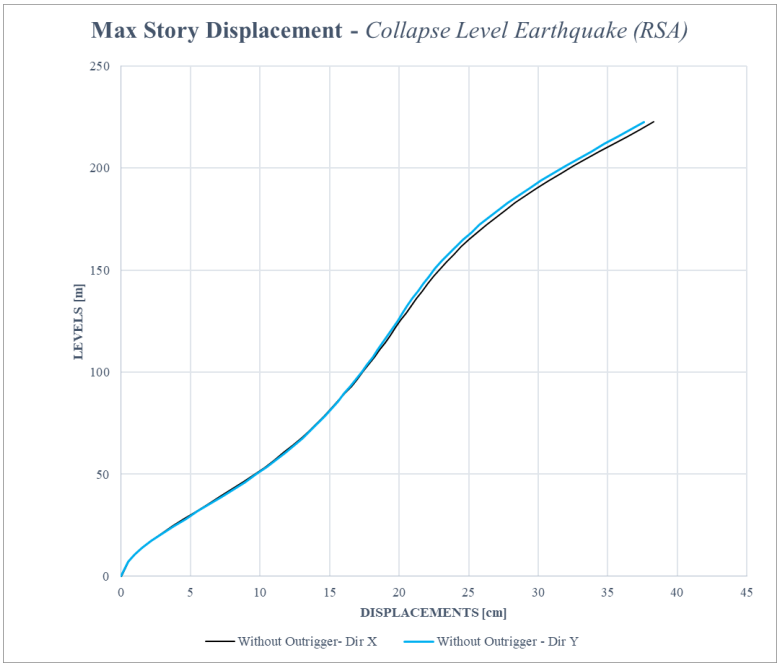

Figure 5. 36 Max Interstory Displacement at Collapse Level Earthquake (RSA)

Table 5.13 shows the maximum values in the X and Y direction for displacement in the Collapse condition:

MAX X	DISPLACEMENT	MAX Y	DISPLACEMENT
w/o OUTRIGGER	38.28cm	w/o OUTRIGGER	37.59cm

Table 5. 13 Maximum displacement values (Collapse - RSA)

The results for displacement in service condition, in X and Y direction are shown in Figure 5.37.

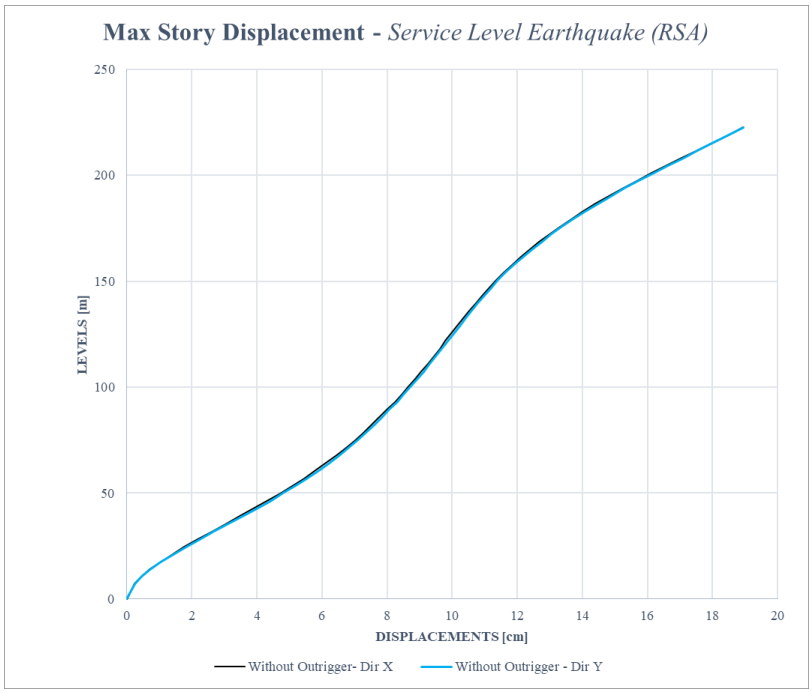

Figure 5. 37 Max Interstory Displacement at Service Level Earthquake (RSA

Table 5.14 shows the maximum values in X and Y direction for displacement in the Service condition:

MAX X	DISPLACEMENT	MAX Y	DISPLACEMENT
w/o OUTRIGGER	18.93cm	w/o OUTRIGGER	18.95cm

Table 5. 14 Maximum displacement values (Service- RSA)

The results for Shear in collapse condition, in X and Y direction are given in Figure 5.38:

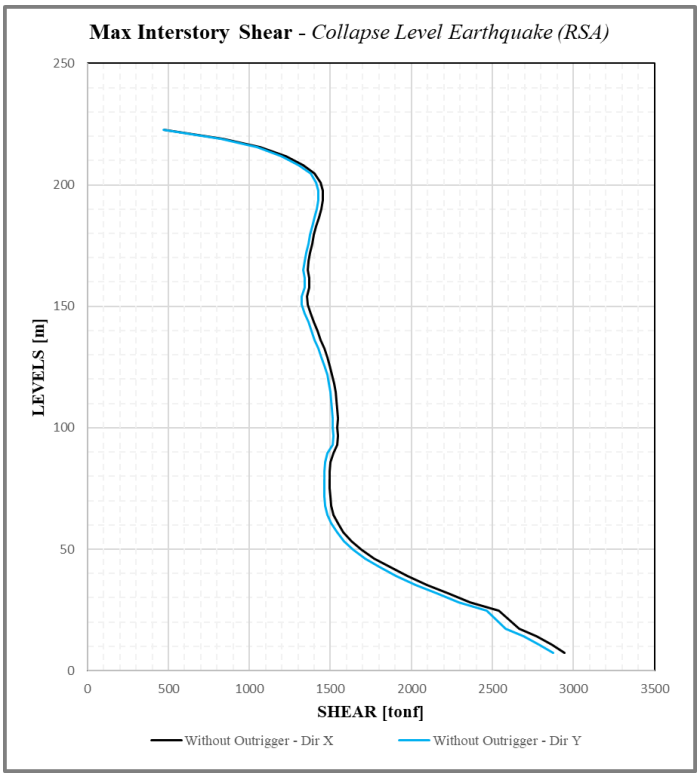

Figure 5. 38 Max Interstory Shear at Collapse Level Earthquake (RSA)

Table 5.15 shows the maximum values in the X and Y direction for the cut in the Collapse condition:

MAX X	SHEAR	MAX Y	SHEAR
w/o OUTRIGGER	2946.26tonf	w/o OUTRIGGER	2877.63tonf

Table 5. 15 Maximum shear values (Collapse - RSA)

The results for Cut in service condition, in X and Y direction are shown in Figure 5.39.

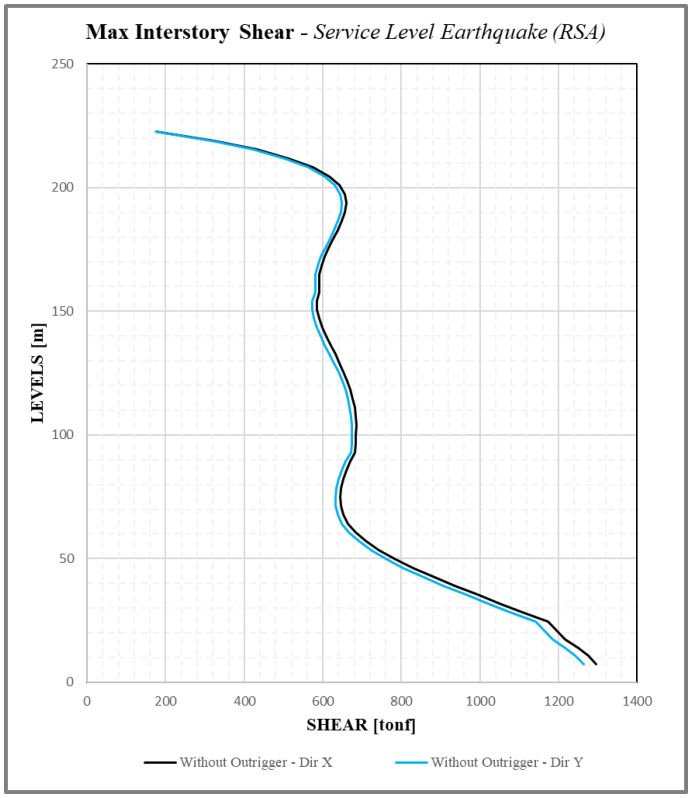

Figure 5. 39 Max Interstory Shear at Service Level Earthquake (RSA)

Table 5.16 shows the maximum values in the X and Y direction for the cut in the Service condition:

MAX X	SHEAR	MAX Y	SHEAR
w/o OUTRIGGER	1296.23tonf	w/o OUTRIGGER	1265.18tonf

Table 5. 16 Maximum shear values (Service- RSA)

5.5.3 Wind demand

In general, for the structural design of skyscrapers the demand for wind load may be more significant than the seismic demand at the earthquake service level (SLE): Therefore, the demand for wind, if it is expected to affect the structural design, must be considered in the first phase of the evaluation of the structure, as explained in the TBI - Guidelines for Performance Based Seismic Design of Tall Buildings, 2017 and in the Performance-Based Seismic Design for Tall Buildings (Golesorkhi et al., 2019). To determine the force of the wind to be applied to the structure was followed step by step the "Manual de diseño de obras civiles - diseño por viento, Mexico". Although the structure has a period and a height such as to have to carry out a study on the wind tunnel, However, we proceeded with a first dynamic analysis useful for a preliminary analysis aimed at determining the drift for the wind and useful for

comparing the plane cut of the wind against that of the earthquake. A more in-depth study, if desired, can be continued by defining this theme which, however, is not the subject of a thesis.

Figure 5.40 (a) shows interstory drift for wind, defining (according to CFE) a limit of 0.002.

Figure 5.40(b) shows the comparison of plane cuts between the seismic load in service condition and the wind loads in service condition.

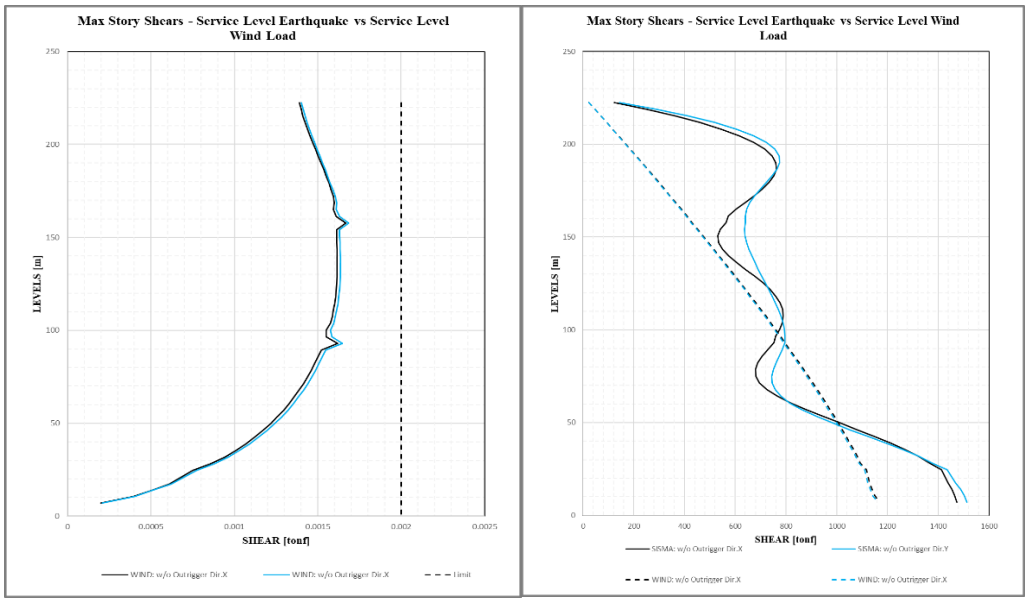

Figure 5. 40 (a) Interstory Drift - Service level of wind; (b) Maximum story shear at Service Level Earthquake vs Wind load

It can be observed that the interstory drift does not exceed the limit provided for by the legislation; also analyzing the cut values for each floor subjected to the force of the wind compared to the seismic combination in service condition, we can deduce that the cut values for the wind are lower than those obtained from the combination of the seismic load. In conclusion, the checks carried out in this chapter will take into account the request defined by applying a seismic action to the structure.

5.5.4 Reinforcement design

This section describes the procedure for defining the design of the reinforcement of structural elements (beams, columns and walls) after the verification of the structure at collapse level. The steel reinforcement was calculated with a traditional method of capacity design approach, following ACI 318-19 requirements, considering the

maximum stresses in structural elements due to gravitational loads and combinations of seismic loads. The effects of seismic loads on the structure were calculated with the Response Spectrum Analysis (RSA) using the inelastic design spectrum introduced in Figure 5.9.

The beam reinforcement design is conducted by dividing the structural element into three parts, as shown in Figure 5.24: two end sections where plastic hinges are expected to form, and a middle section where the stresses due to gravity and seismic loads are generally lower and therefore less steel is required.

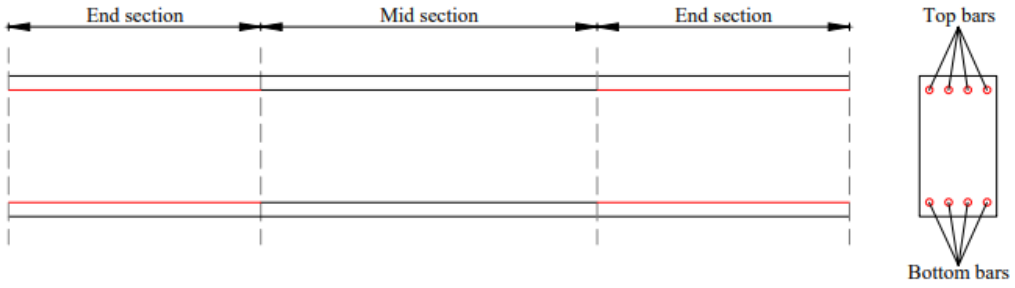

Figure 5. 41 Subdivision of the beam for the reinforcement design

The design of the reinforcement for the column is summarised in Table 5.17 where the minimum amount of steel reinforcement is present for the column sections and obtained from the design procedure. The coefficient ρs represents the total geometric percentage of the reinforcement, defined as:

$$\rho_s = \frac{A_s}{A_c}$$

That is the ratio between the total area of the existing reinforcement and the area of the concrete section.

Table 5. 17 Reinforcement design for Bare frame structure - Column sections

ColumnSection [-]	**b** [cm]	**h** [cm]	**A_c** [cm^2]	**φ** [mm]	**Num. Ofbars** [-]	**$A_{s,tot}$** [cm^2]	**ρ_s** [-]
C 90X160	90	160	14400	804.3	68	54692.4	3.80 %
C 90X140	90	140	12600	490.9	60	29454	2.34 %
C 90X120	90	120	10800	490.9	30	14727	1.36 %
C90X140	90	140	12600	804.3	60	48258	3.83 %
C 90X120	90	120	10800	490.9	38	18654.2	1.73 %

C 90X100	90	100	9000	490.9	26	12763.4	1.42 %

The design of the reinforcement for the wall considers the coefficient ρl indicating the longitudinal dimension, which is given by*:*

$$\rho_l = \frac{2As_l}{E_w * s_l}$$

Where:

- As_l is the longitudinal reinforcement area of the wall;
- E_w is the thickness of the wall;
- s_l is the center to center spacing of horizontal bars;

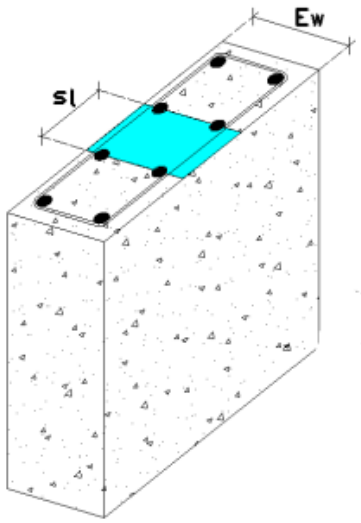

Figure 5. 42 Wall section

5.5.6 Nonlinear Time History Analysis

The ETABS software was used to perform nonlinear chronological analyses, considering the P-Delta geometric nonlinearity. Gravitational loads were applied in the initial phase of the analysis as a nonlinear static case. In each load case, the accelerations were combined in the U1 and U2 directions in order to evaluate the non-linear behavior of the structure, Figure 5.43.

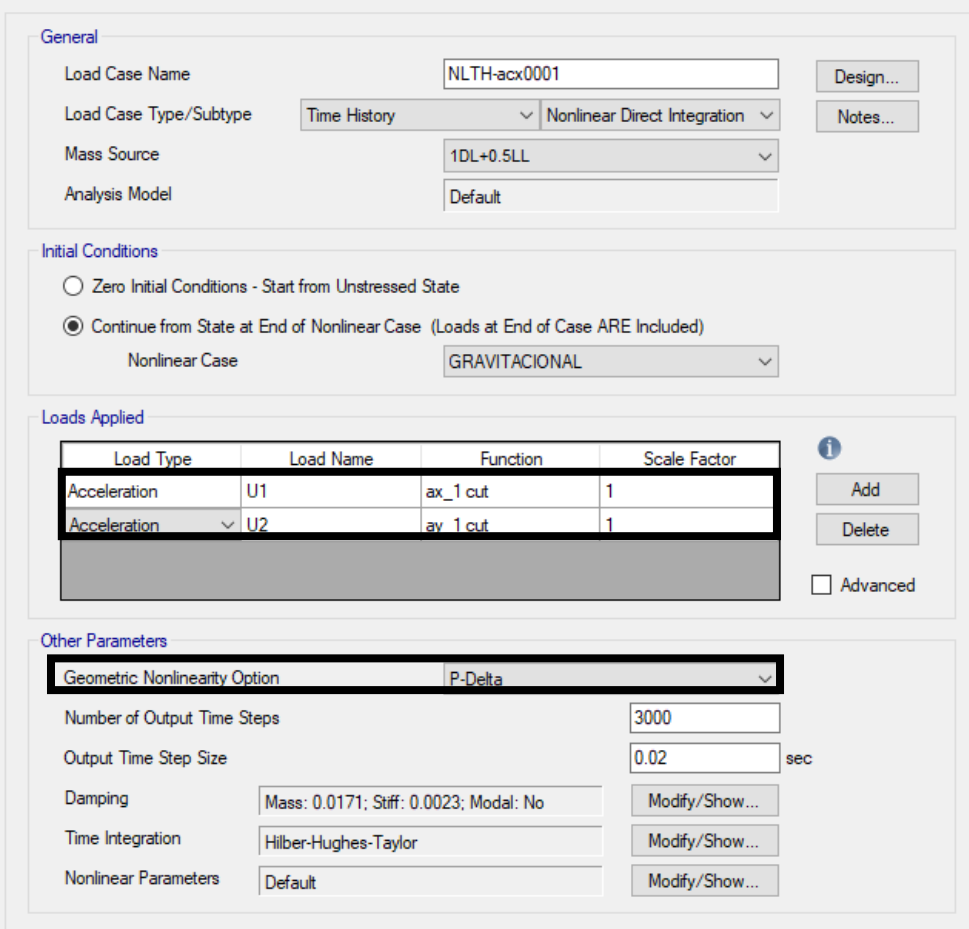

Figure 5. 43 Setting nonlinear time history analysis - ETABS

Damping has been defined as described in paragraph 5.4.2, namely by setting the same modal damping ratio (ξi = 1.3%) in two different natural periods of the structure, that is, they correspond to the first modal period and the period necessary to reach the 90% participating mass in all directions, Figure 5.44.

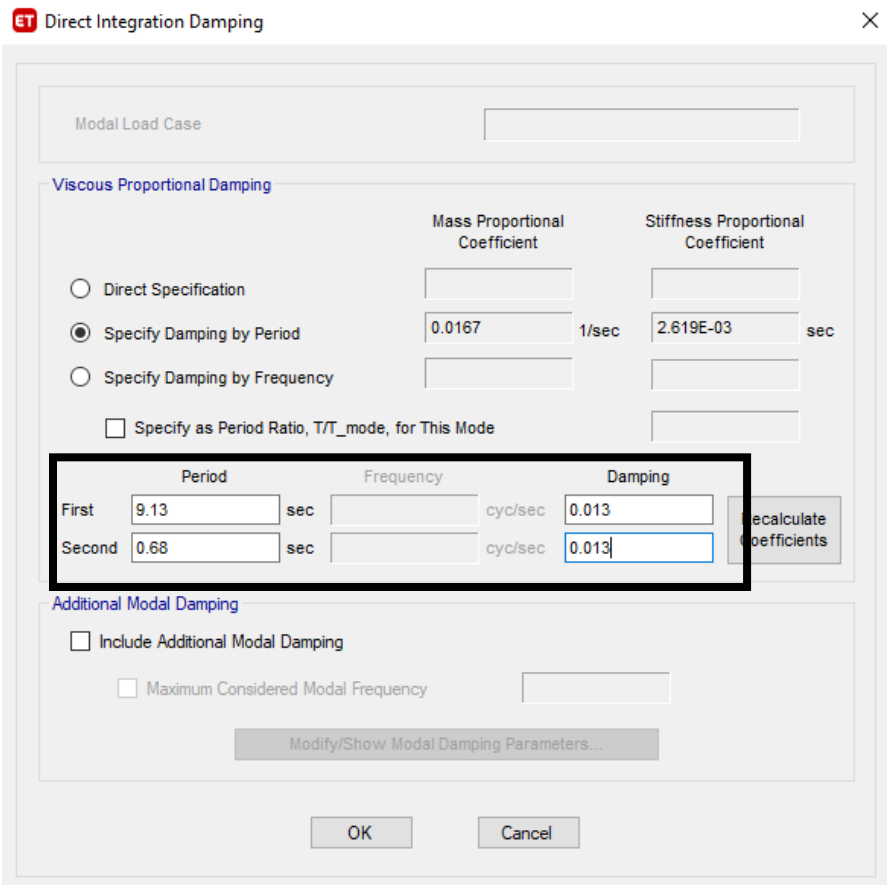

Figure 5. 44 Damping coefficients for Nonlinear time history analysis - ETABS

The set of 10 seismic signals has been used to perform the non-linear analysis, from these are considered both average values (according to the CFE standard) and maximum values (according to the Mexican standard) to evaluate the global and local acceptance criteria. In addition, the results of drift, displacement, shear and acceleration in cover for the considered structure will be analysed and subsequently compared.

❖ OUTPUT

Drift: Figure 5.45 shows the results of the maximum and minimum value of the interstory drift, both in the X direction and in the Y direction for the considered signals.

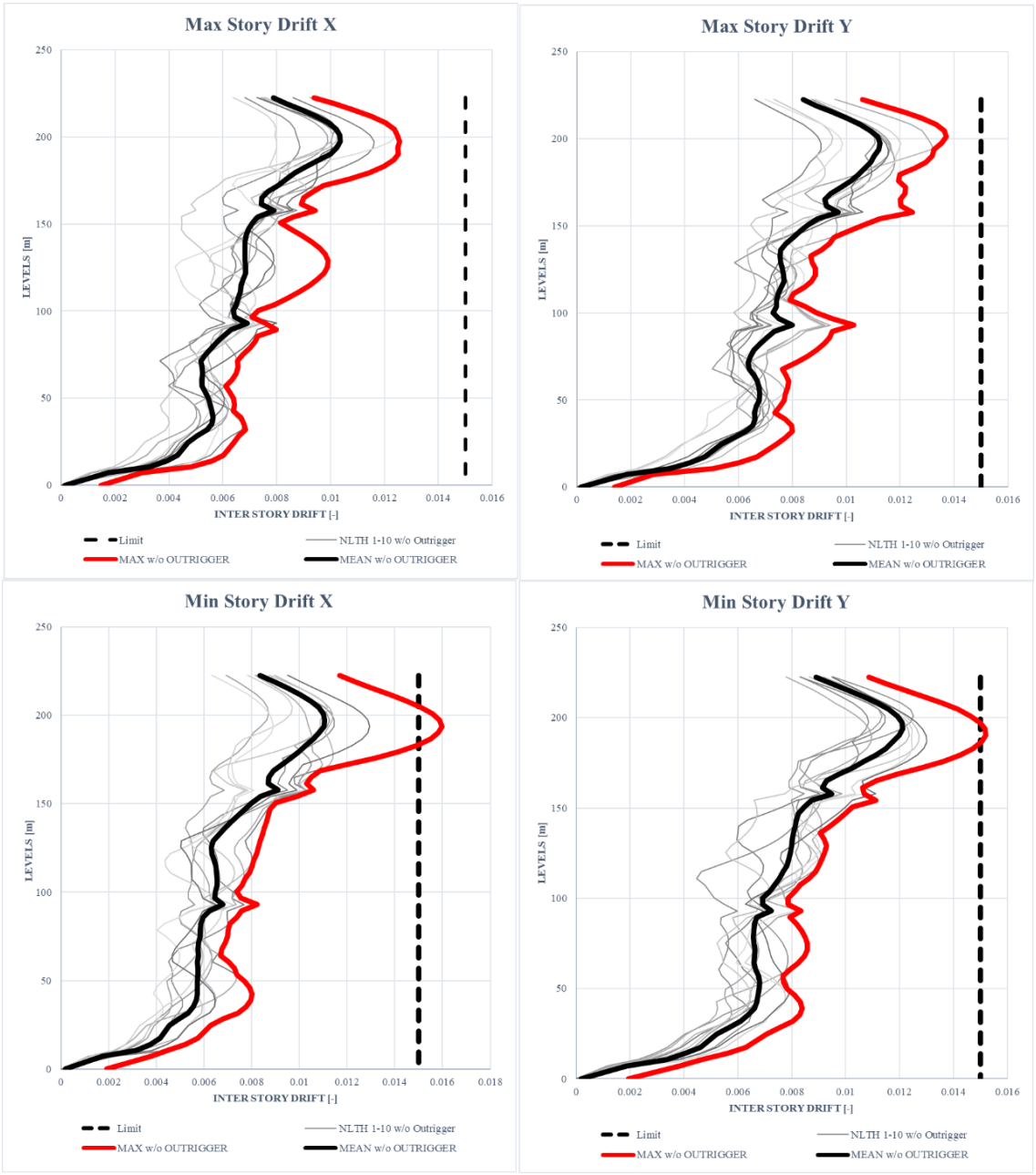

Figure 5. 45 Max and Min Interstory Drift - direction X and Y

You may notice that:

- considering the maximum drift value (in red), the threshold established by the CFE is exceeded in the minimum drift conditions in both x and y direction;
- considering the mean value of drift (in black), interstory drift meets the overall acceptance criteria as it is lower than the limit value established by the standard.

Table 5.18 summarizes the maximum values obtained for drift:

MAX X	DRIFT	MAX Y	DRIFT

w/o OUTRIGGER	0.016	w/o OUTRIGGER	0.015
MEAN X	**DRIFT**	**MEAN Y**	**DRIFT**
w/o OUTRIGGER	0.009	w/o OUTRIGGER	0.011

Table 5. 18 Maximum and mean drift values – Model 1 without Outriggers

Displacement: Figure 5.46 shows the results of the maximum and minimum value of the displacement, is in direction X that in direction Y for the considered signals.

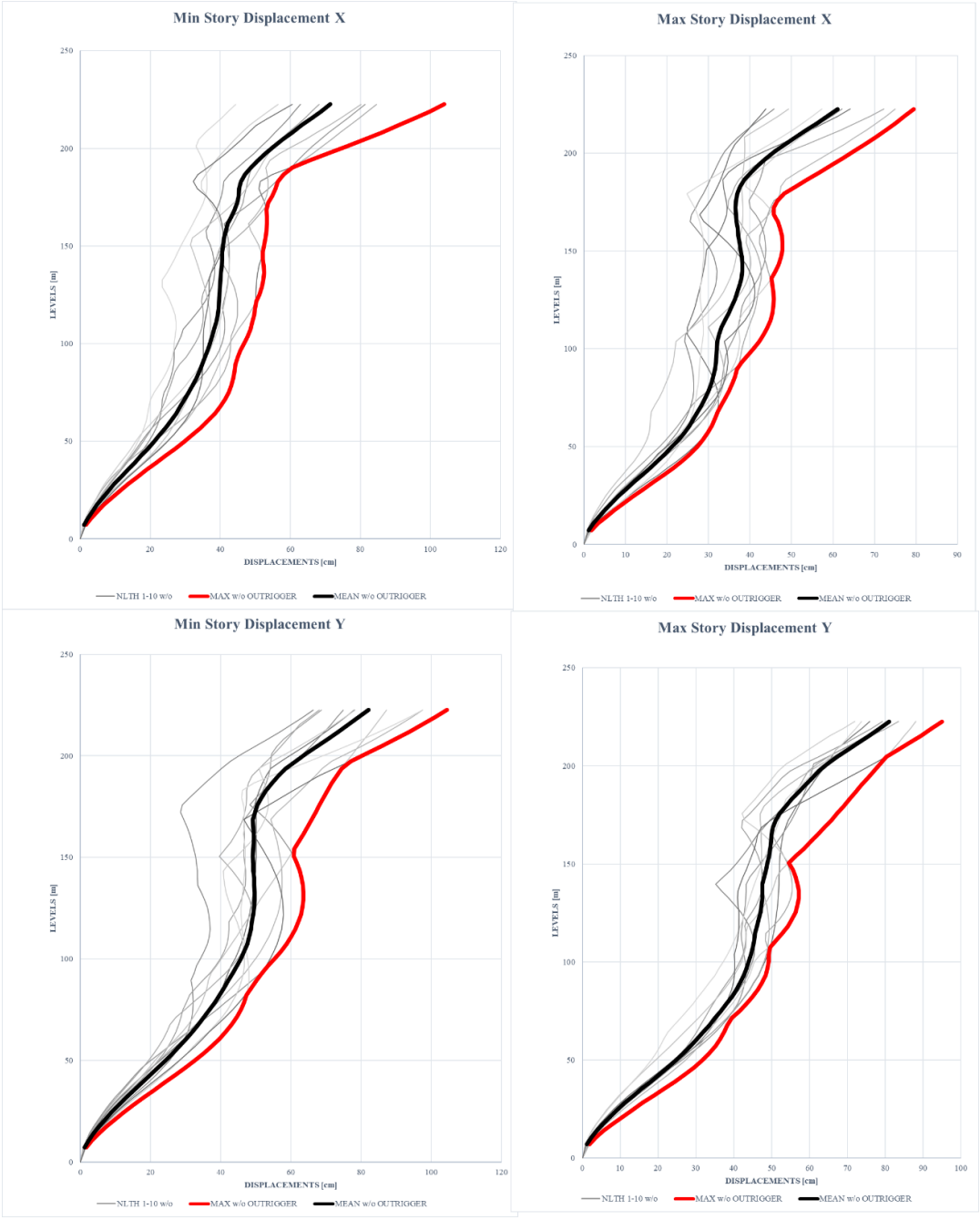

Figure 5. 46 Max and Min values of Displacement - direction X and Y

Table 5.19 summarizes the maximum and average values obtained for displacement:

MAX X	DISPLACEMENT	MAX Y	DISPLACEMENT
w/o OUTRIGGER	103.96cm	w/o OUTRIGGER	104.47cm
MEAN X	**DISPLACEMENT**	**MEAN Y**	**DISPLACEMENT**
w/o OUTRIGGER	63.40cm	w/o OUTRIGGER	83.723cm

Table 5. 19 Maximum and mean displacement values – Model 1 without Outriggers

Shear: Figure 5.47 shows the results of the maximum and minimum value of the cut, is in direction X that in direction Y for the considered signals.

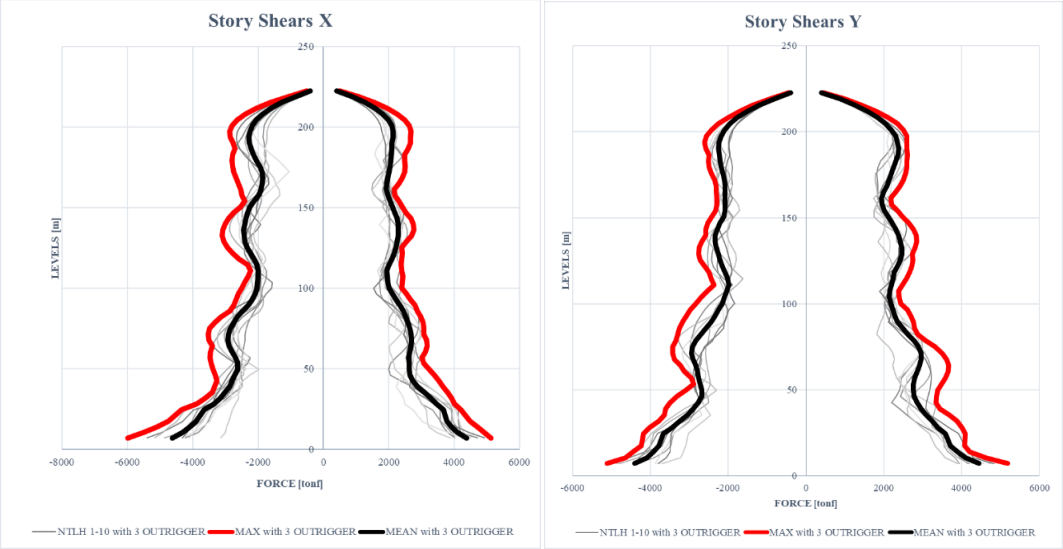

Figure 5. 47 Max and Min values of Story Shear - direction X and Y

Table 5.20 summarizes the maximum and average values obtained for cutting:

MAX X	SHEAR	MAX Y	SHEAR
w/o OUTRIGGER	5975.73tonf	w/o OUTRIGGER	5765.74tonf
MEAN X	**SHEAR**	**MEAN Y**	**SHEAR**
w/o OUTRIGGER	3953.425tonf	w/o OUTRIGGER	4419.442tonf

Table 5. 20 Maximum and mean shear values – Model 1 without Outriggers

Acceleration: Figure 5.48 shows the results of the maximum and minimum value of acceleration evaluated plane by plane along the whole length of the structure, both in the X direction and in the Y direction for the considered signals:

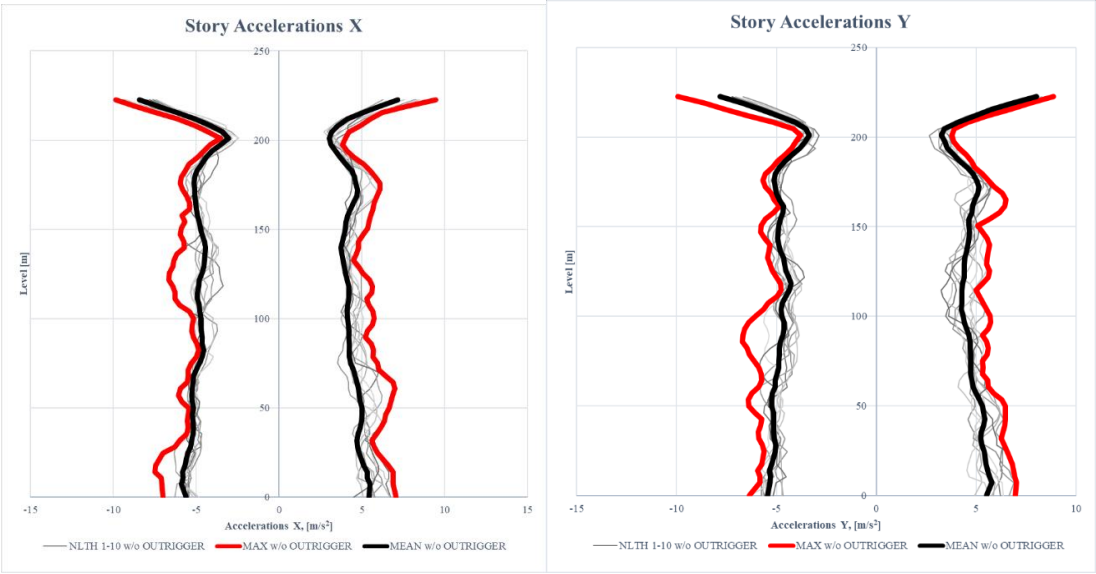

Figure 5. 48 Max and Min values of Story Acceleration - direction X and Y

Table 5.21 summarizes the maximum and average values obtained for acceleration:

MAX X	**ACCELERATION**	**MAX Y**	**ACCELERATION**
w/o OUTRIGGER	9.45 m/s²	w/o OUTRIGGER	8.86 m/s²
MEAN X	**ACCELERATION**	**MEAN Y**	**ACCELERATION**
w/o OUTRIGGER	6.452 m/s²	w/o OUTRIGGER	6.485 m/s²

Table 5. 21 Maximum and mean acceleration values – Model 1 without Outriggers

It was also evaluated how the maximum acceleration varies in coverage as a function of time taking into account an accelerogram taken from the 10 seismic signals provided. In figure 5.49 it is possible to visualize the result for the signal 2.

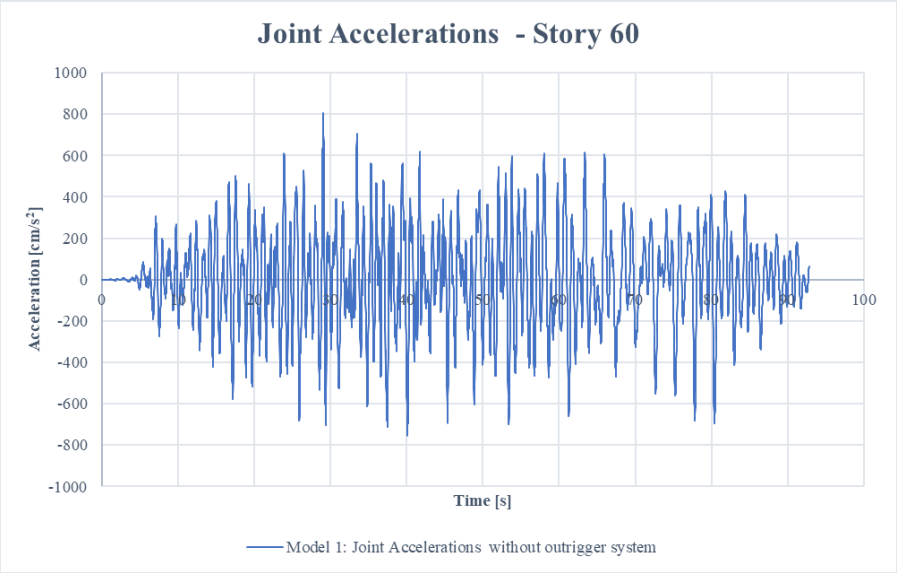

Figure 5. 49 Joint Accelerations without outrigger system

In conclusion, the results of the non-linear analysis meet the criteria of global acceptance. Finally, it is necessary to verify that the property meets the local acceptance criteria. Therefore, plastic rotations in the structural elements (beams, pillars and walls) must be lower than the collapse prevention value (CP). The numerical acceptance criteria for beams and pillars, as described in section 7.2, by ASCE 41-13, while the maximum horizontal displacement for SLB devices is 60 mm.

Table 5.22 shows the maximum and average CP demand ratios of each structural element. The maximum D/C ratio is calculated on the results of the single nonlinear chronological analysis, while the average D/C ratio of the entire set of accelerograms is calculated on the results..

Element [-]	**Mean D/C for CP** [-]	**Max D/C for CP** [-]
Beam	0.15	0.21
Column	0.007	0.064
Wall	0.113	0.132

Table 5. 22 Model 3: Mean and Maximum D/C ratios for Collapse Prevention (CP)

The status of plastic hinges is shown according to the immediate performance levels of occupation (IO), safety of life (LS), prevention of collapse (CP). According to Table 10-8 of ASCE/SEI 41-13 the performance levels are related to the plastic rotation angle (radians) this depends on the breaking condition and the amount of steel reinforcement. For this reason, the plastic hinges developed by the structure have reached the performance level of immediate occupation (IO) without reaching the level of live safety (LS).

Figure 5.50 shows the hysterical response of the plastic hinge for a generic beam. Figure 5.51 shows the hysterical response of the plastic hinge for a generic wall.

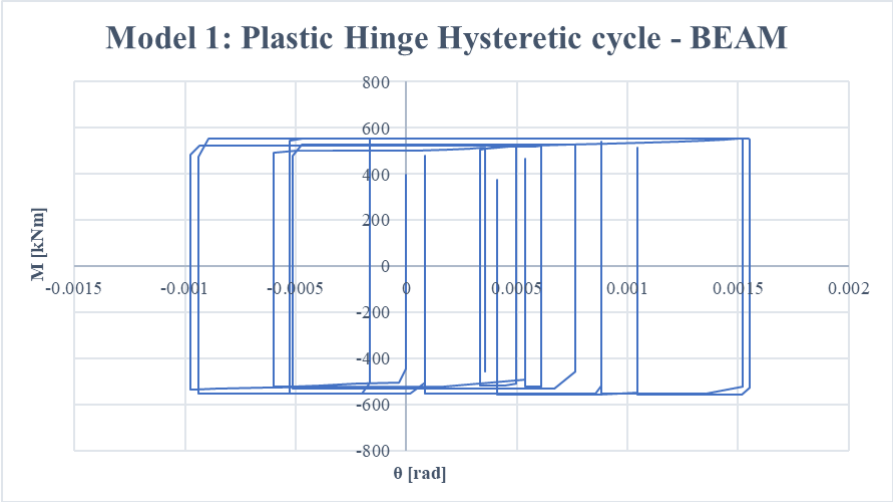

Figure 5. 50 Model 1: Plastic Hinge Hysteretic cycle - BEAM

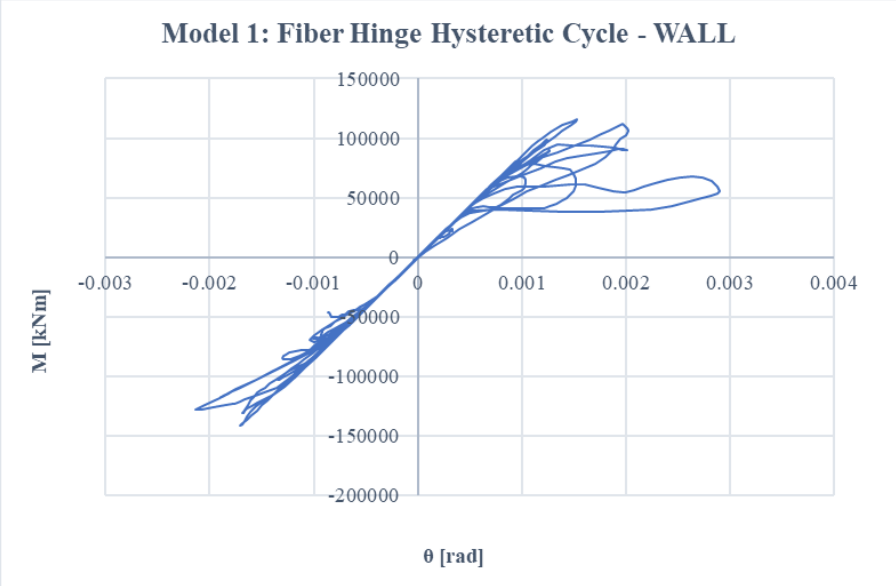

Figure 5. 51 Model 1: Fiber Hinge Hysteretic Cycle - WALL

5.6 MODEL2: Structure with 2 Outriggers and SLB design

5.6.1 Outrigger design

The objective of the present work is to study the use of Outrigger placed in different positions in the building and subject to earthquake. The Outrigger position can reduce interstory drift and lateral displacement. With the use of the ETABS program, used for the analysis, and through an iterative procedure, the typology and the optimal position of the Outriggers in the structure under study were determined.

Given the double symmetry of the building along its entire height, the various types of outrigger systems seen in paragraph 2.4 used a type similar to that studied by Arup, using a combined system of concrete and steel. Initially to increase the stiffness of the building it was thought to build a reinforced concrete wall that flanked the central core to the right and left, both in x direction and y direction. Subsequently for architectural needs and to allow the passage of people, has been defined for the length of 2mt a steel EBF that connects the reinforced concrete wall directly to the column in its center as seen from figures 5.52 and 5.53.

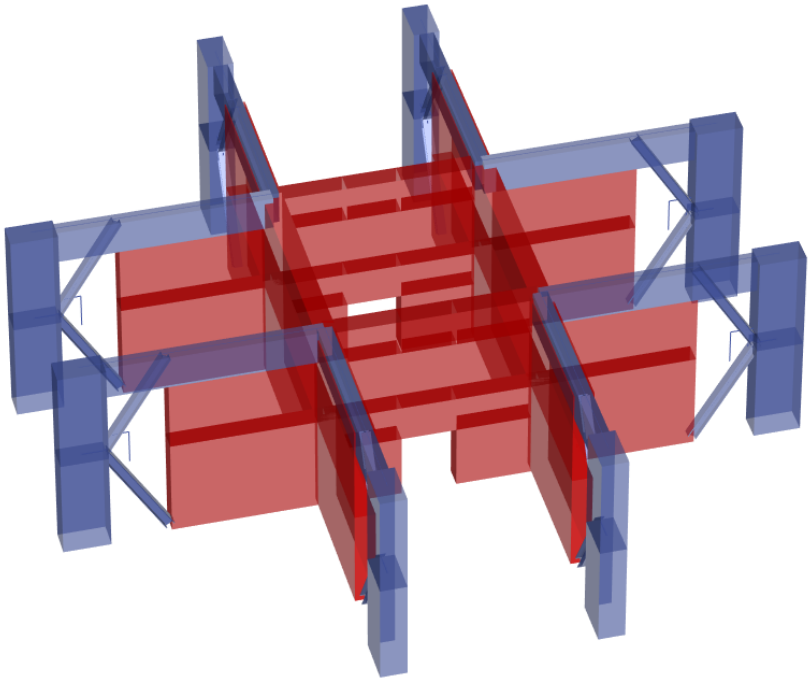

Figure 5. 52 3d of Outrigger system designed for the Paseo de Gracia case study

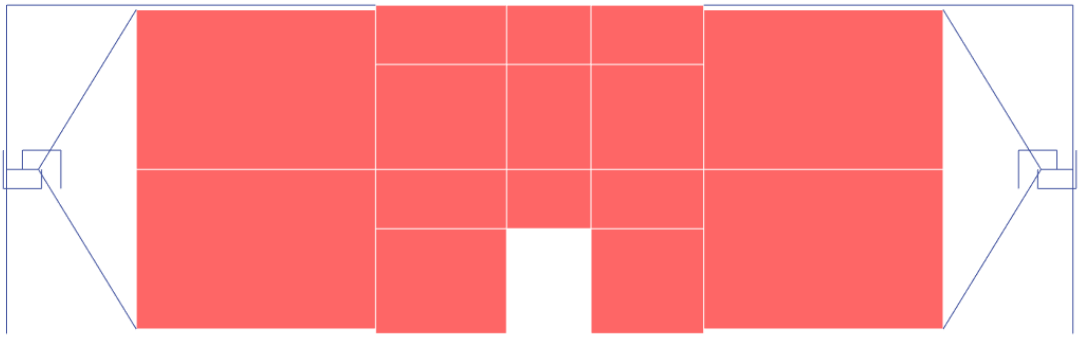

Figure 5. 53 Prospectus of the Outrigger system designed for the Paseo de Gracia case study

The optimal location for the system was evaluated through an iterative procedure and taking into account the architecture of the building. The structure presence of the double heights, two of which were chosen to accommodate the Outrigger system

with SLB heatsinks. More precisely the model analyzed in this paragraph presents the system in the positions in figure 5.54:

- The first Outrigger system was applied in the double height between story 24 and 25, at a height of 93mt;
- The second Outrigger system was applied in the double height between story 42 and 43, at a height of 157.80 meters.

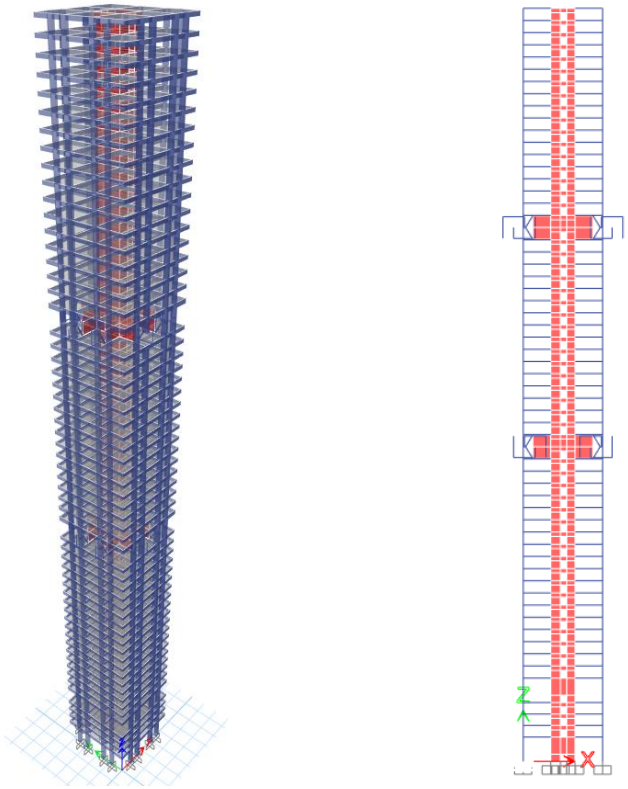

Figure 5. 54 Model 2: Position of the outrigger system

The presence of the Outrigger system also determines the need for stiffening of the wall in the application level, for this reason the structural elements such as columns and beams always maintain the same geometric dimensions, but the wall increases in section and more precisely we see in table 5.23:

Level [-]	**Wall Section** [-]	**s** [cm]	**Concrete** [-]	**f_{ck}** [Mpa]
Story60	M 20	20	C45	45
Story59	M 20	20	C45	45
Story58	M 20	20	C45	45
Story57	M 20	20	C45	45
Story56	M 20	20	C45	45

Story55	M 20	20	C45	45
Story54	M 20	20	C45	45
Story53	M 20	20	C45	45
Story52	M 20	20	C45	45
Story51	M 20	20	C45	45
Story50	M 20	20	C45	45
Story49	M 20	20	C45	45
Story48	M 20	20	C45	45
Story47	M 20	20	C45	45
Story46	M 20	20	C45	45
Story45	M 30	30	C45	45
Story44	M 40	40	C45	45
Story43	M 50	50	C55	55
Story42	M 50	50	C55	55
Story41	M 50	50	C55	55
Story40	M 50	50	C55	55
Story39	M 50	50	C55	55
Story38	M 50	50	C55	55
Story37	M 50	50	C55	55
Story36	M 50	50	C55	55
Story35	M 50	50	C55	55
Story34	M 50	50	C55	55
Story33	M 50	50	C55	55
Story32	M 50	50	C55	55
Story31	M 50	50	C55	55
Story30	M 50	50	C55	55
Story29	M 50	50	C55	55
Story28	M 50	50	C55	55
Story27	M 50	50	C55	55
Story26	M 60	60	C55	55
Story25	M 70	70	C65	65
Story24	M 70	70	C65	65
Story23	M 60	60	C65	65
Story22	M 60	60	C65	65
Story21	M 60	60	C65	65
Story20	M 60	60	C65	65
Story19	M 60	60	C65	65
Story18	M 60	60	C65	65
Story17	M 60	60	C65	65
Story16	M 60	60	C65	65
Story15	M 60	60	C65	65
Story14	M 60	60	C65	65

Story13	M 60	60	C65	65
Story12	M 60	60	C65	65
Story11	M 60	60	C65	65
Story10	M 60	60	C65	65
Story9	M 60	60	C65	65
Story8	M 60	60	C65	65
Story7	M 60	60	C65	65
Story6	M 60	60	C65	65
Story5	M 60	60	C65	65
Story4	M 60	60	C65	65
Story3	M 60	60	C65	65
Story2	M 60	60	C65	65
Story1	M 70	70	C65	65

Table 5. 23 Model 2: Wall Section

5.6.2 SLB design

The use of 4th generation SLB devices has been proposed for the Paseo de Gracia project, coupled to the Outrigger system. The proposed SLB solution sees the heatsink positioned between the diagonal EBF and the column.

The wall stiffness has been compared with the heatsink stiffness (see Table 5.23) using the following formula:

$$k_e = \frac{k_m * k_d}{k_m + k_d} \ ;$$

$$k_m = n * k_d$$

$$k_e = \left(\frac{n}{1+n}\right) k_d$$

Where:

- k_e is elastic stiffness;
- k_m s the stiffness of the wall and is equal to $k_m = \frac{12EI}{h^3}$;
- k_d s the device stiffness that you can see in table 5.24;

2xSLB4_65_20		h_m [cm]	b_m [cm]	e_m [cm]	E_C [kN/cm^2]	I [cm^4]	K_m [kN/cm]	K_d [kN/cm]	n [-]	K_e [kN/cm]
Dissipatore Singolo	**1**	725.26	340	60	2615.51	196520000	16168.27	65902.37	0.245	12983.051
	2	725.26	340	50	2445.22	163766667	12596.32	65902.37	0.191	10575.0456
	3	725.26	340	40	2258.59	131013333	9307.92	65902.37	0.141	8155.98773

Dissipatore Doppio	**4**	725.26	700	60	2615.51	1715000000	141098.02	65902.37	2.141	44921.1413
	5	725.26	700	50	2445.22	1429166667	109926.14	65902.37	1.668	41201.47
SLB4_65_20		h_m	b_m	e_m	E_C	I	K_m	K_d	n	K_e
		[cm]	[cm]	[cm]	[kN/cm^2]	[cm^4]	[kN/cm]	[kN/cm]	[-]	[kN/cm]
Dissipatore Singolo	**1**	725.26	340	60	2615.51	196520000	16168.27	32951.18	0.491	10846.2859
	2	725.26	340	50	2445.22	163766667	12596.32	32951.18	0.382	9112.76306
	3	725.26	340	40	2258.59	131013333	9307.92	32951.18	0.282	7257.7753
Dissipatore Doppio	**4**	725.26	700	60	2615.51	1715000000	141098.02	32951.18	4.282	26712.8302
	5	725.26	700	50	2445.22	1429166667	109926.14	32951.18	3.336	25351.7941

Table 5. 24 Stiffness comparison

The selection procedure of SLB devices was performed using the direct iteration method described in paragraph 4.4.1 , obtaining an initial set of devices. Then the optimal solution was achieved by reducing the size of the heatsinks with a series of nonlinear chronological analysis considering only the non-linear behavior of the heatsinks.

Device	K_1 (KN/cm)	K_2 (KN/cm)	D_y (mm)	F_y (KN)	F_{max} (KN)
SLB4_10_5	2026.65	21.62	0.749	151.79	250.00
SLB4_10_6	2163.53	22.90	0.742	160.54	265.78
SLB4_15_5	2472.60	24.85	0.720	177.92	293.72
SLB4_15_6	2761.73	26.96	0.706	195.09	320.62
SLB4_15_7	3021.88	28.76	0.697	210.76	345.09
SLB4_20_6	3361.00	33.09	0.687	230.93	381.61
SLB4_20_7	3700.15	35.28	0.673	248.98	410.70
SLB4_25_6	4260.80	42.53	0.654	278.74	468.96
SLB4_25_7	4767.68	46.51	0.638	304.31	512.31
SLB4_25_8	5238.65	50.43	0.626	327.73	552.76
SLB4_30_7	5785.96	57.25	0.619	358.28	611.14
SLB4_30_8	6419.52	62.36	0.608	390.28	665.17
SLB4_30_9	6994.22	66.79	0.601	420.37	716.61
SLB4_30_10	7535.22	70.90	0.596	449.29	764.52
SLB4_40_7	7797.49	78.07	0.596	464.68	807.56
SLB4_40_8	8718.88	86.41	0.588	512.48	890.20
SLB4_40_9	9580.18	93.66	0.582	557.71	966.06
SLB4_40_10	10439.63	101.20	0.576	601.31	1043.20
SLB4_40_11	11253.53	109.93	0.571	643.06	1117.73
SLB4_40_12	12033.64	115.64	0.570	685.73	1191.30
SLB4_50_9	12289.99	120.57	0.578	709.95	1236.23
SLB4_50_10	13421.60	130.96	0.572	768.20	1340.09
SLB4_50_11	14537.41	141.39	0.569	827.48	1443.52
SLB4_50_12	15599.37	150.54	0.567	884.08	1540.02
SLB4_60_5	8891.13	91.74	0.598	531.45	932.94
SLB4_60_6	10457.28	106.25	0.586	613.19	1078.09
SLB4_60_11	17684.45	174.36	0.562	993.08	1746.50
SLB4_60_12	19029.62	185.88	0.560	1065.32	1868.98
SLB4_65_11	19829.08	194.60	0.562	1113.76	1957.04
SLB4_65_12	21326.70	209.74	0.560	1194.73	2103.54
SLB4_65_13	22872.65	223.05	0.558	1276.57	2245.62
SLB4_65_14	24379.36	235.06	0.556	1356.52	2382.04
SLB4_65_15	25869.86	249.17	0.554	1433.77	2519.93
SLB4_65_16	27331.55	261.77	0.553	1511.96	2654.85
SLB4_65_18	30180.37	286.67	0.554	1671.12	2912.47
SLB4_65_20	32951.18	306.56	0.553	1822.60	3157.88

Table 5. 25 Design Table for 4th generation of Shear Link Bozzo devices

The optimal solution for each Outrigger system is to install two SLB4_65_20 (see Table 5.25), for a total of 16 devices.

5.6.3 Modal analysis

The first step to follow, as previously done for the bare frame structure, is to define a modal analysis with the aim of studying the dynamic behavior of the structure with the presence of 2 Outrigger systems. Table 5.26 shows the periods and the participating mass of the first three natural modes of vibration of the structure, as

well as the way it presents 90% participating mass The results are obtained considering the actual stiffness values seen in paragraph 5.4.2.

Mode	Period	U_X	U_Y	R_Z	SumU_X	SumU_Y	SumR_Z
[-]	sec	[-]	[-]	[-]	[-]	[-]	[-]
1	8.59	0.00%	68.00%	0.00%	0.00%	68.00%	0.00%
2	8.517	67.00%	0.00%	0.00%	67.00%	68.00%	0.00%
3	3.216	0.00%	0.00%	80.00%	67.00%	68.00%	80.00%
10	0.634	0.00%	4.00%	0.00%	89.00%	93.00%	93.00%

Table 5. 26 Modal analysis results for structure with 2 Outrigger and SLB system

It is possible to observe that the first two modes are translational, while the third mode is rotational, to be precise, the first is translational along Y with 68% of participating mass, the second along X with 67% of participating mass, finally the third rotational around Z, with 80% participating mass.

Figure 5. 55 1st model

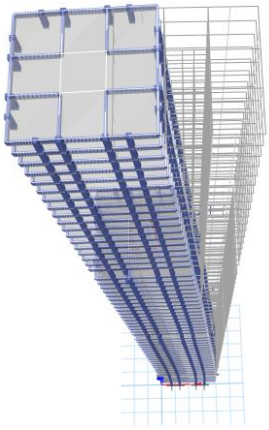

Figure 5. 56 2st mode

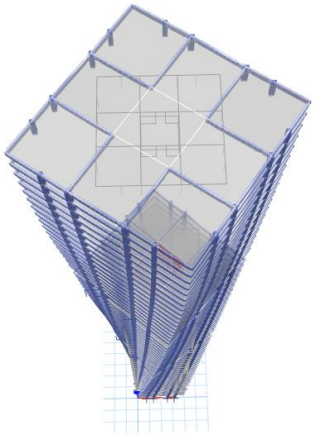

Figure 5. 57 3st mode

The fondamental period is 8.59 seconds, an acceptable value for 60 floors of a reinforced concrete building, while 90% of the participating mass ratio is achieved in all directions considering the first 10 natural modes of structure vibration.

5.6.4 Response spectrum analysis

The next step is to verify the structure at the Collapse Level Earthquake according to the requirements of the CFE, ie defining a limit to 0.015 as required by the standard. The interstory-drift results for the collapse condition, in the X and Y direction are given in Figure 5.58.

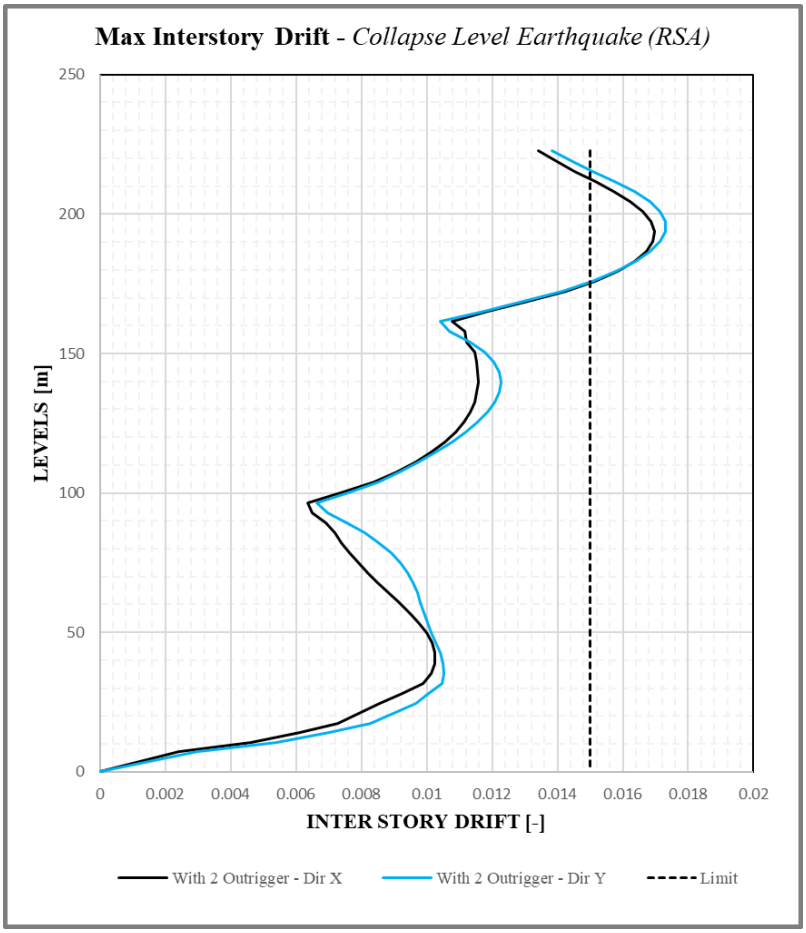

Figure 5. 58 Max Interstory Drift at Collapse Level Earthquake (RSA)

The maximum values in the direction X and Y for drift in the collapse condition are given in Table 5.27:

MAX X	DRIFT	MAX Y	DRIFT
with 2 OUTRIGGER	0.017	with 2 OUTRIGGER	0.017

Table 5. 27 Maximum drift values (Collapse-RSA)

The interstory-drift results are also analyzed for the condition of Service Level Earthquake that, according to the requirements of the CFE, has an acceptable maximum limit of 0.004. Below in Figure 5.59 are the values obtained for the service condition, in direction X and Y.

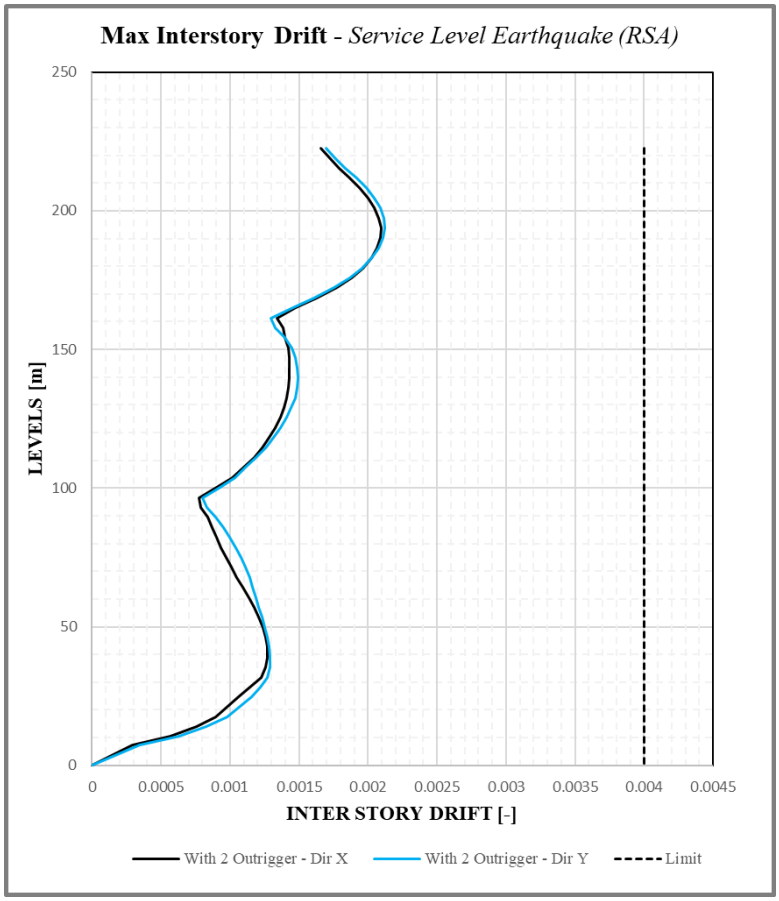

Figure 5. 59 Max Interstory Drift at Service Level Earthquake (RSA)

Table 5.28 shows the maximum values in X and Y direction for drift in Service condition:

MAX X	DRIFT	MAX Y	DRIFT
with 2 OUTRIGGER	0.002	with 2 OUTRIGGER	0.002

Table 5. 28 Maximum drift values (Service-RSA)

It is possible to note that with linear analysis the response in terms of drift in collapse conditions exceeds the limit defined by the legislation, while in the service condition is within the limit prescribed by the legislation.

The results for displacement in the collapse condition, in the X and Y direction are given in Figure 5.60.

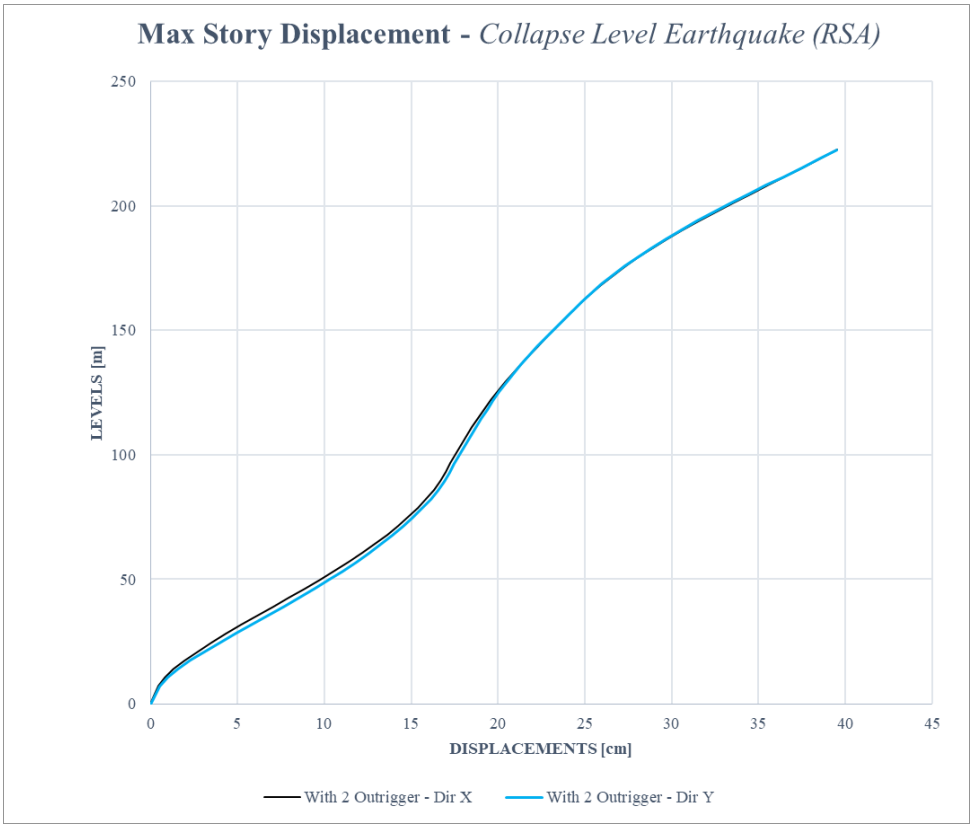

Figure 5. 60 Max Interstory Displacement at Collapse Level Earthquake (RSA)

Table 5.29 shows the maximum values in the X and Y direction for displacement in the Collapse condition:

MAX X	DISPLACEMENT	MAX Y	DISPLACEMENT
with 2 OUTRIGGER	39.52	with 2 OUTRIGGER	39.48

Table 5. 29 Maximum displacement values (Collapse - RSA)

The results for displacement in service condition, in X and Y direction are given in Figure 5.61.

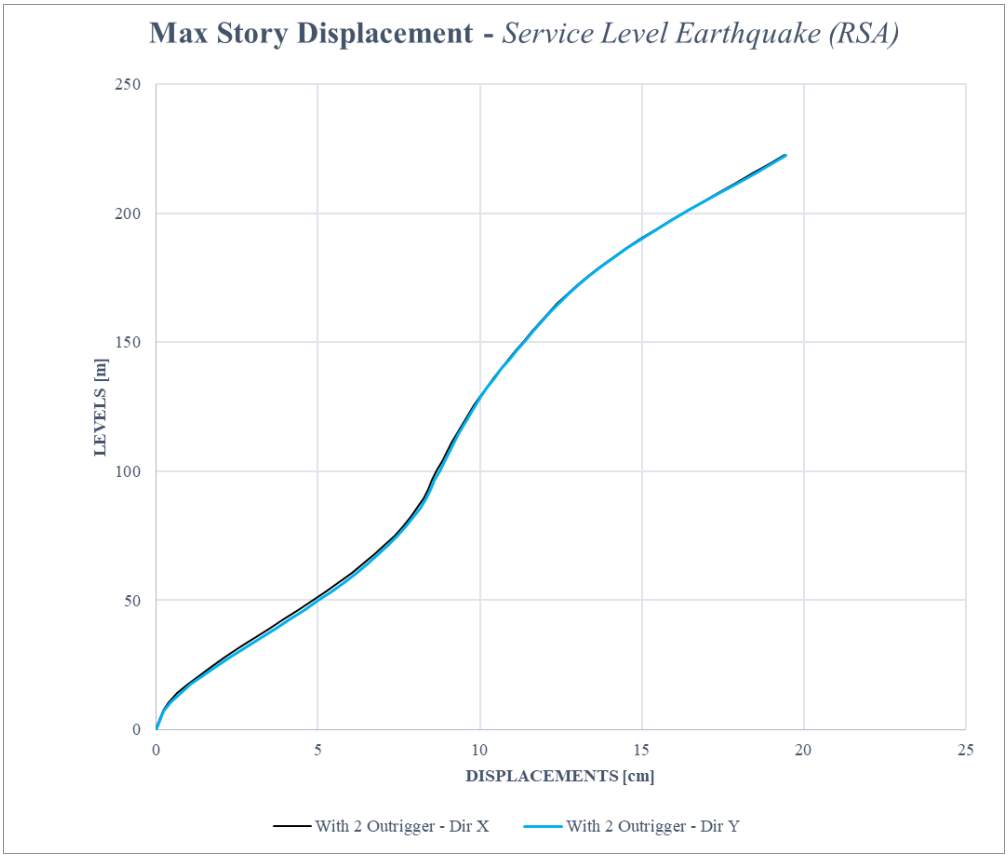

Figure 5. 61 Max Interstory Displacement at Service Level Earthquake (RSA)

Table 5.30 shows the maximum values in X and Y direction for displacement in the Service condition:

MAX X	DISPLACEMENT	MAX Y	DISPLACEMENT
with 2 OUTRIGGER	19.39cm	with 2 OUTRIGGER	19.45cm

Table 5. 30 Maximum displacement values (Service- RSA)

The results for Shear in collapse condition, in X and Y direction are given in Figure 5.62.

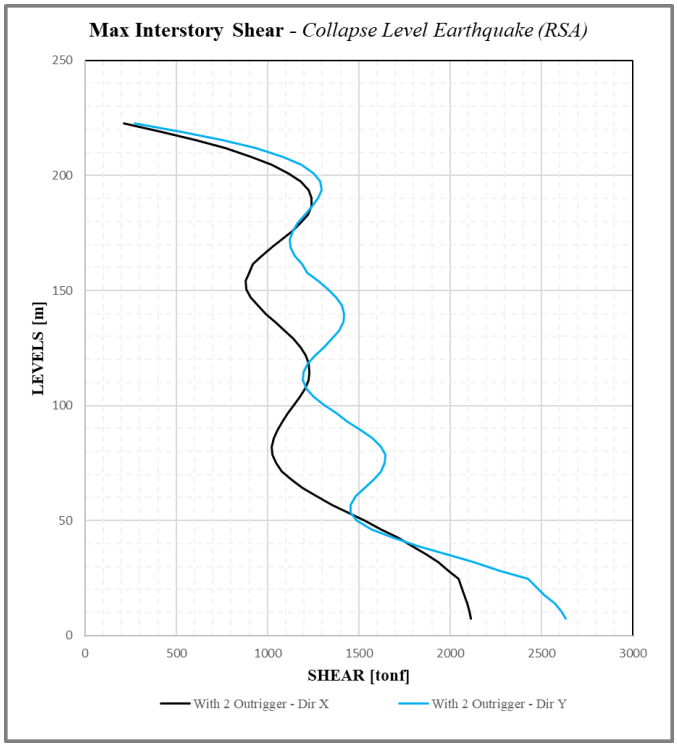

Figure 5. 62 Max Interstory Shear at Collapse Level Earthquake (RSA)

Table 5.31 shows the maximum values in the X and Y direction for the cut in the Collapse condition:

MAX X	SHEAR	MAX Y	SHEAR
with 2 OUTRIGGER	2113.26 tonf	with 2 OUTRIGGER	2634.14 tonf

Table 5. 31 Maximum shear values (Collapse - RSA)

The results for Cut in service condition, in X and Y direction are shown in Figure 5.63.

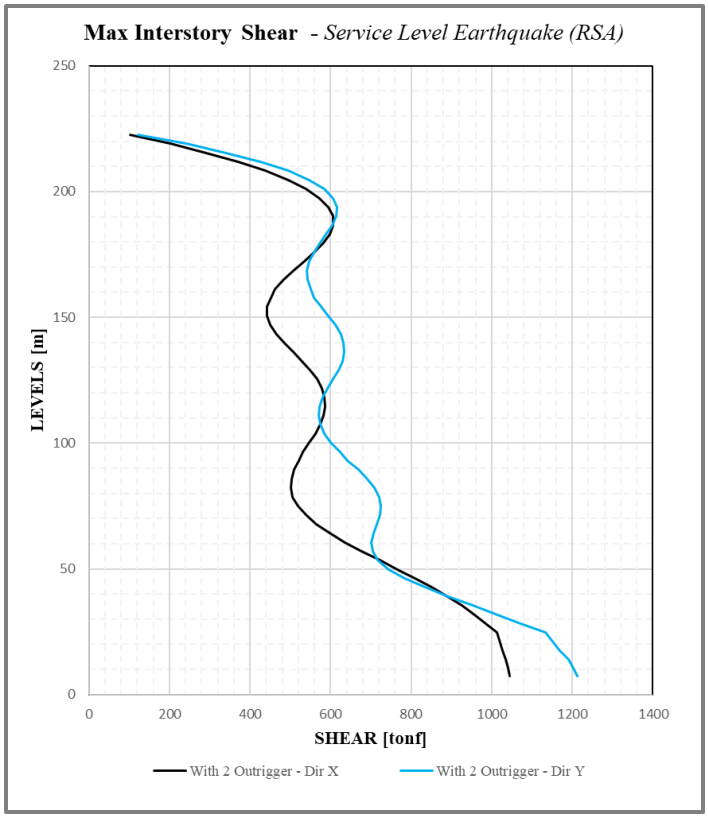

Figure 5. 63 Max Interstory Shear at Service Level Earthquake (RSA)

Table 5.32 shows the maximum values in the X and Y direction for the cut in the Service condition:

MAX X	SHEAR	MAX Y	SHEAR
with 2 OUTRIGGER	1043.76 tonf	with 2 OUTRIGGER	1212.46 tonf

Table 5. 32 Maximum shear values (Service- RSA)

5.6.6 Reinforcement design

This section describes the procedure for defining the design of the reinforcement of structural elements (beams, columns and walls) after the verification of the structure at collapse level. The steel reinforcement was calculated with a traditional method of capacity design approach, following ACI 318-19 requirements, considering the maximum stresses in structural elements due to gravitational loads and combinations of seismic loads. The effects of seismic loads on the structure were calculated with Response Spectrum Analysis (RSA) using the inelastic design spectrum introduced in Figure 5.9.

The beam reinforcement design is conducted by dividing the structural element into three parts, as shown in Figure 5.64: two end sections where the formation of plastic hinges is expected, and a middle section where the stresses due to gravity and seismic loads are generally lower and therefore less steel is required.

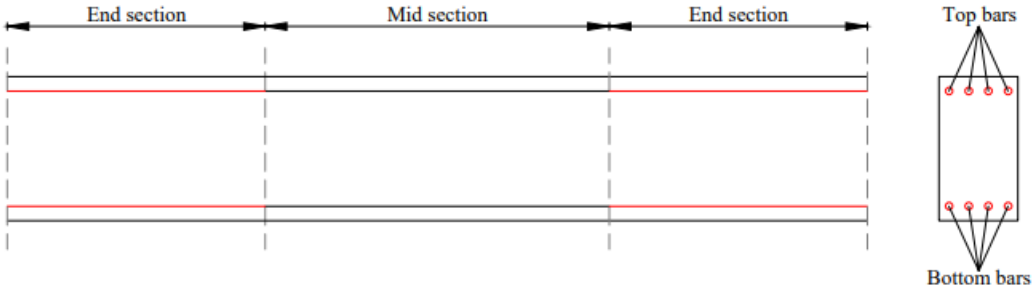

Figure 5. 64 Subdivision of the beam for the reinforcement design

The reinforcement design for the column is summarised in Table 5.33 where the minimum amount of steel reinforcement is present for the column sections and obtained from the design procedure. The coefficient ρs represents the total geometric percentage of the reinforcement, defined as:

$$\rho_s = \frac{A_s}{A_c}$$

That is the ratio between the total area of the existing reinforcement and the area of the concrete section.

ColumnSection [-]	b [cm]	h [cm]	A_c [cm^2]	φ [mm]	Num. Ofbars [-]	$A_{s,tot}$ [cm^2]	ρ_s [-]	
C 90X160	90	160	14400	804.3	56	45040.8	3.13	%
C 90X140	90	140	12600	490.9	34	16690.6	1.32	%
C 90X120	90	120	10800	490.9	24	11781.6	1.09	%
C90X140	90	140	12600	804.3	48	38606.4	3.06	%
C 90X120	90	120	10800	490.9	32	15708.8	1.45	%
C 90X100	90	100	9000	490.9	20	9818	1.09	%

Table 5. 33 Reinforcement design for structure with 2 Outrigger system and SLB - Column sections

The design of the reinforcement for the wall considers the coefficient ρl indicating the longitudinal dimension, which is given by:

$$\rho_l = \frac{2As_l}{E_w * s_l}$$

Where:

- As_l is the longitudinal reinforcement area of the wall;
- E_w is the wall thickness;
- s_l is the center to center spacing of horizontal bars;

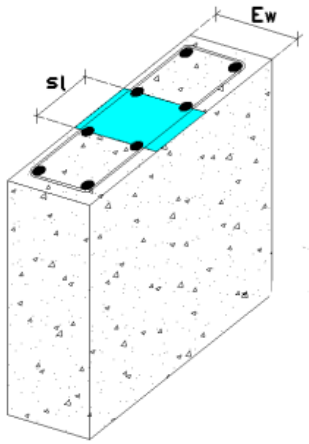

Figure 5. 65 Wall section

5.6.7 Nonlinear Time History Analysis

The ETABS software was used to perform nonlinear chronological analyses, considering the P-Delta geometric nonlinearity. Gravitational loads were applied in the initial phase of the analysis as a nonlinear static case. In each load case, the accelerations were combined in the U1 and U2 directions in order to evaluate the non-linear behavior of the structure, Figure 5.66.

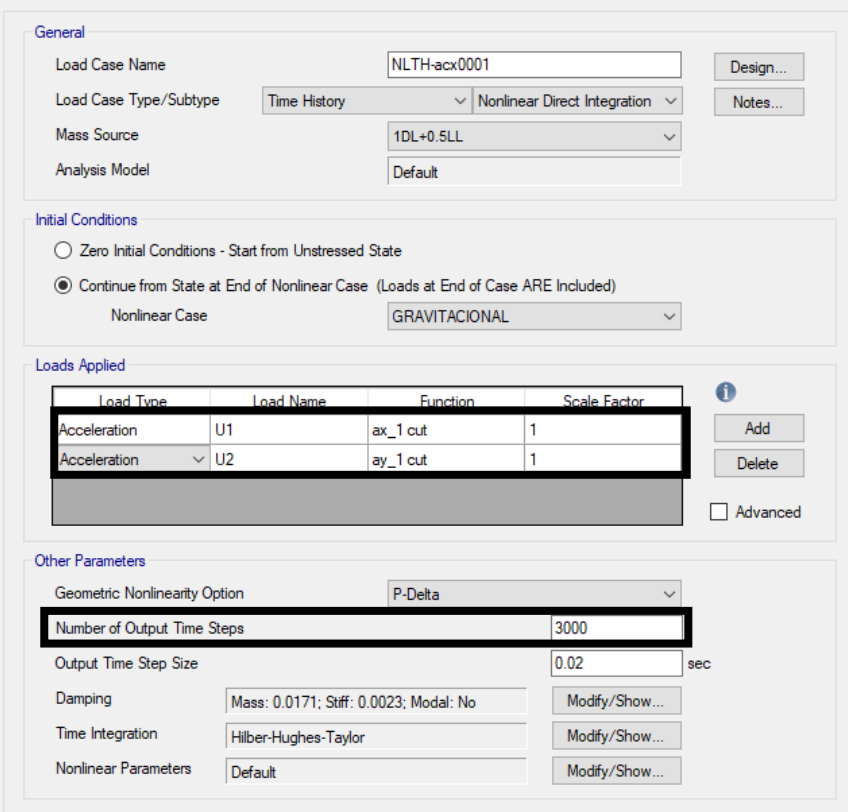

Figure 5. 66 Setting nonlinear time history analysis - ETABS

Damping has been defined as described in paragraph 5.4.2, namely by setting the same modal damping ratio (ξi = 1.3%) in two different natural periods of the structure, that is, they correspond to the first modal period and the period necessary to reach 90% participating mass in all directions, Figure 5.67.

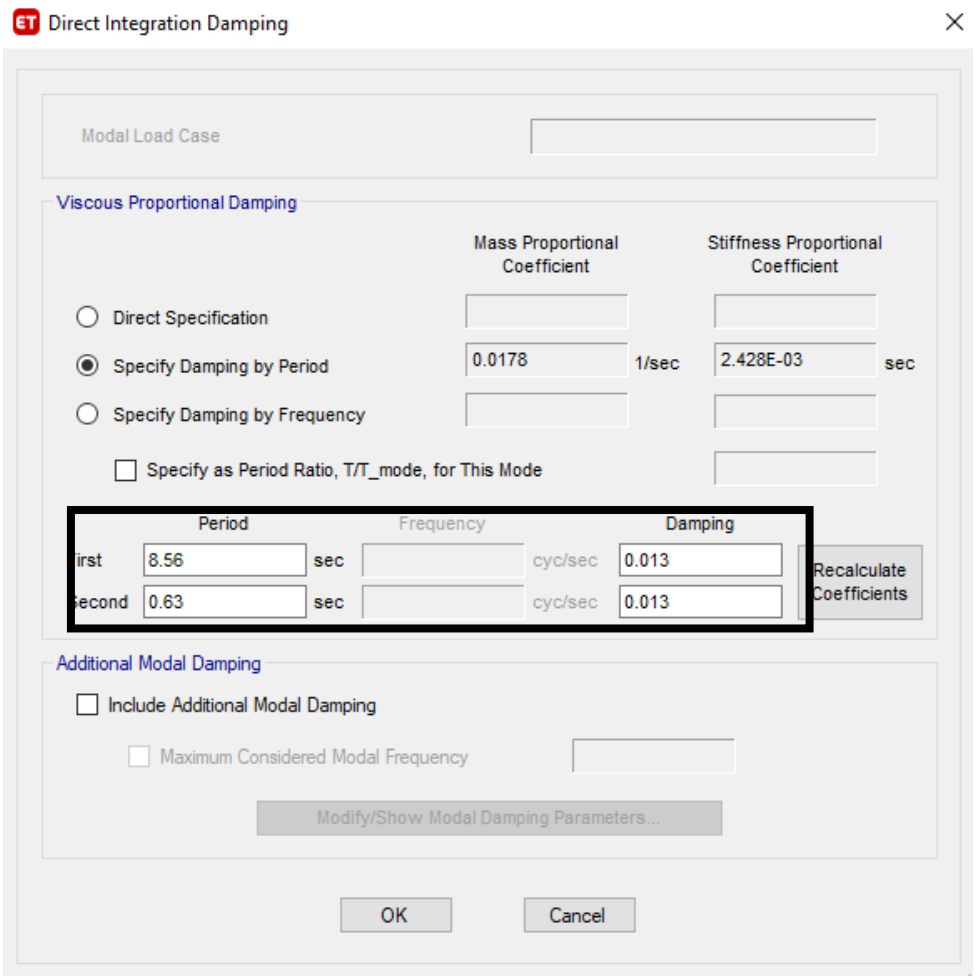

Figure 5. 67 Damping coefficients for Nonlinear time history analysis - ETABS

The set of 10 seismic signals has been used to perform the non-linear analysis, from these are considered the values both average (according to the CFE standard) and maximum (according to the Mexican standard) to evaluate the global and local acceptance criteria. Moreover the results of the drift, the displacement, the cut and the acceleration in cover for the considered structure will be analyzed and subsequently compared.

❖ OUTPUT

Drift: Figure 5.68 shows the results of the maximum and minimum value of the interstory drift, is in direction X that in direction Y for the considered signals.

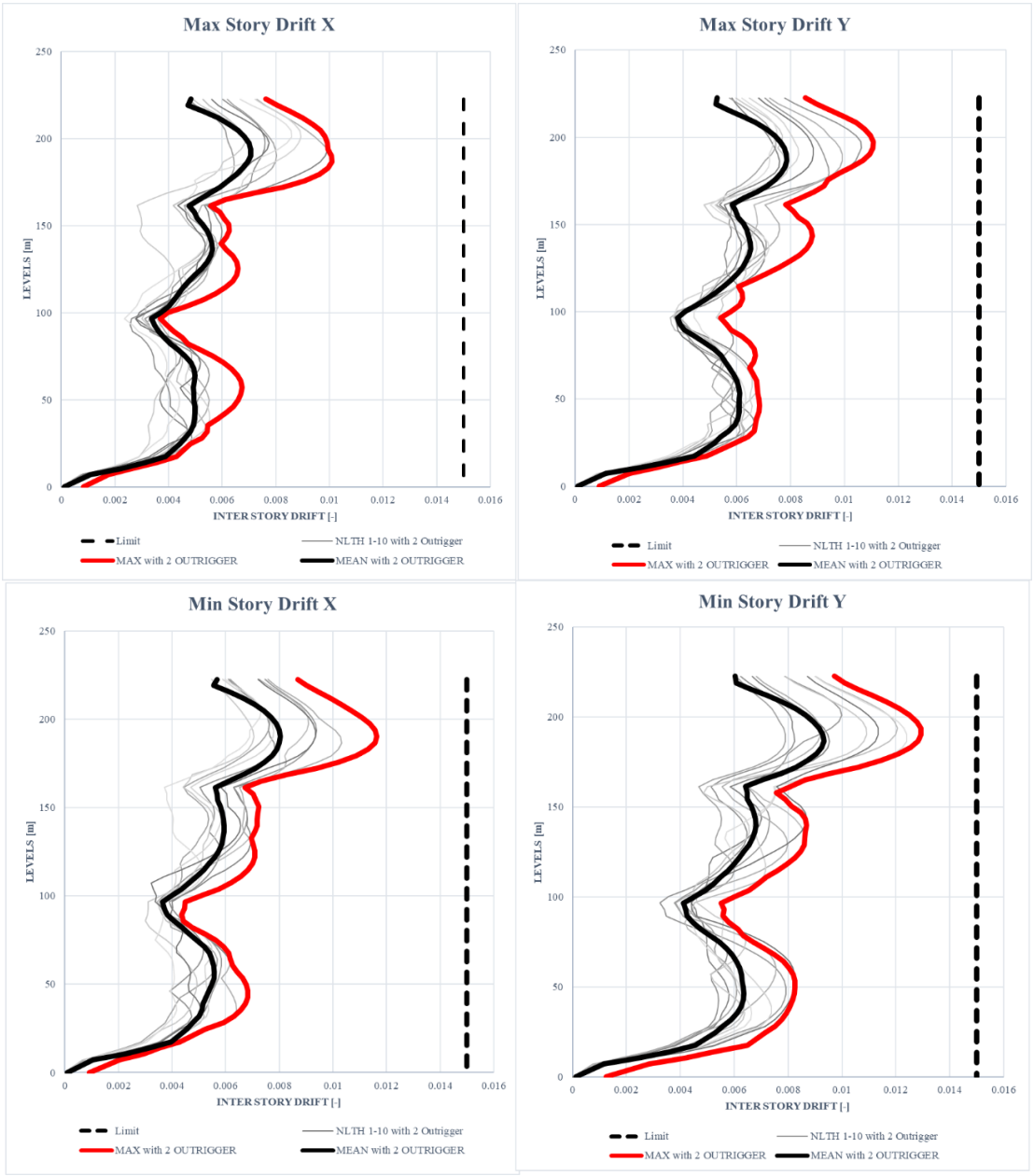

Figure 5. 68 Max and Min Interstory Drift - direction X and Y

You may notice that:

- considering the maximum drift value (in red), the threshold established by the CFE fulfils the acceptance criteria in the minimum drift conditions in both x and y direction;

- considering the mean value of drift (in black), interstory drift meets the overall acceptance criteria as it is lower than the limit value established by the standard.

The maximum values for drift are summarized in Table 5.33:

MAX X	DRIFT	MAX Y	DRIFT
with 2 OUTRIGGER	0.012	with 2 OUTRIGGER	0.013
MEAN X	**DRIFT**	**MEAN Y**	**DRIFT**
with 2 OUTRIGGER	0.008	with 2 OUTRIGGER	0.009

Table 5. 34 Maximum and mean drift values – Model 2 without Outriggers

Displacement: Figure 5.69 shows the results of the maximum and minimum value of the displacement, is in direction X that in direction Y for the considered signals.

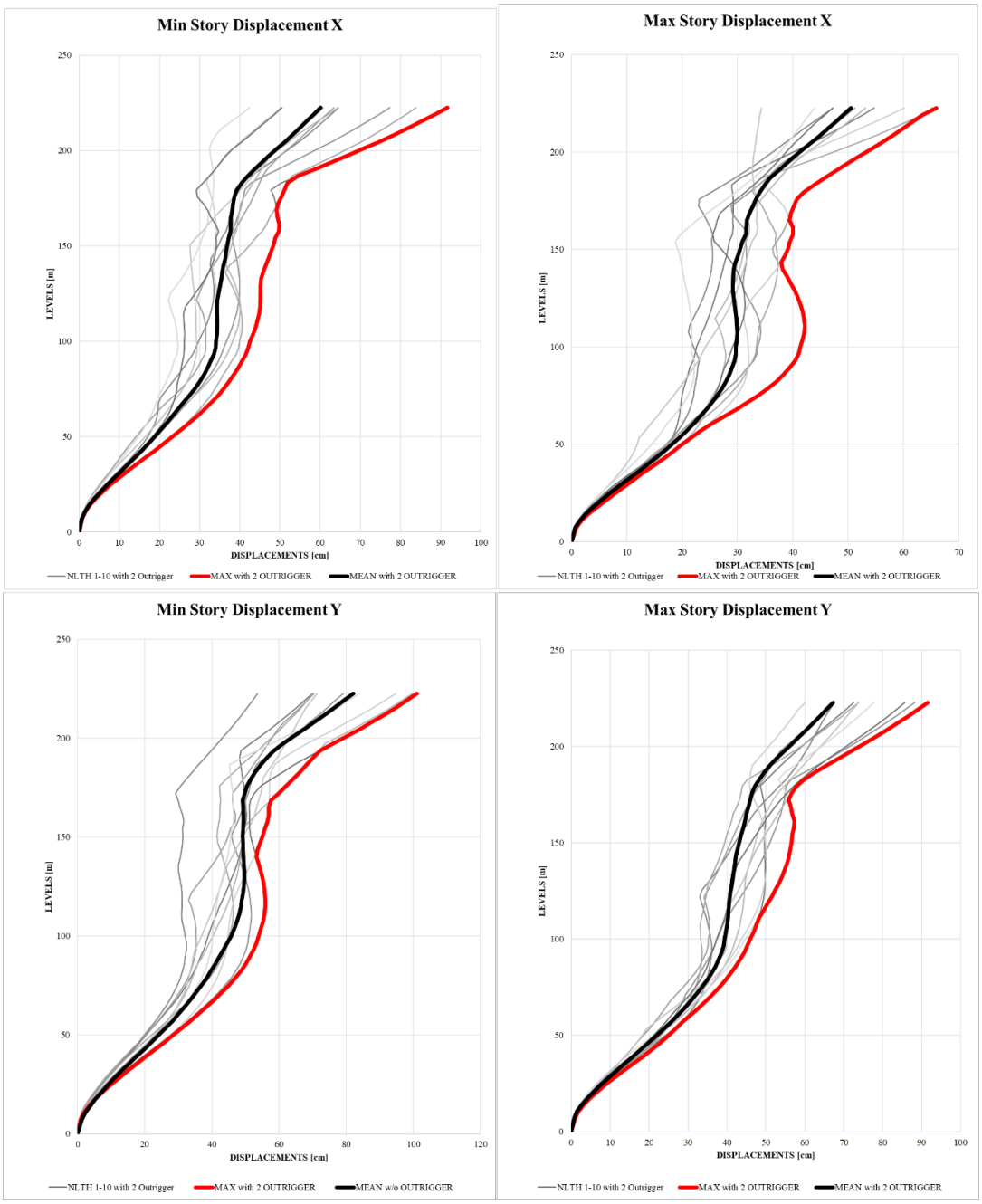

Figure 5. 69 Max and Min values of Displacement - direction X and Y

Table 5.34 summarizes the maximum and average values obtained for displacement:

MAX X	DISPLACEMENT	MAX Y	DISPLACEMENT
with 2 OUTRIGGER	91.62cm	with 2 OUTRIGGER	101.07cm
MEAN X	**DISPLACEMENT**	**MEAN Y**	**DISPLACEMENT**
with 2 OUTRIGGER	59.125cm	with 2 OUTRIGGER	76.553cm

Table 5. 35 Maximum and mean displacement values – Model 2 without Outriggers

Shear: Figure 5.70 shows the results of the maximum and minimum value of the cut, is in direction X that in direction Y for the considered signals.

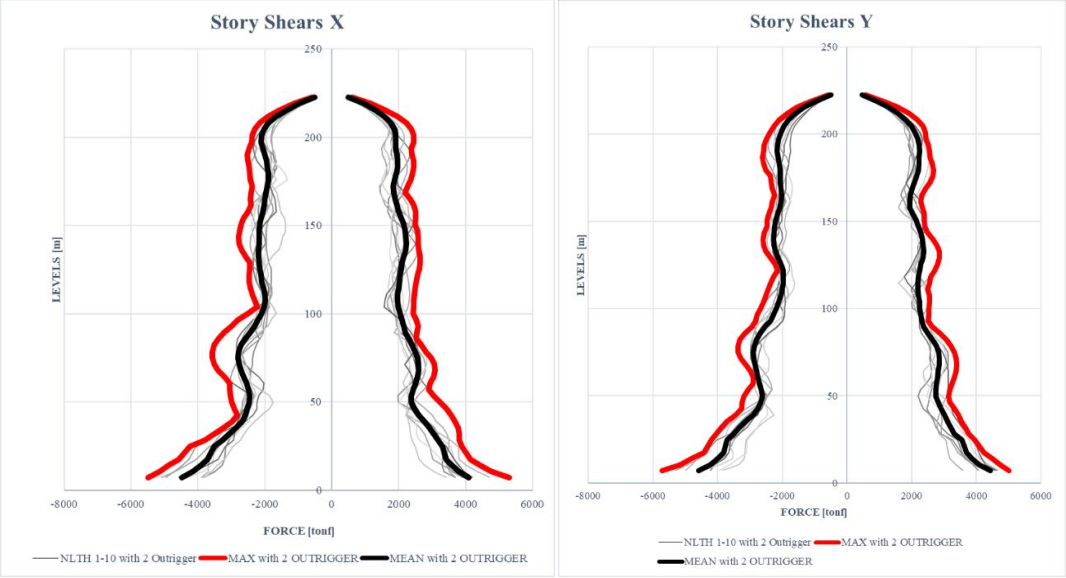

Figure 5. 70 Max and Min values of Story Shear - direction X and Y

Table 5.36 summarizes the maximum and average values obtained for cutting:

MAX X	SHEAR	MAX Y	SHEAR
with 2 OUTRIGGER	5301.95 tonf	with 2 OUTRIGGER	4996.54 tonf
MEAN X	**SHEAR**	**MEAN Y**	**SHEAR**
with 2 OUTRIGGER	4343.751 tonf	with 2 OUTRIGGER	4436.721 tonf

Table 5. 36 Maximum and mean shear values – Model 2 without Outriggers

Acceleration: Figure 5.71 shows the results of the maximum and minimum value of the acceleration, is in direction X that in direction Y for the considered signals:

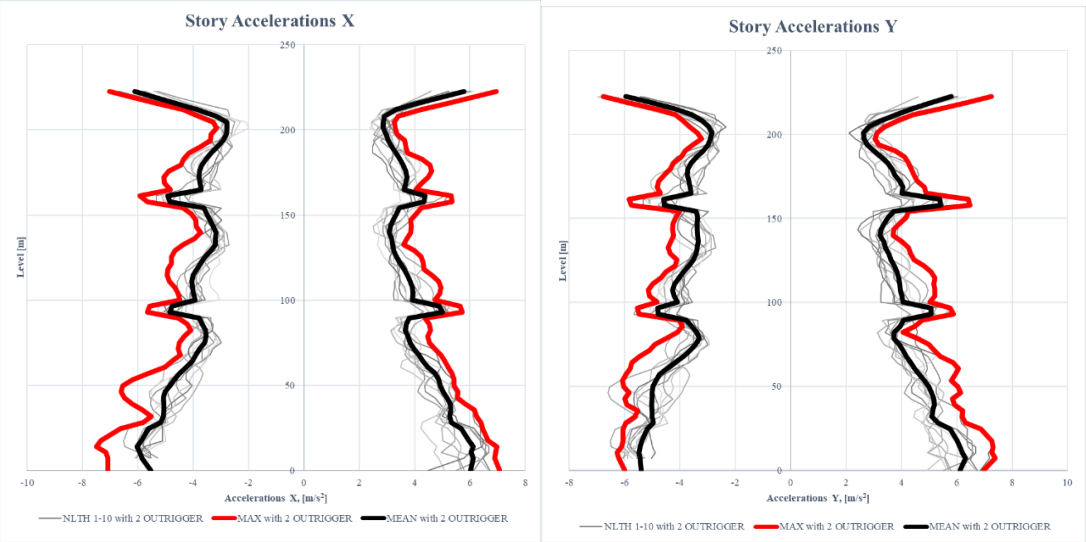

Figure 5. 71 Max and Min values of Story Acceleration - direction X and Y

Table 5.37 summarizes the maximum and average values obtained for acceleration:

MAX X	**ACCELERATION**	**MAX Y**	**ACCELERATION**
with 2 OUTRIGGER	7.06 m/s²	with 2 OUTRIGGER	7.38 m/s²
MEAN X	**ACCELERATION**	**MEAN Y**	**ACCELERATION**
with 2 OUTRIGGER	6.419 m/s²	with 2 OUTRIGGER	6.423 m/s²

Table 5. 37 Maximum and mean acceleration values – Model 2 without Outriggers

It was also evaluated how the maximum acceleration varies in coverage as a function of time taking into account an accelerogram taken from the 10 seismic signals provided. In figure 5.72 it is possible to visualize the result for the signal 2.

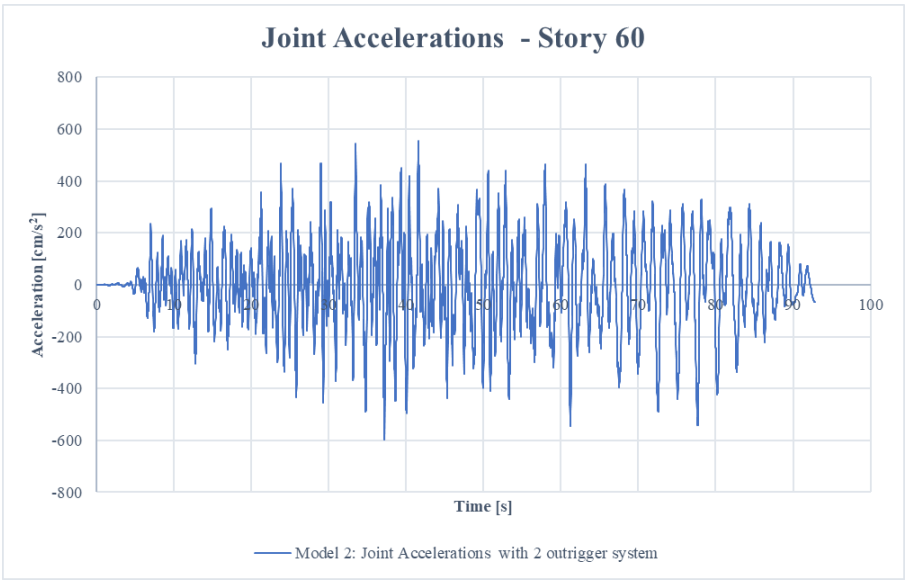

Figure 5. 72 Joint Accelerations with 2 outrigger system

In conclusion, the results of the non-linear analysis meet the criteria of global acceptance. Finally, it is necessary to verify that the property meets the local acceptance criteria. Therefore, plastic rotations in structural elements (beams, pillars and walls) and vertical displacements in SLB devices must be lower than the collapse prevention value (CP). The numerical acceptance criteria for beams and pillars, as described in section 7.2, by ASCE 41-13, while the maximum horizontal displacement for SLB devices is 60 mm.

Table 5.38 shows the maximum and average CP demand ratios of each structural element. The maximum D/C ratio is calculated on the results of the single nonlinear chronological analysis, while on the results the average D/C ratio of the entire set of accelerograms is calculated.

Element	**Mean D/C for CP**	**Max D/C for CP**
[-]	[-]	[-]
Beam	0.129	0.161
Column	0	0
Wall	0.079	0.089
SLB device	0.618	0.836

Table 5. 38 Model 3: Mean and Maximum D/C ratios for Collapse Prevention (CP)

The status of plastic hinges is shown according to the immediate performance levels of occupation (IO), safety of life (LS), prevention of collapse (CP). According to Table 10-8 of ASCE/SEI 41-13 the performance levels are related to the plastic rotation angle (radians) this depends on the breaking condition and the amount of steel reinforcement. For this reason, the plastic hinges developed by the structure have reached the performance level of immediate occupation (IO) without reaching the level of live safety (LS). Figure 5.73 shows the hysterical response of the plastic hinge for a generic beam

Figure 5.74 shows the hysterical response of the plastic hinge for a generic wall. Figures 5.75 and 5.76 show the hysteretic response of the plastic hinge for the SLB device, where the maximum displacement of the SLB device whose hysteretic behaviour has been plotted to verify its displacement.

- K13 refers to the device in the first band of Outrigger and shows a maximum displacement of 49,02mm;

- K16 refers to the device in the second band of Outrigger which shows a maximum displacement of 53,57mm;

It can therefore be inferred that the hysteretic behavior of the link has a greater shift in the second band of Outrigger than the first.

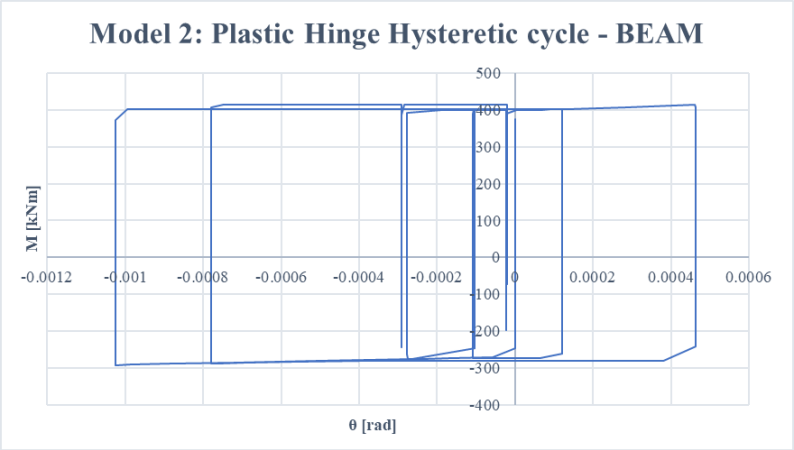

Figure 5. 73 Model 2: Plastic Hinge Hysteretic cycle - BEAM

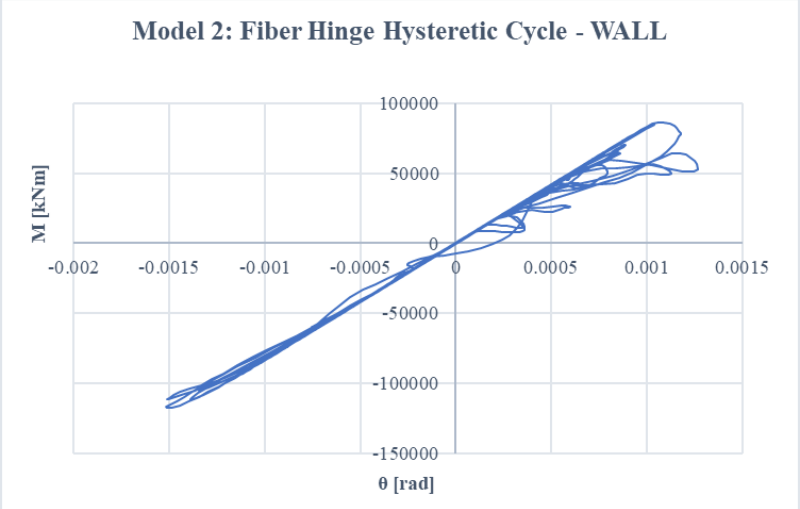

Figure 5. 74 Model 2: Fiber Hinge Hysteretic Cycle - WALL

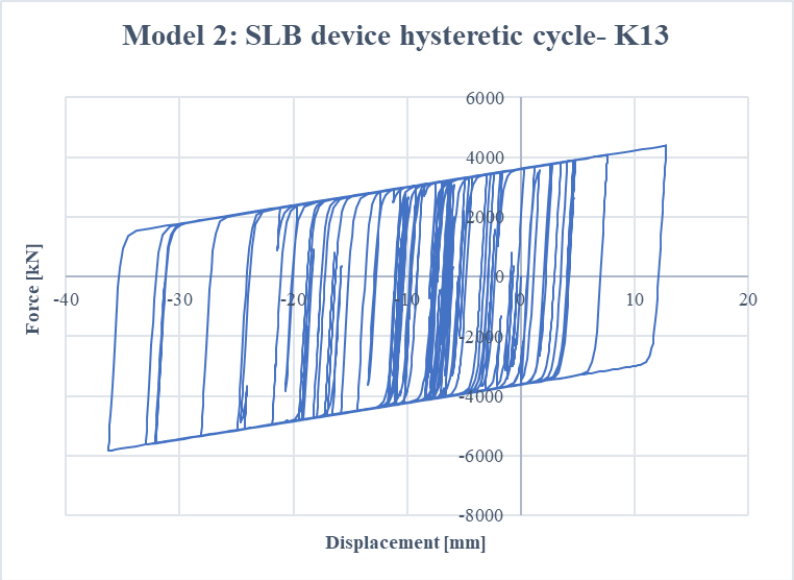

Figure 5. 75 Model 2: SLB device hysteretic cycle- K13

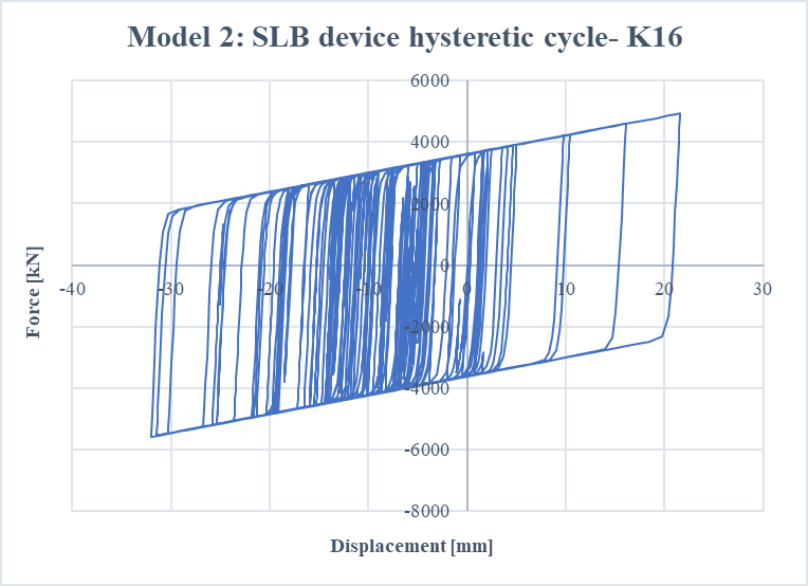

Figure 5. 76 Model 2: SLB device hysteretic cycle- K16

5.7 MODEL3: Structure with 3 Outriggers and SLB design

5.7.1 Outrigger design

This section describes the analysis for a third model presenting 3 Outrigger systems. At the position previously analyzed in the model 2, a third system is added at the top, to evaluate whether the position at the apex of the building can improve the displacement to the last scaffold, as well as the acceleration in coverage.

More precisely the model analyzed in this paragraph presents the system in the positions in figure 5.77:

- The first Outrigger system was applied in the double height between story 24 and 25, at a height of 93.00 meters;
- The second Outrigger system was applied in the double height between story 42 and 43, at a height of 157.80 meters;
- The third Outrigger system was applied to Story 59, at a height of 219.00 meters.

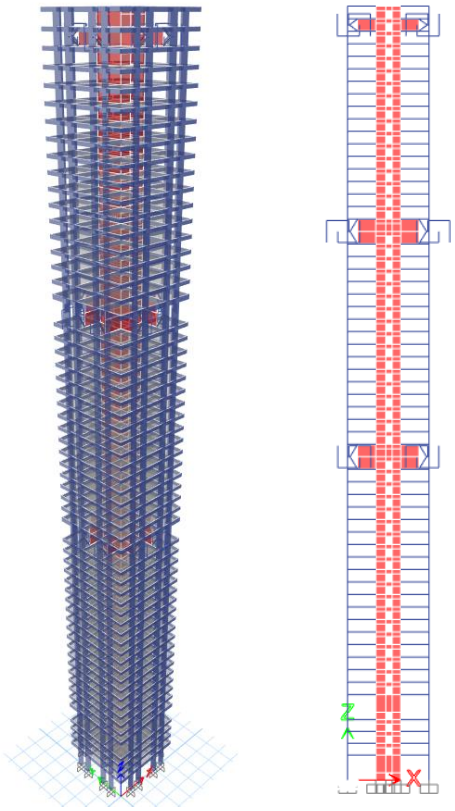

Figure 5. 77 Model 3: Position of the outrigger system

The presence of the Outrigger system also determines the need for stiffening of the wall in the application level, for this reason the structural elements such as columns and beams always maintain the same geometric dimensions, but the wall increases in section and more precisely we see in table 5.39 :

Level	**Wall Section**	**s**	**Concrete**	**f_{ck}**
[-]	**[-]**	**[cm]**	**[-]**	**[Mpa]**
Story60	M 50	50	C55	55
Story59	M 60	60	C55	55
Story58	M 50	50	C55	55
Story57	M 50	50	C55	55

Story56	M 50	50	C55	55
Story55	M 50	50	C55	55
Story54	M 50	50	C55	55
Story53	M 50	50	C55	55
Story52	M 50	50	C55	55
Story51	M 50	50	C55	55
Story50	M 50	50	C55	55
Story49	M 50	50	C55	55
Story48	M 50	50	C55	55
Story47	M 50	50	C55	55
Story46	M 50	50	C55	55
Story45	M 50	50	C55	55
Story44	M 60	60	C55	55
Story43	M 70	70	C55	55
Story42	M 70	70	C55	55
Story41	M 60	60	C55	55
Story40	M 60	60	C55	55
Story39	M 60	60	C55	55
Story38	M 60	60	C55	55
Story37	M 60	60	C55	55
Story36	M 60	60	C55	55
Story35	M 60	60	C55	55
Story34	M 60	60	C55	55
Story33	M 60	60	C55	55
Story32	M 60	60	C55	55
Story31	M 60	60	C55	55
Story30	M 60	60	C55	55
Story29	M 60	60	C55	55
Story28	M 60	60	C55	55
Story27	M 60	60	C55	55
Story26	M 60	60	C55	55
Story25	M 70	70	C65	65
Story24	M 70	70	C65	65
Story23	M 60	60	C65	65
Story22	M 60	60	C65	65
Story21	M 60	60	C65	65
Story20	M 60	60	C65	65
Story19	M 60	60	C65	65
Story18	M 60	60	C65	65
Story17	M 60	60	C65	65
Story16	M 60	60	C65	65
Story15	M 60	60	C65	65

Story14	M 60	60	C65	65
Story13	M 60	60	C65	65
Story12	M 60	60	C65	65
Story11	M 60	60	C65	65
Story10	M 60	60	C65	65
Story9	M 60	60	C65	65
Story8	M 60	60	C65	65
Story7	M 60	60	C65	65
Story6	M 60	60	C65	65
Story5	M 60	60	C65	65
Story4	M 60	60	C65	65
Story3	M 60	60	C65	65
Story2	M 60	60	C65	65
Story1	M 70	70	C65	65

Table 5. 39 Model 3: Wall Section

5.7.2 SLB design

The selection procedure of SLB devices was performed using the direct iteration method described in paragraph 4.4.1 , obtaining an initial set of devices. Then the optimal solution was achieved by reducing the size of the heatsinks with a series of nonlinear chronological analysis considering only the non-linear behavior of the heatsinks.

The optimal solution for each Outrigger system is to install two SLB4_65_20 (see Table 5.25), for a total of 24 devices.

5.7.3 Modal analysis

The first step to follow, as previously done for the bare frame structure and for the structure with 2 Outrigger and SLB system, is to define a modal analysis with the aim of studying the dynamic behavior of the structure with the presence of 2 Outrigger systems. Table 5.40 shows the periods and the participating mass of the first three natural modes of vibration of the structure, as well as the way it presents 90% of the participating mass. The results are obtained by considering the actual stiffness values seen in paragraph 5.4.2.

Mode	Period	U_X	U_Y	R_Z	$SumU_X$	$SumU_Y$	$SumR_Z$
[-]	sec	[-]	[-]	[-]	[-]	[-]	[-]
1	8.815	0.00%	68.00%	0.00%	0.00%	68.00%	0.00%
2	8.739	68.00%	0.00%	0.00%	68.00%	68.00%	0.00%
3	3.221	0.00%	0.00%	81.00%	68.00%	68.00%	81.00%
10	0.616	0.00%	3.00%	0.00%	89.00%	93.00%	94.00%

Table 5. 40 Modal analysis results for structure with 3 Outrigger and SLB system

It is possible to observe that the first two modes are translational, while the third mode is rotational, to be precise, the first is translational along Y with 68% of participating mass, the second along X with 68% of participating mass, finally the third rotational around Z, with 81% participating mass.

Figure 5. 78 1st mode

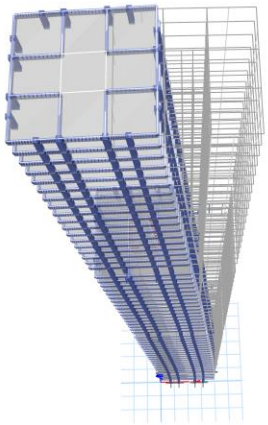

Figure 5. 79 2st mode

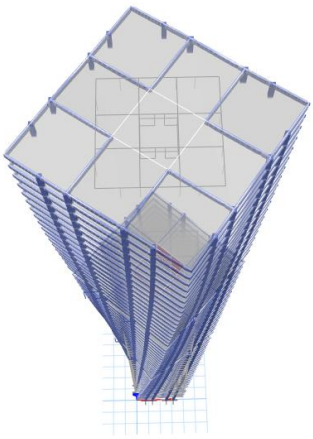

Figure 5. 80 3st mode

The fondamental period is 8.81 seconds, an acceptable value for 60 floors of a reinforced concrete building, while 90% of the participating mass ratio is achieved in all directions considering the first 10 natural modes of structure vibration.

5.7.4 Response spectrum analysis

The next step is to verify the structure at the Collapse Level Earthquake according to the requirements of the CFE, ie defining a limit to 0.015 as required by the standard. The interstory-drift results for the collapse condition, in the X and Y direction are given in Figure 5.81.

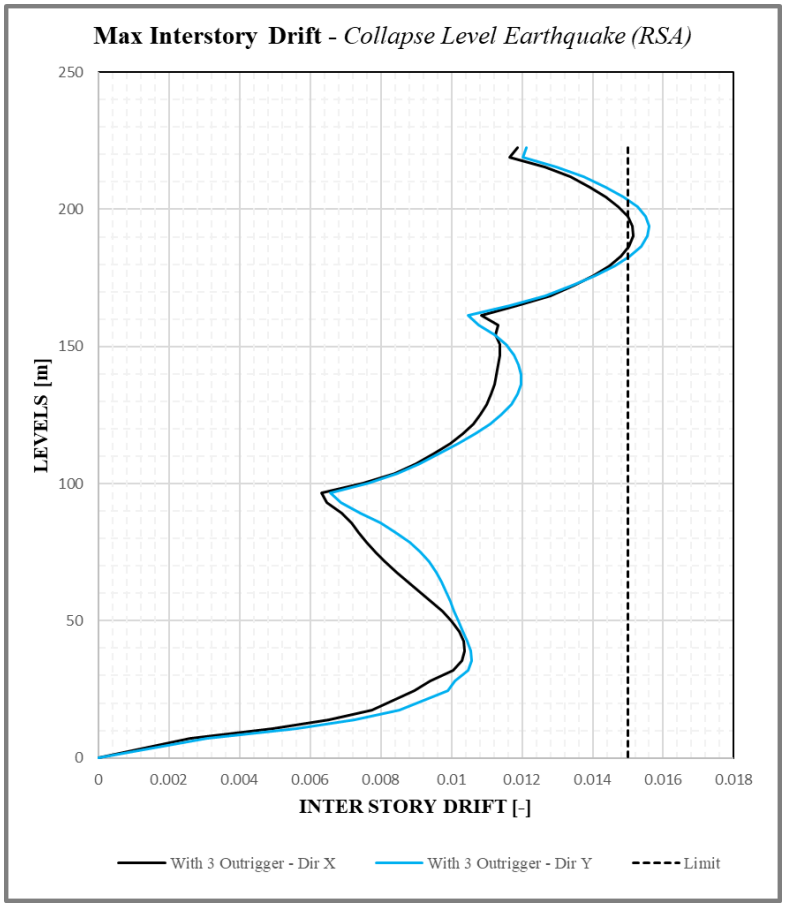

Figure 5. 81 Max Interstory Drift at Collapse Level Earthquake (RSA)

The maximum values in the X and Y direction for drift in the collapse condition are given in Table 5.41:

MAX X	DRIFT	MAX Y	DRIFT
with 3 OUTRIGGER	0.015	with 3 OUTRIGGER	0.016

Table 5. 41 Maximum drift values (Collapse-RSA)

The interstory-drift results are also analyzed for the condition of Service Level Earthquake that, according to the requirements of the CFE, has an acceptable maximum limit of 0.004. Below in Figure 5.82 are the values obtained for the service condition, in direction X and Y.

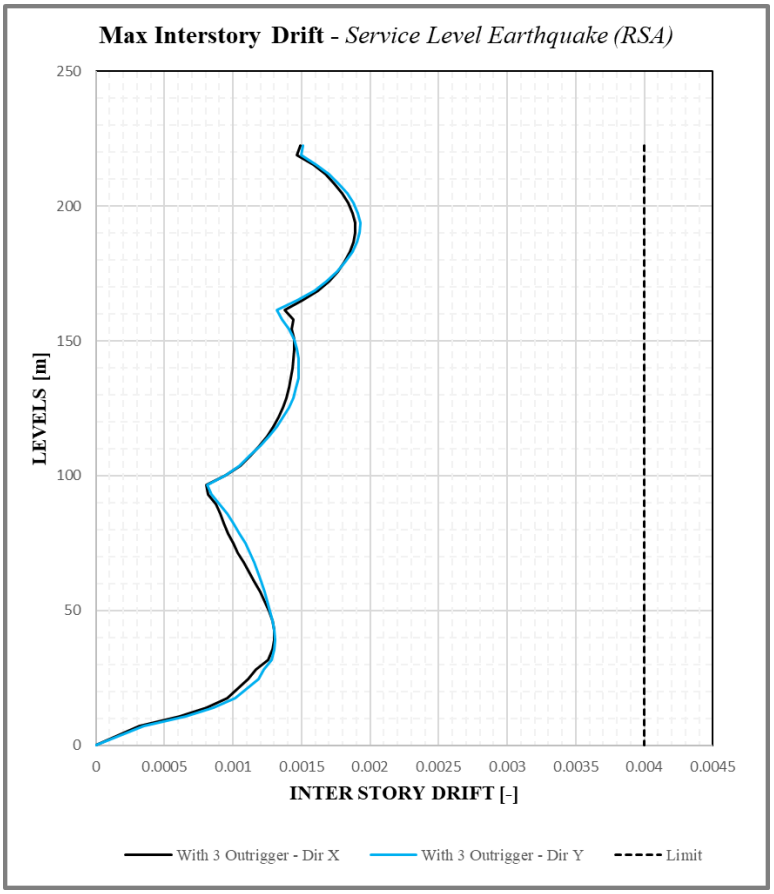

Figure 5. 82 Max Interstory Drift at Service Level Earthquake (RSA)

Table 5.42 shows the maximum values in X and Y direction for drift in Service condition:

MAX X	DRIFT	MAX Y	DRIFT
with 3 OUTRIGGER	0.002	with 3 OUTRIGGER	0.002

Table 5. 42 Maximum drift values (Service-RSA)

It is possible to note that with linear analysis the response in terms of drift in collapse conditions is at the limit in x direction, while in Y direction exceeds the limit defined by the regulations,in the condition of service instead lies within the limit prescribed by law.

The results for displacement in the collapse condition, in the X and Y direction are given in Figure 5.83.

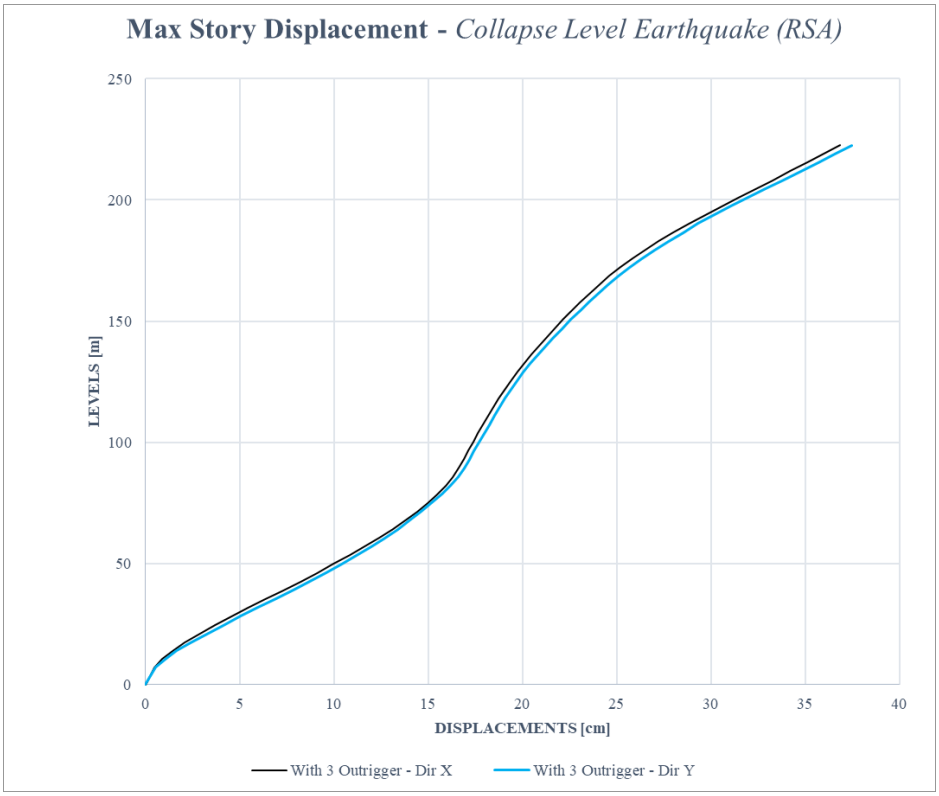

Figure 5. 83 Max Interstory Displacement at Collapse Level Earthquake (RSA)

Table 5.43 shows the maximum values in the X and Y direction for displacement in the Collapse condition:

MAX X	DISPLACEMENT	MAX Y	DISPLACEMENT
with 3 OUTRIGGER	36.84cm	with 3 OUTRIGGER	37.44cm

Table 5. 43 Maximum displacement values (Collapse - RSA)

The results for displacement in service, direction X and Y are given in Figure 5.84.

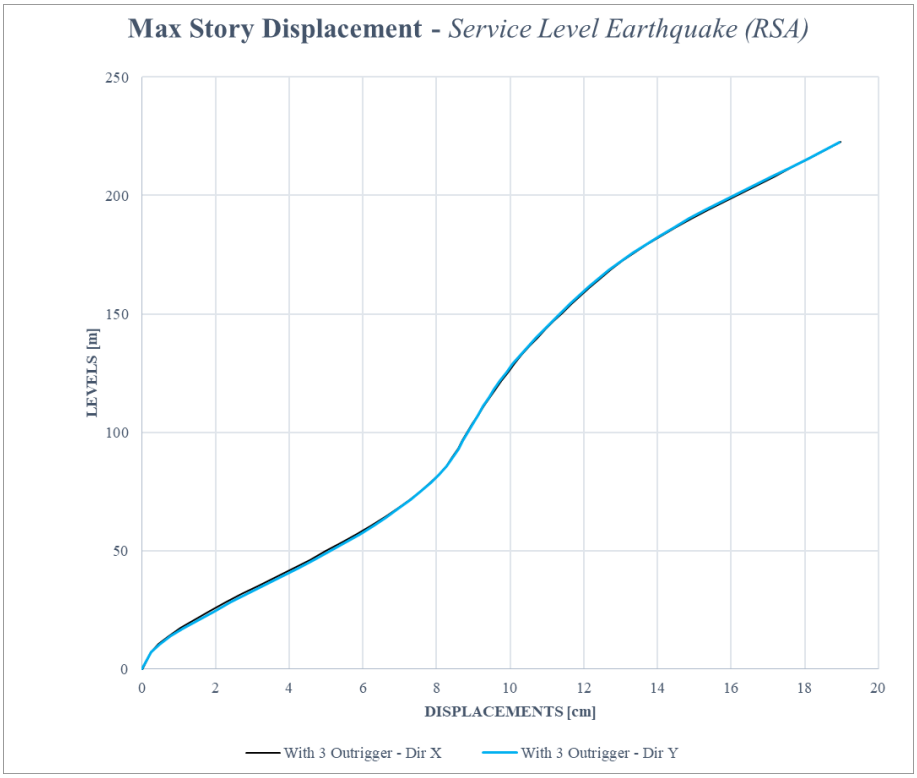

Figure 5. 84 Max Interstory Displacement at Service Level Earthquake (RSA)

Table 5.44 shows the maximum values in X and Y direction for displacement in the Service condition:

MAX X	DISPLACEMENT	MAX Y	DISPLACEMENT
with 3 OUTRIGGER	18.98cm	with 3 OUTRIGGER	18.95cm

Table 5. 44 Maximum displacement values (Service- RSA)

The results for Shear in collapse condition, in X and Y direction are given in Figure 5.85.

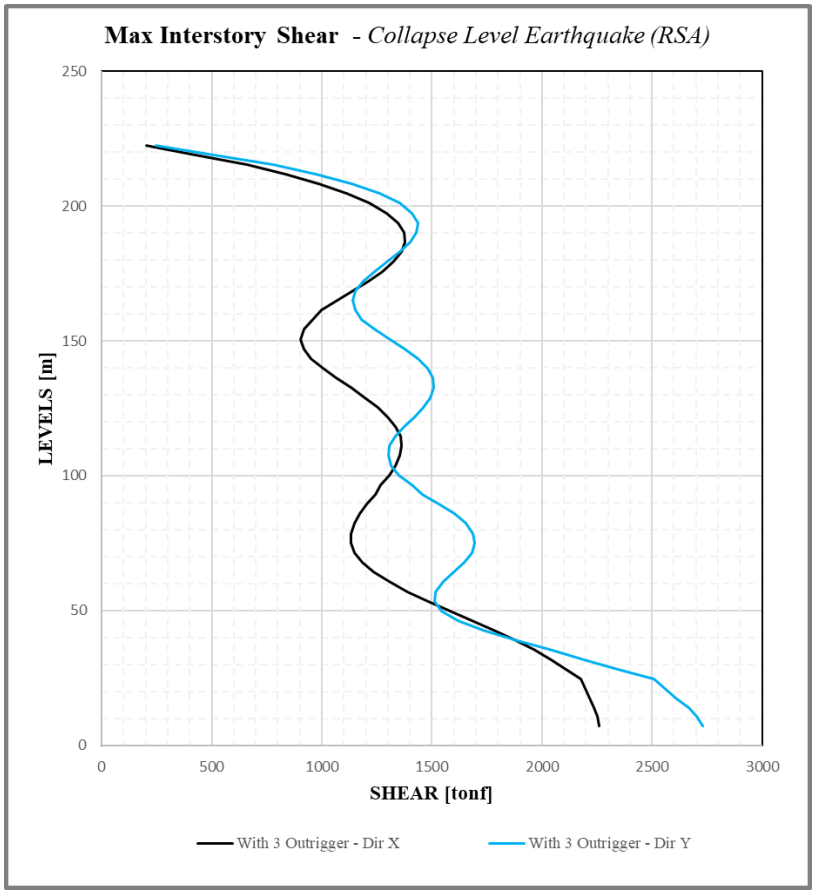

Figure 5. 85 Max Interstory Shear at Collapse Level Earthquake (RSA)

Table 5.45 shows the maximum values in the X and Y direction for the shear in the Collapse condition:

MAX X	SHEAR	MAX Y	SHEAR
with 3 OUTRIGGER	2259.06 tonf	with 3 OUTRIGGER	2729.84 tonf

Table 5. 45 Maximum shear values (Collapse - RSA)

The results for Shear in service condition, in X and Y direction are shown in Figure 5.86.

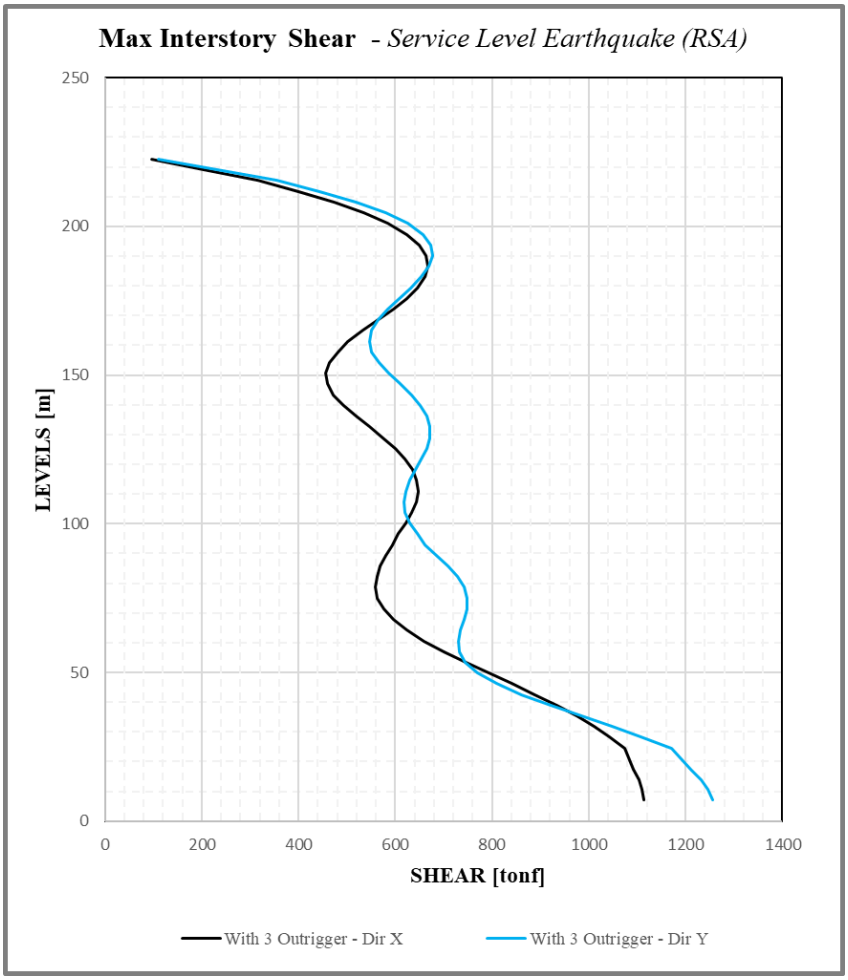

Figure 5. 86 Max Interstory Shear at Service Level Earthquake (RSA)

Table 5.46 shows the maximum values in the X and Y direction for the shear in the Service condition:

MAX X	SHEAR	MAX Y	SHEAR
with 3 OUTRIGGER	1113.14 tonf	with 3 OUTRIGGER	1256.61 tonf

Table 5. 46 Maximum shear values (Service- RSA)

5.7.5 Reinforcement design

This section describes the procedure for defining the design of the reinforcement of structural elements (beams, columns and walls) after the verification of the structure at collapse level. The steel reinforcement was calculated with a traditional method of capacity design approach, following ACI 318-19 requirements, considering the maximum stresses in structural elements due to gravitational loads and combinations of seismic loads. The effects of seismic loads on the structure were calculated with

the Response Spectrum Analysis (RSA) using the inelastic design spectrum introduced in Figure 5.9.

The beam reinforcement design is conducted by dividing the structural element into three parts, as shown in Figure 5.87, two end sections where plastic hinges are expected to form, and a middle section where the stresses due to gravity and seismic loads are generally lower and therefore less steel is required.

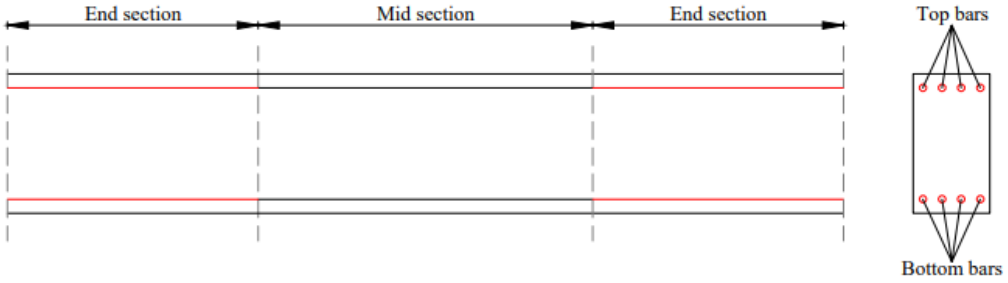

Figure 5. 87 Subdivision of the beam for the reinforcement design

The reinforcement design for the column is summarised in Table 5.46 where the minimum amount of steel reinforcement is present for the column sections and obtained from the design procedure. The coefficient ρ_s represents the total geometric percentage of the reinforcement, defined as:

$$\rho_s = \frac{A_s}{A_c}$$

That is the ratio between the total area of the existing reinforcement and the area of the concrete section.

ColumnSection	**b**	**h**	**A_c**	**φ**	**Num. Ofbars**	**$A_{s,tot}$**	**ρ_s**	
[-]	**[cm]**	**[cm]**	**[cm^2]**	**[mm]**	**[-]**	**[cm^2]**	**[-]**	
C 90X160	90	160	14400	804.3	32	25737.6	1.79	%
C 90X140	90	140	12600	490.9	34	16690.6	1.32	%
C 90X120	90	120	10800	490.9	24	11781.6	1.09	%
C90X140	90	140	12600	804.3	52	41823.6	3.32	%
C 90X120	90	120	10800	490.9	32	15708.8	1.45	%
C 90X100	90	100	9000	490.9	20	9818	1.09	%

Table 5. 47 Reinforcement design for structure with 3 Outrigger system and SLB - Column sections

The design of the reinforcement for the wall considers the coefficient ρl indicating the longitudinal dimension, which is given by:

$$\rho_l = \frac{2As_l}{E_w * s_l}$$

Dove:

- As_l is the longitudinal reinforcement area of the wall;
- E_w is the wall thickness;
- s_l is the center to center spacing of horizontal bars;

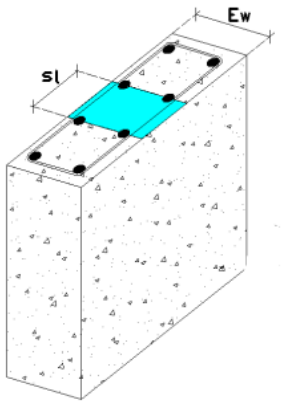

Figure 5. 88 Wall section

5.7.6 Nonlinear Time History Analysis

The ETABS software was used to perform nonlinear chronological analyses, considering the P-Delta geometric non-linearity. Gravitational loads were applied in the initial phase of the analysis as a non-linear static case. In each load case, the accelerations were combined in the U1 and U2 directions in order to evaluate the non-linear behavior of the structure, Figure 5.89.

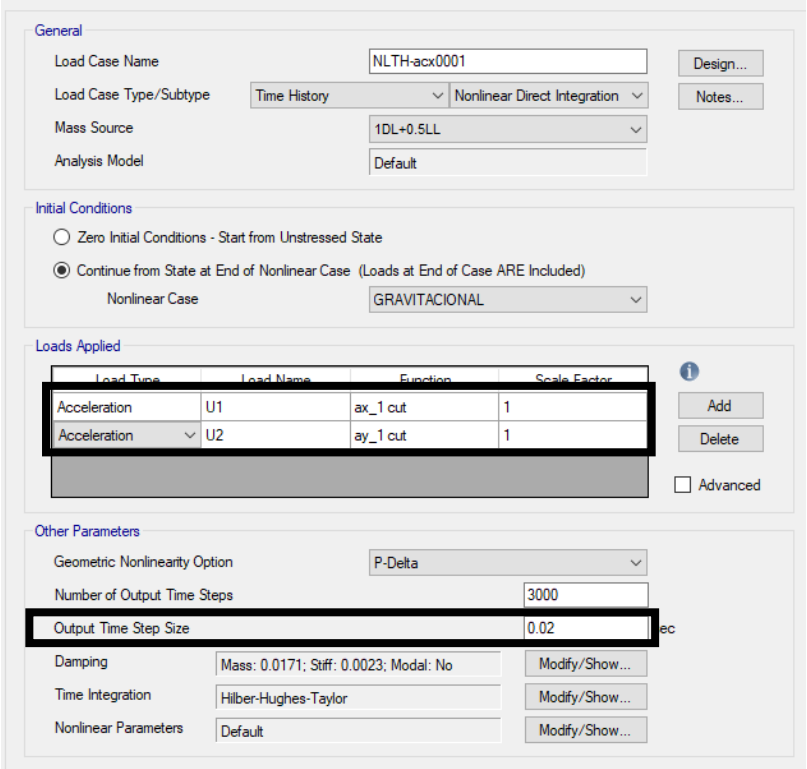

Figure 5. 89 Setting nonlinear time history analysis - ETABS

Damping has been defined as described in paragraph 5.4.2, namely by setting the same modal damping ratio (ξi = 1.3%) in two different natural periods of the structure, that is, they correspond to the first modal period and the period necessary to reach 90% participating mass in all directions, Figure 5.90.

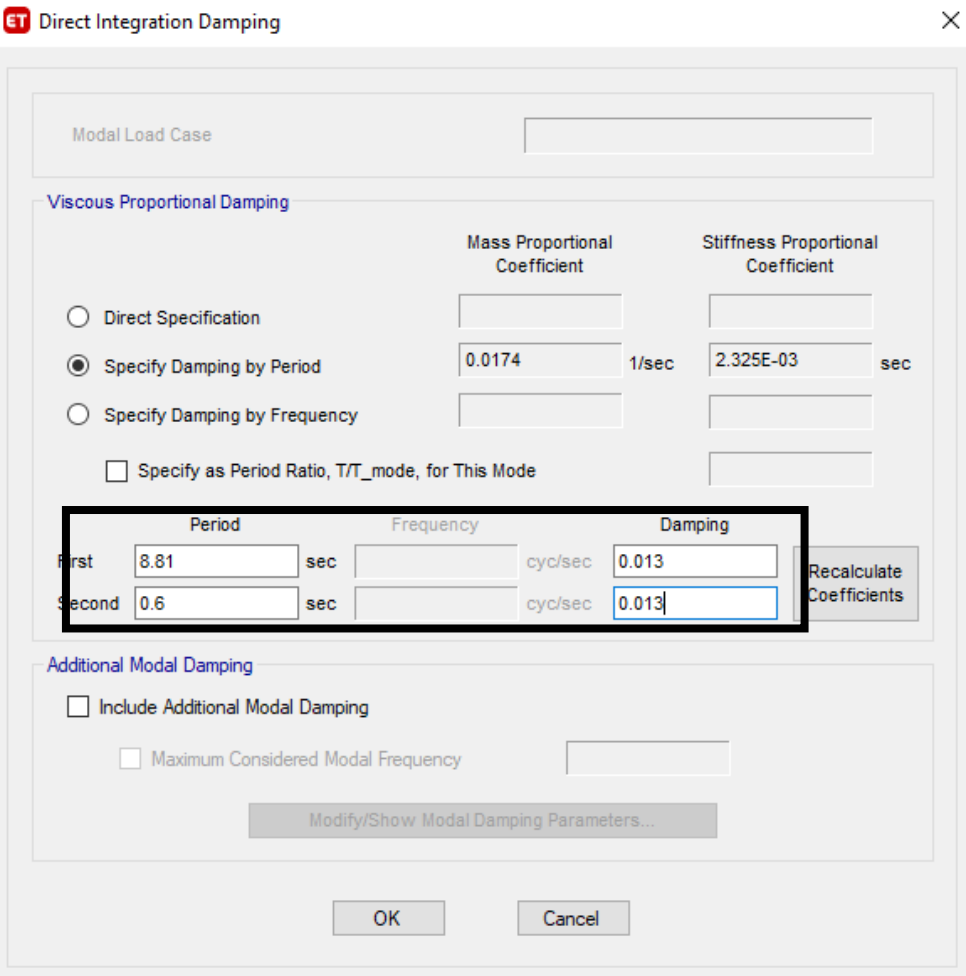

Figure 5. 90 Damping coefficients for Nonlinear time history analysis - ETABS

The set of 10 seismic signals has been used to perform the non-linear analysis, from these are considered the values both average (according to the CFE standard) and maximum (according to the Mexican standard) to evaluate the global and local acceptance criteria. Moreover the results of the drift, the displacement, the shear and the acceleration in cover for the considered structure will be analyzed and subsequently compared.

❖ OUTPUT

Drift: Figure 5.91 shows the results of the maximum and minimum value of the interstory drift, is in direction X that in direction Y for the considered signals.

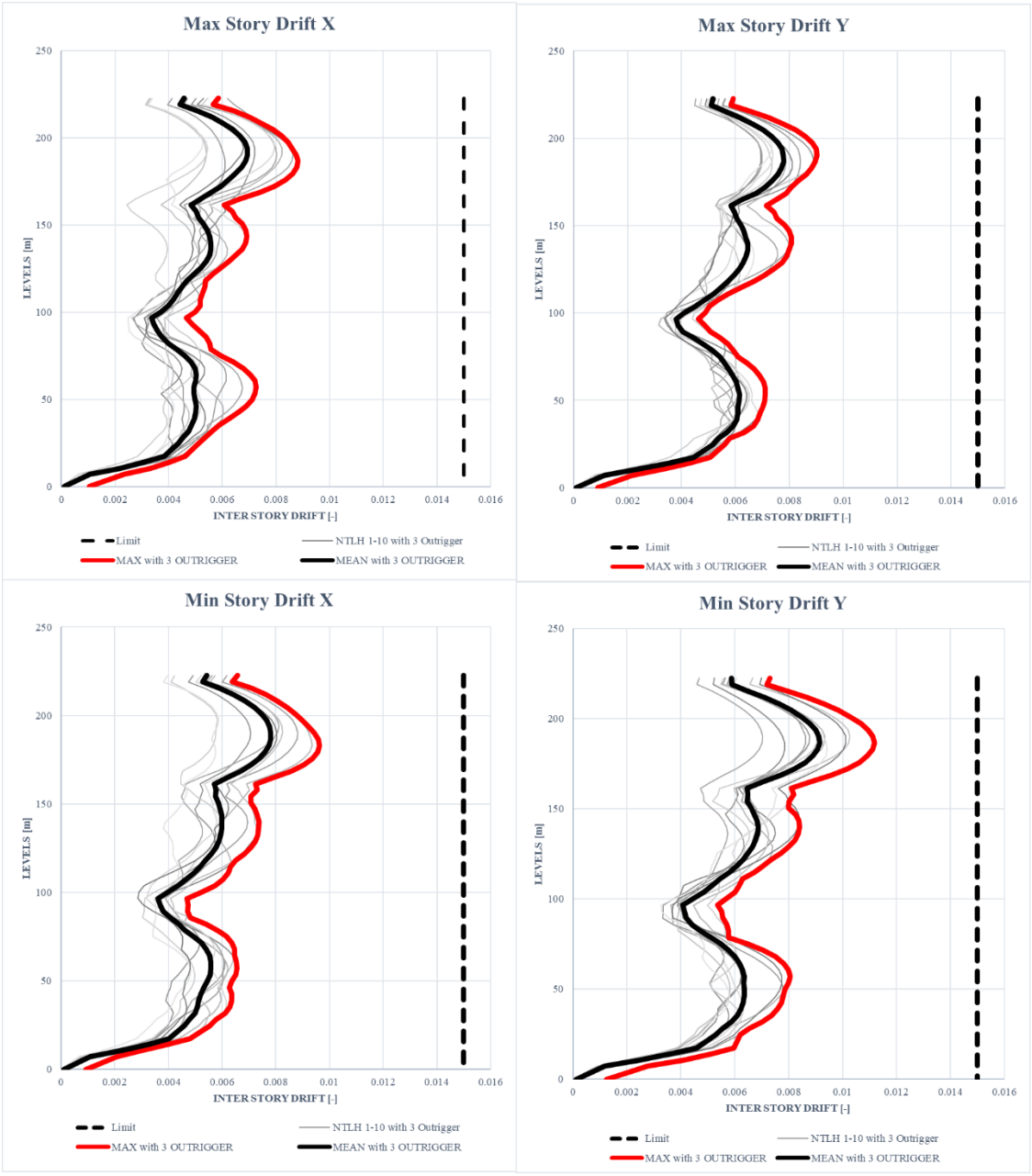

Figure 5. 91 Max and Min Interstory Drift - direction X and Y

You may notice that:

- considering the maximum drift value (in red), the threshold established by the CFE fulfils the acceptance criteria in the minimum drift conditions in both x and y direction;

- considering the mean value of drift (in black), interstory drift meets the overall acceptance criteria as it is lower than the limit value established by the standard.

Table 5.48 summarizes the maximum values obtained for drift:

MAX X	DRIFT	MAX Y	DRIFT
with3 OUTRIGGER	0.010	with3 OUTRIGGER	0.011
MEAN X	**DRIFT**	**MEAN Y**	**DRIFT**
with3 OUTRIGGER	0.011	with3 OUTRIGGER	0.013

Table 5. 48 Maximum and mean drift values – Model 3 without Outriggers

Displacement: Figure 5.92 shows the results of the maximum and minimum value of the displacement, is in direction X that in direction Y for the considered signals.

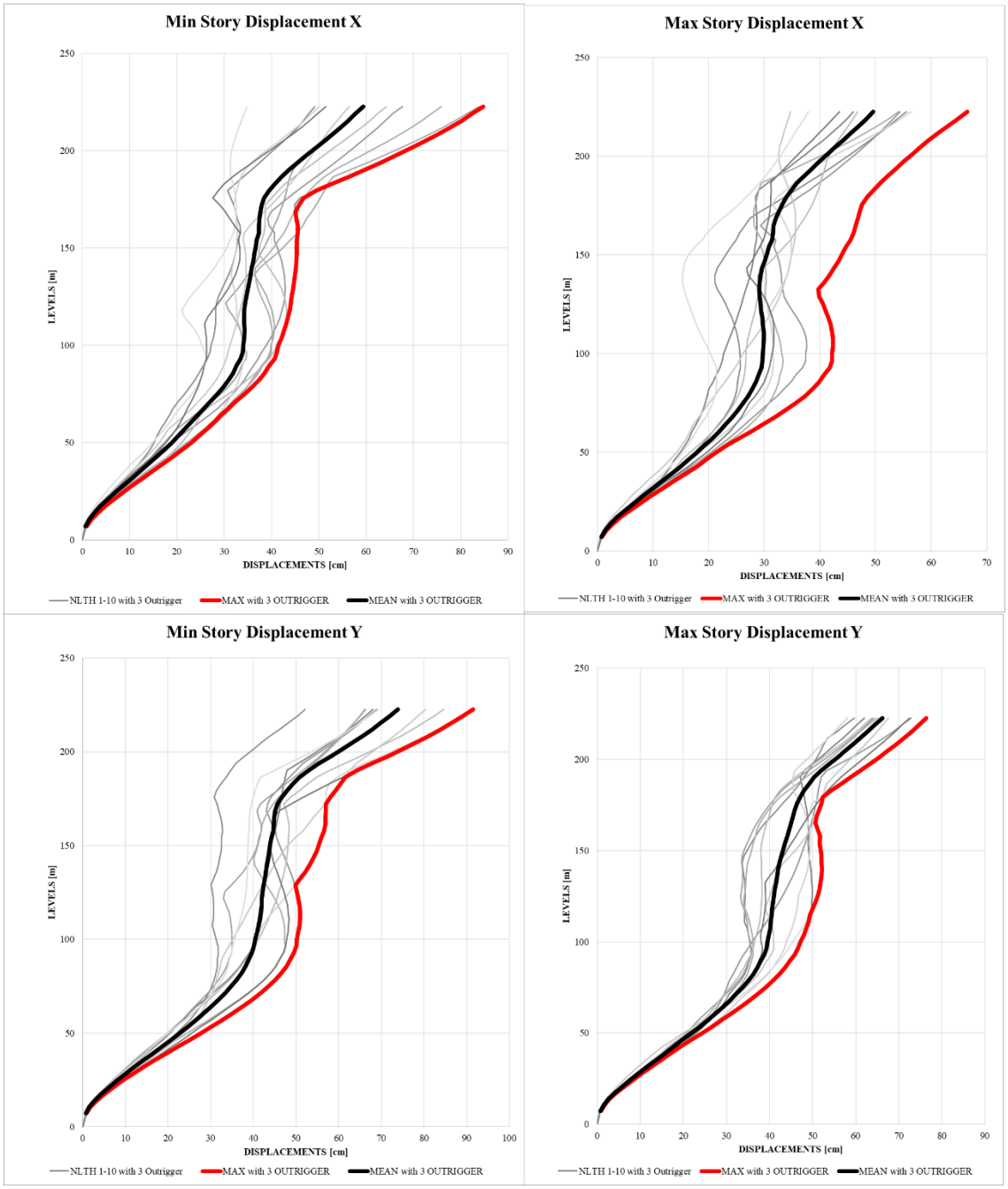

Figure 5. 92 Max and Min values of Displacement - direction X and Y

Table 5.48 summarizes the maximum and average values obtained for displacement:

MAX X	DISPLACEMENT	MAX Y	DISPLACEMENT
with3 OUTRIGGER	84.74 cm	with3 OUTRIGGER	91.55 cm
MEAN X	**DISPLACEMENT**	**MEAN Y**	**DISPLACEMENT**
with3 OUTRIGGER	72.073 cm	with3 OUTRIGGER	88.746 cm

Table 5. 49 Maximum and mean displacement values – Model 3 without Outriggers

Shear: Figure 5.93 shows the results of the maximum and minimum value of the shear, is in direction X that in direction Y for the considered signals.

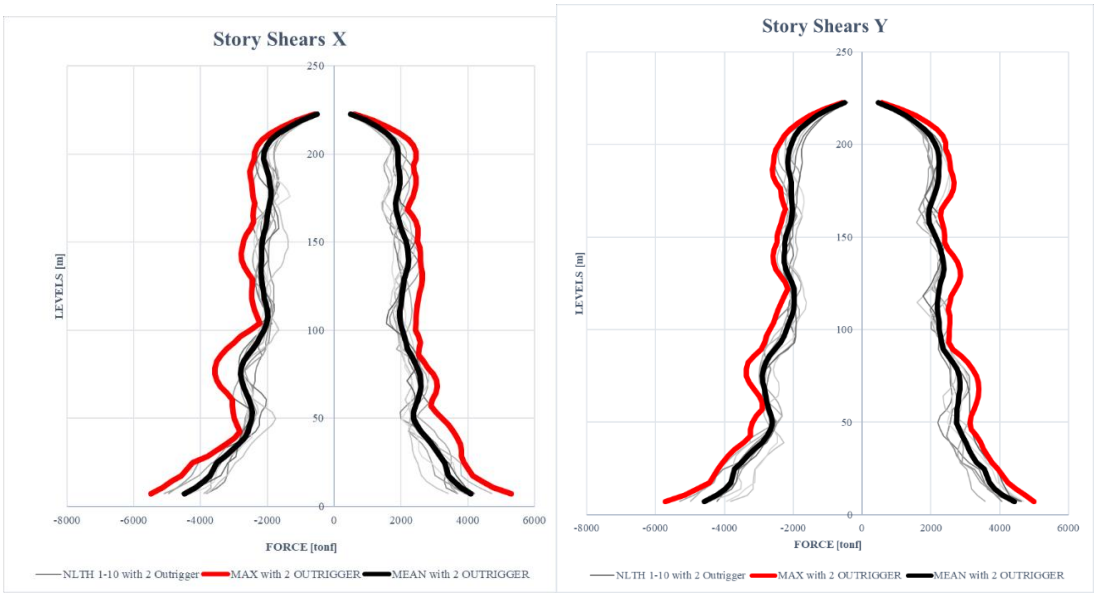

Figure 5. 93 Max and Min values of Story Shear - direction X and Y

Table 5.50 summarizes the maximum and average values obtained for shear:

MAX X	SHEAR	MAX Y	SHEAR
with3 OUTRIGGER	5124.74 tonf	with3 OUTRIGGER	5177.84 tonf
MEAN X	**SHEAR**	**MEAN Y**	**SHEAR**
with3 OUTRIGGER	5018.886 tonf	with3 OUTRIGGER	5151.142 tonf

Table 5. 50 Maximum and mean shear values – Model 3 without Outriggers

Acceleration: Figure 5.94 shows the results of the maximum and minimum value of the acceleration, is in direction X that in direction Y for the considered signals:

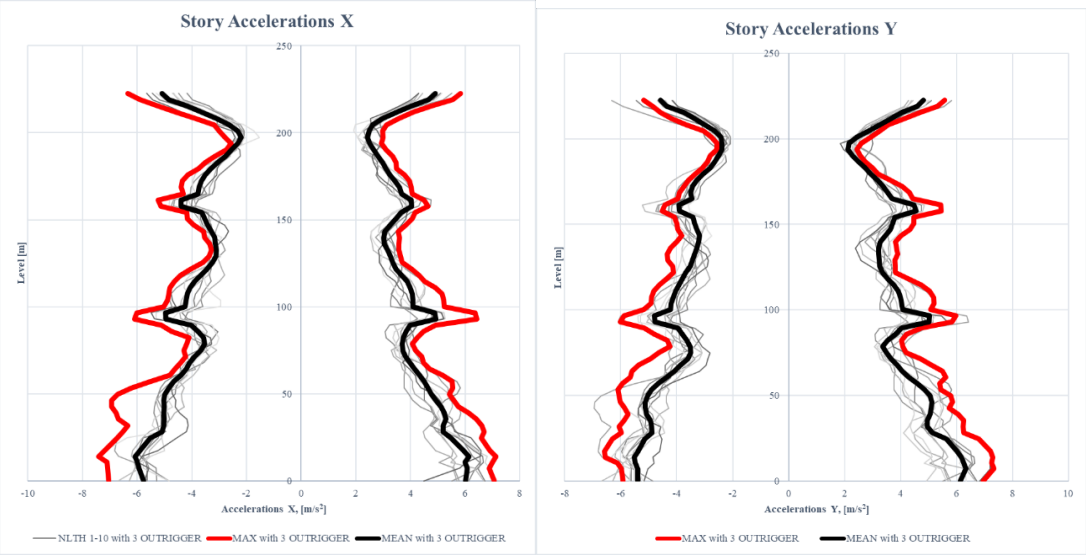

Figure 5. 94 Max and Min values of Story Acceleration - direction X and Y

Table 5.51 summarizes the maximum and average values obtained for acceleration:

MAX X	**ACCELERATION**	**MAX Y**	**ACCELERATION**
with3 OUTRIGGER	7.12 m/s²	with3 OUTRIGGER	7.33 m/s²
MEAN X	**ACCELERATION**	**MEAN Y**	**ACCELERATION**
with3 OUTRIGGER	7.849 m/s²	with3 OUTRIGGER	8.345 m/s²

Table 5. 51 Maximum and mean acceleration values – Model 3 without Outriggers

It was also evaluated how the maximum acceleration varies in roof as a function of time taking into account an accelerogram taken from the 10 seismic signals provided. In figure 5.95 it is possible to visualize the result for the signal 2.

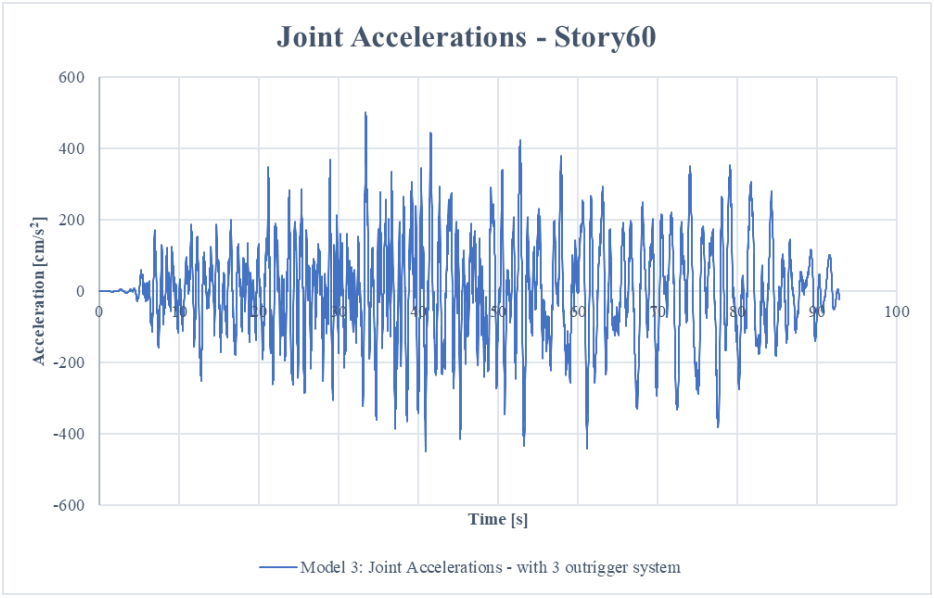

Figure 5. 95 Joint Accelerations with 3 outrigger system

In conclusion, the results of the non-linear analysis meet the criteria of global acceptance. Finally, it is necessary to verify that the property meets the local acceptance criteria. Therefore, plastic rotations in structural elements (beams, pillars and walls) and vertical displacements in SLB devices must be lower than the collapse prevention value (CP). The numerical acceptance criteria for beams and pillars, as described in section 7.2, by ASCE 41-13, while the maximum horizontal displacement for SLB devices is 60 mm.

Table 5.52 shows the maximum and average CP demand ratios of each structural element. The maximum D/C ratio is calculated on the results of the single non-linear chronological analysis, while on the results the average D/C ratio of the entire set of accelerograms is calculated.

Element	**Mean D/C for CP**	**Max D/C for CP**
[-]	[-]	[-]
Beam	0.122	0.17
Column	0	0
Wall	0.082	0.092
SLB device	0.655	0.864

Table 5. 52 Model 3: Mean and Maximum D/C ratios for Collapse Prevention (CP)

The status of plastic hinges is shown according to the immediate performance levels of occupation (IO), safety of life (LS), prevention of collapse (CP). According to Table 10-8 of ASCE/SEI 41-13 the performance levels are related to the plastic rotation angle (radians) this depends on the breaking condition and the amount of steel reinforcement.

For this reason, the plastic hinges developed by the structure have reached the performance level of immediate occupation (IO) without reaching the level of live safety (LS).

Figure 5.96 shows the hysterical response of the plastic hinge for a generic beam. Figure 5.97 shows the hysterical response of the plastic hinge for a generic wall.

In Figures 5.98, 5.99, 5.100 the hysterical response of the plastic hinge for the SLB device is shown, where the maximum displacement of the SLB device, whose hysterical behaviour has been traced to verify its displacement.

- K13 refers to the device in the first Outrigger band and shows a maximum displacement of 54,34mm;

- K16 refers to the device in the second band of Outrigger which shows a maximum displacement of 47,33mm;

- K19 refers to the device in the third band of Outrigger which shows a maximum displacement of 9.72mm.

It can therefore be inferred that by placing SLB in higher heights, the hysterical curve of the plastic hinge that develops in the heatsink always tends to decrease.

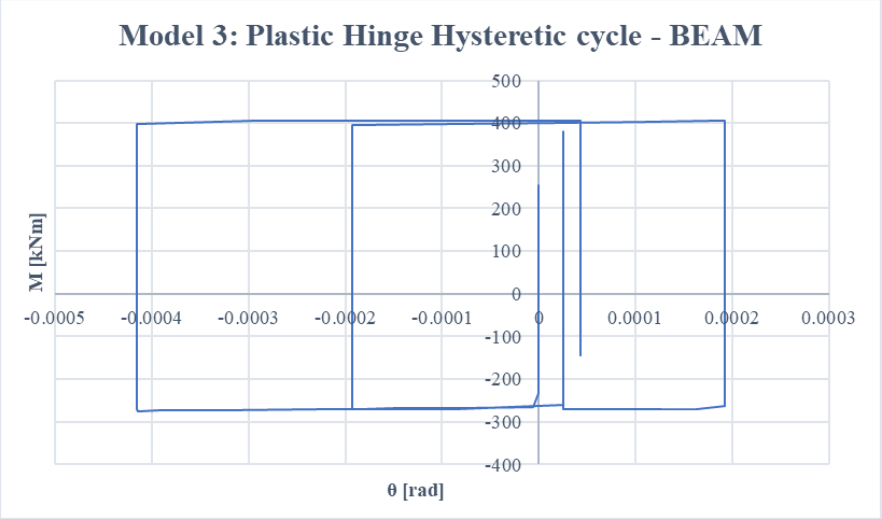

Figure 5. 96 Model 3: Plastic Hinge Hysteretic cycle - BEAM

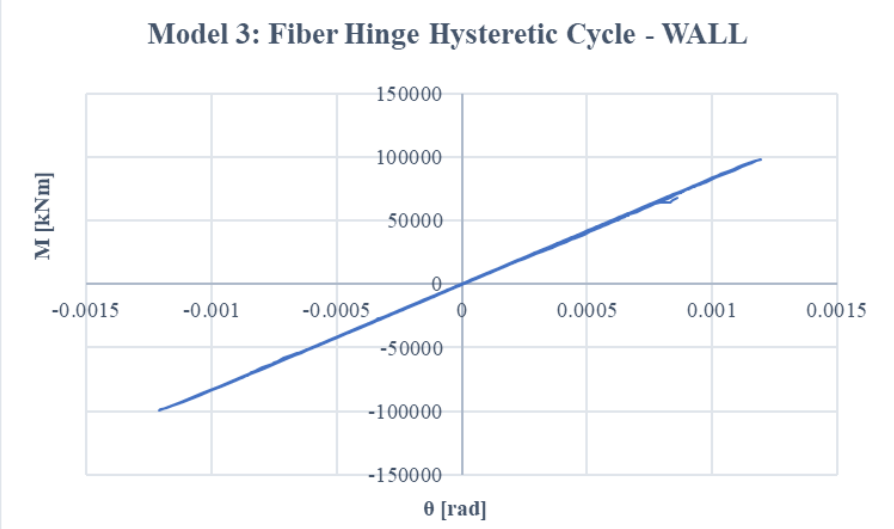

Figure 5. 97 Model 3: Fiber Hinge Hysteretic Cycle - WALL

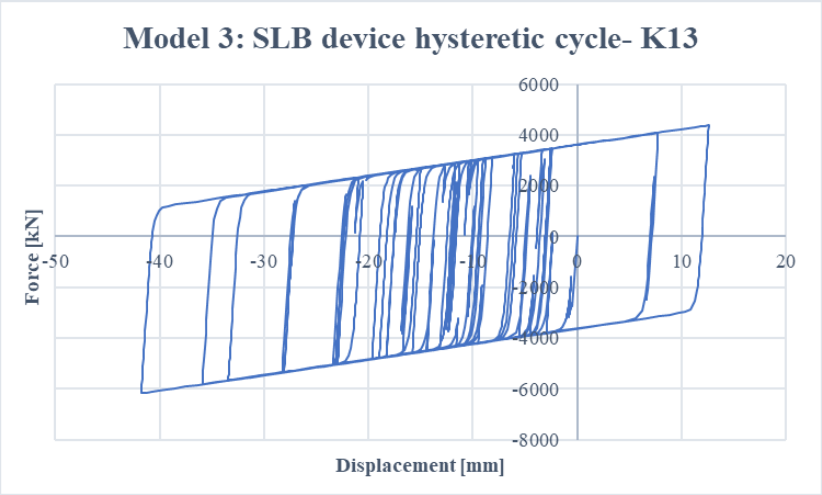

Figure 5. 98 Model 3: SLB device hysteretic cycle- K13

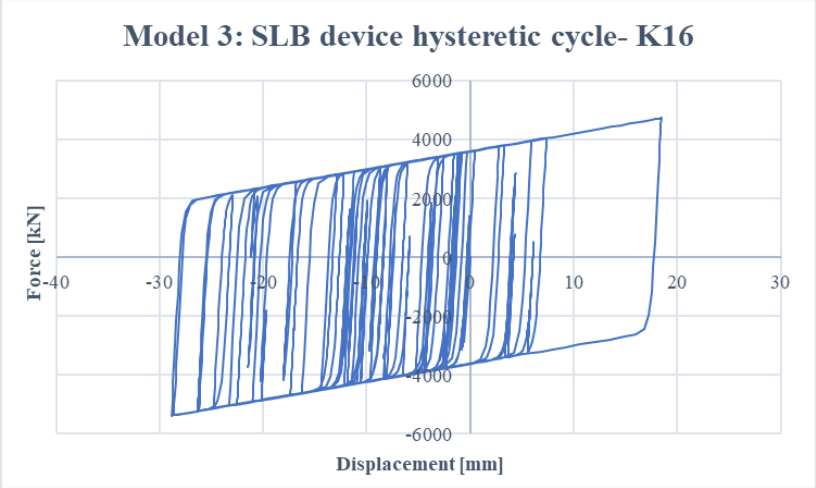

Figure 5. 99 Model 3: SLB device hysteretic cycle- K16

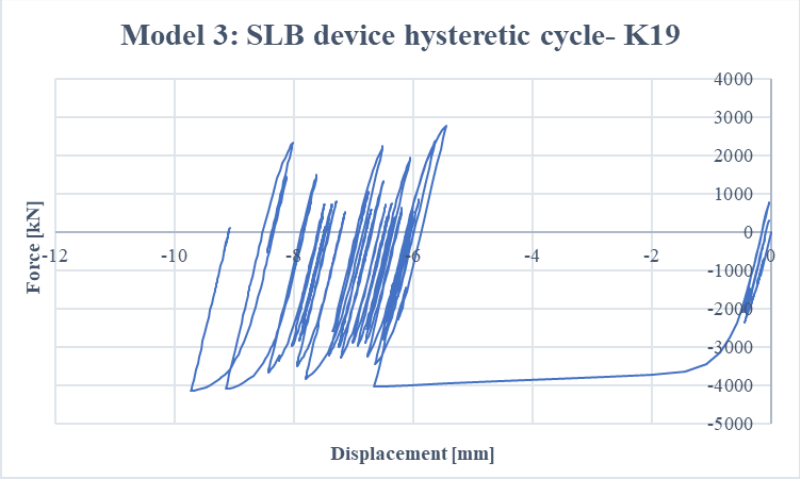

Figure 5. 100 Model 3: SLB device hysteretic cycle- K19

5.8 Comparison between the 3 models

This section presents a comparison between the three structures, with the aim of highlighting pros and cons of the three proposed solutions. In particular, the comparison is conducted considering both the structural behavior and the economic costs of the structural system, showing the advantages provided by the Outrigger system used with SLB devices.

5.8.1 Structural behavior comparison

Modal Analysis:

The first thing that is compared in Table 5.53 is the result of modal analysis, also taking into account the percentage of participating mass for the first three modes of vibrating .

Mode	**Period Model 1 w/o outrigger**	**Period Model 2 with 2 outriggers**	**Period Model 3 with 3 outriggers**	**Period reductionModel 2**	**Period reductionModel 3**	**Partecipating Mass Ratio (m_x,m_y,r_z) Model 1 - w/o outrigger**			**Partecipating Mass Ratio (m_x,m_y,r_z) Model 2 - with 2 outriggers**			**Partecipating Mass Ratio (m_x,m_y,r_z) Model 3 - with 3 outriggers**		
[-]	[s]	[s]	[s]	**[%]**	**[%]**	[-]	[-]	[-]	[-]	[-]	[-]	[-]	[-]	[-]
1	9.13	8.59	8.82	**6%**	**3%**	0%	66 %	0%	0%	68 %	0%	0%	68 %	0%
2	9.05	8.52	8.74	**6%**	**3%**	66 %	0%	0%	67 %	0%	0%	68 %	0%	0%
3	3.27	3.22	3.22	**2%**	**1%**	0%	0%	79 %	0%	0%	80 %	0%	0%	81 %

Table 5. 53 Modal analysis results comparison

The use of the Outrigger system entails a stiffening of the structure, as described in the previous paragraphs, and this is confirmed by the reduction of the period of the first three modes of vibration. In addition, it is important to note that the Outrigger system with SLB has been placed at the central core and symmetrically, for this reason the first two modal forms are translational. This aspect is very important because a fundamental way of torsional vibration could lead to strong stresses due to the torsion of the building under seismic loads.

Linear Analysis:

The comparison made for the three models analysed on the basis of linear analysis under both collapse and service conditions is shown below.

The use of the adopted system for the models 2 and 3 involves a significant reduction of the ratios defined by the output data displayed previously and compared below.

Calculate the reduction for each Story with the following expression:

$$ID_{red} = \frac{ID_{w/o} - ID_{with}}{ID_{w/o}} \quad [\%]$$

Where the positive value defines a reduction in values, while a negative value defines an increase.

- **Drift:**

Figure 5.101 and Table 5.54 show the interpiano drift results for the three models analysed in the Collapse Level Earthquake (RSA) condition in both X and Y direction.

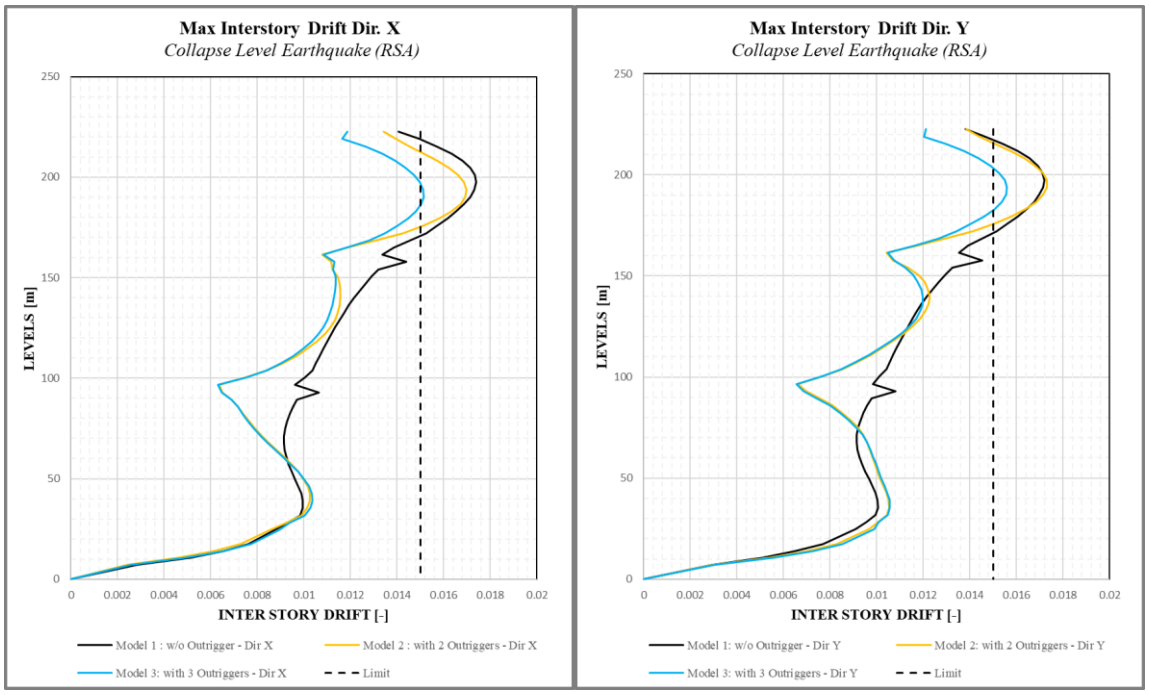

Figure 5. 101 Collapse Level Earthquake (RSA) :Interstory Drift comparison

Collapse Level Earthquake (RSA) :Interstory Drift comparison

Story	Elevation	Model 1: Intrerstory Drift w/o Outrigger		Model 2: Intrerstory Drift with 2 Outrigger		Model 3: Intrerstory Drift with 3 Outrigger		*REDUCTION MODEL 2*		*REDUCTION MODEL 3*		*COMPARISON MODEL 2 VS MODEL 3*	
		X-Dir	Y-Dir	X-Dir	Y-Dir	X-Dir	Y-Dir	*X-Dir*	*Y-Dir*	*X-Dir*	*Y-Dir*	*X-Dir*	*Y-Dir*
[-]	m	[-]	[-]	[-]	[-]	[-]	[-]	*[%]*	*[%]*	*[%]*	*[%]*	*[%]*	*[%]*
Story60	222.60	0.0141	0.0138	0.0134	0.0138	0.0119	0.0121	*5%*	*0%*	*16%*	*14%*	***11%***	***14%***
Story59	219.00	0.0150	0.0147	0.0139	0.0144	0.0116	0.0120	*7%*	*2%*	*22%*	*20%*	***15%***	***18%***
Story58	215.40	0.0157	0.0154	0.0145	0.0151	0.0127	0.0130	*7%*	*2%*	*19%*	*17%*	***12%***	***15%***
Story57	211.80	0.0163	0.0161	0.0152	0.0158	0.0134	0.0138	*7%*	*2%*	*18%*	*16%*	***11%***	***14%***
Story56	208.20	0.0168	0.0166	0.0157	0.0163	0.0139	0.0144	*6%*	*1%*	*17%*	*15%*	***11%***	***13%***
Story55	204.60	0.0172	0.0169	0.0162	0.0168	0.0144	0.0149	*5%*	*1%*	*16%*	*13%*	***11%***	***13%***
Story54	201.00	0.0173	0.0171	0.0166	0.0171	0.0147	0.0153	*4%*	*0%*	*15%*	*12%*	***11%***	***12%***

Story53	197.40	0.0174	0.0172	0.0169	0.0173	0.0150	0.0155	*3%*	*-1%*	*14%*	*11%*	***11%***	***12%***
Story52	193.80	0.0173	0.0171	0.0170	0.0173	0.0151	0.0156	*2%*	*-1%*	*13%*	*10%*	***11%***	***11%***
Story51	190.20	0.0171	0.0170	0.0169	0.0171	0.0151	0.0156	*1%*	*-1%*	*12%*	*9%*	***10%***	***10%***
Story50	186.60	0.0169	0.0167	0.0167	0.0168	0.0150	0.0154	*1%*	*0%*	*11%*	*9%*	***10%***	***9%***
Story49	183.00	0.0165	0.0164	0.0163	0.0164	0.0148	0.0151	*1%*	*0%*	*10%*	*9%*	***9%***	***9%***
Story48	179.40	0.0162	0.0160	0.0158	0.0158	0.0145	0.0146	*2%*	*2%*	*10%*	*10%*	***8%***	***8%***
Story47	175.80	0.0157	0.0156	0.0151	0.0151	0.0140	0.0141	*4%*	*4%*	*11%*	*11%*	***7%***	***7%***
Story46	172.20	0.0152	0.0152	0.0143	0.0141	0.0135	0.0134	*7%*	*7%*	*12%*	*12%*	***5%***	***5%***
Story45	168.60	0.0146	0.0145	0.0131	0.0130	0.0128	0.0127	*10%*	*11%*	*12%*	*13%*	***2%***	***2%***
Story44	165.00	0.0139	0.0139	0.0119	0.0117	0.0119	0.0117	*14%*	*16%*	*15%*	*16%*	***0%***	***0%***
Story43	161.40	0.0134	0.0135	0.0108	0.0104	0.0109	0.0105	*19%*	*23%*	*19%*	*22%*	***-1%***	***-1%***
Story42	157.80	0.0144	0.0145	0.0112	0.0107	0.0113	0.0108	*22%*	*26%*	*21%*	*25%*	***-1%***	***-1%***
Story41	154.20	0.0132	0.0133	0.0112	0.0113	0.0112	0.0112	*15%*	*15%*	*15%*	*15%*	***0%***	***0%***
Story40	150.60	0.0129	0.0129	0.0115	0.0118	0.0114	0.0116	*11%*	*9%*	*12%*	*10%*	***1%***	***2%***
Story39	147.00	0.0126	0.0127	0.0115	0.0120	0.0114	0.0118	*9%*	*5%*	*10%*	*7%*	***1%***	***2%***
Story38	143.40	0.0124	0.0124	0.0116	0.0122	0.0113	0.0119	*7%*	*1%*	*9%*	*4%*	***2%***	***2%***
Story37	139.80	0.0121	0.0122	0.0116	0.0123	0.0113	0.0120	*5%*	*-1%*	*7%*	*1%*	***2%***	***2%***
Story36	136.20	0.0119	0.0119	0.0115	0.0122	0.0112	0.0120	*3%*	*-3%*	*6%*	*0%*	***3%***	***2%***
Story35	132.60	0.0117	0.0117	0.0115	0.0121	0.0111	0.0119	*2%*	*-3%*	*5%*	*-1%*	***3%***	***2%***
Story34	129.00	0.0115	0.0115	0.0113	0.0119	0.0110	0.0117	*2%*	*-3%*	*4%*	*-1%*	***3%***	***1%***
Story33	125.40	0.0113	0.0114	0.0111	0.0116	0.0108	0.0114	*2%*	*-2%*	*4%*	*-1%*	***3%***	***1%***
Story32	121.80	0.0112	0.0112	0.0109	0.0112	0.0106	0.0111	*2%*	*0%*	*5%*	*1%*	***2%***	***1%***
Story31	118.20	0.0110	0.0110	0.0106	0.0108	0.0103	0.0107	*4%*	*2%*	*6%*	*3%*	***2%***	***0%***
Story30	114.60	0.0108	0.0109	0.0102	0.0103	0.0100	0.0102	*6%*	*5%*	*8%*	*6%*	***2%***	***0%***
Story29	111.00	0.0107	0.0107	0.0097	0.0097	0.0095	0.0097	*9%*	*9%*	*11%*	*9%*	***1%***	***0%***
Story28	107.40	0.0105	0.0106	0.0091	0.0092	0.0090	0.0091	*14%*	*13%*	*14%*	*14%*	***1%***	***0%***
Story27	103.80	0.0104	0.0104	0.0084	0.0085	0.0084	0.0085	*19%*	*18%*	*19%*	*18%*	***0%***	***0%***
Story26	100.20	0.0100	0.0101	0.0075	0.0077	0.0075	0.0076	*26%*	*24%*	*25%*	*24%*	***-1%***	***0%***
Story25	96.60	0.0096	0.0098	0.0064	0.0066	0.0063	0.0066	*34%*	*33%*	*34%*	*32%*	***0%***	***-1%***
Story24	93.00	0.0107	0.0108	0.0065	0.0070	0.0065	0.0069	*39%*	*36%*	*39%*	*35%*	***0%***	***0%***
Story23	89.40	0.0097	0.0098	0.0069	0.0076	0.0069	0.0074	*29%*	*23%*	*29%*	*23%*	***0%***	***1%***
Story22	85.80	0.0095	0.0096	0.0072	0.0081	0.0072	0.0080	*25%*	*15%*	*25%*	*16%*	***0%***	***1%***
Story21	82.20	0.0094	0.0094	0.0074	0.0085	0.0074	0.0084	*21%*	*9%*	*21%*	*10%*	***0%***	***1%***
Story20	78.60	0.0093	0.0093	0.0076	0.0089	0.0076	0.0088	*18%*	*4%*	*18%*	*5%*	***0%***	***1%***
Story19	75.00	0.0092	0.0092	0.0079	0.0092	0.0078	0.0091	*14%*	*0%*	*15%*	*1%*	***1%***	***1%***
Story18	71.40	0.0091	0.0091	0.0082	0.0094	0.0081	0.0094	*10%*	*-3%*	*11%*	*-3%*	***1%***	***0%***
Story17	67.80	0.0091	0.0091	0.0085	0.0096	0.0084	0.0096	*7%*	*-5%*	*8%*	*-5%*	***1%***	***0%***
Story16	64.20	0.0092	0.0092	0.0088	0.0097	0.0088	0.0097	*4%*	*-6%*	*4%*	*-6%*	***1%***	***0%***
Story15	60.60	0.0092	0.0092	0.0092	0.0098	0.0091	0.0099	*1%*	*-6%*	*1%*	*-7%*	***1%***	***0%***
Story14	57.00	0.0093	0.0094	0.0095	0.0099	0.0094	0.0100	*-1%*	*-6%*	*-1%*	*-7%*	***0%***	***-1%***
Story13	53.40	0.0095	0.0095	0.0098	0.0100	0.0097	0.0101	*-3%*	*-5%*	*-3%*	*-6%*	***0%***	***-1%***
Story12	49.80	0.0096	0.0097	0.0100	0.0101	0.0100	0.0102	*-4%*	*-5%*	*-4%*	*-6%*	***0%***	***-1%***
Story11	46.20	0.0098	0.0098	0.0102	0.0103	0.0102	0.0103	*-4%*	*-5%*	*-5%*	*-6%*	***-1%***	***-1%***
Story10	42.60	0.0099	0.0100	0.0103	0.0104	0.0103	0.0105	*-4%*	*-4%*	*-5%*	*-6%*	***-1%***	***-1%***

Story9	39.00	0.0100	0.0100	0.0103	0.0105	0.0104	0.0105	*-3%*	*-5%*	*-4%*	*-6%*	***-1%***	***-1%***
Story8	35.40	0.0100	0.0101	0.0101	0.0105	0.0103	0.0106	*-2%*	*-5%*	*-3%*	*-6%*	***-1%***	***-1%***
Story7	31.80	0.0098	0.0100	0.0099	0.0105	0.0100	0.0105	*-1%*	*-5%*	*-2%*	*-6%*	***-2%***	***-1%***
Story6	28.20	0.0093	0.0096	0.0092	0.0101	0.0094	0.0101	*1%*	*-5%*	*-1%*	*-8%*	***-2%***	***-3%***
Story5	24.60	0.0088	0.0091	0.0086	0.0097	0.0089	0.0099	*2%*	*-6%*	*-2%*	*-13%*	***-4%***	***-7%***
Story4	17.40	0.0076	0.0077	0.0073	0.0083	0.0077	0.0085	*4%*	*-7%*	*-2%*	*-12%*	***-6%***	***-5%***
Story3	14.00	0.0065	0.0065	0.0061	0.0070	0.0065	0.0072	*6%*	*-8%*	*0%*	*-11%*	***-6%***	***-3%***
Story2	10.60	0.0051	0.0051	0.0046	0.0054	0.0049	0.0056	*10%*	*-5%*	*4%*	*-9%*	***-6%***	***-3%***
Story1	7.20	0.0028	0.0029	0.0024	0.0030	0.0026	0.0031	*15%*	*-1%*	*8%*	*-9%*	***-6%***	***-8%***

Table 5. 54 Collapse Level Earthquake (RSA) :Interstory Drift comparison

The reduction of interplane drift is more significant at the double heights where Outriggers devices have been inserted. With values that reach a maximum of 39%. For planes where the system is not inserted, however, the reduction is less significant, with a slight increase in interpiano drift for the first 18 stories. As for the difference between Model 2 and Model 3, we see that Model 3 has an improvement of up to 18% at Story 59 (where the third Outrigger is applied) compared to Model 2. By placing a third Outrigger on top of the structure you have an improvement up to a maximum of 20% in Model 3 compared to Model 2 that instead reaches a maximum of 7% in the same area. It can therefore be deduced that in terms of interstory drift for the collapse condition, with Model 1 we exceed the limit imposed by the norm, which also happens with Model 2 albeit in a lower manner; using Model 3 instead the maximum value is almost at the limit.

In table 5.55 the comparison for the maximum values of interstory drift in the condition of Collapse is evidenced:

CollapseLevelEarthquake (RSA)

DRIFT X				
Model 1: w/o OUTRIGGER	Model 2: with 2 OUTRIGGER	Model 3: with 3 OUTRIGGER	**ReductionModel 2**	**ReductionModel 3**
[-]	[-]	[-]	**[%]**	**[%]**
0.017	0.017	0.015	**2%**	**13%**
DRIFT Y				
Model 1: w/o OUTRIGGER	Model 2: with 2 OUTRIGGER	Model 3: with 3 OUTRIGGER	**ReductionModel 2**	**ReductionModel 3**
[-]	[-]	[-]	**[%]**	**[%]**
0.017	0.017	0.016	**1%**	**9%**

Table 5. 55 Maximum comparison values for the interstory drift in the collapse condition

Figure 5.102 and Table 5.57 show the interpiano drift results for the three models analysed in the Service Level Earthquake (RSA) condition.

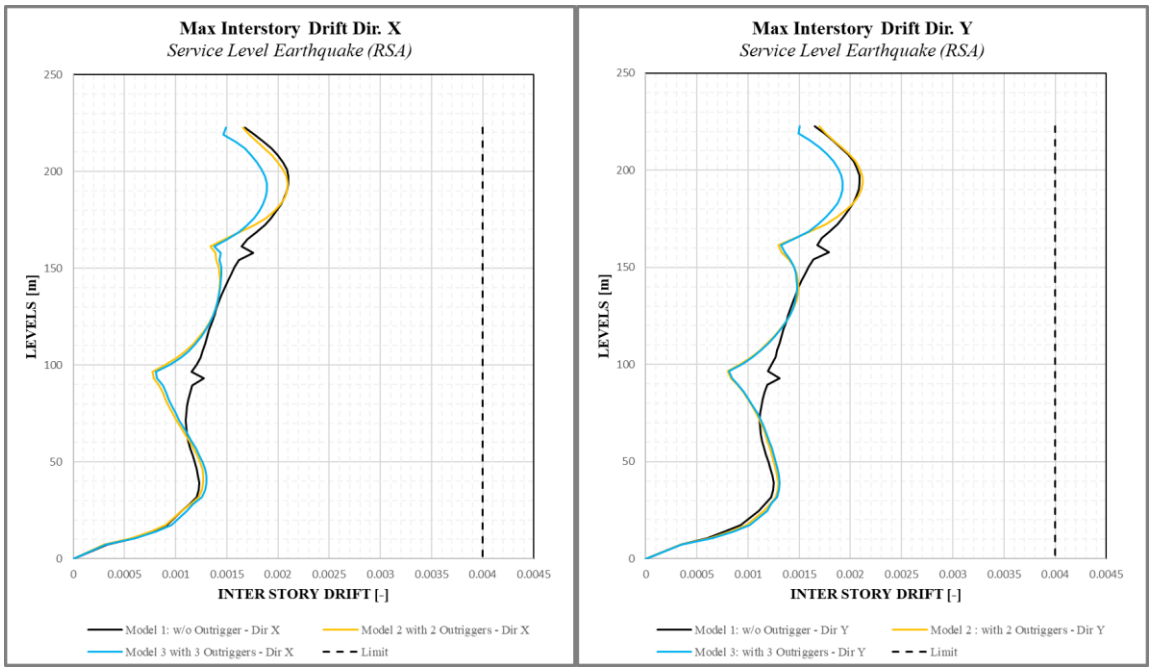

Figure 5. 102 Service Level Earthquake (RSA) :Interstory Drift comparison

Service Level Earthquake (RSA) :Interstory Drift comparison

Story	Elevation	Model 1: Intrerstory Drift w/o Outrigger		Model 2: Intrerstory Drift with 2 Outrigger		Model 3: Intrerstory Drift with 3 Outrigger		*REDUCTION MODEL 2*		*REDUCTION MODEL 3*		*COMPARISON MODEL 2 VS MODEL 3*	
		X-Dir	Y-Dir	X-Dir	Y-Dir	X-Dir	Y-Dir	*X-Dir*	*Y-Dir*	*X-Dir*	*Y-Dir*	*X-Dir*	*Y-Dir*
[-]	m	[-]	[-]	[-]	[-]	[-]	[-]	*[%]*	*[%]*	*[%]*	*[%]*	*[%]*	*[%]*
Story60	222.60	0.0017	0.0017	0.0017	0.0017	0.0015	0.0015	*1%*	*-3%*	*11%*	*10%*	***10%***	***13%***
Story59	219.00	0.0018	0.0017	0.0017	0.0018	0.0015	0.0015	*3%*	*-1%*	*17%*	*16%*	***15%***	***17%***
Story58	215.40	0.0019	0.0018	0.0018	0.0018	0.0016	0.0016	*3%*	*0%*	*15%*	*14%*	***11%***	***14%***
Story57	211.80	0.0019	0.0019	0.0019	0.0019	0.0017	0.0017	*3%*	*0%*	*14%*	*12%*	***10%***	***13%***
Story56	208.20	0.0020	0.0020	0.0019	0.0020	0.0017	0.0018	*3%*	*-1%*	*13%*	*11%*	***10%***	***12%***
Story55	204.60	0.0021	0.0020	0.0020	0.0020	0.0018	0.0018	*3%*	*-1%*	*13%*	*11%*	***10%***	***12%***
Story54	201.00	0.0021	0.0021	0.0020	0.0021	0.0018	0.0019	*2%*	*-1%*	*12%*	*10%*	***10%***	***11%***
Story53	197.40	0.0021	0.0021	0.0021	0.0021	0.0019	0.0019	*1%*	*-1%*	*11%*	*9%*	***10%***	***11%***
Story52	193.80	0.0021	0.0021	0.0021	0.0021	0.0019	0.0019	*0%*	*-2%*	*10%*	*8%*	***10%***	***10%***
Story51	190.20	0.0021	0.0021	0.0021	0.0021	0.0019	0.0019	*0%*	*-1%*	*9%*	*8%*	***9%***	***9%***
Story50	186.60	0.0021	0.0021	0.0021	0.0021	0.0019	0.0019	*0%*	*-1%*	*9%*	*8%*	***9%***	***9%***
Story49	183.00	0.0020	0.0020	0.0020	0.0020	0.0019	0.0019	*0%*	*0%*	*9%*	*8%*	***8%***	***8%***
Story48	179.40	0.0020	0.0020	0.0020	0.0020	0.0018	0.0018	*1%*	*1%*	*8%*	*8%*	***7%***	***7%***
Story47	175.80	0.0019	0.0019	0.0019	0.0019	0.0018	0.0018	*3%*	*3%*	*9%*	*9%*	***6%***	***6%***
Story46	172.20	0.0019	0.0019	0.0018	0.0018	0.0017	0.0017	*5%*	*6%*	*9%*	*10%*	***4%***	***4%***
Story45	168.60	0.0018	0.0018	0.0016	0.0016	0.0016	0.0016	*9%*	*11%*	*9%*	*11%*	***0%***	***0%***
Story44	165.00	0.0017	0.0017	0.0015	0.0015	0.0015	0.0015	*13%*	*15%*	*12%*	*14%*	***-2%***	***-2%***

Story43	161.40	0.0016	0.0017	0.0013	0.0013	0.0014	0.0013	*18%*	*23%*	*16%*	*19%*	***-2%***	***-3%***
Story42	157.80	0.0018	0.0018	0.0014	0.0013	0.0014	0.0014	*21%*	*26%*	*18%*	*23%*	***-3%***	***-3%***
Story41	154.20	0.0016	0.0016	0.0014	0.0014	0.0014	0.0014	*14%*	*15%*	*11%*	*13%*	***-2%***	***-2%***
Story40	150.60	0.0016	0.0016	0.0014	0.0014	0.0014	0.0014	*10%*	*9%*	*8%*	*8%*	***-2%***	***-1%***
Story39	147.00	0.0015	0.0016	0.0014	0.0015	0.0014	0.0015	*7%*	*6%*	*6%*	*5%*	***-1%***	***0%***
Story38	143.40	0.0015	0.0015	0.0014	0.0015	0.0014	0.0015	*5%*	*2%*	*5%*	*2%*	***-1%***	***0%***
Story37	139.80	0.0015	0.0015	0.0014	0.0015	0.0014	0.0015	*3%*	*0%*	*3%*	*0%*	***0%***	***0%***
Story36	136.20	0.0015	0.0015	0.0014	0.0015	0.0014	0.0015	*2%*	*-1%*	*2%*	*-2%*	***0%***	***0%***
Story35	132.60	0.0014	0.0014	0.0014	0.0015	0.0014	0.0015	*1%*	*-2%*	*1%*	*-3%*	***0%***	***-1%***
Story34	129.00	0.0014	0.0014	0.0014	0.0014	0.0014	0.0014	*1%*	*-2%*	*1%*	*-3%*	***0%***	***-1%***
Story33	125.40	0.0014	0.0014	0.0014	0.0014	0.0014	0.0014	*1%*	*-1%*	*1%*	*-2%*	***0%***	***-1%***
Story32	121.80	0.0014	0.0014	0.0013	0.0014	0.0013	0.0014	*2%*	*0%*	*1%*	*-1%*	***0%***	***-1%***
Story31	118.20	0.0013	0.0013	0.0013	0.0013	0.0013	0.0013	*3%*	*2%*	*3%*	*1%*	***-1%***	***-2%***
Story30	114.60	0.0013	0.0013	0.0012	0.0013	0.0012	0.0013	*6%*	*5%*	*5%*	*4%*	***-1%***	***-2%***
Story29	111.00	0.0013	0.0013	0.0012	0.0012	0.0012	0.0012	*9%*	*9%*	*7%*	*7%*	***-1%***	***-2%***
Story28	107.40	0.0013	0.0013	0.0011	0.0011	0.0011	0.0011	*13%*	*13%*	*11%*	*11%*	***-2%***	***-2%***
Story27	103.80	0.0012	0.0013	0.0010	0.0010	0.0011	0.0010	*18%*	*18%*	*16%*	*16%*	***-3%***	***-3%***
Story26	100.20	0.0012	0.0012	0.0009	0.0009	0.0009	0.0009	*25%*	*25%*	*21%*	*22%*	***-3%***	***-3%***
Story25	96.60	0.0012	0.0012	0.0008	0.0008	0.0008	0.0008	*33%*	*33%*	*30%*	*30%*	***-2%***	***-4%***
Story24	93.00	0.0013	0.0013	0.0008	0.0008	0.0008	0.0008	*38%*	*36%*	*36%*	*34%*	***-3%***	***-2%***
Story23	89.40	0.0012	0.0012	0.0008	0.0009	0.0009	0.0009	*28%*	*25%*	*25%*	*22%*	***-3%***	***-2%***
Story22	85.80	0.0011	0.0012	0.0009	0.0010	0.0009	0.0010	*23%*	*18%*	*20%*	*16%*	***-3%***	***-2%***
Story21	82.20	0.0011	0.0011	0.0009	0.0010	0.0009	0.0010	*20%*	*13%*	*17%*	*11%*	***-3%***	***-2%***
Story20	78.60	0.0011	0.0011	0.0009	0.0010	0.0010	0.0011	*16%*	*8%*	*13%*	*5%*	***-3%***	***-2%***
Story19	75.00	0.0011	0.0011	0.0010	0.0011	0.0010	0.0011	*12%*	*3%*	*9%*	*1%*	***-3%***	***-2%***
Story18	71.40	0.0011	0.0011	0.0010	0.0011	0.0010	0.0011	*8%*	*0%*	*6%*	*-2%*	***-2%***	***-2%***
Story17	67.80	0.0011	0.0011	0.0011	0.0011	0.0011	0.0012	*5%*	*-2%*	*2%*	*-5%*	***-2%***	***-2%***
Story16	64.20	0.0011	0.0011	0.0011	0.0012	0.0011	0.0012	*2%*	*-4%*	*0%*	*-6%*	***-2%***	***-2%***
Story15	60.60	0.0011	0.0011	0.0011	0.0012	0.0012	0.0012	*-1%*	*-5%*	*-3%*	*-7%*	***-2%***	***-3%***
Story14	57.00	0.0011	0.0012	0.0012	0.0012	0.0012	0.0012	*-3%*	*-5%*	*-5%*	*-7%*	***-2%***	***-3%***
Story13	53.40	0.0012	0.0012	0.0012	0.0012	0.0012	0.0013	*-4%*	*-4%*	*-6%*	*-7%*	***-2%***	***-3%***
Story12	49.80	0.0012	0.0012	0.0012	0.0013	0.0013	0.0013	*-4%*	*-4%*	*-7%*	*-7%*	***-2%***	***-3%***
Story11	46.20	0.0012	0.0012	0.0013	0.0013	0.0013	0.0013	*-5%*	*-4%*	*-7%*	*-7%*	***-2%***	***-3%***
Story10	42.60	0.0012	0.0012	0.0013	0.0013	0.0013	0.0013	*-4%*	*-4%*	*-7%*	*-7%*	***-2%***	***-3%***
Story9	39.00	0.0012	0.0012	0.0013	0.0013	0.0013	0.0013	*-3%*	*-4%*	*-6%*	*-7%*	***-2%***	***-3%***
Story8	35.40	0.0012	0.0012	0.0013	0.0013	0.0013	0.0013	*-3%*	*-4%*	*-5%*	*-6%*	***-2%***	***-3%***
Story7	31.80	0.0012	0.0012	0.0012	0.0013	0.0013	0.0013	*-2%*	*-4%*	*-4%*	*-6%*	***-2%***	***-2%***
Story6	28.20	0.0011	0.0012	0.0011	0.0012	0.0012	0.0012	*-1%*	*-4%*	*-3%*	*-8%*	***-2%***	***-4%***
Story5	24.60	0.0011	0.0011	0.0011	0.0012	0.0011	0.0012	*0%*	*-5%*	*-5%*	*-12%*	***-5%***	***-7%***
Story4	17.40	0.0009	0.0009	0.0009	0.0010	0.0010	0.0010	*1%*	*-6%*	*-5%*	*-12%*	***-7%***	***-6%***
Story3	14.00	0.0008	0.0008	0.0008	0.0008	0.0008	0.0009	*2%*	*-7%*	*-4%*	*-11%*	***-7%***	***-4%***
Story2	10.60	0.0006	0.0006	0.0006	0.0006	0.0006	0.0007	*6%*	*-4%*	*0%*	*-8%*	***-6%***	***-4%***
Story1	7.20	0.0003	0.0003	0.0003	0.0003	0.0003	0.0004	*10%*	*0%*	*3%*	*-7%*	***-6%***	***-8%***

Table 5. 56 Service Level Earthquake (RSA) :Interstory Drift comparison

From Figure 5.102 it can be defined that the structure equipped with SLB has lower values of interpiano drift in the service condition, this means less damage to both the structural elements and the non-structural components and, in general, lower repair costs in the event of a seismic event.

In table 5.57 the comparison for the maximum values of interstory drift in the condition of Service is evidenced:

ServiceLevelEarthquake (RSA)

DRIFT X				
Model 1: w/o OUTRIGGER	Model 2: with 2 OUTRIGGER	Model 3: with 3 OUTRIGGER	**ReductionModel 2**	**ReductionModel 3**
[-]	[-]	[-]	**[%]**	**[%]**
0.0021	0.0021	0.0019	**0%**	**10%**
DRIFT Y				
Model 1: w/o OUTRIGGER	Model 2: with 2 OUTRIGGER	Model 3: with 3 OUTRIGGER	**ReductionModel 2**	**ReductionModel 3**
[-]	[-]	[-]	**[%]**	**[%]**
0.0021	0.0021	0.0019	**2%**	**8%**

Table 5. 57 maximum comparison values for the interstory drift in the service condition

❖ Displacement

Figure 5.103 and Table 5.58 show displacement results for the three models analysed in the Collapse Level Earthquake (RSA) condition.

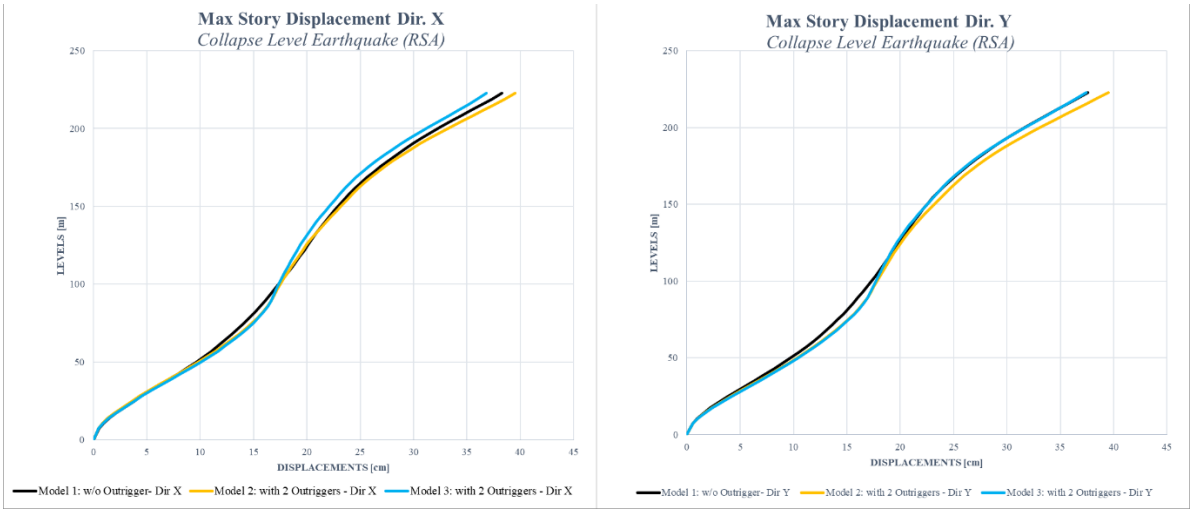

Figure 5. 103 Collapse Level Earthquake (RSA) : Displacements comparison

Collapse Level Earthquake (RSA) : Displacements comparison

Story	**Elevation**	**Model 1: Story Displacement w/o Outrigger**	**Model 2: Story Displacement with 2 Outrigger**	**Model 3: Story Displacement with 3 Outrigger**	***REDUCTION MODEL 2***	***REDUCTION MODEL 3***	***COMPARISON MODEL 2 VS MODEL 3***

		X-Dir	**Y-Dir**	**X-Dir**	**Y-Dir**	**X-Dir**	**Y-Dir**	***X-Dir***	***Y-Dir***	***X-Dir***	***Y-Dir***	***X-Dir***	***Y-Dir***
[-]	m	[-]	[-]	[-]	[-]	[-]	[-]	***[%]***	***[%]***	***[%]***	***[%]***	***[%]***	***[%]***
Story60	222.60	38.28	37.59	39.52	39.48	36.84	37.44	*-3%*	*-5%*	*4%*	*2%*	***7%***	***7%***
Story59	219.00	37.33	36.66	38.54	38.49	35.95	36.55	*-3%*	*-5%*	*4%*	*2%*	***7%***	***7%***
Story58	215.40	36.36	35.71	37.54	37.48	35.09	35.67	*-3%*	*-5%*	*3%*	*2%*	***7%***	***7%***
Story57	211.80	35.39	34.76	36.53	36.46	34.20	34.76	*-3%*	*-5%*	*3%*	*2%*	***7%***	***7%***
Story56	208.20	34.42	33.81	35.52	35.43	33.28	33.83	*-3%*	*-5%*	*3%*	*2%*	***6%***	***7%***
Story55	204.60	33.47	32.87	34.50	34.41	32.36	32.90	*-3%*	*-5%*	*3%*	*2%*	***6%***	***6%***
Story54	201.00	32.53	31.94	33.49	33.40	31.45	31.97	*-3%*	*-5%*	*3%*	*2%*	***6%***	***6%***
Story53	197.40	31.62	31.05	32.50	32.41	30.55	31.06	*-3%*	*-4%*	*3%*	*2%*	***6%***	***6%***
Story52	193.80	30.74	30.18	31.53	31.46	29.67	30.17	*-3%*	*-4%*	*3%*	*2%*	***6%***	***6%***
Story51	190.20	29.90	29.36	30.60	30.54	28.82	29.32	*-2%*	*-4%*	*4%*	*2%*	***6%***	***6%***
Story50	186.60	29.10	28.57	29.71	29.66	28.01	28.51	*-2%*	*-4%*	*4%*	*2%*	***6%***	***6%***
Story49	183.00	28.34	27.82	28.87	28.83	27.24	27.73	*-2%*	*-4%*	*4%*	*2%*	***6%***	***6%***
Story48	179.40	27.62	27.11	28.07	28.05	26.51	27.01	*-2%*	*-3%*	*4%*	*2%*	***6%***	***6%***
Story47	175.80	26.93	26.44	27.33	27.32	25.83	26.33	*-1%*	*-3%*	*4%*	*2%*	***6%***	***6%***
Story46	172.20	26.27	25.80	26.63	26.63	25.19	25.69	*-1%*	*-3%*	*4%*	*2%*	***5%***	***5%***
Story45	168.60	25.64	25.18	25.98	25.98	24.60	25.09	*-1%*	*-3%*	*4%*	*2%*	***5%***	***5%***
Story44	165.00	25.04	24.59	25.37	25.37	24.04	24.53	*-1%*	*-3%*	*4%*	*2%*	***5%***	***5%***
Story43	161.40	24.48	24.04	24.80	24.81	23.53	24.01	*-1%*	*-3%*	*4%*	*2%*	***5%***	***5%***
Story42	157.80	23.95	23.54	24.29	24.30	23.06	23.53	*-1%*	*-3%*	*4%*	*2%*	***5%***	***5%***
Story41	154.20	23.42	23.03	23.77	23.78	22.60	23.05	*-1%*	*-3%*	*4%*	*2%*	***5%***	***5%***
Story40	150.60	22.95	22.58	23.25	23.26	22.15	22.58	*-1%*	*-3%*	*3%*	*2%*	***5%***	***5%***
Story39	147.00	22.50	22.15	22.74	22.75	21.70	22.11	*-1%*	*-3%*	*4%*	*2%*	***5%***	***4%***
Story38	143.40	22.07	21.74	22.24	22.26	21.28	21.66	*-1%*	*-2%*	*4%*	*2%*	***4%***	***4%***
Story37	139.80	21.65	21.35	21.76	21.77	20.87	21.22	*0%*	*-2%*	*4%*	*2%*	***4%***	***4%***
Story36	136.20	21.25	20.97	21.29	21.32	20.47	20.80	*0%*	*-2%*	*4%*	*2%*	***4%***	***4%***
Story35	132.60	20.86	20.60	20.83	20.88	20.09	20.41	*0%*	*-1%*	*4%*	*2%*	***4%***	***4%***
Story34	129.00	20.48	20.24	20.40	20.48	19.73	20.04	*0%*	*-1%*	*4%*	*2%*	***3%***	***3%***
Story33	125.40	20.10	19.89	19.99	20.09	19.39	19.69	*1%*	*-1%*	*4%*	*2%*	***3%***	***3%***
Story32	121.80	19.73	19.53	19.59	19.73	19.06	19.37	*1%*	*-1%*	*3%*	*2%*	***3%***	***3%***
Story31	118.20	19.36	19.18	19.21	19.38	18.75	19.07	*1%*	*-1%*	*3%*	*1%*	***2%***	***3%***
Story30	114.60	18.98	18.82	18.86	19.06	18.46	18.79	*1%*	*-1%*	*3%*	*1%*	***2%***	***2%***
Story29	111.00	18.59	18.46	18.51	18.74	18.18	18.51	*0%*	*-2%*	*2%*	*0%*	***2%***	***2%***
Story28	107.40	18.20	18.09	18.18	18.42	17.91	18.25	*0%*	*-2%*	*2%*	*0%*	***2%***	***2%***
Story27	103.80	17.80	17.70	17.86	18.11	17.64	17.98	*0%*	*-2%*	*1%*	*-1%*	***1%***	***1%***
Story26	100.20	17.39	17.30	17.54	17.80	17.38	17.71	*-1%*	*-3%*	*0%*	*-2%*	***1%***	***1%***
Story25	96.60	16.96	16.90	17.23	17.49	17.12	17.44	*-2%*	*-4%*	*-1%*	*-3%*	***1%***	***1%***
Story24	93.00	16.55	16.50	16.97	17.23	16.90	17.21	*-3%*	*-4%*	*-2%*	*-4%*	***0%***	***0%***
Story23	89.40	16.06	16.03	16.66	16.92	16.64	16.93	*-4%*	*-6%*	*-4%*	*-5%*	***0%***	***0%***
Story22	85.80	15.59	15.59	16.30	16.55	16.31	16.59	*-4%*	*-6%*	*-5%*	*-6%*	***0%***	***0%***
Story21	82.20	15.12	15.13	15.87	16.12	15.92	16.18	*-5%*	*-7%*	*-5%*	*-7%*	***0%***	***0%***

Story20	78.60	14.62	14.65	15.38	15.63	15.47	15.71	*-5%*	*-7%*	*-6%*	*-7%*	***-1%***	***-1%***
Story19	75.00	14.10	14.15	14.84	15.10	14.96	15.19	*-5%*	*-7%*	*-6%*	*-8%*	***-1%***	***-1%***
Story18	71.40	13.55	13.62	14.25	14.53	14.40	14.63	*-5%*	*-7%*	*-6%*	*-8%*	***-1%***	***-1%***
Story17	67.80	12.97	13.06	13.61	13.92	13.79	14.02	*-5%*	*-7%*	*-6%*	*-8%*	***-1%***	***-2%***
Story16	64.20	12.36	12.46	12.92	13.26	13.12	13.37	*-5%*	*-6%*	*-6%*	*-8%*	***-2%***	***-2%***
Story15	60.60	11.71	11.83	12.19	12.58	12.41	12.69	*-4%*	*-6%*	*-6%*	*-8%*	***-2%***	***-2%***
Story14	57.00	11.03	11.16	11.41	11.85	11.64	11.96	*-3%*	*-6%*	*-6%*	*-8%*	***-2%***	***-2%***
Story13	53.40	10.32	10.45	10.59	11.09	10.84	11.20	*-3%*	*-6%*	*-5%*	*-9%*	***-2%***	***-2%***
Story12	49.80	9.56	9.70	9.74	10.29	9.99	10.40	*-2%*	*-6%*	*-4%*	*-9%*	***-3%***	***-3%***
Story11	46.20	8.78	8.92	8.86	9.46	9.11	9.57	*-1%*	*-6%*	*-4%*	*-9%*	***-3%***	***-3%***
Story10	42.60	7.96	8.10	7.96	8.59	8.21	8.71	*0%*	*-6%*	*-3%*	*-9%*	***-3%***	***-3%***
Story9	39.00	7.12	7.25	7.04	7.70	7.29	7.82	*1%*	*-6%*	*-2%*	*-10%*	***-3%***	***-4%***
Story8	35.40	6.26	6.39	6.13	6.78	6.36	6.90	*2%*	*-6%*	*-2%*	*-10%*	***-4%***	***-4%***
Story7	31.80	5.39	5.51	5.22	5.85	5.44	5.97	*3%*	*-6%*	*-1%*	*-11%*	***-4%***	***-5%***
Story6	28.20	4.52	4.63	4.33	4.92	4.54	5.04	*4%*	*-6%*	*0%*	*-11%*	***-5%***	***-5%***
Story5	24.60	3.70	3.79	3.50	4.02	3.70	4.14	*5%*	*-6%*	*0%*	*-12%*	***-5%***	***-6%***
Story4	17.40	2.14	2.16	1.96	2.29	2.10	2.37	*8%*	*-6%*	*2%*	*-11%*	***-6%***	***-5%***
Story3	14.00	1.50	1.51	1.35	1.59	1.44	1.64	*10%*	*-5%*	*4%*	*-10%*	***-6%***	***-5%***
Story2	10.60	0.94	0.97	0.83	0.99	0.88	1.03	*13%*	*-3%*	*6%*	*-9%*	***-6%***	***-6%***
Story1	7.20	0.51	0.53	0.43	0.53	0.47	0.55	*15%*	*0%*	*8%*	*-9%*	***-6%***	***-8%***

Table 5. 58 Collapse Level Earthquake (RSA): Displacements comparison

As for the displacements we can see how the variation between the three models considered in this linear condition is almost imperceptible. At the top you can read a reduction in Model 3 and a small increase in the case of Model 2. At the bottom, however, in both cases you exceed a percentage that reaches the maximum of 12%. The graph shows an increasing trend as the height of the building increases, with similar values in both X and Y direction up to a maximum of 39.52cm for model 2 and 36.84 for model 3 in X direction.

In table 5.59 the comparison for the maximum values of interstory drift in the condition of Collapse is evidenced:

CollapseLevelEarthquake (RSA)

DISPLACEMENT X

Model 1: w/o OUTRIGGER	Model 2: with 2 OUTRIGGER	Model 3: with 3 OUTRIGGER	**ReductionModel 2**	**ReductionModel 3**
[cm]	[cm]	[cm]	**[%]**	**[%]**
38.28	39.52	36.84	**3%**	**4%**

DISPLACEMENT Y

Model 1: w/o OUTRIGGER	Model 2: with 2 OUTRIGGER	Model 3: with 3 OUTRIGGER	**ReductionModel 2**	**ReductionModel 3**

[cm]	[cm]	[cm]	**[%]**	**[%]**
37.59	39.48	37.44	**5%**	**0%**

Table 5. 59 Maximum comparison values for the interstory displacement in the collapse condition

Figure 5.104 and Table 5.60 show displacement results for the three models analysed in the Service Level Earthquake condition (RSA).

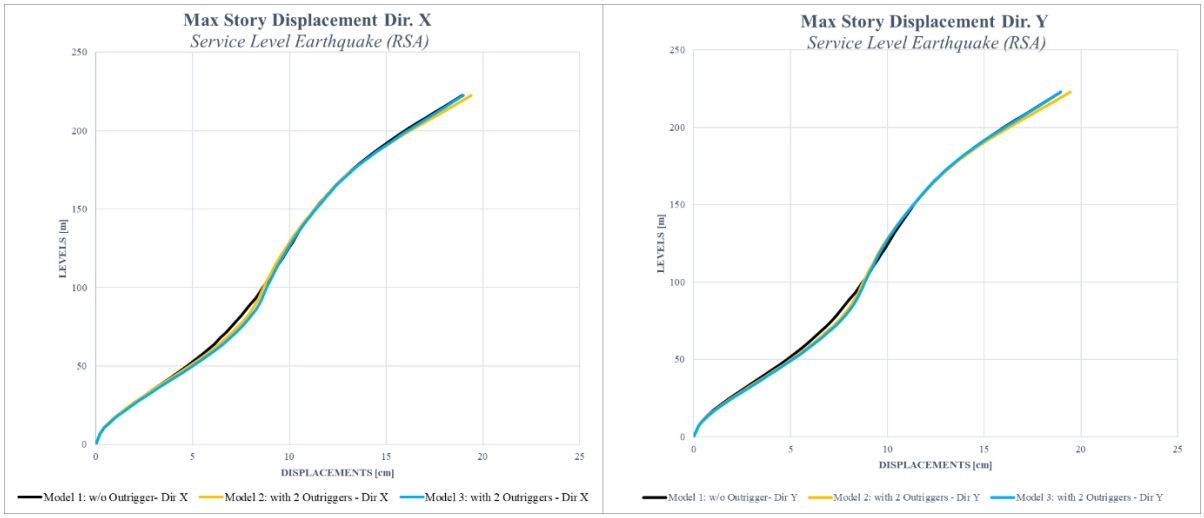

Figure 5. 104 Service Level Earthquake (RSA) :Interstory Displacements comparison

Service Level Earthquake (RSA) :Interstory Displacements comparison

Story	Elevation	Model 1: Story Displacement w/o Outrigger		Model 2: Story Displacement with 2 Outrigger		Model 3: Story Displacement with 3 Outrigger		*REDUCTION MODEL 2*		*REDUCTION MODEL 3*		*COMPARISON MODEL 2 VS MODEL 3*	
		X-Dir	**Y-Dir**	**X-Dir**	**Y-Dir**	**X-Dir**	**Y-Dir**	***X-Dir***	***Y-Dir***	***X-Dir***	***Y-Dir***	***X-Dir***	***Y-Dir***
[-]	m	[-]	[-]	[-]	[-]	[-]	[-]	*[%]*	*[%]*	*[%]*	*[%]*	*[%]*	*[%]*
Story60	222.60	18.93	18.95	19.39	19.45	18.98	18.95	*-2%*	*-3%*	*0%*	*0%*	***2%***	***3%***
Story59	219.00	18.47	18.50	18.90	18.96	18.54	18.50	*-2%*	*-3%*	*0%*	*0%*	***2%***	***2%***
Story58	215.40	18.00	18.03	18.41	18.46	18.10	18.06	*-2%*	*-2%*	*-1%*	*0%*	***2%***	***2%***
Story57	211.80	17.53	17.57	17.91	17.96	17.65	17.60	*-2%*	*-2%*	*-1%*	*0%*	***2%***	***2%***
Story56	208.20	17.05	17.10	17.41	17.45	17.19	17.14	*-2%*	*-2%*	*-1%*	*-1%*	***1%***	***2%***
Story55	204.60	16.58	16.63	16.90	16.94	16.72	16.67	*-2%*	*-2%*	*-1%*	*-1%*	***1%***	***1%***
Story54	201.00	16.12	16.17	16.40	16.44	16.26	16.21	*-2%*	*-2%*	*-1%*	*-1%*	***1%***	***1%***
Story53	197.40	15.66	15.72	15.91	15.95	15.80	15.75	*-2%*	*-1%*	*-1%*	*-1%*	***1%***	***1%***
Story52	193.80	15.23	15.29	15.43	15.47	15.36	15.30	*-1%*	*-1%*	*-1%*	*0%*	***0%***	***1%***
Story51	190.20	14.80	14.87	14.97	15.01	14.92	14.87	*-1%*	*-1%*	*-1%*	*0%*	***0%***	***1%***
Story50	186.60	14.40	14.47	14.52	14.57	14.51	14.45	*-1%*	*-1%*	*-1%*	*0%*	***0%***	***0%***
Story49	183.00	14.02	14.08	14.11	14.16	14.11	14.05	*-1%*	*-1%*	*-1%*	*0%*	***0%***	***0%***
Story48	179.40	13.66	13.72	13.71	13.77	13.73	13.68	*0%*	*0%*	*-1%*	*0%*	***0%***	***0%***
Story47	175.80	13.31	13.38	13.35	13.40	13.37	13.33	*0%*	*0%*	*0%*	*0%*	***0%***	***0%***
Story46	172.20	12.99	13.05	13.00	13.05	13.04	13.00	*0%*	*0%*	*0%*	*0%*	***0%***	***0%***

Story45	168.60	12.67	12.74	12.68	12.73	12.73	12.69	0%	0%	0%	0%	**0%**	**0%**
Story44	165.00	12.38	12.44	12.38	12.43	12.43	12.40	0%	0%	0%	0%	**0%**	**0%**
Story43	161.40	12.10	12.16	12.10	12.15	12.16	12.12	0%	0%	0%	0%	**0%**	**0%**
Story42	157.80	11.85	11.90	11.85	11.90	11.91	11.88	0%	0%	-1%	0%	**0%**	**0%**
Story41	154.20	11.59	11.64	11.60	11.65	11.66	11.63	0%	0%	-1%	0%	**-1%**	**0%**
Story40	150.60	11.35	11.41	11.35	11.40	11.42	11.39	0%	0%	-1%	0%	**-1%**	**0%**
Story39	147.00	11.13	11.19	11.11	11.15	11.18	11.15	0%	0%	0%	0%	**-1%**	**-1%**
Story38	143.40	10.92	10.99	10.87	10.91	10.95	10.91	0%	1%	0%	0%	**-1%**	**-1%**
Story37	139.80	10.72	10.79	10.64	10.67	10.73	10.69	1%	1%	0%	0%	**-1%**	**-1%**
Story36	136.20	10.53	10.59	10.42	10.45	10.52	10.47	1%	1%	0%	1%	**-1%**	**-1%**
Story35	132.60	10.34	10.41	10.21	10.24	10.32	10.27	1%	2%	0%	1%	**-1%**	**-1%**
Story34	129.00	10.16	10.22	10.01	10.04	10.12	10.08	1%	2%	0%	1%	**-1%**	**-1%**
Story33	125.40	9.97	10.04	9.81	9.85	9.94	9.89	2%	2%	0%	1%	**-1%**	**-1%**
Story32	121.80	9.79	9.86	9.63	9.68	9.76	9.72	2%	2%	0%	1%	**-1%**	**-1%**
Story31	118.20	9.61	9.68	9.46	9.51	9.59	9.57	2%	2%	0%	0%	**-1%**	**-1%**
Story30	114.60	9.43	9.50	9.29	9.35	9.43	9.41	1%	2%	0%	0%	**-1%**	**-1%**
Story29	111.00	9.24	9.31	9.13	9.20	9.28	9.27	1%	1%	0%	0%	**-2%**	**-1%**
Story28	107.40	9.05	9.12	8.98	9.05	9.13	9.13	1%	1%	-1%	-1%	**-2%**	**-2%**
Story27	103.80	8.85	8.93	8.82	8.90	8.98	8.99	0%	0%	-1%	-1%	**-2%**	**-2%**
Story26	100.20	8.65	8.72	8.67	8.75	8.84	8.85	0%	0%	-2%	-2%	**-2%**	**-2%**
Story25	96.60	8.44	8.51	8.52	8.60	8.69	8.71	-1%	-1%	-3%	-3%	**-2%**	**-2%**
Story24	93.00	8.24	8.31	8.40	8.48	8.57	8.59	-2%	-2%	-4%	-4%	**-2%**	**-2%**
Story23	89.40	7.99	8.07	8.25	8.33	8.43	8.45	-3%	-3%	-5%	-6%	**-2%**	**-2%**
Story22	85.80	7.76	7.84	8.07	8.15	8.26	8.27	-4%	-4%	-6%	-7%	**-2%**	**-3%**
Story21	82.20	7.52	7.60	7.86	7.95	8.05	8.07	-5%	-4%	-7%	-7%	**-2%**	**-3%**
Story20	78.60	7.27	7.36	7.63	7.71	7.81	7.83	-5%	-5%	-7%	-8%	**-3%**	**-3%**
Story19	75.00	7.01	7.10	7.36	7.45	7.54	7.57	-5%	-5%	-8%	-8%	**-3%**	**-3%**
Story18	71.40	6.73	6.82	7.07	7.16	7.25	7.28	-5%	-5%	-8%	-8%	**-3%**	**-3%**
Story17	67.80	6.44	6.53	6.75	6.85	6.93	6.97	-5%	-5%	-8%	-8%	**-3%**	**-3%**
Story16	64.20	6.12	6.22	6.41	6.52	6.59	6.63	-5%	-5%	-8%	-8%	**-3%**	**-4%**
Story15	60.60	5.80	5.89	6.04	6.17	6.22	6.28	-4%	-5%	-7%	-8%	**-3%**	**-4%**
Story14	57.00	5.45	5.55	5.65	5.80	5.83	5.90	-4%	-5%	-7%	-8%	**-3%**	**-4%**
Story13	53.40	5.08	5.18	5.25	5.41	5.42	5.51	-3%	-4%	-7%	-8%	**-3%**	**-4%**
Story12	49.80	4.70	4.80	4.82	5.01	4.99	5.10	-3%	-4%	-6%	-8%	**-4%**	**-4%**
Story11	46.20	4.30	4.39	4.39	4.59	4.55	4.67	-2%	-4%	-6%	-9%	**-4%**	**-4%**
Story10	42.60	3.89	3.98	3.94	4.15	4.09	4.23	-1%	-4%	-5%	-9%	**-4%**	**-4%**
Story9	39.00	3.47	3.55	3.49	3.70	3.63	3.78	-1%	-4%	-5%	-9%	**-4%**	**-5%**
Story8	35.40	3.03	3.11	3.03	3.25	3.16	3.32	0%	-4%	-4%	-9%	**-4%**	**-5%**
Story7	31.80	2.60	2.67	2.58	2.79	2.70	2.86	1%	-5%	-4%	-10%	**-5%**	**-5%**
Story6	28.20	2.17	2.24	2.14	2.34	2.25	2.40	2%	-5%	-4%	-10%	**-5%**	**-6%**
Story5	24.60	1.77	1.82	1.73	1.90	1.83	1.96	2%	-5%	-4%	-11%	**-6%**	**-6%**
Story4	17.40	1.01	1.03	0.97	1.07	1.04	1.11	4%	-4%	-2%	-10%	**-7%**	**-5%**
Story3	14.00	0.70	0.71	0.66	0.74	0.71	0.77	6%	-4%	-1%	-9%	**-7%**	**-5%**
Story2	10.60	0.44	0.45	0.41	0.46	0.43	0.48	8%	-2%	1%	-8%	**-6%**	**-6%**

Story1	7.20	0.24	0.25	0.21	0.25	0.23	0.25	*10%*	*0%*	*3%*	*-7%*	***-6%***	***-8%***

Table 5. 60 Service Level Earthquake (RSA) :Interstory Displacements comparison

In this condition the trend is similar to the case of collapse, with a maximum value of displacement at the top of 19.45cm for model 2 that is greater than Model 1 that has a displacement of 18.90 and therefore very similar to the value of 18,98cm for model 3. In table 5.61 the comparison for the maximum values of interstory drift in the condition of Service is evidenced:

ServiceLevelEarthquake (RSA)

DISPLACEMENT X				
Model 1: w/o OUTRIGGER	Model 2: with 2 OUTRIGGER	Model 3: with 3 OUTRIGGER	**ReductionModel 2**	**ReductionModel 3**
[cm]	[cm]	[cm]	**[%]**	**[%]**
18.93	19.39	18.98	**2%**	**0%**
DISPLACEMENT Y				
Model 1: w/o OUTRIGGER	Model 2: with 2 OUTRIGGER	Model 3: with 3 OUTRIGGER	**ReductionModel 2**	**ReductionModel 3**
[cm]	[cm]	[cm]	**[%]**	**[%]**
18.95	19.45	18.95	**3%**	**0%**

Table 5. 61 Maximum comparison values for the interstory displacement in the service condition

❖ Shear

Figure 5.105 and Table 5.62 show the interpiano shear results for the three models analysed in the Collapse Level Earthquake condition (RSA).

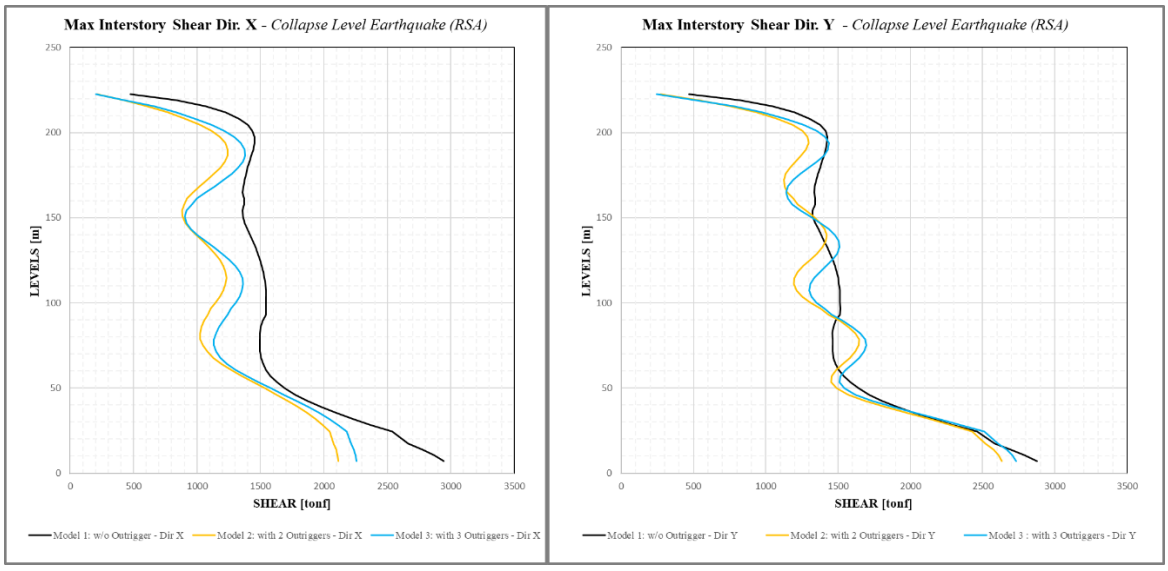

Figure 5. 105 Collapse Level Earthquake (RSA) : Story Shear comparison

Collapse Level Earthquake (RSA) : Story Shear comparison

Story	Elevation	Model 1: Story Shear w/o Outrigger		Model 2: Story Shear with 2 Outrigger		Model 3: Story Shear with 3 Outrigger		*REDUCTION MODEL 2*		*REDUCTION MODEL 3*		*COMPARISON MODEL 2 VS MODEL 3*	
		X-Dir	Y-Dir	X-Dir	Y-Dir	X-Dir	Y-Dir	*X-Dir*	*Y-Dir*	*X-Dir*	*Y-Dir*	*X-Dir*	*Y-Dir*
[-]	m	[-]	[-]	[-]	[-]	[-]	[-]	*[%]*	*[%]*	*[%]*	*[%]*	*[%]*	*[%]*
Story60	222.60	475.8472	468.7436	211.8920	272.5652	203.9830	245.9375	*55%*	*42%*	*57%*	*48%*	***2%***	***6%***
Story59	219.00	837.1817	822.4347	423.2581	535.7770	430.2106	513.5463	*49%*	*35%*	*49%*	*39%*	***-1%***	***4%***
Story58	215.40	1068.8533	1046.4533	606.8292	754.6539	660.6223	780.2518	*43%*	*28%*	*38%*	*27%*	***-5%***	***-1%***
Story57	211.80	1225.1303	1197.3008	768.7734	936.6173	834.8895	975.1628	*37%*	*22%*	*32%*	*20%*	***-5%***	***-1%***
Story56	208.20	1333.3854	1305.9546	907.8919	1080.4583	986.4743	1136.6621	*32%*	*17%*	*26%*	*15%*	***-6%***	***-3%***
Story55	204.60	1401.5310	1376.7827	1023.2420	1186.1095	1114.0900	1263.2334	*27%*	*14%*	*21%*	*10%*	***-6%***	***-4%***
Story54	201.00	1437.5691	1412.8257	1114.2484	1254.9081	1216.8558	1354.4382	*22%*	*11%*	*15%*	*6%*	***-7%***	***-5%***
Story53	197.40	1451.5562	1424.4304	1180.7926	1289.7685	1294.3432	1411.0690	*19%*	*9%*	*11%*	*3%*	***-8%***	***-7%***
Story52	193.80	1451.6856	1423.5109	1223.3293	1295.2680	1346.7379	1435.2881	*16%*	*9%*	*7%*	*1%*	***-9%***	***-8%***
Story51	190.20	1442.3985	1415.8529	1242.7450	1277.6213	1374.2733	1430.4879	*14%*	*10%*	*5%*	*1%*	***-9%***	***-9%***
Story50	186.60	1428.2363	1403.3929	1240.8902	1244.4063	1378.6977	1401.6560	*13%*	*11%*	*3%*	*2%*	***-10%***	***-9%***
Story49	183.00	1412.8726	1389.2673	1220.0039	1204.1779	1361.4661	1354.7476	*14%*	*13%*	*4%*	*4%*	***-10%***	***-9%***
Story48	179.40	1398.2847	1375.7165	1183.3526	1165.9589	1325.3588	1297.8472	*15%*	*15%*	*5%*	*7%*	***-10%***	***-8%***
Story47	175.80	1386.0840	1362.7975	1134.8605	1137.4821	1273.6135	1239.3936	*18%*	*17%*	*8%*	*11%*	***-10%***	***-6%***
Story46	172.20	1375.4912	1350.6439	1079.2840	1124.0649	1210.3498	1188.4102	*22%*	*17%*	*12%*	*14%*	***-10%***	***-3%***
Story45	168.60	1364.3453	1339.3305	1021.4246	1127.7617	1140.5488	1153.1275	*25%*	*16%*	*16%*	*15%*	***-9%***	***0%***
Story44	165.00	1358.6934	1334.5472	966.6750	1148.7065	1068.9138	1139.4233	*29%*	*14%*	*21%*	*16%*	***-8%***	***2%***
Story43	161.40	1369.0317	1343.5223	919.3184	1189.1080	998.4038	1153.6402	*33%*	*11%*	*27%*	*16%*	***-6%***	***4%***
Story42	157.80	1370.1008	1342.6469	900.1697	1218.7459	958.3972	1181.0590	*34%*	*9%*	*30%*	*14%*	***-4%***	***5%***
Story41	154.20	1356.4894	1322.6253	881.8028	1276.1448	917.9660	1240.5870	*35%*	*4%*	*32%*	*9%*	***-3%***	***5%***
Story40	150.60	1360.2440	1324.4009	885.4326	1331.2321	904.9232	1308.6902	*35%*	*-1%*	*33%*	*4%*	***-1%***	***4%***
Story39	147.00	1376.7820	1342.1009	908.0339	1377.0829	917.1550	1376.6323	*34%*	*-3%*	*33%*	*0%*	***-1%***	***3%***
Story38	143.40	1397.9941	1363.6245	945.5890	1408.0680	952.0557	1435.6672	*32%*	*-3%*	*32%*	*-3%*	***0%***	***1%***
Story37	139.80	1419.4651	1383.4290	992.8551	1420.8551	1004.1147	1479.3079	*30%*	*-3%*	*29%*	*-4%*	***-1%***	***-2%***
Story36	136.20	1440.3235	1402.9785	1044.4126	1414.5621	1066.5110	1503.7213	*27%*	*-1%*	*26%*	*-4%*	***-2%***	***-4%***
Story35	132.60	1460.5460	1424.0909	1095.3664	1390.6663	1132.5676	1507.6522	*25%*	*2%*	*22%*	*-3%*	***-3%***	***-6%***
Story34	129.00	1479.5808	1445.7484	1141.7639	1352.8203	1196.6921	1492.2658	*23%*	*6%*	*19%*	*-1%*	***-4%***	***-7%***
Story33	125.40	1496.0583	1465.0349	1180.0214	1307.1310	1253.5499	1461.2467	*21%*	*11%*	*16%*	*2%*	***-5%***	***-8%***
Story32	121.80	1510.1278	1480.5125	1208.4856	1260.4250	1300.7045	1419.7445	*20%*	*15%*	*14%*	*6%*	***-6%***	***-9%***
Story31	118.20	1521.9979	1491.6426	1225.4983	1221.0026	1335.4318	1374.8219	*19%*	*18%*	*12%*	*10%*	***-7%***	***-8%***
Story30	114.60	1531.9265	1499.8964	1230.4119	1197.0147	1356.1453	1335.1610	*20%*	*20%*	*11%*	*13%*	***-8%***	***-7%***
Story29	111.00	1539.4502	1506.5539	1223.4994	1193.7654	1362.5678	1308.4347	*21%*	*21%*	*11%*	*15%*	***-9%***	***-6%***
Story28	107.40	1543.9905	1511.4704	1205.7997	1213.0059	1355.2265	1300.7504	*22%*	*20%*	*12%*	*16%*	***-10%***	***-4%***
Story27	103.80	1544.9188	1513.9172	1179.1978	1252.3883	1335.6011	1314.9089	*24%*	*17%*	*14%*	*15%*	***-10%***	***-2%***
Story26	100.20	1543.1520	1514.5847	1145.9939	1307.7404	1306.0232	1350.0449	*26%*	*14%*	*15%*	*13%*	***-10%***	***-1%***
Story25	96.60	1545.6121	1517.6906	1108.2540	1379.9514	1268.3308	1407.8190	*28%*	*9%*	*18%*	*9%*	***-10%***	***0%***
Story24	93.00	1543.4627	1514.0148	1084.1363	1434.6716	1241.9243	1457.3922	*30%*	*5%*	*20%*	*6%*	***-10%***	***0%***
Story23	89.40	1517.6891	1482.6732	1053.9905	1512.0697	1204.6706	1533.7111	*31%*	*-2%*	*21%*	*-1%*	***-10%***	***1%***
Story22	85.80	1502.3081	1465.5371	1033.5763	1575.5245	1173.2123	1601.5372	*31%*	*-8%*	*22%*	*-7%*	***-9%***	***1%***
Story21	82.20	1496.7428	1461.5724	1023.5834	1620.8278	1148.2868	1654.4766	*32%*	*-11%*	*23%*	*-11%*	***-8%***	***0%***
Story20	78.60	1495.6011	1461.9817	1026.6068	1644.0065	1133.4117	1686.7931	*31%*	*-12%*	*24%*	*-13%*	***-7%***	***0%***

Story19	75.00	1495.7551	1461.7085	1044.8254	1643.5027	1132.4729	1695.3692	*30%*	*-12%*	*24%*	*-13%*	***-6%***	***-1%***
Story18	71.40	1498.1476	1462.4692	1079.2320	1620.8594	1148.6014	1680.4618	*28%*	*-11%*	*23%*	*-12%*	***-5%***	***-1%***
Story17	67.80	1505.8037	1468.7293	1129.4169	1580.8983	1183.4751	1645.8964	*25%*	*-8%*	*21%*	*-9%*	***-4%***	***-2%***
Story16	64.20	1520.9559	1483.2890	1193.6904	1531.8530	1236.9379	1599.2326	*22%*	*-3%*	*19%*	*-5%*	***-3%***	***-2%***
Story15	60.60	1544.9618	1507.0759	1269.4453	1485.1989	1307.0927	1551.6851	*18%*	*1%*	*15%*	*0%*	***-2%***	***-2%***
Story14	57.00	1580.0022	1540.7335	1353.5857	1454.6447	1390.7684	1517.2978	*14%*	*6%*	*12%*	*4%*	***-2%***	***-2%***
Story13	53.40	1629.2496	1585.6067	1443.3891	1453.7821	1484.6483	1510.7608	*11%*	*8%*	*9%*	*7%*	***-3%***	***-1%***
Story12	49.80	1692.1331	1641.4087	1533.3687	1491.1266	1582.1459	1542.5582	*9%*	*9%*	*6%*	*9%*	***-3%***	***0%***
Story11	46.20	1771.3309	1712.8931	1623.9294	1569.9152	1682.9136	1617.6687	*8%*	*8%*	*5%*	*9%*	***-3%***	***0%***
Story10	42.60	1866.6223	1802.0867	1711.9476	1685.5878	1782.8849	1732.8776	*8%*	*6%*	*4%*	*7%*	***-4%***	***1%***
Story9	39.00	1975.7867	1907.4280	1793.6731	1825.3181	1877.2139	1875.5562	*9%*	*4%*	*5%*	*5%*	***-4%***	***1%***
Story8	35.40	2096.9453	2026.7024	1868.1436	1977.5674	1964.2979	2033.5106	*11%*	*2%*	*6%*	*3%*	***-5%***	***1%***
Story7	31.80	2227.2977	2156.4577	1933.9936	2130.5619	2042.1656	2193.9723	*13%*	*1%*	*8%*	*1%*	***-5%***	***0%***
Story6	28.20	2363.9892	2292.5240	1990.2901	2274.3750	2109.4266	2345.9807	*16%*	*1%*	*11%*	*1%*	***-5%***	***0%***
Story5	24.60	2538.5265	2463.5287	2046.6177	2429.0198	2177.4460	2510.5232	*19%*	*1%*	*14%*	*1%*	***-5%***	***0%***
Story4	17.40	2665.1963	2583.7668	2077.3816	2519.9504	2215.0333	2607.6052	*22%*	*2%*	*17%*	*2%*	***-5%***	***0%***
Story3	14.00	2773.8291	2691.9386	2095.5010	2575.8065	2237.2356	2667.3602	*24%*	*4%*	*19%*	*4%*	***-5%***	***0%***
Story2	10.60	2865.8382	2788.6278	2106.2842	2610.5881	2250.4752	2704.5981	*27%*	*6%*	*21%*	*6%*	***-5%***	***-1%***
Story1	7.20	2946.2641	2877.6260	2113.2618	2634.1361	2259.0574	2729.8414	*28%*	*8%*	*23%*	*7%*	***-5%***	***-1%***

Table 5. 62 Collapse Level Earthquake (RSA) : Story Shear comparison

From the above results it can be observed that the interpiano cut tends to have lower values at the levels where the Outrigger is affixed. Model 2 achieves a maximum reduction of 55% in the X direction and at level 60, while model 3 reaches a maximum of 57%, also at the top. The difference between the two models with Outrigger is minimal, reaching a maximum of 10% between the Story 23-28 and the Story 46-50. In general, lower cutting values are obtained for Model 2 than for Model 3.

In table 5.63 the comparison for the maximum values of interstory shear in the condition of Collapse is evidenced:

CollapseLevelEarthquake (RSA)

SHEAR X

Model 1: w/o OUTRIGGER [tonf]	Model 2: with 2 OUTRIGGER [tonf]	Model 3: with 3 OUTRIGGER [tonf]	**ReductionModel 2 [%]**	**ReductionModel 3 [%]**
2946.26	2113.26	2259.06	**28%**	**23%**

SHEAR Y

Model 1: w/o OUTRIGGER [tonf]	Model 2: with 2 OUTRIGGER [tonf]	Model 3: with 3 OUTRIGGER [tonf]	**ReductionModel 2 [%]**	**ReductionModel 3 [%]**
2877.63	2634.14	2729.84	**8%**	**5%**

Table 5. 63 Maximum comparison values for the interstory shear in the collapse condition

Figure 5.106 and Table 5.64 show the cross-plane shear results for the three models analysed in the Service Level Earthquake (RSA) condition.

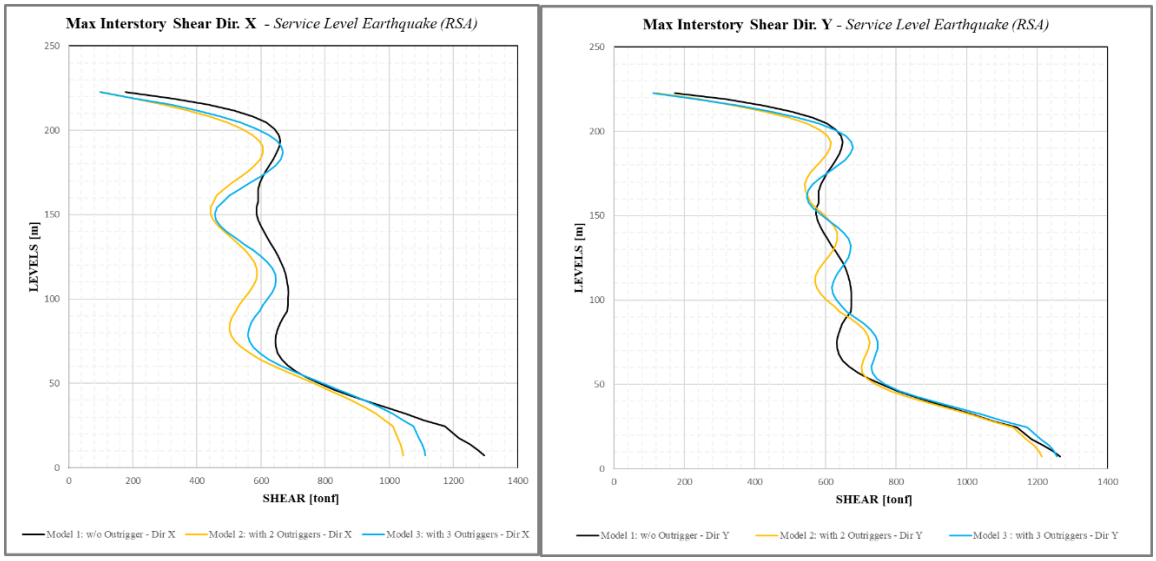

Figure 5. 106 Service Level Earthquake (RSA): Story Shear comparison

Service Level Earthquake (RSA) : Story Shear comparison

Story	Elevation	Model 1: Story Shear w/o Outrigger		Model 2: Story Shear with 2 Outrigger		Model 3: Story Shear with 3 Outrigger		*REDUCTION MODEL 2*		*REDUCTION MODEL 3*		*COMPARISON MODEL 2 VS MODEL 3*	
		X-Dir	Y-Dir	X-Dir	Y-Dir	X-Dir	Y-Dir	*X-Dir*	*Y-Dir*	*X-Dir*	*Y-Dir*	*X-Dir*	*Y-Dir*
[-]	m	[-]	[-]	[-]	[-]	[-]	[-]	*[%]*	*[%]*	*[%]*	*[%]*	*[%]*	*[%]*
Story60	222.60	176.5086	173.3897	102.2047	122.6054	97.6589	111.1154	*42%*	*29%*	*45%*	*37%*	***3%***	***8%***
Story59	219.00	324.3015	317.9492	204.2512	241.8759	206.0662	232.6596	*37%*	*24%*	*36%*	*28%*	***-1%***	***4%***
Story58	215.40	433.0845	423.8560	292.9938	342.1132	316.5798	354.4821	*32%*	*19%*	*27%*	*18%*	***-5%***	***-1%***
Story57	211.80	514.3596	503.1768	371.4266	426.7568	400.3112	444.4373	*28%*	*15%*	*22%*	*14%*	***-6%***	***-2%***
Story56	208.20	574.3262	562.6832	438.9869	495.2870	473.3323	520.1317	*24%*	*12%*	*18%*	*9%*	***-6%***	***-3%***
Story55	204.60	615.8724	604.4599	495.2343	547.6246	535.0472	580.9073	*20%*	*9%*	*13%*	*6%*	***-6%***	***-4%***
Story54	201.00	641.8871	630.4691	539.9031	584.2299	585.0515	626.5315	*16%*	*7%*	*9%*	*2%*	***-7%***	***-5%***
Story53	197.40	655.5420	643.8921	572.9446	606.1621	623.1541	657.2553	*13%*	*6%*	*5%*	*0%*	***-8%***	***-6%***
Story52	193.80	659.7726	648.2394	594.5834	615.1059	649.4571	673.8786	*10%*	*5%*	*2%*	*-2%*	***-8%***	***-7%***
Story51	190.20	656.8613	645.9966	605.2402	613.3097	664.0647	677.5937	*8%*	*5%*	*-1%*	*-3%*	***-9%***	***-8%***
Story50	186.60	649.0775	638.9491	605.8061	603.5620	667.8334	670.3474	*7%*	*6%*	*-3%*	*-3%*	***-10%***	***-9%***
Story49	183.00	638.4468	628.9560	597.3415	588.9447	661.4535	654.3081	*6%*	*6%*	*-4%*	*-2%*	***-10%***	***-9%***
Story48	179.40	626.6924	617.7017	581.3814	572.7732	646.2243	632.4620	*7%*	*7%*	*-3%*	*-1%*	***-10%***	***-8%***
Story47	175.80	615.2511	606.3483	559.7635	558.0393	623.6689	607.9323	*9%*	*8%*	*-1%*	*1%*	***-10%***	***-7%***
Story46	172.20	604.9095	595.9309	534.6918	547.1357	595.6998	584.1106	*12%*	*8%*	*2%*	*3%*	***-10%***	***-5%***
Story45	168.60	595.9542	587.1531	508.3699	541.5066	564.6001	564.2768	*15%*	*8%*	*5%*	*5%*	***-9%***	***-2%***
Story44	165.00	590.2651	581.7141	483.2312	542.0713	532.4964	551.0301	*18%*	*7%*	*10%*	*7%*	***-8%***	***0%***
Story43	161.40	590.6493	581.6344	461.1269	550.2699	500.6611	547.0619	*22%*	*5%*	*15%*	*7%*	***-7%***	***2%***
Story42	157.80	590.4077	580.8622	451.9125	558.1812	482.3505	551.3024	*23%*	*4%*	*18%*	*7%*	***-5%***	***3%***
Story41	154.20	585.0508	573.5702	442.2644	575.6090	463.1782	566.3110	*24%*	*0%*	*21%*	*3%*	***-4%***	***4%***
Story40	150.60	585.5524	572.8946	442.3008	594.4613	455.7639	587.4031	*24%*	*-4%*	*22%*	*0%*	***-2%***	***3%***

Story39	147.00	590.9177	577.7562	450.7521	611.7368	459.1876	610.9696	*24%*	*-6%*	*22%*	*-3%*	***-1%***	***2%***
Story38	143.40	599.2735	585.6298	465.9833	624.9819	472.5364	633.4905	*22%*	*-7%*	*21%*	*-6%*	***-1%***	***1%***
Story37	139.80	609.2895	595.0148	485.7720	632.5923	493.6511	652.1295	*20%*	*-6%*	*19%*	*-7%*	***-1%***	***-1%***
Story36	136.20	620.2174	605.5872	507.7354	633.9071	519.6944	665.0042	*18%*	*-5%*	*16%*	*-7%*	***-2%***	***-3%***
Story35	132.60	631.5055	617.0722	529.6575	629.1743	547.7577	671.2200	*16%*	*-2%*	*13%*	*-6%*	***-3%***	***-4%***
Story34	129.00	642.6219	628.7886	549.7052	619.4597	575.3137	670.8292	*14%*	*1%*	*10%*	*-4%*	***-4%***	***-6%***
Story33	125.40	652.8467	639.7086	566.2083	606.6353	599.9126	664.7419	*13%*	*5%*	*8%*	*-2%*	***-5%***	***-7%***
Story32	121.80	662.0201	649.3680	578.3591	592.8557	620.3711	654.5346	*13%*	*9%*	*6%*	*1%*	***-6%***	***-8%***
Story31	118.20	669.8845	657.3445	585.3765	580.6507	635.4090	642.3056	*13%*	*12%*	*5%*	*4%*	***-7%***	***-8%***
Story30	114.60	676.2790	663.6899	586.9663	572.5233	644.2856	630.6852	*13%*	*14%*	*5%*	*7%*	***-8%***	***-7%***
Story29	111.00	681.0015	668.5450	583.2685	570.1721	646.8698	622.0193	*14%*	*15%*	*5%*	*9%*	***-9%***	***-6%***
Story28	107.40	683.8926	671.8568	574.8032	574.3985	643.4298	618.2883	*16%*	*15%*	*6%*	*10%*	***-10%***	***-5%***
Story27	103.80	684.8308	673.5010	562.5037	584.9234	634.6965	620.6761	*18%*	*13%*	*7%*	*9%*	***-11%***	***-4%***
Story26	100.20	684.0271	673.6252	547.5268	600.9576	621.8202	629.4557	*20%*	*11%*	*9%*	*8%*	***-11%***	***-3%***
Story25	96.60	683.1374	673.2507	531.0416	623.4764	605.8624	645.9005	*22%*	*7%*	*11%*	*5%*	***-11%***	***-2%***
Story24	93.00	681.5310	671.3929	520.9618	641.5996	595.0924	661.1845	*24%*	*4%*	*13%*	*3%*	***-11%***	***-1%***
Story23	89.40	669.5233	658.2825	509.2137	668.4471	580.6267	685.9717	*24%*	*-2%*	*13%*	*-2%*	***-11%***	***-1%***
Story22	85.80	659.3843	647.6026	502.5104	691.7012	569.4055	709.2074	*24%*	*-7%*	*14%*	*-8%*	***-10%***	***-1%***
Story21	82.20	651.9824	640.1921	501.1635	709.5969	561.8140	728.4451	*23%*	*-11%*	*14%*	*-12%*	***-9%***	***-1%***
Story20	78.60	647.0377	635.1525	506.2448	720.6914	559.3642	741.6892	*22%*	*-13%*	*14%*	*-15%*	***-8%***	***-1%***
Story19	75.00	644.7705	632.3195	518.5542	724.5466	563.6139	747.9827	*20%*	*-15%*	*13%*	*-16%*	***-7%***	***-1%***
Story18	71.40	646.1280	632.7467	538.3334	721.9724	575.7118	747.6888	*17%*	*-14%*	*11%*	*-16%*	***-6%***	***-2%***
Story17	67.80	652.4143	637.9653	565.2165	715.0325	596.1472	742.5236	*13%*	*-12%*	*9%*	*-14%*	***-5%***	***-2%***
Story16	64.20	664.6850	649.1100	598.3157	706.9546	624.6492	735.4906	*10%*	*-9%*	*6%*	*-11%*	***-4%***	***-2%***
Story15	60.60	683.6138	666.7930	636.3865	701.8446	660.2628	730.6268	*7%*	*-5%*	*3%*	*-7%*	***-3%***	***-2%***
Story14	57.00	709.6972	691.2915	678.0030	704.0893	701.5462	732.4401	*4%*	*-2%*	*1%*	*-3%*	***-3%***	***-1%***
Story13	53.40	743.3783	722.8036	721.9464	717.5549	747.0582	745.1113	*3%*	*1%*	*0%*	*0%*	***-3%***	***-1%***
Story12	49.80	783.1554	760.0273	765.6540	743.6933	793.8045	770.5524	*2%*	*2%*	*-1%*	*2%*	***-4%***	***-1%***
Story11	46.20	829.6313	803.9886	809.4182	783.2805	841.7754	809.9425	*2%*	*3%*	*-1%*	*2%*	***-4%***	***0%***
Story10	42.60	881.6049	853.9486	851.7948	834.3789	889.1399	861.6330	*3%*	*2%*	*-1%*	*2%*	***-4%***	***0%***
Story9	39.00	936.8511	907.8189	891.0346	892.5074	933.6879	921.1828	*5%*	*2%*	*0%*	*2%*	***-5%***	***0%***
Story8	35.40	994.0691	964.2206	926.7184	953.9952	974.7235	984.7867	*7%*	*1%*	*2%*	*1%*	***-5%***	***0%***
Story7	31.80	1051.5319	1021.2969	958.2226	1014.8635	1011.3588	1048.2287	*9%*	*1%*	*4%*	*0%*	***-5%***	***0%***
Story6	28.20	1107.6314	1077.1619	985.1234	1071.6386	1042.9678	1107.7650	*11%*	*1%*	*6%*	*0%*	***-5%***	***-1%***
Story5	24.60	1173.3689	1142.0921	1012.0117	1132.4470	1074.9054	1171.9012	*14%*	*1%*	*8%*	*0%*	***-5%***	***-1%***
Story4	17.40	1217.3566	1184.4075	1026.6738	1167.9911	1092.5268	1209.4961	*16%*	*1%*	*10%*	*1%*	***-5%***	***-1%***
Story3	14.00	1250.4001	1216.9976	1035.3037	1189.7809	1102.9284	1232.5757	*17%*	*2%*	*12%*	*1%*	***-5%***	***-1%***
Story2	10.60	1275.6624	1242.9820	1040.4364	1203.3193	1109.1269	1246.9178	*18%*	*3%*	*13%*	*2%*	***-5%***	***-1%***
Story1	7.20	1296.2258	1265.1830	1043.7557	1212.4642	1113.1422	1256.6130	*19%*	*4%*	*14%*	*3%*	***-5%***	***-1%***

Table 5. 64 Service Level Earthquake (RSA) : Story Shear comparison

The same can be said for the service condition, in which a lower cut value can be observed for Model 2 than for Model 3 in the x-direction, while for the y-direction in

correspondence of the levels in proximity of the Outrigger system it can be observed that the model 1 introduces values of cut inferior to the other two models.

In table 5.65 it comes evidenced the comparison for the maximum values of interstory shear in the condition of Service:

ServiceLevelEarthquake (RSA)

SHEAR X				
Model 1: w/o OUTRIGGER [tonf]	Model 2: with 2 OUTRIGGER [tonf]	Model 3: with 3 OUTRIGGER [tonf]	**ReductionModel 2 [%]**	**ReductionModel 3 [%]**
1296.23	1043.76	1113.14	**19%**	**14%**
SHEAR Y				
Model 1: w/o OUTRIGGER [tonf]	Model 2: with 2 OUTRIGGER [tonf]	Model 3: with 3 OUTRIGGER [tonf]	**ReductionModel 2 [%]**	**ReductionModel 3 [%]**
1265.18	1212.46	1256.61	**4%**	**1%**

Table 5. 65 Maximum comparison values for the interstory shear in the service condition

Non-linear time history analysis:

Below is an analysis of the comparison made for the three models studied, taking into account the analysis carried out for the Maximum Considered Earthquake, evaluating 10 seismic signals and performing a non-linear time history analysis.

The comparison is made taking into account two rules, the American rules that is the CFE and the Mexican rules; the first defines that the comparison must be carried out taking into account the mean values analyzed, the second, however, through the consideration of the maximum values analyzed. Below are the output data obtained and compared.

- **Drift**

Figure 5.107 and Table 5.66 show the results of inter-story drift in x and y direction for the three models compared and analysed taking into account the maximum values, as defined by the Mexican standard:

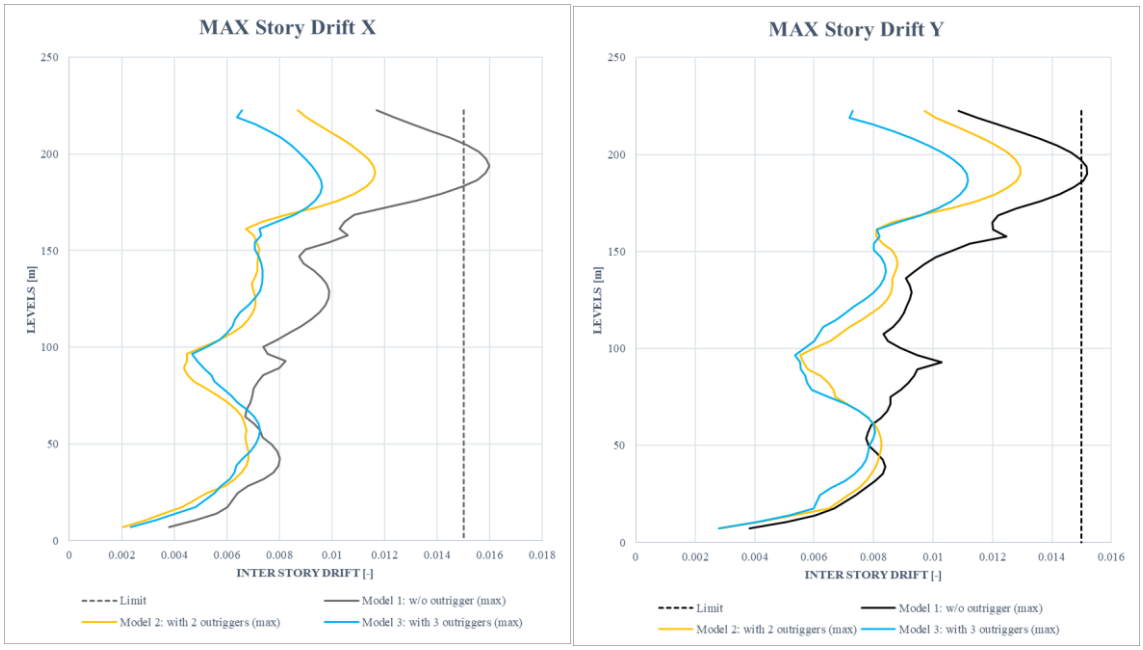

Figure 5. 107 Maximum Drift comparison - Nonlinear time history analysis

Nonlinear time history analysis : Maximum Drift comparison

Story	Elevation	Model 1: Story Drift w/o Outrigger		Model 2: Story Drift with 2 Outrigger		Model 3: Story Drift with 3 Outrigger		*REDUCTION MODEL 2*		*REDUCTION MODEL 3*		*COMPARISON MODEL 2 VS MODEL 3*	
		X-Dir	Y-Dir	X-Dir	Y-Dir	X-Dir	Y-Dir	*X-Dir*	*Y-Dir*	*X-Dir*	*Y-Dir*	*X-Dir*	*Y-Dir*
[-]	m	[-]	[-]	[-]	[-]	[-]	[-]	*[%]*	*[%]*	*[%]*	*[%]*	*[%]*	*[%]*
Story60	222.60	0.012	0.011	0.009	0.010	0.007	0.007	*26%*	*11%*	*44%*	*33%*	***18%***	***22%***
Story59	219.00	0.012	0.011	0.009	0.010	0.006	0.007	*27%*	*12%*	*48%*	*37%*	***21%***	***25%***
Story58	215.40	0.013	0.012	0.009	0.011	0.007	0.008	*28%*	*13%*	*46%*	*35%*	***18%***	***22%***
Story57	211.80	0.014	0.013	0.010	0.011	0.008	0.009	*28%*	*13%*	*45%*	*33%*	***16%***	***19%***
Story56	208.20	0.014	0.014	0.010	0.012	0.008	0.009	*29%*	*14%*	*44%*	*31%*	***16%***	***18%***
Story55	204.60	0.015	0.014	0.011	0.012	0.008	0.010	*29%*	*14%*	*44%*	*30%*	***15%***	***16%***
Story54	201.00	0.016	0.015	0.011	0.013	0.009	0.010	*29%*	*15%*	*44%*	*30%*	***15%***	***15%***
Story53	197.40	0.016	0.015	0.011	0.013	0.009	0.011	*28%*	*15%*	*43%*	*29%*	***15%***	***14%***
Story52	193.80	0.016	0.015	0.012	0.013	0.009	0.011	*28%*	*15%*	*42%*	*28%*	***15%***	***13%***
Story51	190.20	0.016	0.015	0.012	0.013	0.009	0.011	*27%*	*15%*	*40%*	*27%*	***14%***	***12%***
Story50	186.60	0.016	0.015	0.012	0.013	0.010	0.011	*26%*	*15%*	*38%*	*26%*	***13%***	***11%***
Story49	183.00	0.015	0.015	0.011	0.013	0.010	0.011	*24%*	*15%*	*36%*	*25%*	***11%***	***10%***
Story48	179.40	0.014	0.014	0.011	0.012	0.010	0.011	*23%*	*15%*	*33%*	*23%*	***9%***	***8%***
Story47	175.80	0.013	0.014	0.010	0.011	0.009	0.011	*23%*	*16%*	*29%*	*22%*	***7%***	***6%***
Story46	172.20	0.012	0.013	0.009	0.011	0.009	0.010	*22%*	*17%*	*25%*	*21%*	***3%***	***3%***
Story45	168.60	0.011	0.012	0.008	0.010	0.009	0.010	*24%*	*22%*	*21%*	*21%*	***-3%***	***0%***
Story44	165.00	0.010	0.012	0.007	0.009	0.008	0.009	*30%*	*28%*	*25%*	*27%*	***-5%***	***-2%***
Story43	161.40	0.010	0.012	0.007	0.008	0.007	0.008	*35%*	*33%*	*30%*	*33%*	***-5%***	***0%***
Story42	157.80	0.011	0.012	0.007	0.008	0.007	0.008	*34%*	*35%*	*31%*	*34%*	***-3%***	***-1%***
Story41	154.20	0.010	0.011	0.007	0.008	0.007	0.008	*28%*	*26%*	*29%*	*29%*	***1%***	***3%***
Story40	150.60	0.009	0.011	0.007	0.009	0.007	0.008	*20%*	*20%*	*21%*	*25%*	***2%***	***6%***

Story39	147.00	0.009	0.010	0.007	0.009	0.007	0.008	*18%*	*13%*	*18%*	*18%*	***0%***	***5%***
Story38	143.40	0.009	0.010	0.007	0.009	0.007	0.008	*20%*	*9%*	*18%*	*14%*	***-2%***	***4%***
Story37	139.80	0.009	0.009	0.007	0.009	0.007	0.008	*23%*	*7%*	*21%*	*10%*	***-2%***	***4%***
Story36	136.20	0.010	0.009	0.007	0.009	0.007	0.008	*26%*	*5%*	*23%*	*8%*	***-3%***	***3%***
Story35	132.60	0.010	0.009	0.007	0.009	0.007	0.008	*29%*	*6%*	*25%*	*11%*	***-4%***	***4%***
Story34	129.00	0.010	0.009	0.007	0.009	0.007	0.008	*29%*	*7%*	*27%*	*14%*	***-2%***	***6%***
Story33	125.40	0.010	0.009	0.007	0.008	0.007	0.008	*28%*	*8%*	*28%*	*16%*	***0%***	***8%***
Story32	121.80	0.010	0.009	0.007	0.008	0.007	0.007	*27%*	*9%*	*30%*	*19%*	***3%***	***10%***
Story31	118.20	0.010	0.009	0.007	0.008	0.007	0.007	*27%*	*12%*	*32%*	*22%*	***5%***	***10%***
Story30	114.60	0.009	0.009	0.007	0.008	0.006	0.007	*26%*	*14%*	*31%*	*24%*	***6%***	***10%***
Story29	111.00	0.009	0.009	0.007	0.007	0.006	0.006	*26%*	*17%*	*30%*	*27%*	***4%***	***10%***
Story28	107.40	0.008	0.008	0.006	0.007	0.006	0.006	*26%*	*17%*	*28%*	*26%*	***2%***	***9%***
Story27	103.80	0.008	0.008	0.006	0.007	0.006	0.006	*28%*	*23%*	*28%*	*29%*	***0%***	***6%***
Story26	100.20	0.007	0.009	0.005	0.006	0.005	0.006	*31%*	*33%*	*29%*	*36%*	***-2%***	***4%***
Story25	96.60	0.008	0.009	0.004	0.006	0.005	0.005	*41%*	*42%*	*38%*	*43%*	***-3%***	***2%***
Story24	93.00	0.008	0.010	0.004	0.006	0.005	0.006	*46%*	*45%*	*41%*	*46%*	***-5%***	***1%***
Story23	89.40	0.008	0.009	0.004	0.006	0.005	0.006	*45%*	*39%*	*36%*	*41%*	***-10%***	***3%***
Story22	85.80	0.007	0.009	0.005	0.006	0.005	0.006	*39%*	*34%*	*27%*	*39%*	***-12%***	***5%***
Story21	82.20	0.007	0.009	0.005	0.006	0.006	0.006	*34%*	*29%*	*23%*	*37%*	***-11%***	***8%***
Story20	78.60	0.007	0.009	0.005	0.007	0.006	0.006	*25%*	*25%*	*17%*	*34%*	***-9%***	***8%***
Story19	75.00	0.007	0.009	0.006	0.007	0.006	0.006	*19%*	*22%*	*12%*	*24%*	***-7%***	***3%***
Story18	71.40	0.007	0.009	0.006	0.007	0.006	0.007	*12%*	*17%*	*7%*	*17%*	***-5%***	***0%***
Story17	67.80	0.007	0.008	0.006	0.008	0.007	0.008	*6%*	*11%*	*0%*	*11%*	***-6%***	***0%***
Story16	64.20	0.007	0.008	0.007	0.008	0.007	0.008	*2%*	*5%*	*-5%*	*5%*	***-7%***	***0%***
Story15	60.60	0.007	0.008	0.007	0.008	0.007	0.008	*5%*	*-1%*	*-2%*	*-1%*	***-7%***	***1%***
Story14	57.00	0.007	0.008	0.007	0.008	0.007	0.008	*7%*	*-5%*	*0%*	*-3%*	***-7%***	***2%***
Story13	53.40	0.007	0.008	0.007	0.008	0.007	0.008	*9%*	*-7%*	*2%*	*-3%*	***-7%***	***3%***
Story12	49.80	0.008	0.008	0.007	0.008	0.007	0.008	*12%*	*-6%*	*8%*	*0%*	***-4%***	***5%***
Story11	46.20	0.008	0.008	0.007	0.008	0.007	0.008	*14%*	*-2%*	*13%*	*4%*	***-1%***	***5%***
Story10	42.60	0.008	0.008	0.007	0.008	0.007	0.008	*15%*	*2%*	*18%*	*7%*	***3%***	***5%***
Story9	39.00	0.008	0.008	0.007	0.008	0.006	0.008	*15%*	*4%*	*20%*	*9%*	***5%***	***6%***
Story8	35.40	0.008	0.008	0.007	0.008	0.006	0.007	*16%*	*5%*	*19%*	*11%*	***4%***	***7%***
Story7	31.80	0.007	0.008	0.006	0.008	0.006	0.007	*15%*	*4%*	*17%*	*13%*	***2%***	***9%***
Story6	28.20	0.007	0.008	0.006	0.008	0.006	0.007	*13%*	*3%*	*15%*	*15%*	***2%***	***12%***
Story5	24.60	0.006	0.007	0.005	0.007	0.006	0.006	*18%*	*4%*	*14%*	*16%*	***-4%***	***13%***
Story4	17.40	0.006	0.007	0.004	0.006	0.005	0.006	*29%*	*3%*	*20%*	*11%*	***-8%***	***8%***
Story3	14.00	0.006	0.006	0.004	0.005	0.004	0.005	*36%*	*12%*	*28%*	*15%*	***-8%***	***2%***
Story2	10.60	0.005	0.005	0.003	0.004	0.003	0.004	*39%*	*18%*	*31%*	*19%*	***-8%***	***1%***
Story1	7.20	0.004	0.004	0.002	0.003	0.002	0.003	*46%*	*26%*	*39%*	*27%*	***-8%***	***1%***

Table 5. 66 Maximum Drift comparison - Nonlinear time history analysis

It can be observed that models 2 and 3 define a marked improvement compared to Model 1, the drift in fact decreases at the double heights where the Outrigger system

is inserted up to a maximum reduction of 46% for both models compared to the one without system.

If we wanted to analyze a difference between Model 2 and Model 3, they have very similar values up to level 48, where there is an improvement of Model 3 compared to Model 2 due to the presence of the third Outrigger system. The reduction of Model 3 compared to Model 2 comes in fact to 25% just at level 59 where the system is inserted.

Taking into account the maximum values, as defined by the Mexican regulation, it can be observed that Model 1 has both in the X direction and in the Y direction of the values such as to have a drift greater than the limit imposed by the standard and therefore equal to 0,015; while Models 2 and 3 allow to stay well below the threshold imposed.

Figure 5.108 and Table 5.67 show the results of interpiano drift in x and y direction for the three models compared and analysed taking into account the average values, as defined by the CFE:

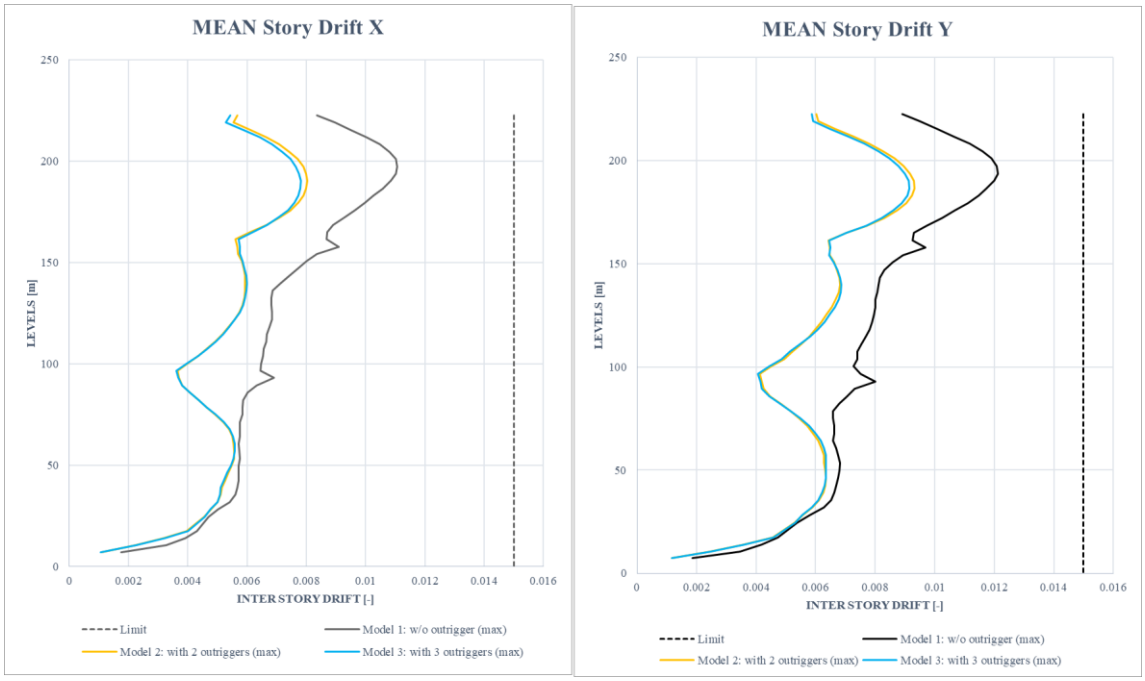

Figure 5. 108 Mean Drift comparison - Nonlinear time history analysis

Nonlinear time history analysis : Mean Drift comparison

Story	Elevation	Model 1: Story Drift w/o Outrigger	Model 2: Story Drift with 2 Outrigger	Model 3: Story Drift with 3 Outrigger	*REDUCTION MODEL 2*	*REDUCTION MODEL 3*	*COMPARISON MODEL 2 VS MODEL 3*

		X-Dir	Y-Dir	X-Dir	Y-Dir	X-Dir	Y-Dir	*X-Dir*	*Y-Dir*	*X-Dir*	*Y-Dir*	*X-Dir*	*Y-Dir*
[-]	m	[-]	[-]	[-]	[-]	[-]	[-]	*[%]*	*[%]*	*[%]*	*[%]*	*[%]*	*[%]*
Story60	222.60	0.008	0.009	0.006	0.006	0.005	0.006	*32%*	*32%*	*35%*	*34%*	***3%***	***2%***
Story59	219.00	0.009	0.009	0.006	0.006	0.005	0.006	*38%*	*36%*	*41%*	*38%*	***3%***	***2%***
Story58	215.40	0.010	0.010	0.006	0.007	0.006	0.006	*36%*	*34%*	*38%*	*36%*	***2%***	***2%***
Story57	211.80	0.010	0.011	0.007	0.007	0.006	0.007	*34%*	*32%*	*36%*	*33%*	***2%***	***1%***
Story56	208.20	0.010	0.011	0.007	0.008	0.007	0.008	*32%*	*30%*	*35%*	*32%*	***2%***	***1%***
Story55	204.60	0.011	0.012	0.007	0.008	0.007	0.008	*31%*	*29%*	*33%*	*30%*	***2%***	***1%***
Story54	201.00	0.011	0.012	0.008	0.009	0.007	0.008	*30%*	*27%*	*32%*	*29%*	***2%***	***1%***
Story53	197.40	0.011	0.012	0.008	0.009	0.008	0.009	*29%*	*26%*	*31%*	*27%*	***2%***	***1%***
Story52	193.80	0.011	0.012	0.008	0.009	0.008	0.009	*27%*	*24%*	*30%*	*26%*	***2%***	***1%***
Story51	190.20	0.011	0.012	0.008	0.009	0.008	0.009	*26%*	*22%*	*28%*	*24%*	***2%***	***1%***
Story50	186.60	0.011	0.012	0.008	0.009	0.008	0.009	*25%*	*21%*	*26%*	*22%*	***2%***	***1%***
Story49	183.00	0.010	0.011	0.008	0.009	0.008	0.009	*23%*	*20%*	*25%*	*21%*	***2%***	***1%***
Story48	179.40	0.010	0.011	0.008	0.009	0.008	0.009	*23%*	*19%*	*24%*	*20%*	***1%***	***1%***
Story47	175.80	0.010	0.011	0.007	0.009	0.007	0.009	*23%*	*18%*	*24%*	*19%*	***1%***	***1%***
Story46	172.20	0.009	0.010	0.007	0.008	0.007	0.008	*24%*	*19%*	*24%*	*20%*	***0%***	***1%***
Story45	168.60	0.009	0.010	0.007	0.008	0.007	0.008	*25%*	*21%*	*25%*	*21%*	***0%***	***0%***
Story44	165.00	0.009	0.009	0.006	0.007	0.006	0.007	*30%*	*24%*	*29%*	*24%*	***-1%***	***0%***
Story43	161.40	0.009	0.009	0.006	0.006	0.006	0.006	*35%*	*31%*	*34%*	*30%*	***-1%***	***0%***
Story42	157.80	0.009	0.010	0.006	0.006	0.006	0.006	*38%*	*33%*	*37%*	*33%*	***-1%***	***0%***
Story41	154.20	0.008	0.009	0.006	0.006	0.006	0.006	*32%*	*28%*	*31%*	*28%*	***-1%***	***0%***
Story40	150.60	0.008	0.009	0.006	0.007	0.006	0.007	*27%*	*23%*	*27%*	*23%*	***0%***	***0%***
Story39	147.00	0.008	0.008	0.006	0.007	0.006	0.007	*24%*	*19%*	*23%*	*19%*	***-1%***	***0%***
Story38	143.40	0.007	0.008	0.006	0.007	0.006	0.007	*20%*	*17%*	*20%*	*16%*	***-1%***	***0%***
Story37	139.80	0.007	0.008	0.006	0.007	0.006	0.007	*17%*	*16%*	*16%*	*15%*	***-1%***	***-1%***
Story36	136.20	0.007	0.008	0.006	0.007	0.006	0.007	*13%*	*16%*	*13%*	*15%*	***-1%***	***-1%***
Story35	132.60	0.007	0.008	0.006	0.007	0.006	0.007	*13%*	*17%*	*13%*	*16%*	***0%***	***-1%***
Story34	129.00	0.007	0.008	0.006	0.007	0.006	0.007	*14%*	*18%*	*14%*	*17%*	***0%***	***-1%***
Story33	125.40	0.007	0.008	0.006	0.006	0.006	0.006	*16%*	*20%*	*16%*	*19%*	***0%***	***-1%***
Story32	121.80	0.007	0.008	0.006	0.006	0.006	0.006	*18%*	*22%*	*18%*	*20%*	***0%***	***-2%***
Story31	118.20	0.007	0.008	0.005	0.006	0.005	0.006	*20%*	*23%*	*20%*	*22%*	***0%***	***-1%***
Story30	114.60	0.007	0.008	0.005	0.006	0.005	0.006	*23%*	*25%*	*22%*	*24%*	***0%***	***0%***
Story29	111.00	0.007	0.008	0.005	0.006	0.005	0.005	*26%*	*27%*	*26%*	*28%*	***0%***	***1%***
Story28	107.40	0.007	0.007	0.005	0.005	0.005	0.005	*29%*	*29%*	*29%*	*31%*	***0%***	***1%***
Story27	103.80	0.007	0.007	0.004	0.005	0.004	0.005	*34%*	*33%*	*34%*	*34%*	***0%***	***1%***
Story26	100.20	0.006	0.007	0.004	0.005	0.004	0.004	*38%*	*38%*	*39%*	*39%*	***0%***	***1%***
Story25	96.60	0.006	0.008	0.004	0.004	0.004	0.004	*43%*	*45%*	*44%*	*46%*	***1%***	***1%***
Story24	93.00	0.007	0.008	0.004	0.004	0.004	0.004	*46%*	*48%*	*47%*	*48%*	***0%***	***1%***
Story23	89.40	0.006	0.007	0.004	0.004	0.004	0.004	*40%*	*42%*	*40%*	*43%*	***0%***	***1%***
Story22	85.80	0.006	0.007	0.004	0.004	0.004	0.004	*32%*	*37%*	*32%*	*37%*	***0%***	***0%***
Story21	82.20	0.006	0.007	0.004	0.005	0.004	0.005	*25%*	*29%*	*25%*	*29%*	***0%***	***0%***
Story20	78.60	0.006	0.007	0.005	0.005	0.005	0.005	*21%*	*22%*	*21%*	*22%*	***0%***	***0%***
Story19	75.00	0.006	0.007	0.005	0.005	0.005	0.005	*16%*	*17%*	*15%*	*17%*	***0%***	***-1%***

Story18	71.40	0.006	0.007	0.005	0.006	0.005	0.006	*10%*	*14%*	*10%*	*13%*	***0%***	***-1%***
Story17	67.80	0.006	0.007	0.005	0.006	0.005	0.006	*6%*	*11%*	*6%*	*9%*	***0%***	***-1%***
Story16	64.20	0.006	0.007	0.005	0.006	0.006	0.006	*5%*	*8%*	*4%*	*6%*	***0%***	***-2%***
Story15	60.60	0.006	0.007	0.006	0.006	0.006	0.006	*3%*	*7%*	*3%*	*6%*	***0%***	***-1%***
Story14	57.00	0.006	0.007	0.006	0.006	0.006	0.006	*3%*	*7%*	*3%*	*6%*	***0%***	***-1%***
Story13	53.40	0.006	0.007	0.006	0.006	0.006	0.006	*3%*	*8%*	*4%*	*7%*	***0%***	***-1%***
Story12	49.80	0.006	0.007	0.005	0.006	0.005	0.006	*4%*	*7%*	*5%*	*6%*	***1%***	***0%***
Story11	46.20	0.006	0.007	0.005	0.006	0.005	0.006	*6%*	*6%*	*7%*	*6%*	***1%***	***0%***
Story10	42.60	0.006	0.007	0.005	0.006	0.005	0.006	*8%*	*6%*	*9%*	*6%*	***1%***	***0%***
Story9	39.00	0.006	0.007	0.005	0.006	0.005	0.006	*9%*	*6%*	*10%*	*6%*	***1%***	***1%***
Story8	35.40	0.006	0.007	0.005	0.006	0.005	0.006	*9%*	*6%*	*9%*	*7%*	***0%***	***0%***
Story7	31.80	0.005	0.006	0.005	0.006	0.005	0.006	*8%*	*6%*	*8%*	*6%*	***0%***	***0%***
Story6	28.20	0.005	0.006	0.005	0.006	0.005	0.006	*5%*	*4%*	*5%*	*4%*	***0%***	***0%***
Story5	24.60	0.005	0.005	0.005	0.005	0.005	0.005	*3%*	*1%*	*3%*	*1%*	***-1%***	***0%***
Story4	17.40	0.004	0.005	0.004	0.005	0.004	0.005	*8%*	*4%*	*7%*	*3%*	***-1%***	***-1%***
Story3	14.00	0.004	0.004	0.003	0.004	0.003	0.004	*18%*	*14%*	*17%*	*14%*	***-1%***	***-1%***
Story2	10.60	0.003	0.003	0.002	0.002	0.002	0.002	*32%*	*29%*	*31%*	*29%*	***-1%***	***-1%***
Story1	7.20	0.002	0.002	0.001	0.001	0.001	0.001	*39%*	*37%*	*39%*	*37%*	***0%***	***-1%***

Table 5. 67 Mean Drift comparison - Nonlinear time history analysis

It can be observed that models 2 and 3 define an improvement over Model 1, the drift in fact decreases at the double heights where the Outrigger system is inserted up to a maximum reduction of 46% for both models compared to the one without system.

If we wanted to analyze a difference between Model 2 and Model 3, the average values evaluated are very similar and almost coincident for the entire height of the building.

Taking into account mean values, as defined by the CFE in all the models deduced, the limit prescribed by the legislation is respected both in direction X and in direction Y. Models 2 and 3 have an mean reduction of 22% compared to Model 1 representative of the structure without reinforcement system structural.

Table 5.68 Shows the maximum value obtained in x and y direction and compared for the Interstory Drift considering both the Mexican standard and the CFE:

Maximum values for Interstory Drift - Mexican Code

	w/o OUTRIGGER	with 2 OUTRIGGER	with3 OUTRIGGER	**REDUCTION Model 2**	**REDUCTION Model 3**	**COMPARISON MODEL 2 VS MODEL 3**
	[-]	[-]	[-]	**[%]**	**[%]**	**[%]**
MAX X	0.016	0.012	0.010	27%	40%	13%
MAX Y	0.015	0.013	0.011	15%	26%	12%

Maximum values for Interstory Drift - CFE

	w/o OUTRIGGER	with 2 OUTRIGGER	with3 OUTRIGGER	**REDUCTION Model 2**	**REDUCTION Model 3**	**COMPARISON MODEL 2 VS MODEL 3**
	[-]	[-]	[-]	**[%]**	**[%]**	**[%]**
MEAN X	0.011	0.008	0.008	27%	29%	2%
MEAN Y	0.012	0.009	0.009	23%	24%	1%

Table 5. 68 Maximum values for Interstory Drift - Mexican Code vs CFE

Analyzing the maximum values obtained both evaluating the maximum and the average of all the values obtained as output we can define a difference between the Mexican Code and the CFE.. The reduction in Models 2 and 3 compared to Model 1 of the system-free structure can be deduced in both cases. Comparing both models with the applied system we note that:

- By evaluating the maximum values, the model with 3 Outrigger has an improvement over the model without Outrigger up to 40% in x direction, while the Model with 2 Outrigger has an improvement up to 27% in the same direction. Also you can notice that the Model 3 has an improvement over the system with 2 Outrigger up to 13% in x direction;
- By evaluating the average values, the model with 3 Outrigger has an improvement over the model without Outrigger up to 29% in x direction, while the Model with 2 Outrigger has an improvement up to 27% in the same direction. Also you can notice that the Model 3 has an improvement over the system with 2 Outrigger of 2% in x direction, and therefore very small.

❖ **Displacement**

Figure 5.109 and Table 5.67 show the results of the interstory displacements in x and y direction for the three models compared and analysed taking into account the maximum values, as defined by the Mexican standard:

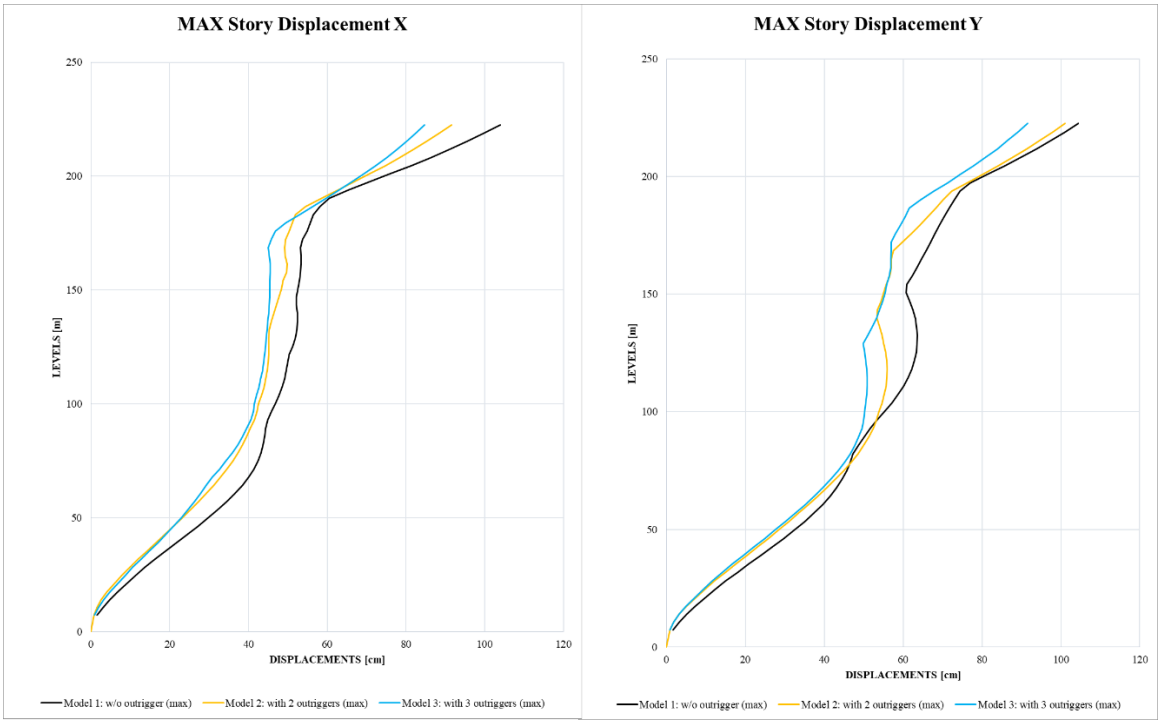

Figure 5. 109 Maximum Displacement comparison - Nonlinear time history analysis

Nonlinear time history analysis : Maximum Displacements comparison

Story	Elevation	Model 1: Story Displacement w/o Outrigger		Model 2: Story Displacement with 2 Outrigger		Model 3: Story Displacement with 3 Outrigger		*REDUCTION MODEL 2*		*REDUCTION MODEL 3*		*COMPARISON MODEL 2 VS MODEL 3*	
		X-Dir	Y-Dir	X-Dir	Y-Dir	X-Dir	Y-Dir	*X-Dir*	*Y-Dir*	*X-Dir*	*Y-Dir*	*X-Dir*	*Y-Dir*
[-]	[m]	[cm]	[cm]	[cm]	[cm]	[cm]	[cm]	*[%]*	*[%]*	*[%]*	*[%]*	*[%]*	*[%]*
Story60	222.60	103.96	104.47	91.62	101.07	84.74	91.55	*12%*	*3%*	*18%*	*12%*	***7%***	***9%***
Story59	219.00	99.85	101.05	88.51	97.93	82.48	89.06	*11%*	*3%*	*17%*	*12%*	***6%***	***9%***
Story58	215.40	95.53	97.48	85.27	94.69	80.16	86.55	*11%*	*3%*	*16%*	*11%*	***5%***	***8%***
Story57	211.80	90.97	93.74	81.89	91.30	77.68	83.84	*10%*	*3%*	*15%*	*11%*	***5%***	***8%***
Story56	208.20	86.22	89.81	78.34	87.75	75.03	80.93	*9%*	*2%*	*13%*	*10%*	***4%***	***8%***
Story55	204.60	81.23	85.70	74.63	84.06	72.23	77.84	*8%*	*2%*	*11%*	*9%*	***3%***	***7%***
Story54	201.00	76.00	81.42	70.77	80.23	69.30	74.59	*7%*	*1%*	*9%*	*8%*	***2%***	***7%***
Story53	197.40	70.69	76.99	66.79	76.29	66.23	71.24	*6%*	*1%*	*6%*	*7%*	***1%***	***7%***
Story52	193.80	65.26	74.44	62.71	72.30	63.03	67.83	*4%*	*3%*	*3%*	*9%*	***0%***	***6%***
Story51	190.20	60.54	72.99	58.58	70.18	59.72	64.40	*3%*	*4%*	*1%*	*12%*	***-2%***	***8%***
Story50	186.60	58.12	71.65	54.47	68.27	56.34	61.56	*6%*	*5%*	*3%*	*14%*	***-3%***	***9%***
Story49	183.00	56.42	70.40	51.91	66.29	52.90	60.45	*8%*	*6%*	*6%*	*14%*	***-2%***	***8%***
Story48	179.40	55.72	69.22	51.16	64.24	49.44	59.31	*8%*	*7%*	*11%*	*14%*	***3%***	***7%***
Story47	175.80	54.85	68.10	50.36	62.09	46.85	58.10	*8%*	*9%*	*15%*	*15%*	***6%***	***6%***
Story46	172.20	53.72	67.01	49.47	59.87	45.80	57.06	*8%*	*11%*	*15%*	*15%*	***7%***	***4%***
Story45	168.60	53.17	65.89	49.20	57.59	45.08	57.04	*7%*	*13%*	*15%*	*13%*	***8%***	***1%***
Story44	165.00	53.37	64.72	49.32	57.00	45.22	56.92	*8%*	*12%*	*15%*	*12%*	***8%***	***0%***
Story43	161.40	53.34	63.50	49.82	56.98	45.49	56.87	*7%*	*10%*	*15%*	*10%*	***8%***	***0%***
Story42	157.80	53.20	62.30	49.66	56.59	45.58	56.54	*7%*	*9%*	*14%*	*9%*	***8%***	***0%***

Story41	154.20	52.91	60.94	48.80	55.72	45.34	55.89	*8%*	*9%*	*14%*	*8%*	***7%***	***0%***
Story40	150.60	52.58	60.77	48.36	55.12	45.37	55.42	*8%*	*9%*	*14%*	*9%*	***6%***	***-1%***
Story39	147.00	52.15	61.74	47.79	54.36	45.35	54.81	*8%*	*12%*	*13%*	*11%*	***5%***	***-1%***
Story38	143.40	52.17	62.49	47.08	53.51	45.28	54.08	*10%*	*14%*	*13%*	*13%*	***3%***	***-1%***
Story37	139.80	52.44	63.06	46.42	53.33	45.12	53.21	*11%*	*15%*	*14%*	*16%*	***2%***	***0%***
Story36	136.20	52.47	63.40	45.79	54.00	44.94	52.20	*13%*	*15%*	*14%*	*18%*	***2%***	***3%***
Story35	132.60	52.29	63.59	45.31	54.61	44.76	51.09	*13%*	*14%*	*14%*	*20%*	***1%***	***6%***
Story34	129.00	51.86	63.57	45.10	55.12	44.54	49.87	*13%*	*13%*	*14%*	*22%*	***1%***	***8%***
Story33	125.40	51.20	63.31	45.11	55.54	44.30	50.22	*12%*	*12%*	*13%*	*21%*	***2%***	***8%***
Story32	121.80	50.32	62.84	45.12	55.83	44.11	50.56	*10%*	*11%*	*12%*	*20%*	***2%***	***8%***
Story31	118.20	49.91	62.15	44.99	55.96	43.85	50.79	*10%*	*10%*	*12%*	*18%*	***2%***	***8%***
Story30	114.60	49.62	61.24	44.78	55.90	43.52	50.90	*10%*	*9%*	*12%*	*17%*	***3%***	***8%***
Story29	111.00	49.21	60.10	44.39	55.65	43.11	50.90	*10%*	*7%*	*12%*	*15%*	***3%***	***8%***
Story28	107.40	48.58	58.74	43.91	55.25	42.64	50.80	*10%*	*6%*	*12%*	*14%*	***3%***	***8%***
Story27	103.80	47.79	57.16	43.28	54.66	42.08	50.56	*9%*	*4%*	*12%*	*12%*	***3%***	***7%***
Story26	100.20	46.81	55.37	42.55	53.90	41.48	50.21	*9%*	*3%*	*11%*	*9%*	***2%***	***7%***
Story25	96.60	45.79	53.40	42.09	53.28	41.18	50.05	*8%*	*0%*	*10%*	*6%*	***2%***	***6%***
Story24	93.00	44.93	51.73	41.49	52.43	40.64	49.57	*8%*	*-1%*	*10%*	*4%*	***2%***	***6%***
Story23	89.40	44.33	50.18	40.44	51.28	39.54	48.65	*9%*	*-2%*	*11%*	*3%*	***2%***	***5%***
Story22	85.80	44.04	48.68	39.53	50.06	38.55	47.77	*10%*	*-3%*	*12%*	*2%*	***2%***	***5%***
Story21	82.20	43.69	47.31	38.46	48.58	37.32	46.63	*12%*	*-3%*	*15%*	*1%*	***3%***	***4%***
Story20	78.60	43.15	46.64	37.28	46.87	35.85	45.22	*14%*	*0%*	*17%*	*3%*	***3%***	***4%***
Story19	75.00	42.42	45.72	35.97	44.95	34.27	43.56	*15%*	*2%*	*19%*	*5%*	***4%***	***3%***
Story18	71.40	41.38	44.58	34.53	42.90	32.60	41.72	*17%*	*4%*	*21%*	*6%*	***5%***	***3%***
Story17	67.80	40.05	43.18	32.92	40.71	30.88	39.67	*18%*	*6%*	*23%*	*8%*	***5%***	***2%***
Story16	64.20	38.46	41.51	31.17	38.41	29.21	37.48	*19%*	*7%*	*24%*	*10%*	***5%***	***2%***
Story15	60.60	36.57	39.59	29.27	36.02	27.84	35.15	*20%*	*9%*	*24%*	*11%*	***4%***	***2%***
Story14	57.00	34.46	37.44	27.29	33.55	26.31	32.70	*21%*	*10%*	*24%*	*13%*	***3%***	***2%***
Story13	53.40	32.15	35.08	25.25	31.02	24.63	30.17	*21%*	*12%*	*23%*	*14%*	***2%***	***2%***
Story12	49.80	29.68	32.52	23.12	28.44	22.85	27.56	*22%*	*13%*	*23%*	*15%*	***1%***	***3%***
Story11	46.20	27.12	29.78	20.95	25.81	20.96	24.90	*23%*	*13%*	*23%*	*16%*	***0%***	***3%***
Story10	42.60	24.45	26.91	18.78	23.11	19.02	22.18	*23%*	*14%*	*22%*	*18%*	***-1%***	***3%***
Story9	39.00	21.73	23.96	16.53	20.38	16.97	19.48	*24%*	*15%*	*22%*	*19%*	***-2%***	***4%***
Story8	35.40	18.99	20.97	14.24	17.64	14.87	16.80	*25%*	*16%*	*22%*	*20%*	***-3%***	***4%***
Story7	31.80	16.31	18.00	11.98	14.93	12.72	14.18	*27%*	*17%*	*22%*	*21%*	***-5%***	***4%***
Story6	28.20	13.69	15.11	9.81	12.26	10.58	11.67	*28%*	*19%*	*23%*	*23%*	***-6%***	***4%***
Story5	24.60	11.26	12.39	7.77	9.72	8.65	9.32	*31%*	*22%*	*23%*	*25%*	***-8%***	***3%***
Story4	17.40	6.77	7.31	4.08	5.07	4.84	4.97	*40%*	*31%*	*28%*	*32%*	***-11%***	***1%***
Story3	14.00	4.83	5.17	2.64	3.28	3.24	3.23	*45%*	*37%*	*33%*	*38%*	***-13%***	***1%***
Story2	10.60	3.06	3.26	1.50	1.87	1.90	1.84	*51%*	*43%*	*38%*	*44%*	***-13%***	***1%***
Story1	7.20	1.58	1.68	0.74	0.90	0.93	0.89	*53%*	*46%*	*41%*	*47%*	***-12%***	***1%***

Table 5. 69 Maximum Displacement comparison - Nonlinear time history analysis

Evaluating the maximum values you can see that the models 2 and 3 define a reduction in displecement compared to Model 1, it is defined to a maximum reduction of 15% for Model 2 and 22% for Model 3.

If we wanted to analyze a difference between Model 2 and Model 3, they have very similar values and differ more precisely in correspondence of the higher levels where there is the third Outrigger for model 3, which has a reduction of up to 9% compared to the model with only 2 Outrigger

Figure 5.110 and Table 5.70 show the results of the interstory displacements in x and y direction for the three models compared and analysed taking into account the average values, as defined by the CFE:

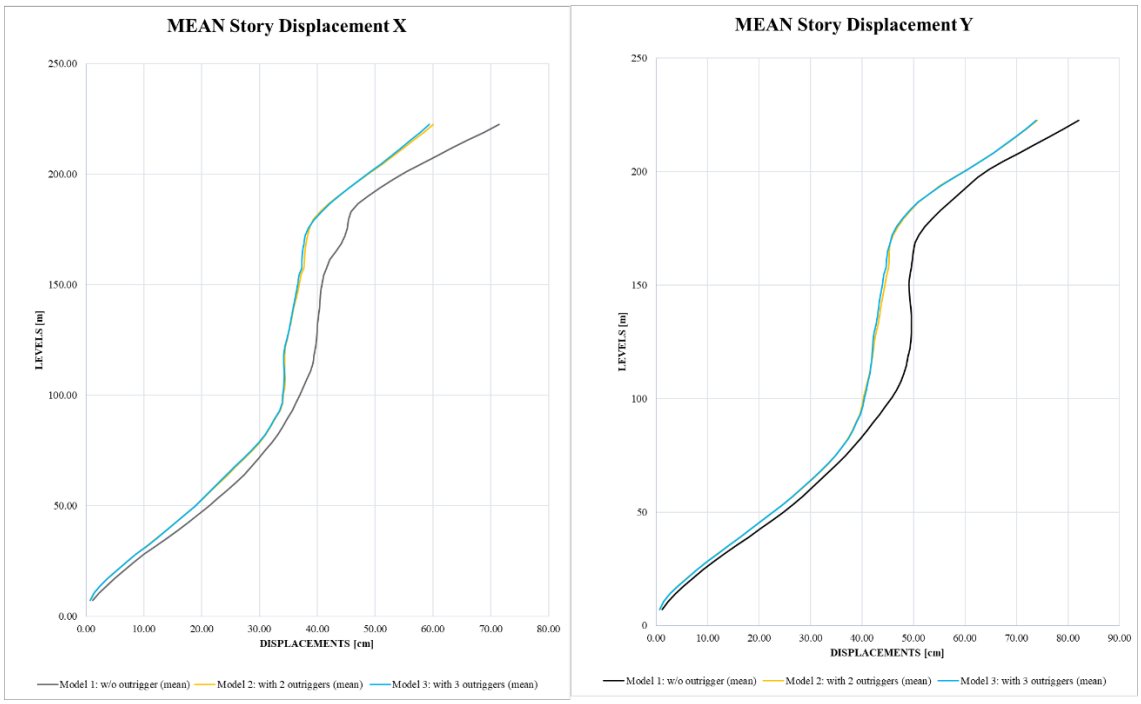

Figure 5. 110 Mean Displacement comparison - Nonlinear time history analysis

Nonlinear time history analysis : Mean Displacements comparison

Story	Elevation	Model 1: Story Displacement w/o Outrigger		Model 2: Story Displacement with 2 Outrigger		Model 3: Story Displacement with 3 Outrigger		*REDUCTION MODEL 2*		*REDUCTION MODEL 3*		*COMPARISON MODEL 2 VS MODEL 3*	
		X-Dir	Y-Dir	X-Dir	Y-Dir	X-Dir	Y-Dir	*X-Dir*	*Y-Dir*	*X-Dir*	*Y-Dir*	*X-Dir*	*Y-Dir*
[-]	[m]	[cm]	[cm]	[cm]	[cm]	[cm]	[cm]	*[%]*	*[%]*	*[%]*	*[%]*	*[%]*	*[%]*
Story60	222.60	71.44	82.08	60.09	74.04	59.40	73.86	*16%*	*10%*	*17%*	*-3%*	1%	-13%
Story59	219.00	68.79	79.31	58.36	72.04	57.75	71.90	*15%*	*9%*	*16%*	*-5%*	1%	-14%
Story58	215.40	66.02	76.43	56.67	69.99	56.16	69.91	*14%*	*8%*	*15%*	*-6%*	1%	-14%
Story57	211.80	63.23	73.54	54.91	67.80	54.49	67.77	*13%*	*8%*	*14%*	*-7%*	1%	-15%
Story56	208.20	60.55	70.52	53.08	65.45	52.75	65.46	*12%*	*7%*	*13%*	*-8%*	1%	-15%

Story55	204.60	57.86	67.46	51.21	63.00	50.97	63.06	*11%*	*7%*	*12%*	*-9%*	0%	-16%
Story54	201.00	55.30	64.68	49.30	60.45	49.15	60.55	*11%*	*7%*	*11%*	*-9%*	0%	-16%
Story53	197.40	52.97	62.46	47.36	57.82	47.30	57.96	*11%*	*7%*	*11%*	*-9%*	0%	-17%
Story52	193.80	50.75	60.63	45.43	55.18	45.46	55.37	*10%*	*9%*	*10%*	*-9%*	0%	-18%
Story51	190.20	48.79	58.84	43.61	53.00	43.73	52.96	*11%*	*10%*	*10%*	*-9%*	0%	-19%
Story50	186.60	47.01	57.07	41.97	51.00	42.16	50.89	*11%*	*11%*	*10%*	*-8%*	0%	-19%
Story49	183.00	45.84	55.31	40.49	49.49	40.74	49.32	*12%*	*11%*	*11%*	*-8%*	-1%	-18%
Story48	179.40	45.39	53.71	39.29	48.15	39.46	47.92	*13%*	*10%*	*13%*	*-6%*	0%	-16%
Story47	175.80	45.20	52.18	38.67	46.98	38.43	46.69	*14%*	*10%*	*15%*	*-3%*	1%	-13%
Story46	172.20	44.79	51.01	38.29	46.04	37.88	45.87	*15%*	*10%*	*15%*	*-2%*	1%	-12%
Story45	168.60	44.11	50.27	38.06	45.50	37.64	45.41	*14%*	*9%*	*15%*	*-3%*	1%	-12%
Story44	165.00	43.20	49.97	37.82	45.29	37.41	44.95	*12%*	*9%*	*13%*	*-4%*	1%	-13%
Story43	161.40	42.17	49.80	37.80	45.30	37.36	44.82	*10%*	*9%*	*11%*	*-6%*	1%	-15%
Story42	157.80	41.62	49.62	37.70	45.17	37.30	44.66	*9%*	*9%*	*10%*	*-7%*	1%	-16%
Story41	154.20	41.06	49.30	37.18	44.73	36.84	44.22	*9%*	*9%*	*10%*	*-8%*	1%	-17%
Story40	150.60	40.82	49.09	36.94	44.48	36.64	43.96	*10%*	*9%*	*10%*	*-8%*	1%	-17%
Story39	147.00	40.58	49.22	36.61	44.21	36.37	43.71	*10%*	*10%*	*10%*	*-8%*	1%	-18%
Story38	143.40	40.50	49.31	36.32	43.91	36.14	43.43	*10%*	*11%*	*11%*	*-7%*	0%	-18%
Story37	139.80	40.41	49.47	35.95	43.63	35.82	43.18	*11%*	*12%*	*11%*	*-7%*	0%	-19%
Story36	136.20	40.22	49.54	35.65	43.38	35.57	42.96	*11%*	*12%*	*12%*	*-7%*	0%	-19%
Story35	132.60	40.03	49.62	35.38	43.08	35.32	42.69	*12%*	*13%*	*12%*	*-7%*	0%	-20%
Story34	129.00	39.92	49.61	35.10	42.73	35.04	42.36	*12%*	*14%*	*12%*	*-6%*	0%	-20%
Story33	125.40	39.84	49.48	34.79	42.42	34.71	42.15	*13%*	*14%*	*13%*	*-6%*	0%	-20%
Story32	121.80	39.67	49.24	34.47	42.20	34.36	42.02	*13%*	*14%*	*13%*	*-6%*	0%	-20%
Story31	118.20	39.46	48.89	34.32	42.02	34.21	41.94	*13%*	*14%*	*13%*	*-6%*	0%	-20%
Story30	114.60	39.21	48.57	34.32	41.77	34.20	41.77	*12%*	*14%*	*13%*	*-7%*	0%	-21%
Story29	111.00	38.80	48.12	34.37	41.45	34.24	41.52	*11%*	*14%*	*12%*	*-7%*	0%	-21%
Story28	107.40	38.22	47.50	34.43	41.07	34.30	41.18	*10%*	*14%*	*10%*	*-8%*	0%	-21%
Story27	103.80	37.63	46.71	34.33	40.69	34.21	40.84	*9%*	*13%*	*9%*	*-9%*	0%	-21%
Story26	100.20	37.02	45.72	34.08	40.27	33.97	40.43	*8%*	*12%*	*8%*	*-9%*	0%	-21%
Story25	96.60	36.33	44.59	33.98	40.00	33.89	40.17	*6%*	*10%*	*7%*	*-11%*	0%	-21%
Story24	93.00	35.65	43.44	33.56	39.53	33.48	39.69	*6%*	*9%*	*6%*	*-11%*	0%	-20%
Story23	89.40	34.81	42.12	32.69	38.76	32.60	38.90	*6%*	*8%*	*6%*	*-12%*	0%	-20%
Story22	85.80	33.99	40.96	31.95	38.09	31.85	38.20	*6%*	*7%*	*6%*	*-12%*	0%	-19%
Story21	82.20	33.11	39.66	31.05	37.21	30.93	37.29	*6%*	*6%*	*7%*	*-13%*	0%	-19%
Story20	78.60	32.09	38.32	29.97	36.13	29.83	36.17	*7%*	*6%*	*7%*	*-13%*	0%	-18%
Story19	75.00	30.95	36.84	28.74	34.88	28.57	34.88	*7%*	*5%*	*8%*	*-13%*	1%	-18%
Story18	71.40	29.79	35.26	27.37	33.46	27.18	33.42	*8%*	*5%*	*9%*	*-12%*	1%	-17%
Story17	67.80	28.62	33.62	25.90	31.92	25.70	31.83	*10%*	*5%*	*10%*	*-11%*	1%	-16%
Story16	64.20	27.35	31.92	24.53	30.25	24.33	30.14	*10%*	*5%*	*11%*	*-10%*	1%	-15%
Story15	60.60	25.94	30.21	23.17	28.48	23.02	28.38	*11%*	*6%*	*11%*	*-9%*	1%	-15%
Story14	57.00	24.39	28.50	21.70	26.60	21.60	26.55	*11%*	*7%*	*11%*	*-9%*	0%	-16%
Story13	53.40	22.75	26.65	20.29	24.64	20.23	24.62	*11%*	*8%*	*11%*	*-8%*	0%	-16%
Story12	49.80	21.17	24.63	18.80	22.61	18.78	22.61	*11%*	*8%*	*11%*	*-7%*	0%	-15%

Story11	46.20	19.47	22.50	17.21	20.54	17.21	20.55	*12%*	*9%*	*12%*	*-6%*	0%	-14%
Story10	42.60	17.74	20.28	15.59	18.44	15.61	18.45	*12%*	*9%*	*12%*	*-4%*	0%	-13%
Story9	39.00	15.89	17.99	13.90	16.30	13.94	16.31	*13%*	*9%*	*12%*	*-3%*	0%	-12%
Story8	35.40	13.97	15.67	12.16	14.17	12.22	14.18	*13%*	*10%*	*13%*	*-2%*	0%	-11%
Story7	31.80	12.02	13.41	10.40	12.04	10.46	12.06	*14%*	*10%*	*13%*	*0%*	-1%	-11%
Story6	28.20	10.10	11.22	8.64	9.95	8.71	9.98	*15%*	*11%*	*14%*	*1%*	-1%	-10%
Story5	24.60	8.32	9.17	6.96	7.97	7.03	8.00	*16%*	*13%*	*15%*	*4%*	-1%	-9%
Story4	17.40	4.99	5.36	3.75	4.19	3.80	4.22	*25%*	*22%*	*24%*	*15%*	-1%	-6%
Story3	14.00	3.55	3.78	2.44	2.68	2.48	2.71	*31%*	*29%*	*30%*	*24%*	-1%	-5%
Story2	10.60	2.25	2.37	1.40	1.51	1.41	1.53	*38%*	*36%*	*37%*	*32%*	-1%	-4%
Story1	7.20	1.16	1.22	0.68	0.73	0.68	0.74	*41%*	*40%*	*41%*	*36%*	0%	-4%

Table 5. 70 Maximum Displacement comparison - Nonlinear time history analysis

Evaluating the average values it can be observed that the models 2 and 3 define a reduction of the displecement regarding the Model 1, it is defined to a maximum reduction of 16% for the Model 2 and 17% for the model 3.

If we wanted to analyze a difference between Model 2 and Model 3, they have almost identical values along the entire height of the building in the X direction, while the system with 3 Outrigger is worse than the system with 2outrigger evaluating the direction, in fact you have a maximum value of -19% at level 51.

Table 5.71 Shows the maximum value obtained in x and y direction and compared for displacement considering both the Mexican standard and the CFE:

Maximum values for Interstory Displacements - Mexican Code

	w/o OUTRIGGER	with 2 OUTRIGGER	with3 OUTRIGGER	**REDUCTION Model 2**	**REDUCTION Model 3**	**COMPARISON MODEL 2 VS MODEL 3**
	[cm]	**[cm]**	**[cm]**	**[%]**	**[%]**	**[%]**
MAX X	103.960	91.622	84.740	12%	18%	7%
MAX Y	104.465	101.071	91.555	3%	12%	9%

Maximum values for Interstory Displacements - CFE

	w/o OUTRIGGER	with 2 OUTRIGGER	with3 OUTRIGGER	**REDUCTION Model 2**	**REDUCTION Model 3**	**COMPARISON MODEL 2 VS MODEL 3**
	[cm]	**[cm]**	**[cm]**	**[%]**	**[%]**	**[%]**
MEAN X	71.435	60.089	59.401	16%	17%	1%
MEAN Y	82.080	74.042	73.860	10%	10%	0%

Table 5. 71 Maximum values for Interstory Displacements - Mexican Code and CFE

Analyzing the maximum values obtained both evaluating the maximum and the average of all the values obtained as output we can define a difference between the Mexican Code and the CFE.

The reduction in Models 2 and 3 compared to Model 1 of the system-free structure can be deduced in both cases. Comparing both models with the applied system we note that:

- By evaluating the maximum values, the model with 3 Outrigger has an improvement over the model without Outrigger up to 18% in x direction, while the Model with 2 Outrigger has an improvement up to 12% in the same direction. Also you can notice that the Model 3 has an improvement over the system with 2 Outrigger up to 9% in y direction;
- By evaluating the average values, the model with 3 Outrigger has an improvement over the model without Outrigger up to 17% in x direction, while the Model with 2 Outrigger has an improvement up to 16% in the same direction. Also you can notice that the 3 model has an improvement over the system with 2 Outrigger of 1% in x direction, and therefore very small and not relevant.

❖ **Shear**

Figure 5.111 and Table 5.71 show the results of the interstory shear in x and y direction for the three models compared and analyzed taking into account the maximum values, as defined by the Mexican standard:

Figure 5. 111 Maximum shear comparison - Nonlinear time history analysis

Nonlinear time history analysis : Maximum Shear comparison

Story	Elevation	Model 1: Story Shear w/o Outrigger				Model 2: Story Shear with 2 Outrigger				Model 3: Story Shear with 3 Outrigger				REDUCTION MODEL 2				REDUCTION MODEL 3				COMPARISON MODEL 2 VS MODEL 3			
		MAX		MIN		MAX		MIN		MAX		MIN		MAX		MIN		MAX		MIN		MAX		MIN	
[-]	m	X-Dir [tonf]	Y-Dir [tonf]	X-Dir [tonf]	Y-Dir [tonf]	X-Dir [tonf]	Y-Dir [tonf]	X-Dir [tonf]	Y-Dir [tonf]	X-Dir [tonf]	Y-Dir [tonf]	X-Dir [tonf]	Y-Dir [tonf]	X-Dir [%]	Y-Dir [%]	X-Dir [%]	Y-Dir [%]	X-Dir [%]	Y-Dir [%]	X-Dir [%]	Y-Dir [%]	X-Dir [%]	Y-Dir [%]	X-Dir [%]	Y-Dir [%]
Story60	222.60	-806.08	-838.98	787.82	702.30	-589.53	-577.91	596.19	575.73	-512.29	-451.03	493.80	449.53	27%	31%	24%	18%	36%	46%	37%	36%	10%	15%	13%	18%
Story59	219.00	-1584.41	-1624.40	1501.38	1378.94	-1136.80	-1113.38	1158.49	1122.32	-925.13	-1073.36	995.04	1005.03	28%	31%	23%	19%	32%	43%	28%	28%	4%	12%	5%	9%
Story58	215.40	-2246.91	-2263.37	2046.25	1953.25	-1569.37	-1531.03	1608.44	1564.78	-1638.67	-1582.65	1566.42	1443.90	30%	32%	21%	20%	27%	39%	23%	26%	-3%	7%	2%	6%
Story57	211.80	-2785.56	-2772.01	2450.11	2423.37	-1912.00	-1893.50	1961.86	1917.40	-2050.80	-1706.88	1951.11	1811.27	31%	33%	20%	21%	26%	38%	20%	25%	-5%	5%	0%	4%
Story56	208.20	-3193.79	-3138.39	2786.85	2777.11	-2155.30	-2095.02	2218.45	2177.59	-2386.19	-2002.52	2258.32	2113.88	33%	33%	20%	22%	25%	36%	19%	24%	-7%	3%	-1%	2%
Story55	204.60	-3467.23	-3393.99	3023.03	3008.65	-2301.33	-2263.03	2381.58	2345.67	-2636.70	-2248.97	2483.05	2345.41	34%	33%	21%	22%	24%	34%	18%	22%	-10%	0%	-3%	0%
Story54	201.00	-3616.89	-3543.22	3294.30	3116.64	-2371.39	-2386.12	2457.56	2424.61	-2797.08	-2436.65	2623.69	2502.18	34%	33%	25%	22%	23%	31%	20%	20%	-12%	-1%	-5%	-2%
Story53	197.40	-3635.10	-3580.37	3493.37	3141.05	-2392.45	-2496.49	2454.18	2441.40	-2869.94	-2560.50	2681.63	2583.30	34%	30%	30%	22%	21%	28%	23%	18%	-13%	-2%	-7%	-5%
Story52	193.80	-3525.98	-3509.72	3609.69	3241.39	-2472.58	-2551.78	2379.54	2521.50	-2856.76	-2607.06	2660.78	2590.55	30%	27%	34%	22%	19%	26%	26%	20%	-11%	-2%	-8%	-2%
Story51	190.20	-3308.33	-3340.99	3639.24	3287.26	-2518.00	-2513.27	2395.70	2550.92	-2760.87	-2575.19	2656.31	2586.27	24%	23%	34%	22%	17%	23%	27%	21%	-7%	0%	-7%	-1%
Story50	186.60	-2991.85	-3077.16	3597.26	3284.09	-2503.27	-2609.87	2442.03	2563.80	-2712.59	-2491.32	2597.66	2607.35	16%	15%	32%	22%	9%	19%	28%	21%	-7%	4%	-4%	-1%
Story49	183.00	-2688.08	-2914.96	3500.37	3235.89	-2465.31	-2585.06	2441.07	2639.64	-2779.61	-2511.68	2479.03	2583.99	15%	11%	30%	18%	4%	14%	29%	20%	-11%	3%	-1%	2%
Story48	179.40	-2749.45	-2866.44	3360.55	3232.23	-2456.13	-2502.26	2403.81	2677.30	-2801.15	-2497.12	2474.16	2588.47	11%	13%	28%	17%	-2%	13%	26%	20%	-13%	0%	-2%	3%
Story47	175.80	-2547.64	-2788.30	3185.06	3204.86	-2424.46	-2366.78	2346.11	2655.98	-2790.32	-2442.03	2503.70	2559.97	5%	15%	26%	17%	-10%	12%	21%	20%	-14%	-3%	-5%	3%
Story46	172.20	-2475.67	-2822.81	2960.92	3105.68	-2379.58	-2342.51	2268.45	2573.26	-2740.89	-2348.81	2481.44	2500.59	4%	17%	23%	17%	-11%	17%	16%	19%	-15%	0%	-7%	2%
Story45	168.60	-2485.03	-2949.87	2756.00	3047.61	-2410.90	-2302.73	2189.61	2429.64	-2672.30	-2293.37	2406.33	2416.72	3%	22%	21%	20%	-8%	22%	13%	21%	-11%	0%	-8%	0%
Story44	165.00	-2696.92	-3003.35	2912.54	3094.61	-2428.40	-2230.94	2334.72	2317.53	-2660.01	-2309.12	2308.01	2309.07	10%	26%	20%	25%	4%	23%	21%	25%	-6%	-3%	1%	0%
Story43	161.40	-2949.03	-3182.70	3018.01	3046.10	-2418.29	-2303.13	2445.07	2271.27	-2528.70	-2297.01	2156.22	2173.75	18%	19%	28%	25%	14%	28%	29%	25%	-4%	0%	10%	3%
Story42	157.80	-2992.20	-3217.35	3024.88	3008.64	-2513.46	-2350.87	2500.64	2334.73	-2492.25	-2290.82	2173.71	2189.05	16%	27%	17%	22%	17%	29%	26%	27%	1%	2%	11%	5%
Story41	154.20	-3048.10	-3267.15	2955.07	2798.42	-2634.46	-2419.37	2458.25	2396.40	-2419.08	-2320.16	2311.42	2356.49	14%	26%	15%	15%	21%	25%	13%	16%	7%	3%	6%	1%
Story40	150.60	-3020.31	-3238.03	2790.03	2779.54	-2713.07	-2462.17	2477.83	2396.20	-2535.71	-2421.95	2417.18	2479.26	10%	24%	11%	14%	16%	25%	13%	11%	6%	1%	2%	-3%
Story39	147.00	-2936.42	-3140.99	2668.63	2864.91	-2756.27	-2473.86	2563.38	2400.31	-2742.48	-2524.84	2519.73	2633.39	6%	21%	4%	16%	7%	20%	6%	8%	0%	-2%	2%	-8%
Story38	143.40	-2820.03	-2988.22	2720.34	3051.50	-2777.23	-2551.81	2571.01	2494.52	-2905.81	-2579.13	2675.62	2756.88	2%	15%	5%	18%	-3%	14%	2%	10%	-5%	-1%	-5%	-9%
Story37	139.80	-3071.31	-2940.90	2732.81	3269.82	-2762.53	-2596.20	2586.35	2661.79	-3020.30	-2578.71	2755.02	2826.16	10%	9%	5%	19%	2%	9%	7%	14%	-8%	1%	-6%	-5%
Story36	136.20	-3276.13	-2890.20	2672.87	3405.77	-2701.02	-2575.36	2593.05	2783.93	-3091.97	-2674.16	2761.62	2838.88	18%	11%	3%	18%	6%	11%	1%	8%	-12%	-3%	-6%	-2%
Story35	132.60	-3425.35	-3091.49	2728.34	3431.05	-2587.73	-2498.89	2628.25	2851.39	-3096.85	-2747.29	2689.19	2797.13	24%	19%	4%	17%	10%	11%	1%	18%	-15%	-8%	-2%	2%
Story34	129.00	-3504.98	-3223.74	2826.21	3371.00	-2446.28	-2370.88	2636.17	2859.80	-3055.55	-2758.30	2530.97	2733.33	30%	26%	7%	15%	13%	14%	10%	19%	-17%	-12%	-4%	4%
Story33	125.40	-3516.95	-3267.97	2921.89	3325.99	-2443.08	-2225.37	2610.94	2807.38	-2951.88	-2711.93	2894.12	2750.74	31%	32%	11%	16%	16%	17%	18%	17%	-14%	-15%	7%	2%
Story32	121.80	-3468.04	-3222.67	2990.85	3306.76	-2468.25	-2155.01	2568.91	2701.64	-2787.93	-2600.57	2804.58	2722.96	29%	33%	14%	18%	20%	19%	20%	18%	-9%	-14%	5%	-1%
Story31	118.20	-3369.74	-3206.86	3013.05	3358.98	-2464.61	-2268.08	2525.75	2591.58	-2579.67	-2491.08	2804.00	2658.55	27%	29%	16%	23%	23%	22%	21%	21%	-3%	-7%	4%	-2%
Story30	114.60	-3230.88	-3276.27	2982.19	3340.86	-2432.91	-2356.13	2491.36	2549.85	-2321.48	-2435.43	2371.00	2571.46	25%	28%	16%	24%	29%	26%	20%	23%	3%	-2%	2%	1%
Story29	111.00	-3140.14	-3324.84	2953.24	3271.46	-2378.43	-2429.02	2468.59	2493.66	-2225.16	-2363.17	2387.34	2473.78	24%	27%	16%	24%	29%	29%	19%	24%	5%	2%	-4%	1%
Story28	107.40	-3154.80	-3282.24	3011.14	3131.87	-2296.88	-2501.29	2455.46	2530.02	-2300.59	-2539.74	2420.58	2377.76	27%	24%	18%	19%	27%	23%	20%	24%	0%	-1%	1%	6%
Story27	103.80	-3492.27	-3342.39	3040.08	3053.19	-2222.91	-2575.08	2446.46	2548.82	-2469.28	-2695.89	2417.07	2391.87	36%	23%	20%	17%	31%	19%	20%	22%	-5%	-4%	1%	5%
Story26	100.20	-3786.17	-3472.63	3028.98	3152.62	-2503.16	-2670.47	2435.08	2532.94	-2508.29	-2837.61	2289.89	2437.14	34%	23%	20%	20%	34%	18%	21%	23%	0%	-5%	1%	3%
Story25	96.60	-4043.75	-3624.86	3219.28	3316.84	-2797.90	-2782.87	2531.58	2537.25	-2605.52	-2975.53	2537.89	2606.23	31%	23%	21%	24%	36%	18%	21%	21%	5%	-5%	0%	-2%
Story24	93.00	-4095.45	-3654.08	3267.59	3355.40	-2835.04	-2984.66	2570.21	2514.06	-2682.58	-3068.55	2661.32	2692.55	27%	22%	21%	25%	34%	16%	19%	20%	7%	-6%	-3%	-5%
Story23	89.40	-4139.81	-3695.06	3348.83	3377.05	-2904.69	-2933.72	2539.15	2645.67	-2748.73	-3166.86	2801.26	2764.00	23%	24%	24%	22%	34%	14%	16%	18%	11%	-6%	-6%	-4%
Story22	85.80	-4140.55	-3695.25	3344.22	3439.82	-2990.33	-3147.14	2523.77	2873.74	-2878.76	-3249.21	2880.17	2784.80	18%	25%	15%	17%	31%	12%	14%	20%	12%	-3%	-11%	3%
Story21	82.20	-4052.01	-3644.81	3268.60	3560.83	-3506.25	-3306.16	2677.96	3068.94	-3141.59	-3293.57	2975.67	2875.03	13%	9%	18%	14%	22%	10%	9%	19%	9%	0%	-9%	5%
Story20	78.60	-3878.74	-3538.22	3104.98	3648.40	-3560.45	-3364.06	2802.61	3211.64	-3336.45	-3345.23	3056.07	3067.99	8%	5%	10%	12%	14%	5%	2%	16%	6%	1%	-8%	4%
Story19	75.00	-3655.68	-3391.76	2846.66	3718.36	-3574.40	-3359.49	2963.27	3320.65	-3483.95	-3428.88	3068.04	3315.84	2%	1%	-4%	11%	5%	-1%	-8%	11%	2%	-2%	-4%	0%
Story18	71.40	-3365.07	-3663.39	2849.80	3760.08	-3516.08	-3282.54	3064.83	3379.34	-3536.30	-3430.16	3070.80	3494.94	-4%	10%	-8%	10%	-5%	6%	-8%	7%	-1%	-4%	0%	-3%
Story17	67.80	-3157.89	-3835.63	2856.90	3754.14	-3393.65	-3133.71	3090.71	3390.08	-3513.08	-3381.25	3160.61	3613.69	-7%	18%	-8%	10%	-11%	12%	-11%	4%	-4%	-6%	-2%	-6%
Story16	64.20	-3193.46	-3946.74	2939.25	3682.62	-3215.43	-2982.75	3036.40	3374.70	-3405.43	-3220.80	3169.15	3664.34	-1%	24%	-3%	8%	-7%	18%	7%	0%	-6%	-6%	-4%	-8%
Story15	60.60	-3207.65	-3976.39	3211.01	3531.38	-3050.05	-2900.40	2929.09	3326.79	-3462.83	-3125.10	3125.45	3648.80	5%	27%	9%	6%	-8%	21%	3%	-3%	-13%	-6%	-6%	-9%
Story14	57.00	-3257.42	-3924.12	3396.13	3352.59	-3048.27	-2901.22	2894.96	3255.54	-3475.96	-2945.53	3011.77	3580.35	6%	26%	15%	3%	-7%	25%	11%	-7%	-13%	-13%	-13%	-10%
Story13	53.40	-3281.84	-3824.11	3713.56	3481.61	-3034.12	-3069.20	3045.58	3167.83	-3445.72	-2893.46	3062.04	3476.30	8%	20%	18%	9%	-5%	24%	18%	0%	-13%	5%	0%	-9%
Story12	49.80	-3244.66	-3653.35	3994.47	3576.23	-2996.69	-3189.26	3233.95	3140.58	-3389.88	-3092.51	3232.17	3383.89	8%	13%	19%	12%	-4%	15%	19%	5%	-12%	3%	0%	-7%
Story11	46.20	-3455.13	-3704.49	4196.69	3635.28	-2922.20	-3246.51	3414.29	3179.02	-3311.60	-3317.73	3389.18	3356.02	15%	12%	19%	13%	4%	10%	19%	8%	-11%	-2%	1%	-5%
Story10	42.60	-3822.48	-3903.33	4384.26	3809.51	-2815.83	-3251.86	3560.32	3319.80	-3263.73	-3492.46	3533.02	3344.96	26%	17%	19%	13%	15%	11%	19%	12%	-12%	-6%	1%	-1%
Story9	39.00	-4141.45	-4171.57	4528.14	4048.21	-2962.76	-3438.81	3682.25	3442.11	-3335.25	-3604.75	3658.37	3432.79	28%	18%	19%	15%	19%	14%	19%	15%	-9%	-4%	1%	0%
Story8	35.40	-4467.49	-4589.97	4643.80	4273.90	-3238.27	-3704.25	3769.45	3541.60	-3401.03	-3636.01	3795.49	3675.52	28%	19%	19%	17%	24%	21%	18%	14%	-13%	-6%	1%	-3%
Story7	31.80	-4775.60	-4958.21	4750.82	4485.61	-3504.19	-3892.86	3804.31	3654.49	-3612.36	-3779.56	3915.31	3874.26	27%	21%	20%	19%	24%	24%	18%	14%	-23%	-25%	2%	-5%
Story6	28.20	-5057.91	-5231.93	4857.39	4671.93	-3794.42	-4048.27	3802.62	3771.55	-3877.59	-4014.81	4012.97	4000.33	25%	23%	22%	19%	23%	23%	17%	14%	-23%	-26%	1%	-4%
Story5	24.60	-5339.73	-5473.13	5043.51	4863.75	-4236.11	-4186.93	3882.24	3946.46	-4347.59	-4182.29	4205.28	4094.40	21%	24%	23%	19%	19%	24%	17%	16%	-23%	-26%	0%	-6%
Story4	17.40	-5554.08	-5495.83	5154.38	4972.14	-4578.95	-4428.83	4135.30	4235.90	-4759.89	-4226.43	4480.77	4077.41	18%	20%	15%	14%	20%	23%	13%	18%	-33%	-26%	4%	-7%
Story3	14.00	-5764.16	-5483.59	5315.57	5144.55	-4878.94	-4805.64	4428.50	4481.04	-5111.70	-4441.17	4720.67	4198.21	15%	12%	17%	13%	11%	19%	11%	18%	-43%	-26%	5%	-5%
Story2	10.60	-6042.32	-5585.44	5569.35	5306.34	-5129.46	-5160.02	4765.66	4735.42	-5502.31	-4637.16	4902.86	4633.28	15%	8%	14%	12%	9%	17%	12%	14%	-65%	9%	7%	2%
Story1	7.20	-6386.20	-5655.41	5975.73	5765.74	-5487.23	-5714.70	5301.95	4996.54	-5994.62	-5110.14	5124.74	5177.84	14%	2%	11%	13%	6%	13%	14%	10%	-85%	10%	3%	-3%

Table 5. 72 Maximum shear comparison - Nonlinear time history analysis

Evaluating the maximum values we can observe that the models 2 and 3 define a reduction of the cut compared to the Model 1, it is defined in fact to an average reduction compared to the Model 1 of 18% for the structure with 2 Outrigger and 17% for the structure with 3 Outrigger.

If we want to analyze a difference between Model 2 and Model 3, we note that in most levels the Model with 3 Outrigger has higher cutting values than the Model with 2 Outrigger.

Figure 5.112 and Table 5.73 show the results of the interstory shear in x and y direction for the three models compared and analysed taking into account the average values, as defined by the CFE:

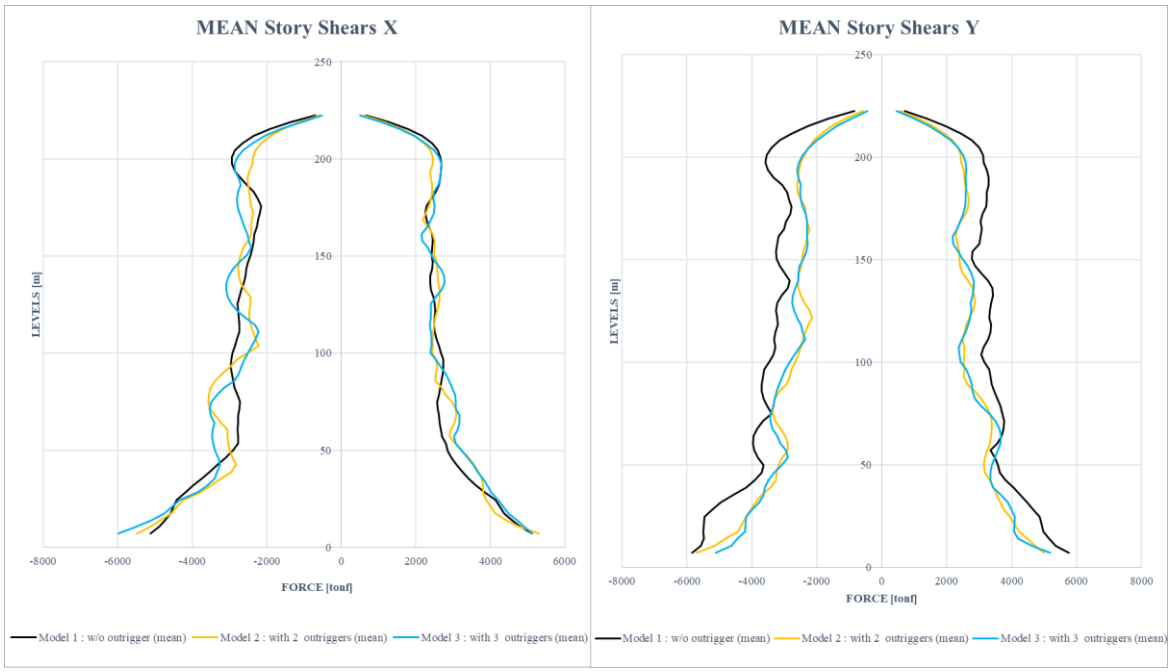

Figure 5. 112 Mean shear comparison - Nonlinear time history analysis

Nonlinear time history analysis : Mean Shear comparison

Story	Elevation	Model 1: Story Shear w/o Outrigger				Model 2: Story Shear with 2 Outrigger				Model 3: Story Shear with 3 Outrigger				REDUCTION MODEL 2				REDUCTION MODEL 3				COMPARISON MODEL 2 VS MODEL 3			
		MAX		MIN		MAX		MIN		MAX		MIN		MAX		MIN		MAX		MIN		MAX		MIN	
[–]	m	X-Dir [tonf]	Y-Dir [tonf]	X-Dir [tonf]	Y-Dir [tonf]	X-Dir [tonf]	Y-Dir [tonf]	X-Dir [tonf]	Y-Dir [tonf]	X-Dir [tonf]	Y-Dir [tonf]	X-Dir [tonf]	Y-Dir [tonf]	X-Dir [%]	Y-Dir [%]	X-Dir [%]	Y-Dir [%]	X-Dir [%]	Y-Dir [%]	X-Dir [%]	Y-Dir [%]	X-Dir [%]	Y-Dir [%]	X-Dir [%]	Y-Dir [%]
Story60	222.60	-703.88	-634.65	662.82	668.71	-504.99	-501.93	494.97	475.15	-407.50	-390.95	402.60	398.90	28%	21%	25%	29%	42%	38%	39%	40%	14%	17%	14%	11%
Story59	219.00	-1370.10	-1231.50	1278.86	1295.19	-977.86	-964.71	952.96	917.11	-848.93	-810.19	880.79	877.26	29%	22%	25%	29%	38%	34%	31%	32%	9%	13%	6%	3%
Story58	215.40	-1922.45	-1722.32	1779.09	1804.55	-1357.07	-1324.14	1308.23	1276.14	-1269.00	-1223.94	1268.32	1268.03	29%	23%	26%	29%	33%	29%	29%	30%	4%	8%	2%	0%
Story57	211.80	-2353.26	-2113.54	2161.58	2205.30	-1660.27	-1599.46	1573.88	1577.05	-1604.70	-1519.20	1574.18	1584.58	29%	24%	27%	28%	32%	28%	27%	28%	2%	4%	0%	0%
Story56	208.20	-2663.48	-2413.60	2426.55	2503.98	-1883.26	-1808.96	1763.26	1811.35	-1856.78	-1763.63	1815.06	1841.02	29%	25%	27%	28%	30%	27%	25%	26%	1%	2%	-2%	-1%
Story55	204.60	-2857.96	-2636.91	2580.25	2704.47	-2029.10	-1957.66	1876.31	1986.25	-2049.25	-1954.86	1986.18	2039.82	29%	26%	27%	27%	28%	26%	23%	25%	-1%	0%	-4%	-2%
Story54	201.00	-2944.70	-2768.48	2653.94	2823.23	-2101.52	-2047.10	1912.24	2109.37	-2182.39	-2096.31	2086.20	2200.06	29%	26%	28%	25%	26%	24%	21%	22%	-3%	-2%	-7%	-3%
Story53	197.40	-2931.86	-2818.20	2680.36	2878.82	-2110.37	-2111.72	1913.15	2190.24	-2256.69	-2185.78	2121.12	2301.97	28%	25%	24%	23%	20%	20%	20%	20%	-5%	-3%	-8%	-4%
Story52	193.80	-2849.62	-2798.46	2666.21	2877.24	-2066.33	-2150.18	1913.42	2225.15	-2283.89	-2234.82	2123.78	2355.40	28%	23%	24%	23%	20%	20%	20%	20%	-8%	-3%	-8%	-5%
Story51	190.20	-2708.63	-2743.04	2651.91	2804.63	-2001.59	-2157.88	1948.72	2244.72	-2270.48	-2245.79	2092.54	2382.23	26%	21%	27%	20%	16%	18%	21%	15%	-10%	-3%	-5%	-5%
Story50	186.60	-2535.07	-2694.85	2617.17	2697.64	-1945.70	-2134.13	1972.21	2231.89	-2223.17	-2224.70	2085.80	2368.85	23%	17%	25%	17%	12%	17%	20%	12%	-11%	-3%	-4%	-5%
Story49	183.00	-2359.51	-2607.01	2526.83	2615.62	-1920.20	-2091.55	1964.70	2222.64	-2137.74	-2208.48	2071.85	2313.58	19%	20%	15%	14%	9%	15%	15%	12%	-9%	-4%	-4%	-3%
Story48	179.40	-2240.60	-2557.86	2408.20	2562.29	-1897.37	-2061.80	1924.82	2205.42	-2051.84	-2174.36	2054.08	2248.88	15%	19%	20%	14%	8%	15%	15%	12%	-7%	-4%	-5%	-2%
Story47	175.80	-2161.83	-2505.11	2388.55	2503.08	-1893.59	-2055.92	1864.80	2156.07	-1958.21	-2132.18	2034.64	2191.40	12%	18%	19%	14%	9%	15%	11%	12%	-3%	-3%	-7%	-1%
Story46	172.20	-2190.75	-2514.88	2245.10	2488.28	-1935.45	-2053.04	1828.99	2081.14	-1879.27	-2095.43	2011.82	2140.23	12%	18%	19%	16%	14%	17%	10%	14%	3%	3%	-2%	-2%
Story45	168.60	-2223.64	-2581.79	2282.38	2458.27	-1966.85	-2039.43	1852.12	2013.26	-1857.84	-2081.07	1972.62	2075.27	12%	21%	19%	18%	17%	19%	14%	16%	5%	5%	-2%	-3%
Story44	165.00	-2277.05	-2610.27	2351.07	2384.54	-2002.64	-2027.55	1885.36	1951.05	-1871.30	-2086.50	1935.71	1999.18	15%	22%	20%	18%	18%	20%	18%	16%	6%	6%	-2%	-2%
Story43	161.40	-2336.96	-2606.88	2438.44	2364.90	-2027.82	-2033.62	1942.31	1939.38	-1917.06	-2079.52	1923.95	1939.30	13%	22%	20%	18%	18%	20%	21%	16%	6%	5%	-2%	1%
Story42	157.80	-2352.28	-2597.65	2448.53	2364.45	-2061.04	-2075.69	1993.27	1947.45	-1990.62	-2078.27	1960.03	1951.86	12%	20%	19%	18%	15%	18%	20%	17%	3%	0%	1%	0%
Story41	154.20	-2388.68	-2534.39	2436.29	2389.96	-2122.01	-2148.82	2067.25	2033.67	-2132.41	-2076.16	2030.54	2015.14	11%	15%	15%	15%	11%	18%	17%	16%	0%	3%	2%	1%
Story40	150.60	-2436.87	-2496.00	2417.41	2457.38	-2158.63	-2207.60	2143.56	2132.04	-2244.33	-2109.25	2109.66	2103.57	11%	12%	11%	13%	8%	15%	13%	14%	-4%	4%	1%	1%
Story39	147.00	-2513.53	-2445.83	2453.65	2552.63	-2172.71	-2238.33	2189.17	2216.18	-2319.24	-2208.96	2188.43	2211.27	14%	8%	11%	13%	8%	10%	11%	13%	-6%	1%	0%	0%
Story38	143.40	-2550.51	-2404.18	2442.57	2651.32	-2175.71	-2251.87	2212.34	2284.96	-2376.00	-2282.44	2253.73	2301.24	15%	6%	9%	14%	7%	5%	8%	13%	-8%	-1%	-2%	-1%
Story37	139.80	-2574.91	-2449.82	2387.15	2721.69	-2178.93	-2269.90	2217.51	2325.60	-2410.22	-2329.66	2279.91	2384.02	15%	7%	7%	15%	6%	5%	4%	12%	-9%	-2%	-3%	-2%
Story36	136.20	-2627.43	-2556.01	2376.12	2797.02	-2188.01	-2260.66	2199.14	2358.27	-2438.42	-2337.58	2286.19	2420.26	17%	12%	7%	16%	7%	9%	4%	13%	-10%	-3%	-4%	-2%
Story35	132.60	-2684.16	-2652.07	2406.04	2845.88	-2188.11	-2307.03	2147.60	2374.13	-2429.76	-2303.52	2281.31	2459.15	18%	17%	11%	17%	9%	13%	5%	14%	-9%	-4%	-6%	-3%
Story34	129.00	-2743.50	-2771.32	2469.54	2862.26	-2164.83	-2129.22	2093.07	2346.41	-2403.20	-2244.16	2257.22	2458.42	21%	23%	15%	18%	12%	19%	9%	14%	-9%	-6%	-7%	-4%
Story33	125.40	-2785.74	-2852.62	2501.89	2905.07	-2147.15	-2041.22	2068.69	2286.37	-2334.71	-2202.45	2214.42	2418.80	23%	28%	17%	21%	16%	23%	11%	17%	-7%	-6%	-6%	-5%
Story32	121.80	-2775.59	-2901.29	2517.67	2920.61	-2123.04	-1976.27	2032.66	2240.86	-2233.95	-2156.15	2160.77	2353.69	24%	32%	19%	23%	20%	26%	14%	19%	-4%	-6%	-5%	-4%
Story31	118.20	-2761.94	-2920.25	2498.07	2945.91	-2090.61	-1973.14	2017.55	2216.10	-2120.00	-2086.02	2086.54	2268.60	24%	32%	19%	25%	23%	29%	16%	23%	-1%	-4%	-3%	-2%
Story30	114.60	-2739.67	-2893.08	2479.12	2918.73	-2040.98	-1968.80	1998.67	2193.10	-2037.73	-2008.58	2004.39	2233.52	26%	32%	23%	25%	26%	31%	19%	23%	0%	-1%	0%	-1%
Story29	111.00	-2743.24	-2905.80	2506.44	2856.00	-2007.24	-1995.33	1971.77	2196.87	-2005.44	-1988.09	1935.74	2193.08	27%	31%	23%	22%	26%	32%	23%	23%	0%	0%	1%	0%
Story28	107.40	-2807.10	-2964.29	2553.77	2828.61	-1988.64	-1956.98	1956.98	2210.63	-2005.82	-2039.69	1943.61	2148.05	29%	31%	23%	22%	29%	31%	24%	24%	-1%	0%	1%	2%
Story27	103.80	-2862.60	-3004.24	2611.22	2813.40	-2014.54	-2119.94	1978.18	2237.75	-2013.18	-2092.23	1966.67	2138.75	30%	29%	24%	20%	30%	30%	25%	24%	0%	1%	0%	4%
Story26	100.20	-2914.14	-3038.60	2659.76	2783.97	-2087.94	-2189.76	2040.96	2249.43	-2042.17	-2146.19	2002.66	2173.63	28%	28%	23%	19%	30%	29%	25%	22%	2%	1%	1%	3%
Story25	96.60	-2958.70	-3049.63	2731.09	2785.59	-2212.39	-2271.50	2103.75	2278.70	-2098.04	-2247.88	2106.78	2238.31	25%	26%	23%	23%	29%	26%	23%	20%	4%	1%	0%	1%
Story24	93.00	-2969.24	-3050.85	2738.78	2793.33	-2297.78	-2363.73	2143.54	2307.04	-2180.17	-2332.38	2209.96	2278.01	23%	23%	22%	17%	27%	24%	19%	18%	4%	1%	-2%	1%
Story23	89.40	-2938.96	-2996.54	2715.96	2794.63	-2439.08	-2534.21	2188.45	2270.97	-2205.72	-2438.63	2240.59	2348.87	17%	15%	19%	15%	22%	19%	14%	16%	5%	3%	-6%	1%
Story22	85.80	-2903.43	-2925.47	2686.38	2798.60	-2576.26	-2688.60	2296.96	2498.10	-2476.75	-2580.34	2441.02	2488.95	11%	8%	15%	11%	15%	12%	9%	11%	3%	4%	-5%	0%
Story21	82.20	-2864.08	-2858.18	2655.96	2799.28	-2703.26	-2801.24	2397.79	2635.89	-2634.60	-2702.41	2519.05	2616.74	6%	2%	10%	6%	8%	5%	5%	7%	2%	3%	-5%	1%
Story20	78.60	-2785.72	-2809.79	2615.17	2803.56	-2778.86	-2858.57	2480.61	2757.61	-2754.82	-2830.54	2582.80	2769.26	0%	-2%	5%	2%	1%	-1%	1%	1%	1%	1%	-4%	0%
Story19	75.00	-2717.34	-2786.26	2575.13	2807.89	-2802.82	-2893.45	2552.81	2828.06	-2852.29	-2917.06	2642.53	2890.04	-3%	-4%	1%	-1%	-5%	-5%	-3%	-3%	-2%	-1%	-3%	-2%
Story18	71.40	-2732.13	-2788.35	2578.71	2850.99	-2774.91	-2885.38	2583.99	2853.38	-2915.98	-2941.40	2685.41	2953.36	-2%	-3%	0%	0%	-7%	-5%	-4%	-4%	-5%	-2%	-4%	-4%
Story17	67.80	-2768.23	-2824.88	2624.59	2893.27	-2714.92	-2837.76	2598.40	2851.01	-2928.88	-2899.08	2698.21	2960.26	2%	0%	3%	1%	-6%	-2%	-3%	-2%	-5%	-2%	-4%	-4%
Story16	64.20	-2779.71	-2857.36	2637.20	2895.97	-2632.00	-2791.65	2584.75	2815.85	-2884.26	-2829.20	2673.15	2910.41	5%	2%	3%	3%	-4%	-1%	-1%	-1%	-5%	-1%	-4%	-3%
Story15	60.60	-2784.43	-2880.65	2670.83	2894.12	-2551.36	-2756.17	2496.48	2794.78	-2808.11	-2785.53	2634.82	2852.18	8%	4%	7%	3%	-1%	3%	1%	1%	-5%	-1%	-5%	-2%
Story14	57.00	-2771.28	-2954.68	2709.18	2946.93	-2488.12	-2705.58	2425.51	2767.26	-2689.22	-2756.97	2613.31	2783.79	10%	8%	10%	6%	3%	7%	4%	6%	-7%	-2%	-7%	-1%
Story13	53.40	-2773.46	-3033.83	2797.40	3047.98	-2440.93	-2642.73	2371.36	2752.21	-2616.55	-2716.45	2616.16	2765.29	12%	13%	15%	10%	6%	10%	6%	9%	-6%	-2%	-9%	-2%
Story12	49.80	-2918.15	-3145.67	2854.92	3144.42	-2476.80	-2613.04	2382.47	2751.06	-2620.11	-2670.57	2620.11	2759.04	15%	17%	17%	13%	10%	15%	8%	10%	-5%	-2%	-8%	-4%
Story11	46.20	-3112.08	-3277.04	2943.57	3292.86	-2530.99	-2661.26	2468.68	2826.04	-2716.30	-2682.32	2640.01	2777.30	19%	19%	16%	14%	13%	18%	10%	16%	-5%	-2%	-6%	-4%
Story10	42.60	-3318.09	-3438.91	3082.42	3444.87	-2573.11	-2761.17	2591.98	2908.85	-2799.64	-2768.25	2730.22	2854.89	22%	20%	16%	16%	16%	20%	11%	17%	-7%	0%	-4%	2%
Story9	39.00	-3534.19	-3593.08	3246.28	3603.90	-2678.81	-2901.96	2761.20	3012.81	-2875.07	-2906.10	2869.91	2961.73	24%	19%	15%	16%	19%	19%	12%	18%	-6%	0%	-3%	1%
Story8	35.40	-3753.04	-3767.07	3425.72	3771.35	-2867.45	-3131.89	2922.98	3112.07	-3014.07	-3040.33	3077.56	3091.45	24%	17%	15%	17%	20%	19%	10%	18%	-4%	2%	-5%	1%
Story7	31.80	-3984.50	-3952.96	3625.94	3963.36	-3059.36	-3322.71	3046.72	3209.71	-3152.02	-3240.27	3280.49	3239.11	23%	16%	16%	19%	21%	18%	10%	18%	-2%	2%	-6%	-1%
Story6	28.20	-4186.17	-4099.08	3855.58	4147.19	-3266.45	-3504.19	3167.69	3324.49	-3357.88	-3446.65	3450.65	3388.44	22%	15%	18%	20%	20%	16%	11%	18%	-2%	1%	-7%	-2%
Story5	24.60	-4422.76	-4242.87	4142.50	4352.11	-3519.62	-3708.64	3308.73	3552.81	-3659.99	-3660.12	3668.90	3577.94	20%	13%	20%	18%	17%	14%	11%	18%	-3%	1%	-5%	-1%
Story4	17.40	-4597.16	-4360.72	4375.02	4467.38	-3713.86	-3911.88	3415.42	3701.29	-3818.09	-3893.19	3776.33	3705.67	19%	12%	22%	17%	15%	13%	14%	17%	-4%	1%	-8%	0%
Story3	14.00	-4744.15	-4483.84	4582.59	4605.86	-3909.00	-3989.00	3383.23	3862.24	-4089.87	-3914.84	3918.71	3888.13	18%	11%	22%	16%	14%	13%	14%	17%	-4%	2%	-7%	-1%
Story2	10.60	-4885.71	-4625.95	4809.80	4821.38	-4146.68	-4228.95	3783.50	4083.19	-4308.93	-4085.97	4094.63	4104.47	15%	9%	21%	15%	12%	12%	12%	15%	-3%	2%	-6%	-1%
Story1	7.20	-5119.62	-4842.89	5120.70	5105.93	-4477.61	-4584.39	4088.28	4436.78	-4626.89	-4396.62	4379.59	4439.10	13%	5%	20%	13%	10%	9%	14%	13%	-3%	4%	-6%	0%

Table 5. 73 Mean shear comparison - Nonlinear time history analysis

Evaluating the maximum values we can observe that the models 2 and 3 define a reduction of the cut compared to the Model 1, it is defined in fact to an average reduction compared to the Model 1 of 17% for the structure with 2 Outrigger and 16% for the structure with 3 Outrigger.

If we want to analyze a difference between Model 2 and Model 3, we note that in most levels the Model with 3 Outrigger has higher cutting values than the Model with 2 Outrigger.

Table 5.74 Shows the maximum value obtained in x and y direction and compared for shear considering both the Mexican standard and the CFE:

Maximum values for Interstory Shear - Mexican Code

	w/o OUTRIGGER	with 2 OUTRIGGER	with3 OUTRIGGER	**REDUCTION Model 2**	**REDUCTION Model 3**	**COMPARISON MODEL 2 VS MODEL 3**
	[tonf]	**[tonf]**	**[tonf]**	**[%]**	**[%]**	**[%]**
MAX X	6386.201	5487.231	5994.624	14%	6%	-8%
MAX Y	5855.412	5714.702	5177.843	2%	12%	9%

Maximum values for Interstory Shear - CFE

	w/o OUTRIGGER	with 2 OUTRIGGER	with3 OUTRIGGER	**REDUCTION Model 2**	**REDUCTION Model 3**	**COMPARISON MODEL 2 VS MODEL 3**
	[tonf]	**[tonf]**	**[tonf]**	**[%]**	**[%]**	**[%]**
MEAN X	634.649	668.714	475.146	-5%	25%	31%
MEAN Y	5120.699	4477.608	4626.890	13%	10%	-3%

Table 5. 74 Maximum values for Interstory Shear - Mexican Code and CFE

Analyzing the maximum values obtained both evaluating the maximum and the average of all the values obtained as output we can define a difference between the Mexican Code and the CFE.

The reduction in Models 2 and 3 compared to Model 1 of the system-free structure can be deduced in both cases. Comparing both models with the applied system we note that:

- evaluating the maximum values, the model with 3 Outrigger has an improvement over the model without Outrigger up to 12% in the y direction, while the Model with 2 Outrigger has an improvement up to 14% in the x direction . You can also notice that the Model 3 has an improvement over the system with 2 Outrigger up to 9% in y direction, but at the same time has a worsening and therefore an increase in the cut up to -8% in x direction.

Evaluating the average values, the model with 3 Outrigger has an improvement over the model without Outrigger up to 25% in x direction, while the Model with 2 Outrigger has an improvement up to 13% in y direction . Also you can notice that the Model 3 has an improvement over the system with 2 Outrigger of 31% in x direction, while it has a worsening of -3% in y direction.

The CFE defines an ulterior revision regarding the minimal cut to the base that is deduced from the following relationship :

$$\frac{V_0}{W_T}$$

Where:

- V_0 is the maximum cut obtained by dynamic analysis;
- W_T is the total weight of the structure that varies according to the 2 models analyzed.

Basal shearrevision - CFE

		w/o OUTRIGGER	with 2 OUTRIGGER	with3 OUTRIGGER
V_0	[tonf]	6386.20	5714.70	5994.62
W_T	[tonf]	44407.43	45411.17	47279.99
		0.144	**0.126**	**0.127**

Table 5. 75 Basal shearrevision - CFE

❖ Acceleration

Figure 5.113 and Table 5.76 show the results of interstory acceleration in x and y direction for the three models compared and analyzed taking into account the maximum values, as defined by the Mexican standard

:

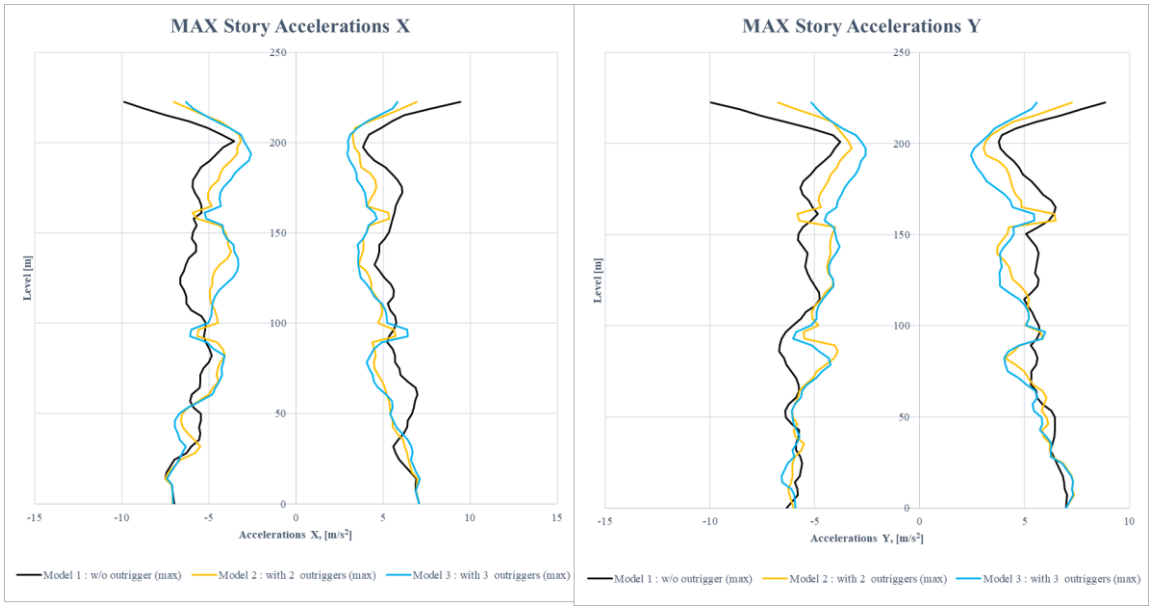

Figure 5. 113 Maximum acceleration comparison - Nonlinear time history analysis

Nonlinear time history analysis : Maximum Acceleration comparison

Story	Elevation	Model 1: Story Acceleration w/o Outrigger				Model 2: Story Acceleration with 2 Outrigger				Model 3: Story Acceleration with 3 Outrigger				REDUCTION MODEL 2				REDUCTION MODEL 3				COMPARISON MODEL 2 VS MODEL 3			
		MAX		MIN		MAX		MIN		MAX		MIN		MAX		MIN		MAX		MIN		MAX		MIN	
[-]	m	X-Dir [m/s²]	Y-Dir [m/s²]	X-Dir [m/s²]	Y-Dir [m/s²]	X-Dir [m/s²]	Y-Dir [m/s²]	X-Dir [m/s²]	Y-Dir [m/s²]	X-Dir [m/s²]	Y-Dir [m/s²]	X-Dir [m/s²]	Y-Dir [m/s²]	X-Dir [%]	Y-Dir [%]	X-Dir [%]	Y-Dir [%]	X-Dir [%]	Y-Dir [%]	X-Dir [%]	Y-Dir [%]	X-Dir [%]	Y-Dir [%]	X-Dir [%]	Y-Dir [%]
Story60	222.60	9.45	8.86	-9.88	-9.05	6.95	7.24	-7.03	-6.76	5.83	5.58	-6.33	-5.17	26%	18%	29%	32%	38%	37%	36%	48%	12%	19%	19%	7%	16%
Story59	219.00	7.76	7.71	-8.72	-8.61	6.06	6.38	-6.17	-5.89	5.55	5.32	-5.90	-4.87	22%	17%	29%	32%	29%	31%	32%	43%	7%	14%	14%	3%	12%
Story58	215.40	6.21	6.67	-7.47	-7.56	5.17	5.43	-5.29	-4.94	4.78	4.69	-5.26	-4.57	17%	19%	29%	35%	23%	30%	30%	40%	6%	11%	11%	1%	5%
Story57	211.80	5.51	5.54	-6.14	-6.42	4.24	4.43	-4.37	-4.17	4.10	4.14	-4.59	-4.17	23%	20%	29%	35%	26%	25%	25%	35%	2%	5%	-4%	-1%	0%
Story56	208.20	4.91	4.57	-5.06	-5.16	3.41	3.88	-3.80	-3.90	3.55	3.56	-3.84	-3.66	30%	15%	25%	24%	28%	22%	24%	29%	-3%	7%	-1%	2%	5%
Story55	204.60	4.21	3.90	-4.28	-4.14	3.27	3.39	-3.28	-3.65	3.12	3.27	-3.18	-3.04	22%	13%	23%	12%	26%	16%	26%	26%	4%	3%	2%	2%	15%
Story54	201.00	4.00	3.77	-3.54	-3.79	3.30	3.13	-3.16	-3.38	2.97	2.94	-2.99	-2.77	18%	17%	11%	11%	26%	22%	16%	27%	8%	5%	5%	5%	16%
Story53	197.40	3.83	3.86	-4.17	-4.04	3.36	3.04	-3.36	-3.22	3.00	2.60	-2.80	-2.57	12%	21%	19%	20%	22%	33%	33%	36%	9%	11%	14%	11%	16%
Story52	193.80	4.11	4.14	-4.54	-4.24	3.65	3.17	-3.38	-3.54	2.94	2.45	-2.56	-2.57	11%	23%	26%	16%	28%	41%	44%	39%	17%	18%	18%	18%	23%
Story51	190.20	4.51	4.49	-4.94	-4.55	3.68	3.78	-3.72	-3.82	3.10	2.55	-2.73	-2.79	18%	16%	25%	16%	31%	43%	45%	39%	13%	27%	27%	20%	23%
Story50	186.60	5.12	4.75	-5.45	-4.94	3.73	4.11	-4.14	-3.96	3.34	2.73	-3.17	-2.89	27%	14%	24%	20%	35%	42%	42%	41%	8%	29%	18%	15%	22%
Story49	183.00	5.49	4.93	-5.65	-5.21	4.26	4.26	-4.34	-4.24	3.46	3.00	-3.50	-3.08	22%	14%	23%	19%	37%	39%	38%	41%	14%	25%	15%	12%	18%
Story48	179.40	5.82	5.32	-5.90	-5.55	4.55	4.34	-4.45	-4.35	3.49	3.19	-3.77	-3.34	22%	18%	25%	22%	40%	40%	36%	40%	18%	22%	12%	12%	18%
Story47	175.80	6.09	5.61	-5.95	-5.69	4.61	4.44	-4.87	-4.58	3.77	3.63	-4.14	-3.58	24%	21%	18%	19%	38%	35%	30%	37%	14%	14%	12%	12%	17%
Story46	172.20	6.10	5.88	-5.81	-5.57	4.49	4.57	-5.05	-4.77	3.97	4.06	-4.34	-3.73	26%	22%	13%	14%	35%	35%	25%	33%	9%	9%	9%	12%	19%
Story45	168.60	5.91	6.29	-5.57	-5.28	4.27	4.83	-5.04	-4.82	4.03	4.32	-4.39	-3.89	28%	23%	9%	9%	32%	31%	21%	26%	4%	8%	12%	12%	18%
Story44	165.00	5.74	6.47	-5.43	-5.12	4.05	4.88	-4.82	-4.70	4.06	4.43	-4.31	-3.96	30%	25%	11%	8%	29%	32%	21%	23%	0%	7%	10%	14%	29%
Story43	161.40	5.65	6.41	-5.43	-4.86	5.32	6.41	-5.93	-5.03	4.50	5.44	-5.24	-4.42	6%	0%	-5%	-20%	20%	15%	9%	3%	15%	15%	15%	13%	24%
Story42	157.80	5.54	6.17	-5.87	-5.16	5.34	6.48	-5.66	-5.76	4.64	5.47	-5.13	-4.52	4%	-5%	4%	-12%	16%	11%	13%	12%	13%	16%	9%	9%	24%
Story41	154.20	5.44	5.65	-5.70	-5.56	4.25	4.26	-4.37	-4.02	4.17	4.47	-4.19	-4.09	22%	25%	23%	28%	23%	21%	26%	26%	1%	1%	-4%	3%	-1%
Story40	150.60	5.34	5.06	-5.92	-5.78	4.05	4.18	-4.06	-4.16	4.06	4.48	-4.17	-4.00	24%	17%	31%	28%	24%	11%	30%	31%	0%	0%	-6%	-2%	3%
Story39	147.00	5.08	5.29	-5.97	-5.80	3.86	3.93	-3.92	-4.26	3.85	4.33	-3.95	-3.96	24%	26%	34%	27%	24%	18%	34%	32%	0%	-8%	-8%	-1%	5%
Story38	143.40	4.79	5.54	-5.75	-5.59	3.87	3.72	-3.90	-4.28	3.55	4.02	-3.58	-3.82	19%	33%	32%	23%	26%	28%	38%	32%	7%	6%	-5%	6%	8%
Story37	139.80	4.79	5.67	-5.74	-5.33	3.85	3.69	-3.73	-4.24	3.60	3.82	-3.54	-4.00	19%	35%	35%	20%	25%	33%	38%	25%	5%	3%	-2%	3%	5%
Story36	136.20	4.67	5.61	-6.17	-5.39	3.72	4.01	-3.94	-4.33	3.56	3.85	-3.35	-4.22	20%	29%	36%	20%	24%	31%	46%	22%	3%	3%	10%	2%	2%
Story35	132.60	4.49	5.55	-6.34	-5.45	3.60	4.25	-4.37	-4.43	3.58	3.90	-3.29	-4.34	20%	23%	31%	19%	20%	30%	48%	20%	0%	6%	17%	2%	2%
Story34	129.00	4.79	5.51	-6.42	-5.33	4.01	4.34	-4.67	-4.36	3.64	3.80	-3.37	-4.32	16%	21%	27%	18%	24%	31%	48%	19%	8%	10%	20%	1%	1%
Story33	125.40	5.05	5.66	-6.64	-5.21	4.24	4.44	-4.79	-4.12	3.70	3.82	-3.60	-4.13	16%	21%	28%	21%	27%	32%	46%	21%	11%	11%	11%	0%	0%
Story32	121.80	5.46	5.61	-6.66	-5.01	4.32	4.80	-4.79	-4.17	4.05	3.82	-4.05	-4.11	21%	14%	28%	17%	26%	32%	39%	18%	5%	18%	11%	1%	1%
Story31	118.20	5.62	5.32	-6.43	-4.79	4.33	5.06	-4.92	-4.51	4.31	4.27	-4.41	-4.37	23%	5%	23%	6%	23%	20%	31%	9%	0%	15%	8%	3%	3%
Story30	114.60	5.58	4.98	-6.30	-4.76	4.62	5.21	-4.95	-4.69	4.51	4.74	-4.64	-4.62	17%	-4%	21%	2%	19%	5%	26%	3%	2%	9%	5%	1%	1%
Story29	111.00	5.29	5.15	-6.28	-4.98	4.87	5.16	-4.87	-5.00	4.92	5.04	-4.79	-4.83	8%	0%	22%	0%	7%	2%	24%	9%	-1%	2%	1%	1%	3%
Story28	107.40	5.42	5.34	-6.00	-5.42	4.95	5.19	-4.66	-5.14	5.15	5.18	-4.84	-4.91	9%	3%	22%	5%	5%	3%	19%	9%	-4%	0%	-3%	4%	4%
Story27	103.80	5.67	5.50	-5.43	-5.65	4.91	5.20	-4.54	-5.11	5.22	5.20	-4.88	-4.92	14%	5%	16%	10%	8%	5%	10%	13%	-5%	0%	-6%	3%	3%
Story26	100.20	5.74	5.68	-5.18	-6.02	4.73	5.03	-4.49	-4.82	5.23	5.08	-5.03	-5.18	18%	11%	13%	20%	9%	11%	3%	14%	-9%	-1%	-10%	-6%	-6%
Story25	96.60	5.62	5.73	-5.23	-6.39	5.64	5.75	-5.58	-5.53	6.37	5.98	-6.01	-5.89	0%	0%	-7%	13%	-13%	-4%	-15%	8%	-13%	-4%	-8%	-8%	-6%
Story24	93.00	5.33	5.59	-5.27	-6.58	5.73	5.88	-5.66	-5.49	6.43	5.85	-6.10	-6.02	-7%	-5%	-7%	13%	-21%	-5%	-16%	9%	-13%	1%	-8%	-11%	-8%
Story23	89.40	5.22	5.30	-5.18	-6.68	4.38	4.75	-4.53	-4.04	4.91	4.75	-5.12	-5.15	16%	10%	15%	39%	6%	10%	1%	23%	-10%	0%	-11%	-17%	-17%
Story22	85.80	5.56	5.51	-4.95	-6.70	4.52	4.49	-4.20	-3.91	4.48	4.22	-4.74	-4.80	19%	19%	15%	42%	19%	23%	4%	28%	1%	5%	-11%	-13%	-4%
Story21	82.20	5.69	5.61	-4.84	-6.48	4.58	4.06	-4.08	-4.08	4.25	4.04	-4.11	-4.34	19%	28%	16%	37%	25%	28%	15%	33%	6%	0%	-1%	4%	-4%
Story20	78.60	5.68	5.55	-5.00	-6.35	4.48	4.57	-4.34	-4.49	4.07	4.08	-4.18	-4.23	21%	18%	13%	29%	28%	27%	17%	33%	7%	9%	3%	4%	4%
Story19	75.00	5.94	5.32	-5.31	-6.13	4.52	4.98	-4.50	-4.91	4.18	4.19	-4.29	-4.64	24%	6%	15%	20%	30%	21%	19%	24%	6%	15%	4%	4%	4%
Story18	71.40	6.02	5.32	-5.49	-5.89	4.73	5.19	-4.54	-5.10	4.42	4.72	-4.23	-4.93	21%	3%	17%	13%	27%	11%	23%	16%	5%	5%	6%	6%	3%
Story17	67.80	6.41	5.30	-5.48	-5.76	4.95	5.40	-4.46	-5.45	4.48	5.10	-4.42	-5.37	23%	-2%	19%	5%	30%	4%	19%	7%	6%	6%	1%	2%	2%
Story16	64.20	6.87	5.57	-5.54	-5.74	5.09	5.85	-4.76	-5.73	4.71	5.50	-4.80	-5.39	26%	-5%	14%	0%	31%	1%	17%	3%	6%	6%	3%	2%	2%
Story15	60.60	6.98	5.60	-5.98	-5.88	5.22	6.06	-5.02	-5.80	5.17	5.62	-4.80	-5.67	25%	-8%	16%	1%	26%	0%	20%	4%	8%	8%	4%	2%	2%
Story14	57.00	6.84	5.85	-6.07	-6.24	5.34	5.94	-5.60	-5.95	5.53	5.39	-5.51	-5.94	22%	-1%	8%	5%	19%	8%	9%	5%	1%	9%	2%	0%	0%
Story13	53.40	6.76	6.29	-5.88	-6.40	5.42	5.81	-6.19	-6.08	5.54	5.43	-6.23	-6.10	20%	8%	-5%	5%	18%	14%	-6%	5%	-3%	6%	-1%	0%	0%
Story12	49.80	6.65	6.45	-5.45	-6.37	5.42	6.04	-6.54	-6.03	5.42	5.80	-6.72	-6.06	19%	6%	-20%	5%	18%	10%	-23%	5%	-2%	0%	-3%	0%	0%
Story11	46.20	6.43	6.45	-5.47	-6.08	5.56	6.13	-6.61	-5.85	5.59	5.86	-6.93	-6.02	14%	5%	-21%	4%	13%	9%	-27%	1%	-1%	4%	-6%	-3%	-3%
Story10	42.60	6.37	6.46	-5.55	-5.74	5.54	5.83	-6.50	-6.01	5.75	5.74	-6.95	-5.86	13%	10%	-17%	-5%	10%	11%	-25%	-2%	-3%	3%	-9%	3%	3%
Story9	39.00	6.17	6.42	-5.49	-5.78	5.83	5.92	-6.20	-5.91	6.12	6.05	-6.78	-5.73	6%	8%	-13%	-2%	1%	6%	-23%	1%	-5%	-2%	-10%	3%	3%
Story8	35.40	5.86	6.34	-5.57	-5.90	6.16	6.22	-5.84	-5.52	6.40	6.27	-6.69	-5.87	-5%	2%	-5%	6%	-9%	1%	-20%	0%	-4%	-1%	-15%	-6%	-6%
Story7	31.80	5.58	6.23	-6.01	-5.89	6.25	6.20	-5.51	-5.64	6.62	6.24	-6.34	-6.06	-12%	1%	8%	4%	-19%	0%	-6%	-3%	-7%	-1%	-14%	-7%	-7%
Story6	28.20	5.72	6.39	-6.28	-5.69	6.40	6.31	-5.81	-5.96	6.69	6.25	-6.53	-5.98	-12%	1%	8%	-5%	-17%	2%	-4%	-5%	-5%	1%	-11%	0%	0%
Story5	24.60	5.95	6.53	-6.99	-5.61	6.46	6.86	-6.63	-6.05	6.60	6.80	-6.72	-6.30	-9%	-5%	5%	-8%	-11%	-4%	4%	-12%	-2%	1%	-1%	-4%	-4%
Story4	17.40	6.59	6.82	-7.45	-5.73	6.66	7.26	-7.34	-6.06	6.91	7.22	-7.18	-6.57	-1%	-7%	2%	-6%	-5%	-6%	4%	-15%	-4%	1%	2%	-9%	-9%
Story3	14.00	6.89	6.87	-7.51	-5.95	6.98	7.30	-7.51	-6.11	7.12	7.30	-7.40	-6.56	-1%	-6%	0%	-3%	-3%	-6%	1%	-10%	-2%	1%	1%	-7%	-7%
Story2	10.60	6.87	6.92	-7.11	-5.84	6.93	7.26	-7.17	-6.27	7.01	7.25	-7.11	-6.12	-1%	-5%	0%	-7%	-2%	-5%	0%	-5%	-1%	0%	1%	3%	3%
Story1	7.20	6.88	7.02	-7.10	-5.81	6.90	7.38	-7.08	-6.21	6.88	7.33	-7.07	-5.98	0%	-5%	0%	-7%	0%	-4%	0%	-3%	0%	1%	0%	4%	4%

Table 5. 76 Maximum acceleration comparison - Nonlinear time history analysis

Evaluating the maximum values we can see that the models 2 and 3 define a reduction of acceleration compared to Model 1, it is defined in fact to an average reduction compared to Model 1 of 13% for the structure with 2 Outrigger and 18% for the structure with 3 Outrigger.

If we wanted to analyze a difference between Model 2 and Model 3, we note that in most levels the Model with 3 Outrigger has lower acceleration values than the Model with 2 Outrigger, up to a maximum of 27% in the Y direction evaluating the positive values. On average, the overall reduction of Model 3 compared to Model 2 is 4%.

Figure 5.114 and Table 5.77 show the results of interstory acceleration in x and y direction for the three models compared and analysed taking into account the average values, as defined by the CFE:

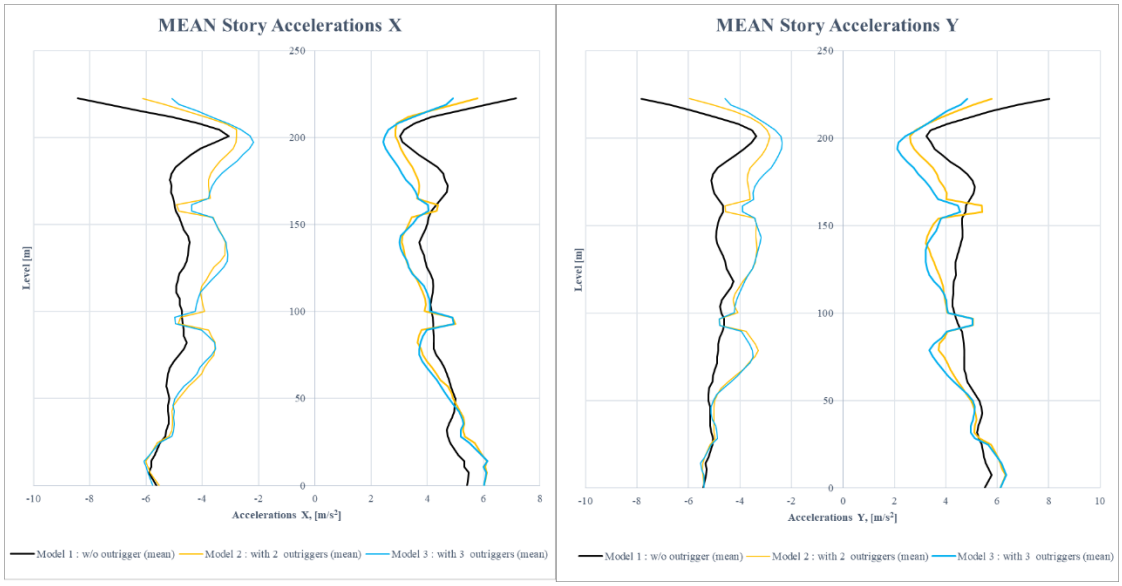

Figure 5. 114 Mean acceleration comparison - Nonlinear time history analysis

Nonlinear time history analysis : Mean Acceleration comparison																																			
Story	Elevation	Model 1: Story Acceleration				Model 2: Story Acceleration				Model 3: Story Acceleration				REDUCTION								COMPARISON											
		MAX		MIN		MAX		MIN		MAX		MIN		MAX		MIN						MAX		MIN									
[-]	[m]	X-Dir [m/s²]	Y-Dir [m/s²]	X-Dir [m/s²]	Y-Dir [m/s²]	X-Dir [m/s²]	Y-Dir [m/s²]	X-Dir [m/s²]	Y-Dir [m/s²]	X-Dir [m/s²]	Y-Dir [m/s²]	X-Dir [m/s²]	Y-Dir [m/s²]	X-Dir [%]	Y-Dir [%]	X-Dir [%]	Y-Dir [%]					X-Dir [%]	Y-Dir [%]	X-Dir [%]	Y-Dir [%]								
Story60	222.60	7.16	8.02	-8.43	-7.82	5.78	5.79	-6.12	-5.97	4.92	4.82	-5.09	-4.58	19%	28%	27%	24%	31%	40%	40%	42%	12%	12%	12%	18%								
Story59	219.00	6.09	6.83	-7.32	-6.74	4.94	5.09	-5.36	-5.05	4.67	4.59	-4.83	-4.36	19%	25%	27%	25%	23%	33%	34%	35%	4%	7%	7%	10%								
Story58	215.40	5.08	5.75	-6.19	-5.79	4.07	4.42	-4.61	-4.21	4.06	4.03	-4.18	-3.74	20%	23%	25%	27%	20%	30%	32%	35%	0%	7%	7%	8%								
Story57	211.80	4.15	4.92	-5.09	-4.91	3.32	3.82	-3.86	-3.59	3.51	3.66	-3.65	-3.37	20%	23%	24%	27%	15%	26%	28%	31%	-4%	3%	4%	4%								
Story56	208.20	3.54	4.06	-4.13	-4.07	2.91	3.27	-3.19	-3.20	2.96	3.26	-3.08	-3.00	18%	20%	23%	21%	17%	20%	26%	26%	-1%	0%	3%	5%								
Story55	204.60	3.17	3.40	-3.40	-3.52	2.86	2.82	-2.79	-2.96	2.61	2.87	-2.63	-2.64	10%	17%	18%	16%	18%	25%	23%	25%	8%	-1%	5%	9%								
Story54	201.00	3.04	3.24	-3.07	-3.36	2.86	2.62	-2.78	-2.84	2.48	2.44	-2.31	-2.41	6%	19%	10%	16%	18%	25%	25%	28%	12%	6%	15%	13%								
Story53	197.40	3.11	3.42	-3.52	-3.56	2.96	2.64	-2.80	-2.90	2.42	2.16	-2.19	-2.37	5%	23%	20%	18%	22%	37%	38%	33%	17%	14%	17%	15%								
Story52	193.80	3.41	3.56	-4.06	-3.84	3.04	2.77	-2.92	-2.99	2.51	2.12	-2.32	-2.39	11%	22%	28%	22%	26%	40%	43%	38%	16%	18%	15%	16%								
Story51	190.20	3.69	3.88	-4.41	-4.20	3.17	3.00	-3.12	-3.15	2.66	2.27	-2.55	-2.50	14%	23%	29%	25%	28%	41%	42%	40%	14%	19%	13%	16%								
Story50	186.60	4.04	4.17	-4.69	-4.55	3.32	3.27	-3.36	-3.39	2.82	2.51	-2.76	-2.64	18%	22%	28%	25%	30%	40%	41%	42%	12%	18%	13%	17%								
Story49	183.00	4.37	4.53	-4.96	-4.86	3.46	3.49	-3.54	-3.60	2.97	2.74	-3.06	-2.80	21%	23%	29%	26%	32%	39%	38%	42%	11%	17%	10%	16%								
Story48	179.40	4.56	4.82	-5.10	-5.05	3.58	3.65	-3.70	-3.71	3.10	2.94	-3.30	-3.06	22%	24%	27%	27%	32%	39%	35%	39%	10%	15%	8%	13%								
Story47	175.80	4.64	5.03	-5.15	-5.11	3.68	3.76	-3.77	-3.73	3.25	3.18	-3.50	-3.27	21%	25%	27%	27%	30%	37%	32%	36%	9%	11%	5%	9%								
Story46	172.20	4.73	5.13	-5.10	-5.06	3.72	3.92	-3.78	-3.68	3.44	3.38	-3.65	-3.43	21%	23%	26%	27%	27%	34%	29%	32%	6%	11%	3%	5%								
Story45	168.60	4.69	5.08	-5.12	-4.99	3.69	4.05	-3.76	-3.64	3.59	3.54	-3.74	-3.50	21%	20%	27%	27%	23%	30%	27%	30%	2%	10%	3%	6%								
Story44	165.00	4.50	4.94	-5.03	-4.84	3.63	4.02	-3.71	-3.60	3.67	3.70	-3.77	-3.47	19%	19%	26%	26%	18%	25%	25%	28%	-1%	7%	-1%	6%								
Story43	161.40	4.32	4.80	-4.98	-4.65	3.39	4.02	-4.91	-4.59	4.02	4.48	-4.39	-3.91	-2%	-12%	1%	1%	7%	7%	12%	16%	9%	12%	9%	14%								
Story42	157.80	4.15	4.77	-4.95	-4.67	4.33	4.55	-4.84	-4.57	4.04	4.55	-4.38	-3.90	-5%	-14%	2%	2%	3%	5%	11%	17%	7%	18%	9%	14%								
Story41	154.20	4.05	4.62	-4.83	-4.80	3.45	3.72	-3.60	-3.42	3.65	3.81	-3.64	-3.42	15%	20%	25%	29%	10%	18%	25%	29%	-5%	-2%	-1%	2%								
Story40	150.60	4.01	4.62	-4.74	-4.87	3.35	3.52	-3.52	-3.36	3.48	3.73	-3.54	-3.37	16%	24%	26%	31%	13%	19%	25%	31%	-3%	-5%	0%	5%								
Story39	147.00	3.92	4.66	-4.65	-4.91	3.24	3.38	-3.40	-3.39	3.26	3.63	-3.43	-3.28	17%	27%	27%	31%	17%	22%	26%	33%	-1%	-5%	-1%	0%								
Story38	143.40	3.81	4.64	-4.52	-4.94	3.12	3.27	-3.27	-3.39	3.06	3.46	-3.28	-3.17	18%	30%	28%	31%	20%	25%	27%	36%	2%	0%	4%	4%								
Story37	139.80	3.71	4.58	-4.46	-4.90	3.10	3.23	-3.18	-3.35	3.02	3.29	-3.16	-3.22	17%	30%	29%	32%	19%	28%	29%	34%	2%	-1%	0%	3%								
Story36	136.20	3.78	4.51	-4.49	-4.79	3.16	3.36	-3.19	-3.35	3.05	3.22	-3.14	-3.28	16%	26%	29%	30%	19%	29%	30%	31%	3%	3%	1%	1%								
Story35	132.60	3.87	4.44	-4.52	-4.66	3.20	3.43	-3.19	-3.38	3.16	3.22	-3.10	-3.36	17%	23%	30%	27%	19%	27%	31%	28%	1%	5%	2%	1%								
Story34	129.00	3.92	4.39	-4.55	-4.58	3.25	3.54	-3.35	-3.41	3.27	3.23	-3.12	-3.44	17%	19%	26%	26%	16%	26%	31%	25%	0%	7%	5%	1%								
Story33	125.40	3.98	4.38	-4.66	-4.53	3.34	3.63	-3.58	-3.53	3.35	3.26	-3.24	-3.51	16%	17%	23%	22%	16%	26%	31%	23%	0%	8%	7%	0%								
Story32	121.80	4.11	4.40	-4.82	-4.39	3.49	3.74	-3.73	-3.68	3.47	3.35	-3.44	-3.67	15%	15%	22%	16%	16%	24%	29%	16%	0%	9%	6%	0%								
Story31	118.20	4.19	4.32	-4.86	-4.26	3.63	3.83	-3.87	-3.87	3.68	3.53	-3.67	-3.80	14%	11%	20%	9%	12%	18%	25%	11%	-1%	7%	4%	2%								
Story30	114.60	4.21	4.29	-4.92	-4.35	3.73	3.90	-4.02	-4.04	3.87	3.76	-3.89	-3.92	11%	9%	18%	7%	8%	12%	21%	10%	-3%	3%	3%	2%								
Story29	111.00	4.20	4.28	-4.92	-4.53	3.84	3.93	-4.06	-4.20	3.99	3.93	-4.07	-4.04	9%	8%	18%	7%	5%	8%	17%	11%	-4%	0%	0%	4%								
Story28	107.40	4.15	4.27	-4.81	-4.70	3.92	3.96	-4.02	-4.26	4.06	4.01	-4.16	-4.12	6%	7%	16%	9%	2%	6%	14%	12%	-3%	-1%	-3%	3%								
Story27	103.80	4.12	4.26	-4.80	-4.77	3.94	4.01	-3.98	-4.21	4.08	4.04	-4.21	-4.20	4%	6%	17%	12%	1%	5%	12%	12%	-4%	-1%	-5%	0%								
Story26	100.20	4.14	4.33	-4.72	-4.73	3.91	4.06	-3.93	-4.09	4.09	4.09	-4.25	-4.21	6%	6%	17%	13%	1%	6%	10%	11%	-4%	-1%	-7%	-3%								
Story25	96.60	4.19	4.40	-4.72	-4.61	4.89	5.06	-4.77	-4.80	4.89	5.04	-4.97	-4.80	-17%	-15%	-1%	-4%	-17%	-15%	-5%	-4%	0%	-4%	-2%	0%								
Story24	93.00	4.21	4.50	-4.69	-4.62	5.01	5.06	-4.85	-4.79	4.93	5.03	-4.95	-4.79	-19%	-12%	-3%	-4%	-17%	-12%	-5%	-4%	2%	1%	-2%	0%								
Story23	89.40	4.21	4.62	-4.66	-4.69	3.80	4.07	-3.77	-3.77	3.98	4.03	-4.02	-3.96	10%	12%	19%	20%	6%	13%	14%	16%	-4%	1%	-5%	-4%								
Story22	85.80	4.24	4.68	-4.65	-4.79	3.70	3.95	-3.67	-3.59	3.84	3.83	-3.78	-3.79	13%	16%	21%	25%	9%	18%	19%	21%	-3%	3%	-2%	3%								
Story21	82.20	4.23	4.70	-4.56	-4.85	3.65	3.74	-3.55	-3.40	3.75	3.54	-3.57	-3.63	14%	20%	22%	30%	11%	25%	22%	25%	-2%	4%	0%	-5%								
Story20	78.60	4.24	4.71	-4.65	-4.85	3.77	3.71	-3.54	-3.30	3.71	3.36	-3.53	-3.52	11%	21%	24%	32%	13%	29%	24%	27%	1%	8%	0%	-5%								
Story19	75.00	4.32	4.71	-4.82	-4.89	3.84	3.92	-3.59	-3.43	3.71	3.50	-3.67	-3.49	11%	17%	26%	30%	14%	26%	24%	29%	3%	9%	-2%	-1%								
Story18	71.40	4.48	4.71	-5.01	-4.88	3.98	4.05	-3.77	-3.65	3.82	3.67	-3.90	-3.61	11%	14%	25%	25%	15%	22%	22%	26%	4%	8%	-3%	1%								
Story17	67.80	4.60	4.72	-5.16	-4.97	4.16	4.18	-3.92	-3.87	3.99	3.87	-4.09	-3.86	9%	12%	24%	22%	13%	18%	21%	22%	4%	6%	-3%	0%								
Story16	64.20	4.68	4.78	-5.21	-5.05	4.31	4.32	-4.03	-4.18	4.16	4.05	-4.20	-4.08	8%	10%	23%	17%	11%	15%	19%	19%	3%	6%	-3%	0%								
Story15	60.60	4.78	4.84	-5.25	-5.07	4.47	4.46	-4.26	-4.47	4.34	4.30	-4.36	-4.39	7%	8%	19%	12%	9%	11%	16%	14%	3%	3%	-3%	0%								
Story14	57.00	4.83	4.98	-5.28	-5.20	4.73	4.64	-4.49	-4.74	4.49	4.59	-4.65	-4.66	2%	7%	15%	9%	7%	8%	12%	10%	5%	1%	-3%	2%								
Story13	53.40	4.91	5.15	-5.23	-5.23	4.86	4.82	-4.68	-4.88	4.63	4.86	-4.84	-4.90	1%	6%	11%	7%	6%	6%	7%	6%	5%	5%	-1%	0%								
Story12	49.80	4.99	5.30	-5.17	-5.22	4.93	4.99	-4.85	-4.98	4.77	5.05	-4.98	-5.05	1%	6%	6%	5%	4%	5%	4%	3%	3%	6%	-3%	1%								
Story11	46.20	4.99	5.37	-5.23	-5.16	5.04	5.09	-5.01	-5.01	4.94	5.12	-5.03	-5.12	-1%	5%	4%	3%	1%	5%	4%	1%	2%	6%	-3%	0%								
Story10	42.60	4.96	5.41	-5.22	-5.15	5.17	5.16	-5.07	-5.01	5.12	5.10	-5.12	-5.01	-4%	5%	3%	3%	4%	6%	4%	1%	1%	1%	1%	1%								
Story9	39.00	4.88	5.35	-5.19	-5.16	5.29	5.19	-5.06	-5.02	5.24	5.06	-5.02	-5.08	-8%	3%	2%	3%	3%	5%	3%	2%	1%	2%	1%	1%								
Story8	35.40	4.77	5.26	-5.19	-5.16	5.32	5.13	-5.06	-5.01	5.29	5.07	-5.00	-4.95	-12%	3%	3%	3%	-1%	6%	4%	4%	1%	3%	1%	1%								
Story7	31.80	4.68	5.21	-5.29	-5.12	5.27	5.10	-5.08	-5.01	5.19	4.96	-5.02	-4.91	-12%	2%	4%	2%	-1%	5%	5%	4%	2%	3%	1%	2%								
Story6	28.20	4.73	5.29	-5.33	-5.04	5.33	5.32	-5.18	-4.96	5.19	5.14	-5.09	-4.88	-13%	-1%	3%	2%	-10%	3%	4%	3%	3%	3%	2%	2%								
Story5	24.60	4.82	5.40	-5.51	-5.06	5.68	5.76	-5.61	-5.18	5.49	5.64	-5.52	-5.13	-18%	-7%	-2%	-2%	-14%	-4%	0%	-1%	4%	2%	2%	2%								
Story4	17.40	5.11	5.49	-5.70	-5.23	5.96	6.03	-5.88	-5.38	5.94	6.02	-5.90	-5.38	-17%	-10%	-3%	-3%	-16%	-10%	-3%	-3%	0%	0%	0%	0%								
Story3	14.00	5.30	5.56	-5.83	-5.34	6.11	6.12	-6.03	-5.44	6.13	6.18	-6.08	-5.53	-15%	-10%	-3%	-2%	-16%	-11%	-4%	-4%	0%	1%	-1%	-1%								
Story2	10.60	5.31	5.66	-5.81	-5.29	6.05	6.20	-5.94	-5.48	5.99	6.25	-5.99	-5.48	-14%	-9%	-2%	-4%	-13%	-10%	-3%	-4%	1%	0%	-1%	-1%								
Story1	7.20	5.48	5.78	-5.89	-5.32	6.13	6.32	-5.86	-5.45	6.09	6.34	-5.93	-5.39	-12%	-9%	1%	-2%	-11%	-10%	-1%	-1%	1%	0%	-1%	-1%								

Table 5. 77 Mean acceleration comparison - Nonlinear time history analysis

Evaluating the average values obtained, it can be observed that models 2 and 3 define a reduction in acceleration compared to Model 1, is defined as an average reduction compared to Model 1 of 13% for the structure with 2 Outrigger and 16% for the structure with 3 Outrigger.

If we wanted to analyze a difference between Model 2 and Model 3, we note that in most levels the Model with 3 Outrigger has acceleration values lower than the Model with 2 Outrigger up to a maximum of 19% in the direction and evaluating the positive values, in general, however, the reduction of the system with 3 Outrigger compared to the system with 2 Outrigger is equal to 3%.

Table 5.78 Shows the maximum value obtained in x and y direction and compared for acceleration considering both the Mexican standard and the CFE:

Maximum values for Interstory Acceleration - Mexican Code

	w/o OUTRIGGER	with 2 OUTRIGGER	with3 OUTRIGGER	**REDUCTION Model 2**	**REDUCTION Model 3**	**COMPARISON MODEL 2 VS MODEL 3**
	[m/s^2]	**[m/s^2]**	**[m/s^2]**	**[%]**	**[%]**	**[%]**
MAX X	9.876	7.505	7.402	24%	25%	1%
MAX Y	9.946	7.380	7.329	26%	26%	1%

Maximum values for Interstory Acceleration - CFE

	w/o OUTRIGGER	with 2 OUTRIGGER	with3 OUTRIGGER	**REDUCTION Model 2**	**REDUCTION Model 3**	**COMPARISON MODEL 2 VS MODEL 3**
	[m/s^2]	**[m/s^2]**	**[m/s^2]**	**[%]**	**[%]**	**[%]**
MEAN X	8.433	6.127	6.134	27%	27%	0%
MEAN Y	8.019	6.319	6.341	21%	21%	0%

Table 5. 78 Maximum values for Interstory Acceleration - Mexican Code and CFE

Analyzing the maximum values obtained both evaluating the maximum and the average of all the values obtained as output we can define a difference between the Mexican Code and the CFE.

The reduction in Models 2 and 3 compared to Model 1 of the system-free structure can be deduced in both cases. Comparing both models with the applied system we note that:

- By evaluating the maximum values, the model with 3 Outrigger has an improvement over the model without Outrigger up to 26% in the y direction, as well as the Model with 2 Outrigger. You can also notice that the Model 3

has an irrelevant improvement over the system with 2 Outrigger, equal to 1% for both directions.

- Evaluating the average values, the model with 3 Outrigger has an improvement over the model without Outrigger up to 27% in the y direction, as well as the Model with 2 Outrigger. You can also notice that the 3 model shows no improvement on the maximum value obtained compared to the system with 2 Outrigger, in fact the comparison is equal to 0% for both directions.

Figure 5.115 shows the results compared for the maximum acceleration in coverage analyzed for the three models and defined as time changes considering the acceleration corresponding to the accelerogram 2:

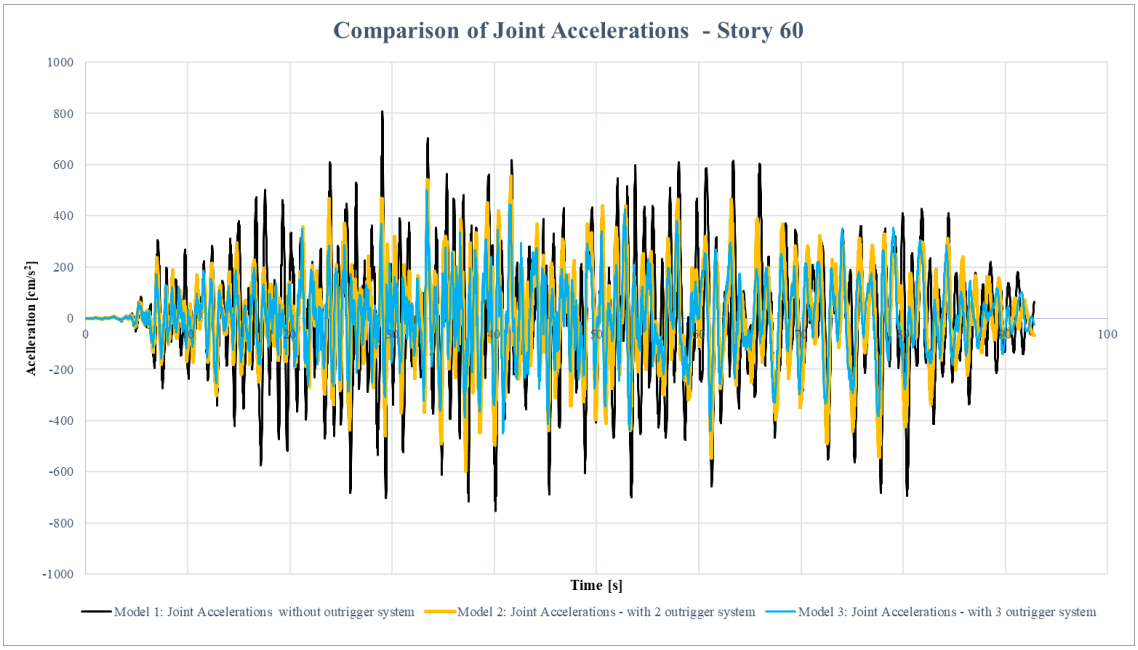

Figure 5. 115 Comparison for maximum acceleration in roof

❖ **Demand to capacity ratio –Collapse Prevention**

Considering the request for collapse prevention (CP) with capacity ratios of beams, columns and walls for the three structures at MCE level. In particular, as shown in Table 5.79, the collapse prevention D/C ratios are lower for the structure equipped with Outrigger with SLB, although the quantities of structural steel reinforcement elements are smaller than the corresponding ones used in the bare frame structure. This aspect confirms that in the structure with SLB devices the damage is mainly

concentrated in the heatsinks, while in the other structural elements are partially preserved.

Element [-]	Modello 1: w/ooutrigger Mean D/C for CP [-]	Modello 1: w/ooutrigger Max D/C for CP [-]	Modello 2: with 2outriggers Mean D/C for CP [-]	Modello 2: with 2outriggers Max D/C for CP [-]	Modello 3: with 3 outriggers Mean D/C for CP [-]	Modello 3: with 3 outriggers Max D/C for CP [-]
Beam	0.150	0.210	0.129	0.161	0.122	0.170
Column	0.007	0.064	0	0	0	0
Wall	0.113	0.132	0.079	0.089	0.082	0.092
SLB device	-	-	0.618	0.836	0.655	0.864

Table 5. 79 Comparison of Collapse Prevention D/C ratios for structure

- **Hysteretic cycle of the most stressed element**

Figure 5.116 shows the comparison of hysteretic behaviour for the structural element as the most stressed beam. You may notice that there is a significant curve reduction for the structure with 2 Outrigger, but even greater for the structure with 3 Outrigger.

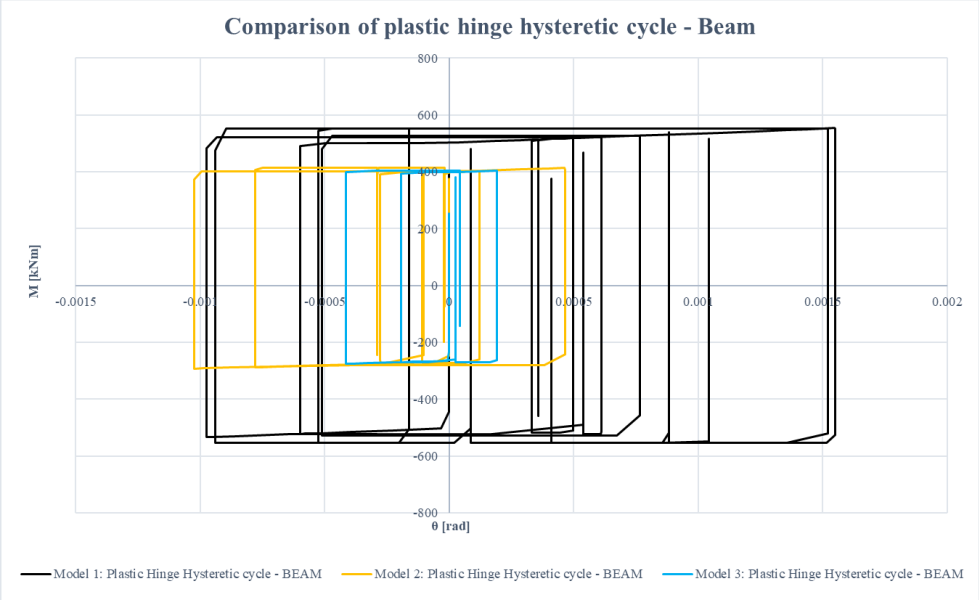

Figure 5. 116 Comparison of hysteretic cycles of the most stressed plastic hinges in Beam

In figure 5.117 it is represented the comparison of the hysteretic behavior for the structural element which wall, referred to the central core, more stressed. You may notice that there is a significant curve reduction for the structure with 2 Outrigger, but even greater for the structure with 3 Outrigger.

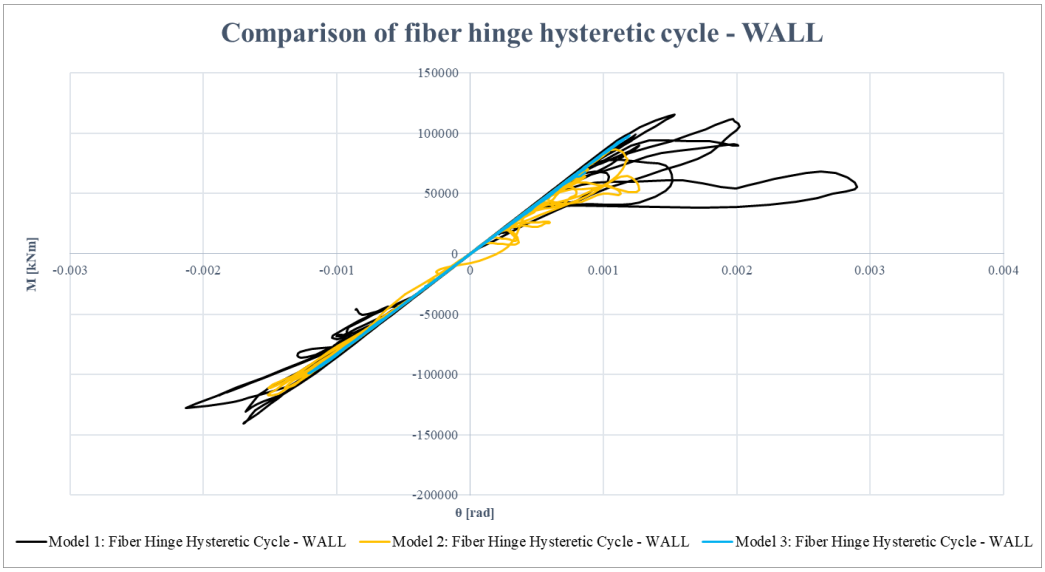

Figure 5. 117 Comparison of hysteretic cycles of the most stressed fibre hinges in Wall

5.9 Economic comparison

Section 5.8.1 describes the advantages of using SLB devices for structural behaviour following a seismic action. However, in order to make earlier results more meaningful, the three proposed solutions are compared in this chapter from an economic point of view. For this reason, the following Table 5.80 summarizes the costs of the materials considered for the case study, provided by an engineering company based in Mexico:

Material	Cost	
Concrete C35	238.43	$/m^3
Concrete C45	265	$/m^3
Concrete C55	292.37	$/m^3
Concrete C65	319.63	$/m^3
Steel reinforce	1.75	$/kg
Steel fordiagonals	2.19	$/kg
SLB Device	1500	$

Table 5. 80 Material costs for Paseo de Gracia project

The first step is to calculate the quantities of steel and cement used for the three structures analysed. The amount of concrete used for beams, columns and walls is different depending on the model and is calculated using the following expression:

$$V_c = A_c * \sum l_i$$

$$m_c = \rho_{conc} * V_c$$

Where:

- l_i is the net length of the i-th structural element;
- A_c is the cross section of the element;
- ρ_{conc} is the density of the concrete;
- V_c and m_c represent the volume and mass of the concrete respectively.

The calculated amount of concrete for beams and columns is summarised in Tables 5.81, 5.82 and 5.83, while the amount of concrete for walls is defined in Table 5.84,5.85 and 5.86 below:

Amount of concrete for the structure - Model 1: w/o outrigger

Section [-]	b [cm]	h [cm]	A_c [cm^2]	Totallength [cm]	ρ_{conc} [ton/m^3]	V_c [m^3]	m_c [ton]	$m_{c,tot}$ [ton]
C 90X160 C65	90	160	14400	77640		1118	2683	
C 90X140 C65	90	140	12600	78000		983	2359	
C 90X120 C55	90	120	10800	51480		556	1334	
C90X140 C55	90	140	12600	57840		729	1749	
C 90X120 C45	90	120	10800	48960	2.4	529	1269	21,00
C 90X100 C45	90	100	9000	48960		441	1058	
T 50X120 C35	50	120	6000	61110		367	880	
T 50X90 C35	50	90	4500	857613		3859	9262	
T 30X70 C35	30	70	2100	82078		172	414	

Table 5. 81 Amount of concrete for the element frame - Model 1: w/o outrigger

Amount of concrete for the structure - Model 2: with 2 outriggers

Section [-]	b [cm]	h [cm]	A_c [cm^2]	Totallength [cm]	ρ_{conc} [ton/m^3]	V_c [m^3]	m_c [ton]	$m_{c,tot}$ [ton]
C 90X160 C65	90	160	14400	77280		1113	2671	
C 90X140 C65	90	140	12600	77280		974	2337	
C 90X120 C55	90	120	10800	51840		560	1344	
C90X140 C55	90	140	12600	51840		653	1568	
C 90X120 C45	90	120	10800	48960	2.4	529	1269	20,80
C 90X100 C45	90	100	9000	48960		441	1058	
T 50X120 C35	50	120	6000	61110		367	880	
T 50X90 C35	50	90	4500	857613		3859	9262	
T 30X70 C35	30	70	2100	82078		172	414	

Table 5. 82 Amount of concrete for the element frame - Model 2: with 2 outriggers

Amount of concrete for the structure - Model 3: with 3 outriggers

Section	b	h	A_c	Totallength	ρ_{conc}	V_c	m_c	$m_{c,tot}$
[-]	[cm]	[cm]	[cm^2]	[cm]	[ton/m^3]	[m^3]	[ton]	[ton]
C 90X160 C65	90	160	14400	77280		1113	2671	
C 90X140 C65	90	140	12600	77280		974	2337	
C 90X120 C55	90	120	10800	51840		560	1344	
C90X140 C55	90	140	12600	51840		653	1568	
C 90X120 C45	90	120	10800	48960	2.4	529	1269	20,80
C 90X100 C45	90	100	9000	48960		441	1058	
T 50X120 C35	50	120	6000	61110		367	880	
T 50X90 C35	50	90	4500	857613		3859	9262	
T 30X70 C35	30	70	2100	82078		172	414	

Table 5. 83 Amount of concrete for the element frame - Model 3: with 3 outriggers

Amount of concrete for the wall - Model 1: w/o outrigger

Section	Height	Thikness	A_c	Totallength	ρ_{conc}	V_c	m_c	$m_{c,tot}$
[-]	[m]	[m]	[m^2]	[m]	[ton/m^3]	[m^3]	[ton]	[ton]
Wall 70cm C65	3.6	0.7	2.52	91.34		230.17680	552	
Wall 60cm C65	3.6	0.6	2.16	562.85		1215.75600	2918	
Wall 50cm C55	3.6	0.5	1.8	451.76	2.4	813.16800	1951.6	6224.13
Wall 40cm C45	3.6	0.4	1.44	25.09		36.12960	86.71	
Wall 30cm C45	3.6	0.3	1.08	25.09		27.09720	65.03	
Wall 20cm C45	3.6	0.2	0.72	376.47		271.05840	650.54	

Table 5. 84 Amount of concrete for the wall - Model 1: w/o outrigger

Amount of concrete for the wall - Model 2: with 2 outriggers

Section	Height	Thikness	A_c	Totallength	ρ_{conc}	V_c	m_c	$m_{c,tot}$
[-]	[m]	[m]	[m^2]	[m]	[ton/m^3]	[m^3]	[ton]	[ton]
Wall 70cm C65	3.6	0.7	2.52	89.7		226.0440	542.51	
Wall 60cm C65	3.6	0.6	2.16	552.18		1192.7088	2862.50	
Wall 60cm C55	3.6	0.6	2.16	25.09		54.1944	130.07	6180.63
Wall 50cm C55	3.6	0.5	1.8	426.68	2.4	768.0240	1843.26	
Wall 40cm C45	3.6	0.4	1.44	25.09		36.1296	86.71	
Wall 30cm C45	3.6	0.3	1.08	25.09		27.0972	65.03	
Wall 20cm C45	3.6	0.2	0.72	376.48		271.0656	650.56	

Table 5. 85 Amount of concrete for the wall - Model 2: with 2 outriggers

Amount of concrete for the wall - Model 3: with 3 outriggers

Section	Height	Thikness	A_c	Totallength	ρ_{conc}	V_c	m_c	$m_{c,tot}$
[-]	[m]	[m]	[m^2]	[m]	[ton/m^3]	[m^3]	[ton]	[ton]
Wall 70cm C65	3.6	0.7	2.52	89.29	2.4	225	540	

Wall 60cm C65	3.6	0.6	2.16	552.18		1193	2863	
Wall 70cm C55	3.6	0.7	2.52	50.2		127	304	
Wall 60cm C55	3.6	0.6	2.16	451.78		976	2342	7674.56
Wall 50cm C55	3.6	0.5	1.8	376.48		678	1626	

Table 5. 86 Amount of concrete for the wall - Model 3: with 3 outriggers

The geometric percentage of steel reinforcement for structural elements is more different for the three proposed solutions (see Tables 5.87, 5.88 and 5.89for beams, Tables 5.90, 5.91, 5.92 for columns and Tables 5.93, 5.94, 5.95 for walls). As with concrete, the amount of steel used was calculated as:

$$m_S = \rho_{steel} * A_s * \sum l_i$$

Where:

- l_i is the net length of the i-th structural element;
- A_s is the cross section of the element;
- ρ_{steel} is the density of steel;
- m_s is the mass of steel:

Amount of steel rinforcement for the structure Model 1: w/o outrigger - BEAM

Model 1: w/o outrigger						
Beam Section	**b**	**h**	**A_c**	**Totallength**	**$m_{s,tot}$**	**$m_{s,tot}$**
[-]	**[cm]**	**[cm]**	**[cm^2]**	**[cm]**	**[ton]**	**[kg]**
T 50X120 C35	50	120	6000	61110		
T 50X90 C35	50	90	4500	857613	602.47	602,472.00
T 30X70 C35	30	70	2100	82078		

Table 5. 87 Amount of steel reinforcement for the structure Model 1: w/o outrigger – BEAM

Amount of steel rinforcement for the structure - Model 2: with 2 outrigger - BEAM

Model 2: with 2 outrigger						
Beam Section	**b**	**h**	**A_c**	**Totallength**	**$m_{s,tot}$**	**$m_{s,tot}$**
[-]	**[cm]**	**[cm]**	**[cm^2]**	**[cm]**	**[ton]**	**[kg]**
T 50X120 C35	50	120	6000	61110		
T 50X90 C35	50	90	4500	857613	578.92	578,915.00
T 30X70 C35	30	70	2100	82078		

Table 5. 88 Amount of steel reinforcement for the structure – Model 2: with 2 outrigger – BEAM

Amount of steel rinforcement for the structure - Model 3: with 3 outrigger - BEAM

Model 3: with 3 outrigger						
Beam Section	**b**	**h**	**A_c**	**Totallength**	**$m_{s,tot}$**	**$m_{s,tot}$**
[-]	**[cm]**	**[cm]**	**[cm^2]**	**[cm]**	**[ton]**	**[kg]**

T 50X120 C35	50	120	6000	61110		
T 50X90 C35	50	90	4500	857613	556.16	556,161.00
T 30X70 C35	30	70	2100	82078		

Table 5. 89 Amount of steel reinforcement for the structure - Model 3: with 3 outrigger - BEAM

Amount of steel rinforcement for the structure Model 1: w/o outrigger - COLUMN

ColumnSection	b	h	A_c	Totallength	ρ	$A_{s,tot}$	V_s	ρ_{steel}	m_s	$m_{c,tot}$	$m_{c,tot}$
[-]	[cm]	[cm]	[cm^2]	[cm]	[%]	[cm^2]	[m^3]	[ton/m^3]	[ton]	[ton]	[kg]
C 90X160 C65	90	160	14400	77640	3.63	522.72	40.58		319		
C 90X140 C65	90	140	12600	78000	3.64	458.64	35.77		281		
C 90X120 C55	90	120	10800	51480	1.7	183.6	9.45		74		
C90X140 C55	90	140	12600	57840	1.54	194.04	11.22	7.85	88	863.54	863,541.95
C 90X120 C45	90	120	10800	48960	1.32	142.56	6.98		55		
C 90X100 C45	90	100	9000	48960	1.36	122.4	5.99		47		

Table 5. 90 Amount of steel reinforcement for the structure Model 1: w/o outrigger – COLUMN

Amount of steel rinforcement for the structure - Model 2: with 2 outrigger - COLUMN

ColumnSection	b	h	A_c	Totallength	ρ	$A_{s,tot}$	V_s	ρ_{steel}	m_s	$m_{c,tot}$	$m_{c,tot}$
[-]	[cm]	[cm]	[cm^2]	[cm]	[%]	[cm^2]	[m^3]	[ton/m^3]	[ton]	[ton]	[kg]
C 90X160 C65	90	160	14400	77280	3.63	522.72	40.40		317		
C 90X140 C65	90	140	12600	77280	3.64	458.64	35.44		278		
C 90X120 C55	90	120	10800	51840	1.7	183.6	9.52		75		
C90X140 C55	90	140	12600	51840	1.54	194.04	10.06	7.85	79	850.85	850,852.08
C 90X120 C45	90	120	10800	48960	1.32	142.56	6.98		55		
C 90X100 C45	90	100	9000	48960	1.36	122.4	5.99		47		

Table 5. 91 Amount of steel reinforcement for the structure - Model 2: with 2 outrigger - COLUMN

Amount of steel rinforcement for the structure - Model 3: with 3 outrigger - COLUMN

ColumnSection	b	h	A_c	Totallength	ρ	$A_{s,tot}$	V_s	ρ_{steel}	m_s	$m_{s,tot}$	$m_{s,tot}$
[-]	[cm]	[cm]	[cm^2]	[cm]	[%]	[cm^2]	[m^3]	[ton/m^3]	[ton]	[ton]	[kg]
C 90X160 C65	90	160	14400	77280	3.19	459.36	35.50		279		
C 90X140 C65	90	140	12600	77280	3.14	395.64	30.58		240		
C 90X120 C55	90	120	10800	51840	1.42	153.36	7.95		62		
C90X140 C55	90	140	12600	51840	1.29	162.54	8.43	7.85	66	725.69	725,688.31
C 90X120 C45	90	120	10800	48960	1.04	112.32	5.50		43		
C 90X100 C45	90	100	9000	48960	1.02	91.8	4.49		35		

Table 5. 92 Amount of steel reinforcement for the structure – Model 3: with 3 outrigger – COLUMN

Amount of steel rinforcement for the structure Model 1: w/o outrigger - WALL

Model 1: w/o outrigger

Wall Section	b	h	A_c	Totallength	ρ	$A_{s,tot}$	V_s	ρ_{steel}	m_s	$m_{s,tot}$	$m_{s,tot}$
[-]	[m]	[m]	[m^2]	[m]	[%]	[m^2]	[m^3]	[ton/m^3]	[ton]	[ton]	[kg]
Wall 70cm C65	3.6	0.7	2.52	91.34	0.66	0.16632	15.1916688	7.85	119	691.33	691,334.67

Wall 60cm C65	3.6	0.6	2.16	562.85	0.25	0.054	30.3939	239	
Wall 50cm C55	3.6	0.5	1.8	451.76	0.34	0.0612	27.647712	217	
Wall 40cm C45	3.6	0.4	1.44	25.09	0.49	0.07056	1.7703504	14	
Wall 30cm C45	3.6	0.3	1.08	25.09	0.62	0.06696	1.6800264	13	
Wall 20cm C45	3.6	0.2	0.72	376.47	0.42	0.03024	11.3844528	89	

Table 5. 93 Amount of steel reinforcement for the structure Model 1: w/o outrigger – WALL

Amount of steel rinforcement for the structure - Model 2: with 2 outrigger - WALL

Model 2: with 2 outrigger											
Wall Section	**b**	**h**	**A_c**	**Totallength**	**ρ**	**$A_{s,tot}$**	**V_s**	**ρ_{steel}**	**m_s**	**$m_{s,tot}$**	**$m_{s,tot}$**
[-]	**[m]**	**[m]**	**[m^2]**	**[m]**	**[%]**	**[m^2]**	**[m^3]**	**[ton/m^3]**	**[ton]**	**[ton]**	**[kg]**
Wall 70cm C65	3.6	0.7	2.52	89.7	0.33	0.08316	7.459452		59		
Wall 60cm C65	3.6	0.6	2.16	552.18	0.27	0.05832	32.2031376		253		
Wall 60cm C55	3.6	0.6	2.16	25.09	0.25	0.054	1.35486		11		
Wall 50cm C55	3.6	0.5	1.8	426.68	0.3	0.054	23.04072	7.85	181	619.74	619,735.64
Wall 40cm C45	3.6	0.4	1.44	25.09	0.67	0.09648	2.4206832		19		
Wall 30cm C45	3.6	0.3	1.08	25.09	0.7	0.0756	1.896804		15		
Wall 20cm C45	3.6	0.2	0.72	376.48	0.39	0.02808	10.5715584		83		

Table 5. 94 Amount of steel reinforcement for the structure – Model 2: with 2 outrigger – WALL

Amount of steel rinforcement for the structure - Model 3: with 3 outrigger - WALL

Model 3: with 3 outrigger											
Wall Section	**b**	**h**	**A_c**	**Totallength**	**ρ**	**$A_{s,tot}$**	**V_s**	**ρ_{steel}**	**m_s**	**$m_{s,tot}$**	**$m_{s,tot}$**
[-]	**[m]**	**[m]**	**[m^2]**	**[m]**	**[%]**	**[m^2]**	**[m^3]**	**[ton/m^3]**	**[ton]**	**[ton]**	**[kg]**
Wall 70cm C65	3.6	0.7	2.52	89.29	0.64	0.16128	14.4006912		113		
Wall 60cm C65	3.6	0.6	2.16	552.18	0.27	0.05832	32.2031376		253		
Wall 70cm C55	3.6	0.7	2.52	50.2	0.53	0.13356	6.704712	7.85	53	890.01	890,009.02
Wall 60cm C55	3.6	0.6	2.16	451.78	0.31	0.06696	30.2511888		237		
Wall 50cm C55	3.6	0.5	1.8	376.48	0.44	0.0792	29.817216		234		

Table 5. 95 Amount of steel reinforcement for the structure - Model 3: with 3 outrigger - WALL

Listed below are the quantities used for the metal diagonals used as support for the Outrigger system in Model 2 and Model 3 (see tables 5.95 and 5.96):

Amount of steel for structure - Model 2: with 2 outriggers - Diagonal

Section	**Total Depth**	**Top FlangeWidth**	**Top FlangeThickness**	**Web Thickness**	**n**	**A_{flange}**	**A_{web}**	**A_{tot}**	**Totallength**	**V_s**	**ρ_{steel}**	**m_s**	**$m_{s,tot}$**
[-]	**cm**	**cm**	**cm**	**cm**	**[-]**	**[cm^2]**	**[cm^2]**	**[cm^2]**	**[cm]**	**[m^3]**	**[ton/m^3]**	**[ton]**	**[kg]**
S305X158 A36	32.7	31	2.51	1.55	64	155.62	50.685	206.305	13140.012	3	7.85	21	21,280.17

Table 5. 96 Amount of steel for structure - Model 2: with 2 outriggers - Diagonal

Amount of steel for structure - Model 3: with 3 outriggers - Diagonal

Section	Total Depth	Top FlangeWidth	Top FlangeThickness	Web Thickness	n	A_{flange}	A_{web}	A_{tot}	Totallength	V_s	ρ_{steel}	m_s	$ms_{,tot}$
[-]	cm	cm	cm	cm	[-]	[cm^2]	[cm^2]	[cm^2]	[cm]	[m^3]	[ton/m^3]	[ton]	[kg]
S305X158 A36	32.7	31	2.51	1.55	96	155.62	50.685	206.305	17777.333	4	7.85	29	28,790.29

Table 5. 97 Amount of steel for structure - Model 3: with 3 outriggers - Diagonal

Listed below are the comparisons of the quantities of material used for the three models. Table 5.98 shows the comparison of concrete quantities for beams and columns, Table 5.99 shows the comparison for concrete quantities for walls, Table 5.100 shows the comparison of reinforcement quantities used for beams and pillars and table 5.101 shows the comparison of reinforcement quantities used for walls:

Design comparison of frame element - Model 1 vs Model 2 &Model 1 vs Model 3

	Model 1: w/o outrigger		Model 2: with 2 outrigger		Model 3: with 3 outrigger		Comparison			
Section	m_{1c}	$m_{1c,tot}$	m_{2c}	$m_{2c,tot}$	m_{3c}	$m_{3c,tot}$	$\Delta m_{1s}/\Delta m_{2s}$	$\Delta m_{1s,tot}/\Delta m_{2s,tot}$	$\Delta m_{1s}/\Delta m_{3s}$	$\Delta m_{1s,tot}/\Delta m_{3s,tot}$
[-]	[ton]	[ton]	[ton]	[ton]	[ton]	[ton]	[-]	[-]	[-]	[-]
C 90X160 C65	2683		2671		2671		0%		0%	
C 90X140 C65	2359		2337		2337		1%		1%	
C 90X120 C55	1334		1344		1344		-1%		-1%	
C90X140 C55	1749		1568		1568		12%		12%	
C 90X120 C45	1269	21,008	1269	20,802	1269	20,802	0%	1%	0%	1%
C 90X100 C45	1058		1058		1058		0%		0%	
T 50X120 C35	880		880		880		0%		0%	
T 50X90 C35	9262		9262		9262		0%		0%	
T 30X70 C35	414		414		414		0%		0%	

Table 5. 98 Design comparison of frameelement- Model 1 vs Model 2 & Model 1 vs Model 3

Design comparison of wall - Model 1 vs Model 2 &Model 1 vs Model 3

	Model 1: w/o outrigger		Model 2: with 2 outrigger		Model 3: with 3 outrigger		Comparison	
Section	m_{1c}	$m_{1c,tot}$	m_{2c}	$m_{2c,tot}$	m_{3c}	$m_{3c,tot}$	$\Delta m_{1s,tot}/\Delta m_{2s,tot}$	$\Delta m_{1s,tot}/\Delta m_{3s,tot}$
[-]	[ton]	[ton]	[ton]	[ton]	[ton]	[ton]	[-]	[-]
Wall 70cm C65	552		543		540			
Wall 60cm C65	2918		2863		2863			
Wall 70cm C55	0		0		304			
Wall 60cm C55	0		130.07		2342			
Wall 50cm C55	1952	6,224	1843.26	6,181	1626	7,675	**1%**	**-23%**
Muro 40cm C45	87		87		0			
Muro 30cm C45	65		65		0			
Muro 20cm C45	651		651		0			

Table 5. 99 Design comparison of wall - Model 1 vs Model 2 & Model 1 vs Model 3

Rinforcement design comparison - Model 1 vs Model 2 &Model 1 vs Model 3

	Model 1: w/o outrigger		Model 2: with 2 outrigger		Model 3: with 3 outrigger		Comparison	
Section	**m_{1s}**	**$m_{1s,tot}$**	**m_{2s}**	**$m_{2s,tot}$**	**m_{3s}**	**$m_{3s,tot}$**	**$\Delta m_{1s,tot}/\Delta m_{2s,tot}$**	**$\Delta m_{1s,tot}/\Delta m_{3s,tot}$**
[-]	**[ton]**	**[ton]**	**[ton]**	**[ton]**	**[ton]**	**[ton]**	**[-]**	**[-]**
C 90X160 C65	319		317		279			
C 90X140 C65	281		278		240			
C 90X120 C55	74		75		62			
C90X140 C55	88		79		66			
C 90X120 C45	55	1,466	55	1,430	43	1,282	**2%**	**13%**
C 90X100 C45	47		47		35			
T 50X120 C35								
T 50X90 C35	602		0		0			
T 30X70 C35								

Table 5. 100 Reinforcement design comparison of frame– Model 1 vs Model 2 & Model 1 vs Model 3

Rinforcementdesigncomparison - Model 1 vs Model 2 &Model 1 vs Model 3

	Model 1: w/o outrigger		Model 2: with 2 outrigger		Model 3: with 3 outrigger		Comparison	
Section	**m_{1s}**	**$m_{1s,tot}$**	**m_{2s}**	**$m_{2s,tot}$**	**m_{3s}**	**$m_{3s,tot}$**	**$\Delta m_{1s,tot}/\Delta m_{2s,tot}$**	**$\Delta m_{1s,tot}/\Delta m_{3s,tot}$**
[-]	**[ton]**	**[ton]**	**[ton]**	**[ton]**	**[ton]**	**[ton]**	**[-]**	**[-]**
Muro 70cm C65	119		59		113			
Muro 60cm C65	239		253		253			
Muro 70cm C55	-		-		53			
Muro 60cm C55	-	691	11	620	237	890	**10%**	**-29%**
Muro 50cm C55	217		181		234			
Muro 40cm C45	14		19		-			
Muro 30cm C45	13		15		-			
Muro 20cm C45	89		83		-			

Table 5. 101 Reinforcement design comparison of wall – Model 1 vs Model 2 & Model 1 vs Model 3

It is possible to say that the use of the Outrigger system with the use of SLB devices allows a reduction in the amount of concrete in the beams and columns not very relevant and therefore by 1%, more relevant instead is in the walls of Model 3 in which there is a stiffening of the same until having a quantitative worsening of the -23% compared to Model 1. There is also a reduction in the amount of steel for beams and columns of 2% for model 2 and 13% for model 3, while in the case of walls there is a reduction of 10% for Model 2 and an increase of 29% for Model 3, both compared to the system-free structure. However, for solutions with the Outrigger system and SLB devices, in addition to the devices, the quantities of steel due to the

diagonals and walls that define the structural reinforcement system studied in this chapter and its application must also be evaluated. Specifically, for each wall (16 for Model 2 and 24 for Model 3) the amount of concrete was evaluated with the above equation, as well as for steel used for reinforcement and steel used in the diagonals. Finally, considering the material costs in Table 5.80, the following Table 5.102 summarises the total costs of the three solutions analysed:

Material	Cost		Model 1: w/o outrigger		Model 2: with 2 outrigger		Model 3: with 3 outrigger	
Concrete C35	238.43	$/m^3	1,048,682.45	$	1,048,682.45	$	1,048,682.45	$
Concrete C45	265	$/m^3	345,478.70	$	345,480.61	$	256,893.12	$
Concrete C55	292.37	$/m^3	613,373.55	$	595,053.18	$	875,083.53	$
Concrete C65	319.63	$/m^3	1,133,647.32	$	1,120,403.13	$	1,120,072.89	$
Steel rinforce	1.75	$/kg	2,565,524.41	$	2,502,092.39	$	2,243,236.30	$
Steel fordiagonals	2.19	$/kg	-	$	46,603.58	$	63,050.73	$
SLB Device	1500	$	-	$	24,000.00	$	36,000.00	$
TOTAL			**5,706,706.43**	**$**	**5,682,315.33**	**$**	**5,643,019.01**	**$**
COMPARISON				**$**	**0.4%**	**$**	**1.1%**	**$**

Table 5. 102 Economic comparison between the three solutions

In conclusion, it is important to note that the use of the Outrigger system coupled to SLB devices leads to an improvement in the seismic behavior of the structure, as explained in paragraph 5.8.1; from the economic point of view the realization of the 3 models defines a very similar economic expenditure for the 3 case studies. In particular, the structure with 2 systems Ourigger with SLB leads to a saving on construction costs of 0.4%, while the structure with 3 Outrigger with SLB defines a saving of 1.1%. The objective of the comparison must demonstrate that the three structures can be compared and it can be defined that the use of the Outrigger system with SLB heatsinks improves the structural behavior of the building at the same cost of the structure with and without system, also economically justifies the assumption of the Outrigger system with SLB.

6. CONCLUSIONS

In this thesis work we introduce the concept of Outrigger, which has been historically used in the construction of canoes and gradually extended to tall buildings and skyscrapers to mitigate the structural response and add stability. The literature survey conducted on the outrigger structure demonstrates its importance in controlling the response of tall buildings and shows that it is effective in high-rise buildings as a lateral load resistance technique by mitigating the vibration response of the building.

The introduction of new concepts of damped outriggers, i.e. with seismic energy dissipation devices, and in particular the Bozzo Shear Linksdevices, has represented a greater advantage to the field of application by reducing the vibration of the building with the addition of the reduction of lateral design forces. Due to the reduction of the lateral design forces, there is an increase in the structural damping, which has also led to the reduction in the size of the structural members and in the construction costs. While the SLB damped outrigger concept is still an upcoming project and a relatively new methodology in structural control and monitoring, it has enormous potential.

The theoretical study of this system is analysed through its application in a real case study (present in chapter 5). The system represents an excellent solution for seismic protection of tall buildings and is particularly advantageous due to its flexibility in covering a wide range of force capacities, which makes it adaptable to different levels of demand.

The combined use of the damped outrigger defines the following conclusions:

- the application of the outrigger to the building, as explained in paragraph 2.3, defines a greater stiffness to the structure and consequently determines a reduction of the displacements;
- the use of the SLB device, as described in chapter 4, lies in providing local ductility while avoiding local buckling in a simple way, in addition to the fact that the device itself is manufactured in a controlled and economical way.

The application of this system, can economically lead to small savings on material costs if its use is compared to the structure without a system. Consequently, it can be

deduced that for the same construction price, it is convenient to use this system which defines significant improvements from a structural point of view in terms of inter-floor drift, displacements, minimum shear at the base and accelerations. As well as the use of this system, combined with shear absorbers, leads to an overall improvement of the seismic behaviour of the structure by providing a large energy dissipation capacity due to its hysteretic behaviour, which generally translates into the concentration of most of the damages structures within the device, preserving the remaining structural elements from damage. This generally results in an economic saving in any restoration costs of the structural elements and non-structural components.

The case study analysed in this thesis concerns a new reinforced concrete building located in the city of Nuevo Porto Vallarta, Mexico. The analysis was carried out by analysing 3 Models, of which, Model 1 is given by the bare frame structure and therefore without the application of the outrigger system and SLB devices; Model 2 is given by the structure with the application of 2 systems; finally Model 3 with the application of 3 systems. The study was carried out analysing the structure both through linear analysis (in collapse conditions and in service conditions) and through non-linear time history analysis. Both have been verified through two regulations, the American one, namely the CFE and the Mexican regulation. The results of this study led to:

- a reduction in the period of up to 6% for Model 2 and 3% for Model 3;
- a maximum reduction of the interstory drift for the linear analysis in the collapse condition up to 39%, while in the service condition up to 38%; for non-linear analysis up to 46% for model 2 and up to 48% for model 3;
- a maximum reduction of the displacement for the linear analysis in the collapse condition up to 15%, while in the service condition up to 10%; for the non-linear analysis instead up to 53% for model 2 and up to 47% for model 3;
- a maximum reduction of the plane shear for the linear analysis in the collapsed condition up to 57%, while in the service condition up to 45%; while for the non-linear analysis up to 36% for model 2 and up to 46% for model 3;

- a maximum acceleration reduction for the non-linear analysis of up to 42% for model 2 and up to 48% for model 3;
- a saving on material costs of 0.4% in the case of the structure with 2 systems and of 1.1% in the case of the structure with 3 systems;

Finally, the maximum and mean collapse prevention through D/C ratios are lower for the system-equipped structure, even though the amounts of steel reinforcement in the structural members are considerably lower than the corresponding ones used in the bare-frame structure. This aspect confirms that in the structure with SLB devices the damage is mainly concentrated in the dissipators, while the other structural elements are partially preserved.

In conclusion we can say that, investigating all the analyses carried out, the use of the Outrigger system with SLB devices defines an improvement not only from the structural point of view, but also an economic advantage that determines, at the same cost of construction, a structure more rigid and more resistant to horizontal forces. Finally, comparing the two hypotheses studied with the insertion of the system, it is possible to say that with Model 2 and Model 3, evaluating the average responses of the structure is indifferent the choice of the two systems, By referring instead to the maximum values taken as reference, we prefer the Model 3 that, in small percentage, exceeds the performance of the Model 2, despite having the same construction cost.

REFERENCES

Hi Sun Choi, Goman Ho, Leonard Joseph & Neville Mathias, ***Outrigger Design for High-Rise Buildings, (An output of the CTBUH Outrigger Working Group)***

Wael Alhaddad, Yahia Halabi, Hu Xu, HongGang Lei, 2020. ***A Comprehensive Introduction to Outrigger and Belt-Truss System in Skyscrapers***

Arup, Level 5, 80 Tat Chee Avenue, Kowloon Tong, Hong Kong SAR, China, 2016. ***TheEvolution of Outrigger System in Tall Buildings***

B. G. Kavyashree, Shantharam Patil, Vidya S. Rao, 2021. ***Evolution of Outrigger Structural System: A State-of-the-Art Review***

Hi Sun Choi, Leonard Joseph, 2012. ***Outrigger System Design Considerations***

Archit Dangi, Sagar Jamle, 2019. ***Stability Enhancement of Optimum Outriggers and Belt Truss Structural System***

Monografía M-00 de ACHE, 2021. ***Estructuras con sistemas de protección sísmica***

Constantinou M.C., Soong T.T., Dargush G.F., ***"Passive Energy Dissipation Systems for Structural Design and Retrofit"***, Multidisciplinary center for earthquake engineering research (MCEER).

Alehashem et al., 2008. ***Behavior and Performance of Structures Equipped with ADAS & TADAS Dampers*** (a Comparison with Conventional Structures)

American Society of Civil Engineers, 2013. ***Seismic Evaluation and Retrofit of Existing Buildings Anil K. Chopra, 1995. Dynamics of structures*** (1st edition)

Bozzo Guillermo, Alva Rodrigo, Gnazzo Massimino, Dávalos Elizabeth, Bozzo Luis M., 2022. ***Evaluación del desempeño de tres tipos de disipadores de energía para la protección sísmica de edificios de gran altura***

Bozzo Guillermo, Alva Rodrigo, Chianese Riccardo, Bozzo Luis M., 2022. ***Two complex high rise buildings case studies equipped with SLB seismic devices***

Bozzo Guillermo, 2021. ***Una nueva generación de disipadores slb "shear link" para el diseño sismorresistente***

Bozzo Luis M, J. Ramirez, J. Bairan, G. Bozzo, E. Muñoz, 2020. ***Precast buildings equipped with SLB seismic devices***

Bozzo Luis M., H. Gonzales, M. Pantoja Medina, E. Muñoz, J. Ramirez, 2019. ***Modeling, analysis and seismic design of structures using energy dissipators SLB***

Bozzo Luis M., 2019. ***Análysis y diseño utilizando disipadores sísmicos tipo SLB***

TBI – RaminGolesorkhi, Leonard Joseph, Ron Klemencic, David Shook& John Viise, 2017.***Guidelinesfor Performance BasedSeismicDesignofTallBuildings***.

CFE 15, ***Manual de Diseño de Obras Civiles***, Capítulo C.1.3 Diseño por Sismo. Sección 3.1: Espectros de diseño símico para el territorio mexicano; Sección 3.3: Estructura Tipo1-Edificios

Cristian Cruz and Eduardo Miranda, Ph.D, 2017. ***Evaluation of Damping Ratios for the Seismic Analysis of Tall Buildings***

ACI 318-19***Code Requirements for Structural Concrete***

ASCE/SEI 41-13, ***American Society of Civil Engineers, Structural Engineers Institute***

Adapted from: https://www.csi-italia.eu/academy/analisi-pushover/analisi-pushover-parte-iii/

ACKNOWLEDGEMENTS

Esprimo la mia più sincera gratitudine ai miei due relatori, Il Prof. Giorgio Serino ed il Prof. Antonio Formisano, per la fiducia datami in questo percorso, per aver creduto in me e nelle mie capacità, vi ringrazio per l'aiuto fondamentale nella stesura della tesi e per la grande disponibilità mostratami.
Special thanks to my co-supervisor Prof. Luis Bozzo for his availability, for giving me the opportunity to have an unforgettable experience and for having had the opportunity to work in his studio, to be able to improve my knowledge, and challenge myself in this thesis topic.

Ringrazio la mia famiglia per avermi sempre supportata e per essere stata sempre dalla mia parte, nelle gioie e nelle ansie.
A mio cugino Giovanni, per essere come un fratello. Il mio confidente numero uno, sempre pronto ad ascoltarmi, sempre pronto ad esserci.

Un ringraziamento va a chi ha reso questo percorso, un'esperienza di vita indimenticabile, grazie alle persone stupende che ho incontrato e che sempre avranno un posto indelebile nel mio cuore.

Alla mia Casa Sollazzo e a tutte le mie splendide coinquiline, presenti e passate, in particolare:
Adelina, per essere stata sempre con me nonostante la distanza. Un punto fisso sul quale so poter fare sempre affidamento. Il bene che ci unisce rimarrà eterno.
Noemi, alla fantastica persona che sei, dolce e premurosa. Mi hai sempre tenuta d'occhio come una sorella maggiore e ti sei sempre accertata che stessi bene in ogni passo della mia vita. Sei speciale e sono felice di averti potuta scoprire con gli anni.
Maria e Marialea, con voi i sorrisi non mancano mai. Ci siete sempre state e mi avete regalato la leggerezza e la spensieratezza che solo Casa Sollazzo sa dare.
Simona, grazie per essere così esuberante e motivante. Nei momenti tristi sei riuscita a darmi quella forza in più per credere in me stessa e prendere la vita più con il sorriso che con le lamentele.

Alle mie compagne di avventura Carmen, Mesa, Mariangela e Annamaria. Questo

percorso lo abbiamo iniziato insieme e fino alla fine ci siamo sempre state. L'una per l'altra. E' stato bello condividere questi anni con voi, alla splendida amicizia che ci lega e che mai finirà. Ad altri mille traguardi e momenti felici insieme e alle femmene grosse che diventeremo!!

A tutti i miei amici di SSB, al gruppo Sciò Sciò Ciucciué, al legame profondo che ci unisce, ai momenti belli passati insieme e a quelli brutti che ci lasceranno presto. Sono felice di aver conosciuto meglio ognuno di voi e di avere tantissimi ricordi da rivivere insieme.

In particolare ringrazio Sara, la mia speciale commarella. Grazie per la tua costante presenza. Alla certezza che sei per me, la casa dove so poter sempre tornare. Al nostro anno di cambiamenti e momenti speciali, da vivere insieme sempre mano nella mano.

A Chicca, la mia amica da sempre. Grazie per aver avuto un posto speciale nella mia vita. Alla distanza che non ci cambierà.

A Barbara, siamo riuscite a portare avanti le nostre vite separate senza mai staccarci davvero. Al bene vero e sincero. Grazie per esserci sempre nei momenti importanti della mia vita.

Ad Alice e Giuditta, che hanno reso speciale la mia esperienza a Barcellona. Alla vita che ci ha fatte incontrare e alla speranza di non perderci mai.

Ad Arnaldo, il mio amico vero. Grazie per avermi sempre supportata, appoggiata e spesso anche sopportata. Grazie per esserci stato e per esserci sempre. Che le cose non cambino mai.

A Quentin, la mia camomilla. Grazie per aver reso il periodo più stressante della mia vita, un po' più leggero. La tua presenza è fondamentale per la mia sanità mentale. Alla tua leggerezza, simpatia e dolcezza e alla speranza che qualcosa di speciale non cambi mai, tia.